

The Crosslinking of Polyethylene by
Ultraviolet Radiation .

by

Waleed J. Georgie

A Thesis submitted to the Department of Pure and Applied Chemistry, University of Strathclyde, in accordance with the requirements for the Degree of Doctor of Philosophy.

1983

IMAGING SERVICES NORTH

Boston Spa, Wetherby
West Yorkshire, LS23 7BQ
www.bl.uk

BEST COPY AVAILABLE.

VARIABLE PRINT QUALITY

Acknowledgement

I would like to give my grateful thanks to the Department of Pure and Applied Chemistry, especially to my supervisor Professor N.B. Graham for his guidance and advice, throughout the project.

Also I would like to thank Imperial Chemical Industries PLC, for their grant and support in my project, especially my Industrial supervisor. Mr. F. Sherliker and his group in Runcorn.

I would also express my thanks to Dr. W.I. Bengough, Dr. R.W. Richards and Dr. D. Walsh for their valuable discussion during the work.

My thanks also go to Miss J. Douglas and Mrs. B. Sweeney for the typing of the thesis.

Last but not least I would like to thank my parents for their financial and moral support, without which the completion of this work would not have been possible.

Abstract

Crosslinking of low density polyethylene by ultraviolet light was carried out. The polyethylene was incorporated with high functionality monomer (crosslinking agent) and photoinitiator. Saturated and unsaturated hydrocarbon model systems were used in the project, in order that a better understanding of the crosslinking process could be established.

A comparison between photoinitiation crossing and Gamma irradiation process of the model systems and polyethylene was also carried out.

It was found that the properties of the photo-initiated crosslinked polyethylene were significantly improved, especially the flow properties and the environmental stress cracking resistance (ESCR). Other properties such as Tensile strength, Glass transition temperature (T_g) and melting temperature (T_m) were not greatly affected.

The significant improvement in the flow properties was due to the formation of the microphase of the high functional crosslinking agent which was incorporated in the polyethylene matrix. The formation of such a microphase was only achieved within the amorphous region of the polyethylene.

CONTENTS

	<u>Page No.</u>
Chapter 1 Introduction	1
1.1 Radiolysis of hydrocarbons	4
1.2 General Aspects of Light Absorption Processes	7
1.2.1 Excited States and Possibilities for Photo- initiation	8
1.2.2 The Nature and Reactivity of Excited States of Aromatic Carbonyl Compounds	12
1.3 Photoinduced Hydrogen Abstraction by Aromatic Carbonyl Compounds	17
1.3.1 General Mechanism	17
1.3.2 Photoinitiation by Xanthone	18
1.4 Polymerization of Allyl Compounds	21
1.4.1 Polymerization of Allyl Acetate	30
1.4.2 Polymerization of Tri- allyl Cyanurate	34
References	42
Chapter 2 Model Systems I	45
2.1 Introduction	45
2.2 Experimental	45
2.2.1 Materials	45
2.2.2 Apparatus	46
2.2.3 Photoinitiations	47

2.2.4	Octane, Xanthone and TAC Solutions for UV and Gamma irradiation	57
2.3	Discussion	65
	References	76
Chapter 3	Model Systems II	77
3.1	Introduction	77
3.2	Experimental	78
3.2.1	Materials	78
3.2.2	The Irradiation of Allyl- acetate, Xanthone and Hydrocarbon for Quali- tative Analysis	79
3.2.3	The Irradiation of Allyl- acetate, Xanthone and Octane for quantitative Analysis	83
3.3	Discussion	97
3.3.1	Discussion Based on the NMR Qualitative Results	97
3.3.2	Discussion Based on the GLC Qualitative Results	101
3.3.3	Discussion Based on the UV Quantitative Results	102
	References	120
Chapter 4	Crosslinking of Polyethylene	121
4.1	Introduction	121
4.2	Structure of Polyethylene	122

4.3	General Aspects of Crosslinking in Polyethylene	124
4.3.1	Radiation Effect in Poly- ethylene	124
4.3.2	Photochemically Cured Polyethylene	129
4.3.3	Methods for Analysing and Characterizing the Cross- linked Polyethylene	133
4.4	Characterisation of Polyethylene TAC Network Cured by Ultraviolet Light	149
4.5	Experimental	150
4.5.1	Materials Used	150
4.5.2	Equipment Used	151
4.5.3	Preparation of Poly- ethylene Batches	152
4.5.4	Curing of Polyethylene by Ultraviolet Light	153
4.5.5	Measuring the Gel Content	155
4.5.6	Analysis of the Gel Part	164
4.5.7	Light Penetration Through the Polyethylene Films	182
4.5.8	Post Curing of Poly- ethylene Films	185
4.5.9	The Effect of Crosslinking on the Mechanical Properties	189

4.5.10	The Characterization of the Sol Part by GPC	190
4.5.11	The Crosslinking Effect on Tg and Tm	194
4.5.12	The Crosslinking Effect on the Degree of Crystal- linity	194
	References	195
Chapter 5	Rheology Studies	198
5.1	Theory	198
5.2	Instrumentation	203
5.3	Experimental	205
	References	239
Chapter 6	Discussion and Conclusions	240
6.1	Discussion Based on the Results Obtained from the Polyethylene Networks	240
6.1.1	Gel and Sol Character- ization Results	243
6.1.2	Polyethylene Network Characterization Results	249
6.1.3	Flow Properties of the Polyethylene Network	252
6.2	Conclusions	255
	References	261

CHAPTER 1

INTRODUCTION

The irradiation of polymers has been a much studied subject over the past thirty-five years. The effects can be beneficial in causing an improvement in the physical properties of polymers or alternatively a desirable photo-degradation.

While most polymers, including polystyrene, may be crosslinked by radiation, polymers of tetrafluoro-ethylene are not crosslinked but rather degraded, as was also observed with polymethyl methacrylate and polyisobutylene.

Charlesby (1,2) found that polyethylene will crosslink by high energy radiation, using fast electron accelerators. The properties such as Young's modulus, density, melting point and other mechanical properties improve as a result. The crosslinking of polyethylene by other methods, such as thermal crosslink using peroxides or by ultra violet radiation (3,4) were followed.

Although the study of the photolysis of synthetic high polymers is important with respect to the effect of sunlight in promoting polymer degradation, photo-crosslinked polymers have not generated as much interest to industry as the high energy radiation crosslinked polymers. One of the reasons for this, is the limitation in the efficiency of the photo-crosslinking process.

Although the crosslinking of polyethylene has been accomplished by means of ultraviolet radiation with the addition of a photosensitizer (4), Oster found that the efficiency of the ultraviolet curing is as good as the

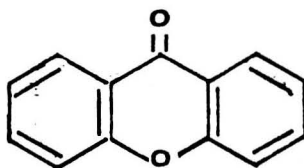
energetic and ionizing gamma rays. However, disadvantages do exist. The penetrating power of ultraviolet radiation was poor compared to the other high energy curing methods, but the cost of curing, using ultraviolet light should be quite low. Oster also found that there are potential advantages in the ultraviolet technique which lie in the cost and safety. Speed however, will be limited to a less extent as compared with thermally cured systems.

The effect of various types of radiation on polymers is the result of free radicals generated in the system and so it is not surprising that additives which can chemically generate free radicals or interact with radicals can themselves cause similar effects to electromagnetic radiation or electron beam. Thus thermally decomposable organic peroxides were found to cause crosslinking of polyethylene and the addition of carbon black to all of these initiating systems improved the efficiency of crosslinking (8).

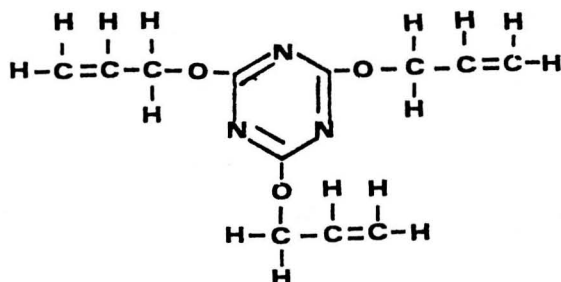
The use of polyfunctional monomers allows crosslinking of polymers not normally cured by radiation. Radiation crosslinking in the presence of a polyfunctional coagent has been studied with polyethylene (9, 51) polyvinylchloride (11, 12), cellulose acetate (13), polymethylmethacrylate (14) and several other polymers (15).

The interest in the system with which this thesis is concerned started with ICI looking at different photoinitiators and finding that by the use of coagents the efficiency of the crosslinking was improved. Xanthone was used as it gave a better performance than the other

twelve photoinitiators tested. Xanthone is also a thermally stable compound at the processing temperature of low density polyethylene. Triallyl cyanurate was chosen as a polymerisable additive because of the high functionality due to the presence of three allyl groups.



Xanthone



Tri-allyl Cyanurate (TAC)

The technical and commercial promise of such a system led to this programme in which the photosensitization and crosslinking mechanism was studied, together with the resulting physical properties morphology and rheology. Low density polyethylene was used for the work reported herein.

To aid understanding of the fundamentals of such a process, work was carried out by using smaller and simpler molecular models to study the mechanism of crosslinking. Hydrocarbons represent simple analogues of polyethylene. Therefore, a study of the behaviour of such compounds under irradiation should in principle lead to a better understanding of crosslinking. Extensive work has been reported

by different people (5,6) on the effects of ionizing radiation on hydrocarbons, from which a mechanism was established and related to the crosslinking of polyethylene.

Model system which will be discussed in the following chapters will be treated with UV radiation and the products compared with products obtained after γ -radiation.

1.1 Radiolysis of Hydrocarbons

Polyethylene molecules are essentially long chain aliphatic hydrocarbons of the type $(CH_2)_n$. Branching and unsaturation does exist in the chemical structure. The extent of branching is strongly dependent upon the polymerization conditions. In general polymer prepared by free radical polymerization under high pressure is known as low density polyethylene. The polymer prepared by metal alkyl catalysts using low pressure, which has a greater crystallinity, is known as high density polyethylene. The extent of crystallinity as determined by x-ray diffraction is strongly dependent upon the chemical structure and particularly upon the extent of branching.

The series of simple hydrocarbon molecules used should contain the chemical features of the polyethylene molecule. Saturated and unsaturated hydrocarbons and others with tertiary, secondary and primary carbon atoms were used.

Hydrocarbons subjected to high energy radiation were found to undergo complicated chain scission and chain extension reactions. The products from such reactions were a mixture of molecules with lower and higher molecular weights, than the starting hydrocarbons. Gases such as hydrogen were also observed to form during the process.

Free carbon has never been observed in these processes. Kevan and Libby (16) studied the irradiation of n-Hexane at two different temperatures, in the solid state at 77 K and liquid state 293 K. Their analysis was based on gas liquid chromatography (GLC) where it was found that their products were mainly branched n-Hexane dimers. Lower molecular weight species together with hydrogen was also found.

Known isomers of n-dodecane were synthesised and compared with the radiolysis branched dodecanes. It was found that the product of dimers formed have no dose dependences in the solid state radiation, while some dependence exists when radiation was carried out in the liquid state.

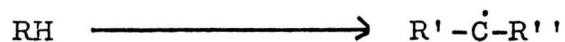
Also, some isomers of the C_{12} were formed at higher concentrations in the solid state than the liquid state. Other isomers however will form higher concentrations in liquid rather than the solid state.

Salovey and colleagues (17, 18) studied the chemical changes occurring in n-Hexadecane by γ -radiation. Again from their analyses which were based on GLC, it was found that the formation of saturated and unsaturated low molecular weight products (C_1-C_5), intermediate hydrocarbons ($C_{17}-C_{31}$), hydrogen and branched Dotria-contanes C_{32} 's were the crosslinking products of n-Hexane which was the major effect attributed to C-H rupture. Salovey (19) found similar behaviour on the irradiation of n-heptadecane.

The basic reaction in the radiolysis of saturated hydrocarbons will cause the formation of two different

types of free radical depending on whether a carbon-hydrogen or carbon-carbon bond is ruptured.

a) Carbon-hydrogen bond rupture

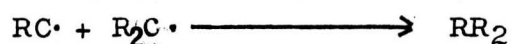
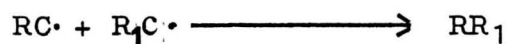
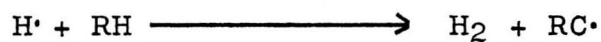


b) Carbon-carbon bond rupture

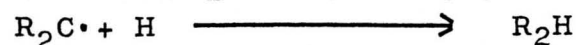
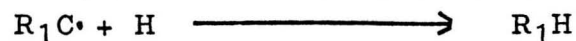


Where $R'-\dot{C}-R''$ is a free radical containing the same number of carbon atoms as the original hydrocarbon RH while $R_1C\cdot$ and $R_2C\cdot$ will have a smaller number of carbon atoms.

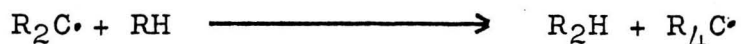
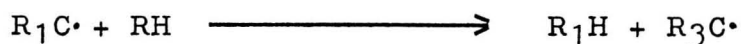
Hydrogen and condensation products may arise by the following steps



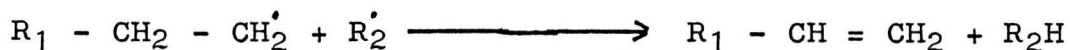
The reaction of the last type accounts for the formation of the dimer products. Products with n-number of C-atoms (C_n) may result from recombination of $R_1C\cdot$ and $R_2C\cdot$ with hydrogen radicals.



or from hydrogen abstraction



or else from disproportionation reactions



This analysis will be used in the following chapters, since the photolysis products from hydrocarbon, photo-initiator and crosslinking agent, will be compared to similar samples which were irradiated by ^{60}Co $\dot{\gamma}$ -irradiation.

1.2 General Aspects of Light Absorption Processes

Since the main object of this work is the photo-curing of polyethylene, a look at the light absorption processes are helpful. A photochemical process is a chemical reaction, which is initiated by light radiation.

Photochemistry is at the crossroads of chemistry and physics, since it is concerned with the interaction of electromagnetic radiation with matter. So by discussing photochemical processes, physical processes such as the absorption and emission of light should also be considered.

In molecular spectra of simple molecules (diatomic) consideration should be taken of the energies associated with the rotation of the molecule as a whole and with the periodic vibrations of the atoms constituting the molecule, in addition to the intramolecular motion of the electrons. Examples of such electronic energy levels of atoms are molecular, electronic, vibrational and rotational energy levels which are quantized and each set can be represented by expressions involving integers, e.g. the electronic, vibrational and rotational quantum number. Fig. 1.1

represents the energy levels and transitions in a diatomic molecule. Electronic absorption covers the region 7500\AA - 1100\AA , i.e. it falls in between the red end of the visible spectrum and the far ultraviolet or Schumann region.

Vibrational level absorption is from 3 to 30 microns which is in the infra-red region. Pure rotational levels are in the far infra-red beyond 30 microns.

In Polyatomic molecules, there are more electronic energy levels and closer spacing between them. These will lead to a greater overlapping of energy levels of the various electron states as in Fig. 1.2. The photophysical processes are classified in table 1.1 using hypothetical polyatomic molecules ABC. The primary photochemical processes are classified in table 1.2.

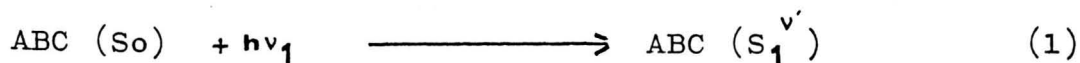
1.2.1 Excited States and Possibilities for Photo-initiation

It can be seen from the Fig. 1.2 that molecules have minimum electronic energy when in the ground state. Changes in the electronic configuration will occur when an electron from the highest occupied molecular orbital in the ground state shifts to the lowest vacant molecular orbital.

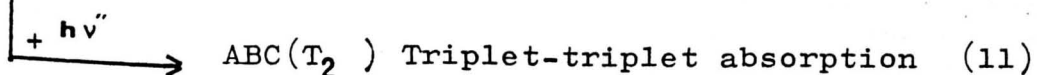
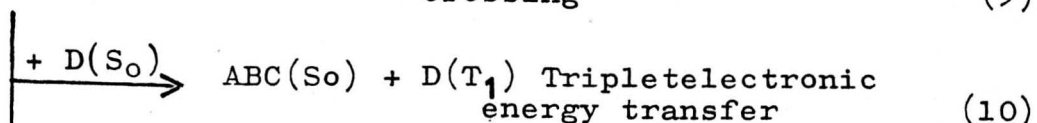
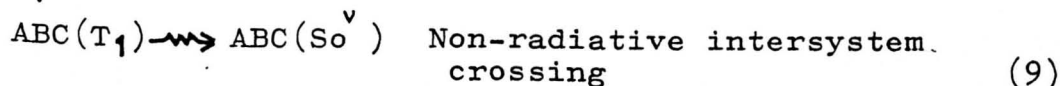
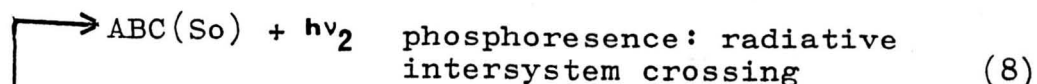
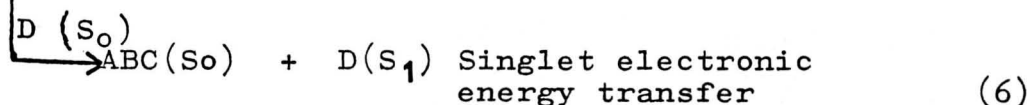
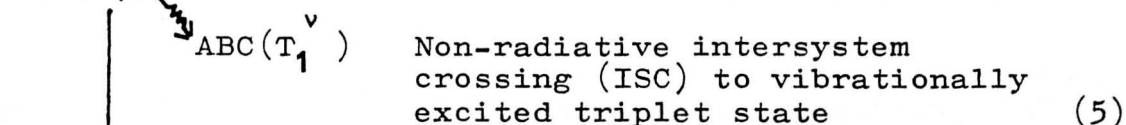
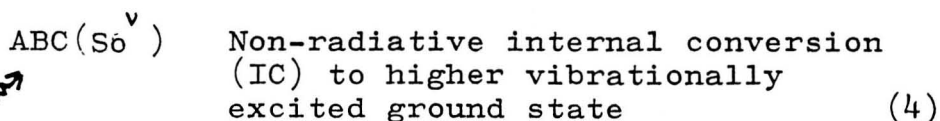
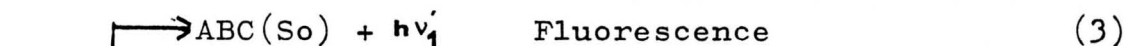
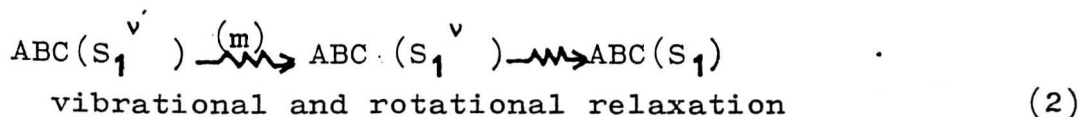
This change in electronic configuration will produce the first excited state, either singlet (S), or triplet (T), the triplet is of lower energy in accord with Hund's rule. Further excited states of greater energy may be formed by similar excitation processes (e.g. S_2 , S_3 , T_2 , T_3 , etc.). Singlet states are usually of higher energy than the equivalent triplet states because of

TABLE 1.1: Photophysical Processes of Polyatomic molecules as reported by Calvert and Pitts

Absorption of radiation and promotion to first excited singlet.



Photophysical Processes:



S_0, S_1, S_2 = Singlet electronic states

T_1, T_2 = Triplet electronic states

superscript v = Excess vibrational energy.

TABLE 1.2: Primary Photochemical Processes as reported
by Calvent and Pitts (20)

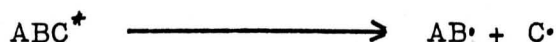
	→	$AB\cdot + C\cdot$	Dissociation into radicals	(1)
	→	$E + F$	Intramolecular decomposition into molecules	(2)
	→	ACB	Intramolecular rearrangement	(3)
	→	$ABC' (S_1) \circ$ or		
	→	$ABC' (T_1) \longrightarrow$	$ABC' (S_0)$ Photoisomerization	(4)
	→	$\xrightarrow{RH} (ABCH)\cdot + R\cdot$	Hydrogen atom abstraction	(5)
$ABC(S_1)$ or $ABC(T_1)$	→	$\xrightarrow{ABC} (ABC)_2$	Photodimerization (Photoaddition)	(6)
	→	$\xrightarrow{D} ABC + \text{products}$	Photosensitized reaction	(7)
	→	$ABC^+ + e^-$	Photoionization reaction	(8)
	→	$\xrightarrow{D} ABC^+ \text{ or } (-) + D^- \text{ or } (+)$	(External) electron transfer	(9)
	→	$AB^+ + C^-$	internal electron transfer	(10)

greater repulsion in the singlet states. Once the lowest excited singlet state is formed, it may lose its excitation energy in one of four possible processes.

- a) Radiationless, conversion back to ground singlet state.
- b) Radiative conversion back to ground singlet state (Fluorescence).
- c) Quenching of the excited singlet state by interaction with other constituents of the system.
- d) Conversion to the corresponding triplet excited state (intersystem crossing). These are mainly the processes for the generation of excited triplet states. The triplet will have a longer lifetime than the singlet state since a spin inversion must accompany any deactivation of the triplet.

It can be shown in table 1.2 that the photoexcited molecule whether in its S_1 or T_1 may initiate polymerization in different processes. In free radical polymerization, three processes may be used.

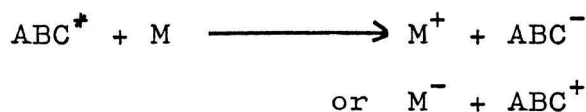
- I) Homolytic fragmentation of the photoexcited molecule i.e. dissociation into radicals.



- II) Hydrogen abstraction by the photoexcited molecule ABC^* from monomer, solvent so as to produce two radicals.

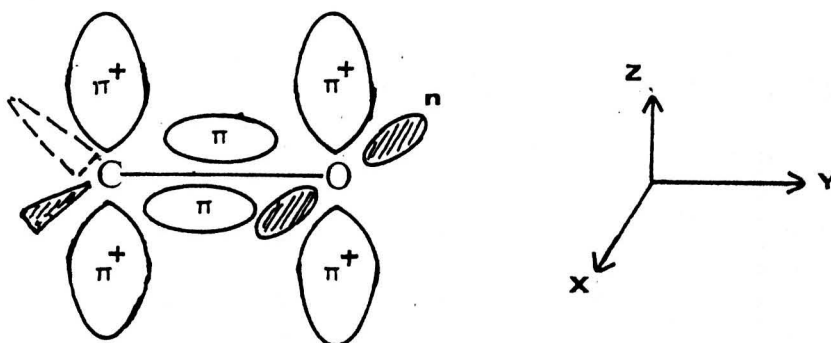


III) Electron transfer between photoexcited molecules and monomer, solvent or activation so as to produce a pair of ion radicals



1.2.2 The Nature and Reactivity of Excited States of Aromatic Carbonyl Compounds

Carbonyl compounds have electrons in orbitals, associated with the heteroatom, which are not involved in the bonding system of the molecule as shown below.

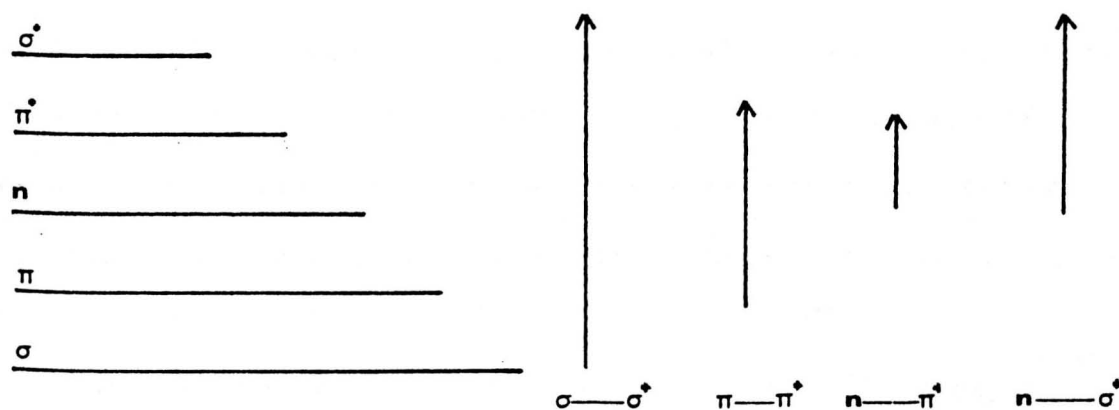


There are two electrons in each of the non-bonding A-orbitals (represented as a 2p orbital) of the oxygen atom. Absorption of radiation can lead to the promotion of one of these electrons into either a σ^+ or a π^+ . Singlet-singlet transition involving the promotion of a

non-bonding 2p electron of the oxygen atom to the carbonyl group's antibonding orbital is known as the $n \longrightarrow \pi^+$ transition. The other two transitions which may occur are $\pi \longrightarrow \pi^+$ and $n \longrightarrow \sigma^+$.

Molecules with n, π^+ first excited states generally differ significantly from those whose lowest states are π, π^+ [20]. In particular the natural life-time and the degree of localization of excitation are greater and the $S_1 \longrightarrow T_1$ energy gaps are less than for n, π^+ states.

For most molecules, the energies of the various bonding and anti-bonding orbitals increase in the order: -

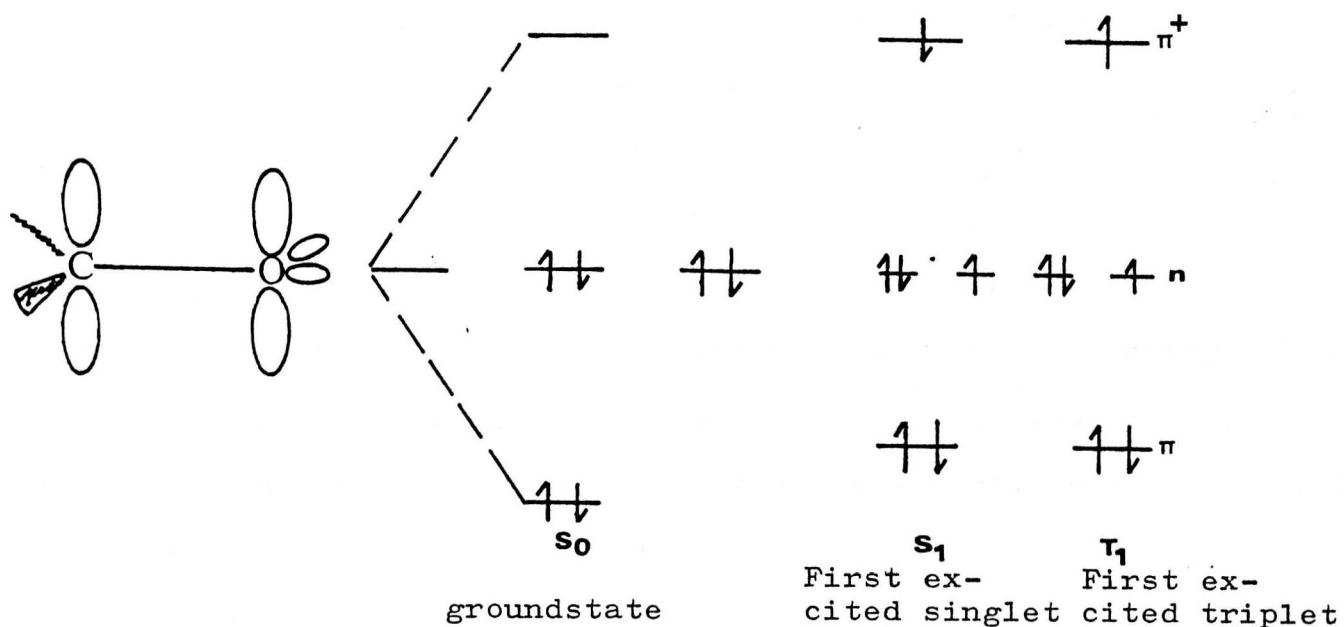


Usually $n \longrightarrow \pi^+$ transitions are lower in energy than the corresponding $\pi \longrightarrow \pi^+$ transitions but the positions may differ when the molecule has a high degree of conjugation in which case the π -orbital has a higher energy than the n -orbital.

In the above diagram, which represents the orbitals of a carbonyl group, it is indicated that the promotion of an electron from n to π^+ orbital will have the effect of removing the electron density from the oxygen atom, which means that (n, π^+) excited states have the reactivity of hydrogen bonding reactions (21).

On the other hand, the promotion of electrons a π to π^+ orbital has the effect of increasing the electron density at the oxygen atom which leads to the increase of the polar nature of the carbonyl group. Therefore by using a polar solvent, the energies of the transition will be effected and the differing electron distributions of excited states are manifested. Increasing the solvent polarity causes a decrease in the energy of $\pi \longrightarrow \pi^+$ transitions (red shift) mainly because polar solvents will reduce the energy of the more polar excited state by increased solvation. Increasing the solvent polarity will also shift the $n \longrightarrow \pi^+$ transition to shorter wavelength (blue shift) because the decrease in energy of n -orbital consequents hydrogen bonding or other dipolar interaction.

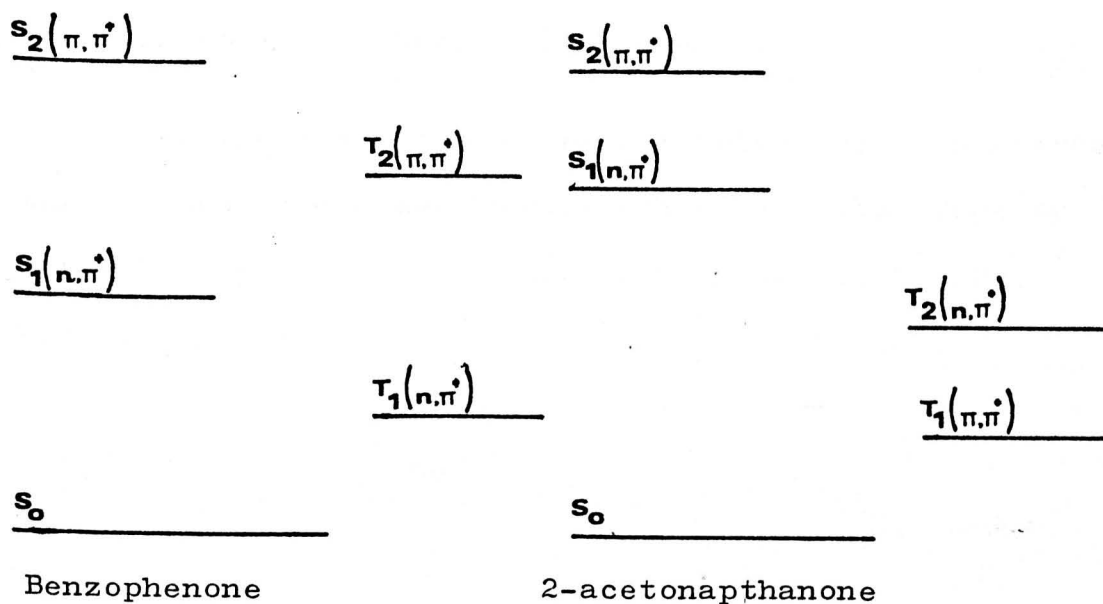
The $n \longrightarrow \pi^+$ excitation of a carbonyl group is shown below, in which both singlet and triplet excited states are possible.



The efficiency of intersystem crossing (i.e. $S_1 \longrightarrow T_1$) in the $n \longrightarrow \pi^+$ excited state is high. As already mentioned, the triplet states have the longest lifetimes. Triplet states are useful intermediates in organic photochemistry. The $n \longrightarrow \pi^+$ excitation is energetically more favoured than $\pi \longrightarrow \pi^+$ excitation of the carbonyl group.

Benzophenone derivatives are aromatic carbonyl compounds which generally give lowest energy $n \longrightarrow \pi^+$ transitions with complete conversion $S_1 \longrightarrow T_1$, which has been used extensively in organic photochemistry. Carbonyl triplet states of the ($n \longrightarrow \pi^+$) type readily abstract hydrogen atoms from reactive substrates such as alcohols and ethers.

Two types of aromatic carbonyl compounds give rise to the lowest energy excited states not having (n, π^+) character. In amino substituted benzophenones, whenever the degree of conjugation in aromatic carbonyl compounds is more extensive than the Ph - C = O group, the lowest lying triplet excited states are frequently (π, π^+) in nature. These compounds do not readily undergo the typical photoinduced hydrogen abstraction with alcohol and ethers. Compounds which are classified to give such behaviour include fluorenone, xanthone, phenyl benzophenone and α, β -naphthyl compounds. As seen below, the triplet excited states of benzophenone and 2-aceto-napthane are different in character.

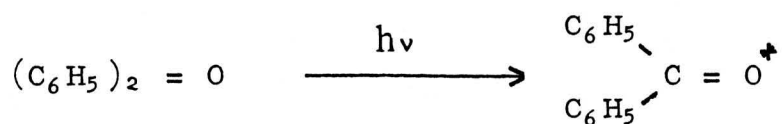


Having mentioned xanthone, the photoreduction of this compound, was reported by different workers and summarised by Cohen (22) and will now be dealt with in the following section.

1.3 Photoinduced Hydrogen Abstraction by Aromatic Carbonyl Compounds

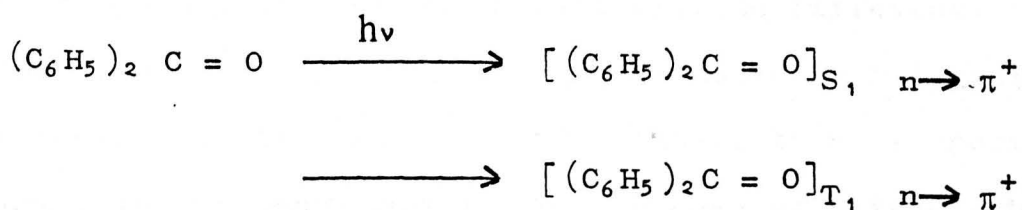
1.3.1 General Mechanism

The best known hydrogen abstraction reaction of aromatic carbonyls was discussed by Backstrom (20), in 1934, when he suggested that the hydrogen abstracting species in the photoreduction of benzophenone by alcohols was in his terms, the 'biradical' now identified as the benzophenone triplet.



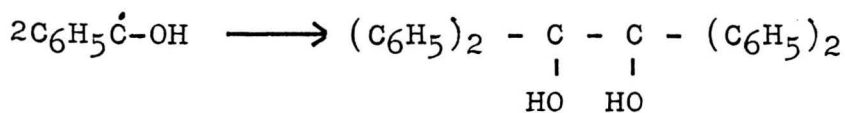
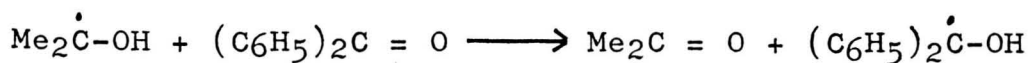
The photoreduction of benzophenone involves the formation of benzopinacol on ultraviolet irradiation of its solutions in ethers and alcohols.

Comprehensive studies were carried out by different workers and summarized by Ledwith (21). The steps by which benzophenone photoreduces isopropanol by free radical intermediates are summarized as follows:-



the general expression for the photo activated species $(\text{C}_6\text{H}_5)_2\text{C}=\text{O}^{\bullet}$





The photoreduction of benzophenone by isopropanol is accompanied by the formation of a coloured compound which was an adduct of the radicals formed from the hydrogen abstraction process. The precise reaction mechanism is still a matter of controversy.

1.3.2 Photoinitiation by Xanthone

Xanthone was found to have similar properties to benzophenone, when photoinitiated by ultraviolet light but was less efficient because of lower rates of hydrogen abstraction (23). Xanthone has been reported not to be photoreduced by certain alcohols such as 2-propanol (24). However, it was found to be photoreduced by ethanol, methanol, dioxan and hydrocarbons (25). Also xanthone was photoreduced by N_1N -dimethyl aniline to give xanthopinacol (26).

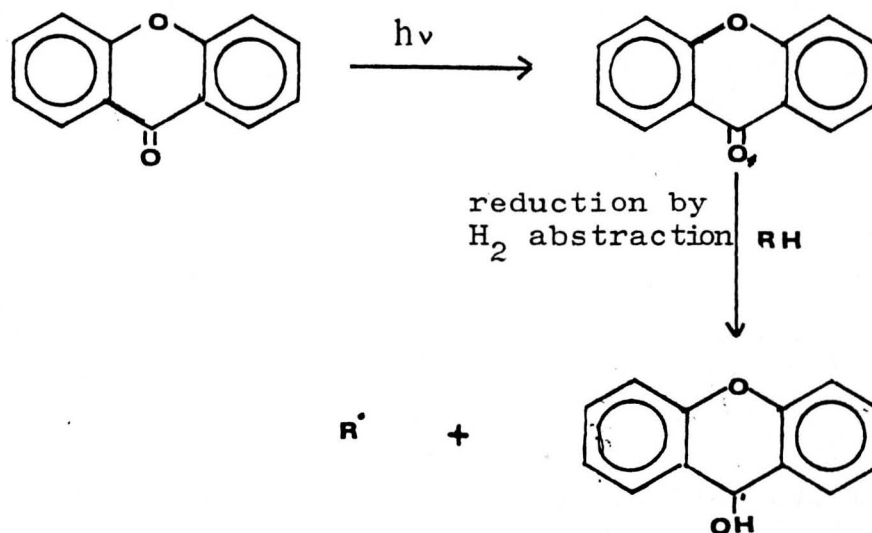
Zanker and Ehrhardt in their work (25), found that by irradiating Xanthone in polar solvent and non-polar solvent the photoreduction product will be different. In the case of the polar ethanol, its molecule interacts preferentially with Xanthone. The interaction is specific to the polar carbonyl group. In the case of hexane, which was used as a non-polar medium, the Xanthone molecule is free without any interaction and that was due to the solvation forces between the media and the reacting radicals (47). This phenomenon was apparently the cause for two main different mechanisms established for the

photoreaction of Xanthone.

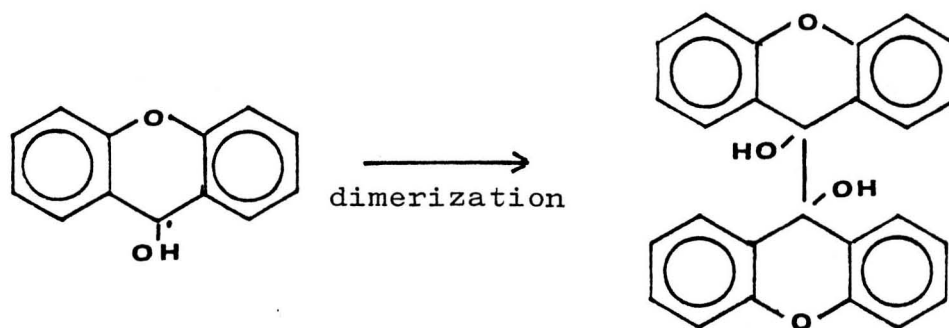
Zanker and Ehrhardt (25) reached the following reaction conclusions.

In the case of Xanthone present in the polar solvent it absorbs at the free electron pair of the carbonyl group, a quantum $n \longrightarrow \pi^+$ transition state and passes over to the triplet state. This will abstract a hydrogen from the solvent resulting in the reductive formation of the xanthydiol or a hydroxy xanthyl radical.

This radical will have two ways of reacting, firstly dimerization by combination of two equal xanthyl radicals to form dihydroxy dixanthyl and secondly an association of the xanthyl radical with a solvent radical generated due to the hydrogen abstraction. These two reaction mechanisms are shown below:-

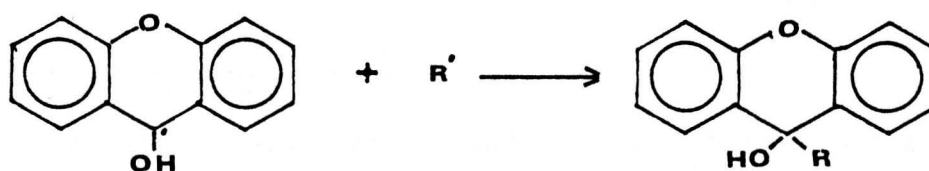


Reaction Path (1)



9,9'-dihydroxydioxanthone

Reaction Path (2)



Reaction path (2) seems to be favoured in the case of polar solvent as a strong interaction of the solvent molecule with the carbonyl group will take place.

Zanker and Ehrhandt, also studied the stability of dihydroxy dixathene by U.V. light. It was found that the dixanthene in the presence of oxygen, will oxidize to xanthone. It was also found that the dixanthene was stable photochemically in the absence of oxygen.

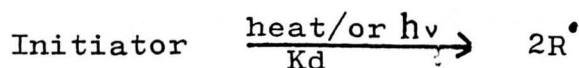
1.4 Polymerization of Allyl Compounds

Some chemistry, mainly of Triallylcyanurate and allyl acetate will be covered in this section since both were involved in this work. Before looking at the polymerization of these two compounds, the polymerization process as a whole will be considered.

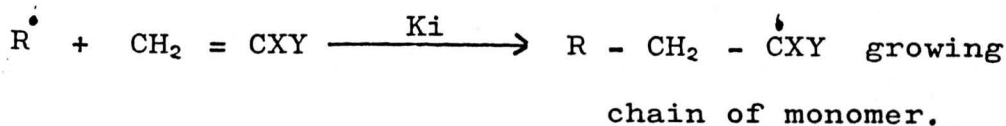
It is now generally accepted that there are four main reactions involved in chain polymerization; initiation, propagation, chain transfer and termination. (27)

(i) Initiation by free radicals

This occurs when free radicals are liberated e.g. Benzoyl peroxide initiated thermally to form Benzoyl radical (R). These free radicals will react in the presence of monomer to form a growing chain of monomer. The decomposition of a free radical initiator can be represented thus



The radical R[•] will react with the monomer as follows:-

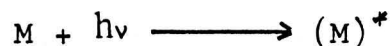


Where X and Y represent substituent atoms or groups according to the monomer being considered e.g. X = H Y = Ph in the case of styrene.

Polymerization can also be initiated by photochemical means, as described in the case of benzophenone and xanthone in Section 1.3

In general free radicals can be produced by means of ultraviolet irradiation in three ways.

- a) Photolysis of some monomers results in the formation of an excited state $(M)^*$ by the absorption of light quanta.



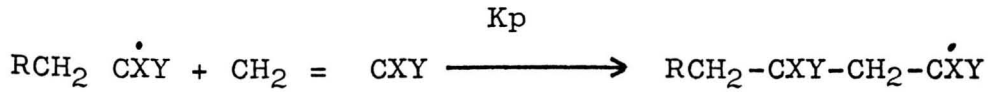
The excited species undergoes homolysis to produce radicals capable of initiating the polymerization of the monomer.



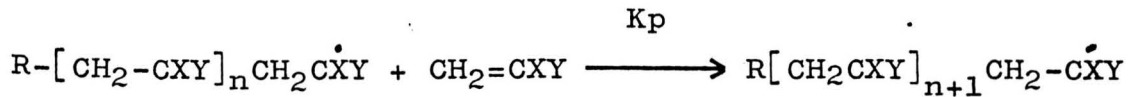
- b) Photolytic dissociation of initiator e.g. benzoyl peroxide which leads to similar free radicals generated on the thermal dissociation, such as benzoyl radicals.
- c) Photosensitizers e.g. in the case of benzophenone and xanthone which were used in this work. In general, photosensitizer Z, undergoes excitation by ultraviolet light to form an activated species which will activate the monomer by one of photochemical means described in Table 1.2 in the form of radicals.

ii) Propagation

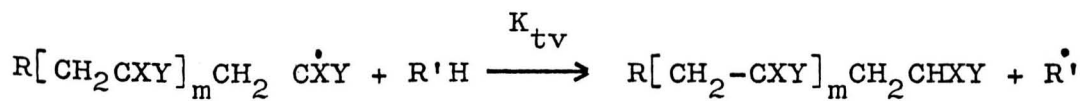
This is the process in which the polymer chain is built up by the addition of more monomer molecules to the growing chain which was produced in the initiation step.



after n steps

iii) Chain Transfer

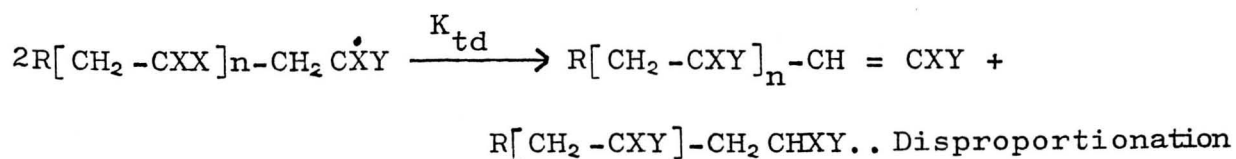
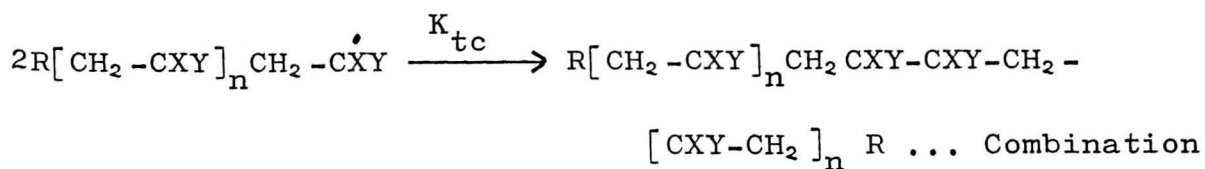
This occurs when the propagating radicals react with solvent, monomer, initiator or polymer growing chain to form a polymer which will no longer grow. In this case, the free radical is not removed from the system but a chain transfer reaction takes place, thus limiting the length of the polymer chain and the molecular weight.



Here R'H represents any chain transfer agent and R'· is the radical derived from it.

iv) Termination

This is the termination process of the growing polymer radical by its combination with another growing radical. Termination may also occur by disproportionation of the growing polymer radical.



where K_d is the rate constant for the catalyst dissociation.

K_i is the rate constant for the initiation.

K_p is the rate constant for propagation.

K_{tv} is the rate constant of chain transfer.

K_{tc} is the rate constant for termination by coupling.

K_{tp} is the rate constant for termination by disproportionation.

v) Inhibition and Retardation

The addition of certain substances suppresses the polymerization of monomers. These substances act by reacting with the initiating and propagating radicals and converting them either to nonradical species or radicals of low reactivity which will not propagate. These substances are classified according to their effectiveness. Inhibitors stop every radical and polymerization is completely halted until all the inhibitors are consumed, whereas retarders are less efficient and stop only a portion of the radicals. Retarders will slow the polymerization rate without an inhibition period.

vi) Kinetics of Free Radical Polymerization

The kinetic model used for the free radical polymerization is shown below. In order to obtain a kinetic expression for the overall rate of polymerization, it is necessary to use the following assumptions: -

- a) k_p and k_t are independent of the size of the radical.
- b) It is a cornerstone of simple polymerization theory that the reactivity of a growing polymer chain depends almost completely on the last unit added and not on previously added units, or on the length of the chain. Therefore, k_p remains the same for a chain of any length.
- c) Monomer is consumed only in the propagation step and the rate of propagation may be considered as the rate of polymerization.
- d) Reaction proceeds slowly enough to reach a steady state, where the radical population does not change rapidly with time. This allows the rate of initiation to be equated to the rate of termination, provided no chain transfer occurs.

$$\text{i.e. } \frac{d[R\cdot]}{dt} \text{ and } \frac{d[M\cdot]}{dt} = 0$$

$$\text{then } 2 k_d [I] - k_i [R\cdot][M] = \frac{d[R\cdot]}{dt} = 0$$

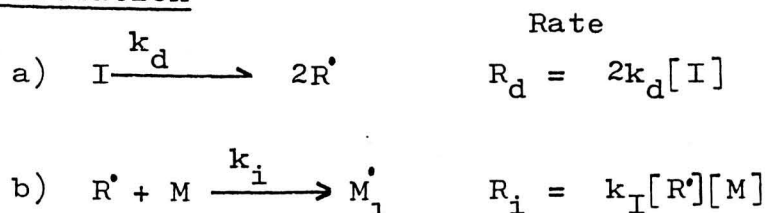
$$k_i [R\cdot][M] - 2 k_t [M\cdot]^2 = \frac{d[M\cdot]}{dt} = 0$$

where $[R\cdot]$ concentration of free radicals generated

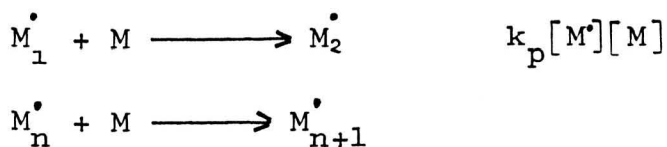
$[M\cdot]$ concentration of monomer free radical.

With the use of these assumptions the kinetic scheme for free radical polymerization will be as follows:-

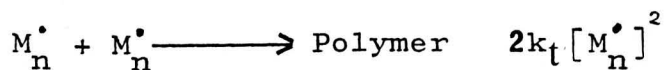
Initiation



Propagation



Termination



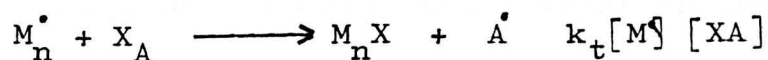
where $[R\cdot]$ represents a radical derived from the initiator

M monomer molecule

$M_n\cdot$ growing polymer radical of n monomer units

$M_1\cdot$ radical derived from the monomer

Chain Transfer



where XA may be monomer, initiator, solvent or other substance, and X is the atom or species transferred.

The rate of polymerization R_p is equal to the rate of monomer removed in the propagation step and is given by

$$R_p = \frac{-d[M]}{dt} = k_p [M^*]_s [M]$$

$[M^*]_s$ is the steady state radical concentration

Under steady state conditions, there is first order dependence on monomer and half order dependence on initiator i.e.

$$R_p = k_p \left(\frac{k_i}{k_t} \right)^{0.5} [M][I]^{0.5}$$

if only a certain fraction of initiator fragments can successfully react with the monomer then the equation becomes:-

$$R_p = k_p \left(\frac{fk_i}{k_t} \right)^{0.5} [M][I]^{0.5}$$

In experimental studies, the monomer concentration is measured as a function of time for various starting concentrations of monomer and initiator and at various temperatures.

The polymerization rate could be followed experimentally by measuring the changes in any of the few properties of the system such as density, refractive index, viscosity or light absorption.

Density measurements are among the most accurate sensitive and most commonly used of the techniques. In practice the volume of the polymerizing system is measured by carrying out the reaction in a dilatometer.

Polymerizations usually follow first order kinetics whereas the initiation step is normally of half order. However, for various reasons such as a diffusion-controlled reaction, or more complex mechanisms, the polymerization order may be more or less than one. Such order deviations are often valuable in unravelling the sequence of reaction steps. A useful check on the order is to plot the polymerization rate after the initial rate against different initial concentration of monomer and initiator. The slope (index) of such a plot will give the order of the reaction.

If the polymerization was carried out in solution, the solvent may act in two ways. Firstly, it may take no part in the reaction, whereby it is only acting as a diluent for the monomer, or it may form free radicals which can take part in the reactions, such as chain transfer agents and may also affect the purity of the polymer. The kinetics of polymerizations must be altered to accommodate such interference.

Dilution of monomer may cause initiation and propagation and consequently short chains may form. Short chains may also result from chain transfer reactions to solvent.

If the chain length is short, the rate of reaction of monomer cannot be equated to its consumption in the propagation step alone, and terms allowing for consumption of monomer in the initiation and chain transfer reactions must be added.

The rates of initiation and polymerization for photosensitized polymerization differ from the one already mentioned above, as the Quantum yield for radical production ϕ should be taken into account.

The rate of initiation will be given by

$$R_i = 2 \phi I_{\leftarrow} = 2 \phi E I_0 [I]$$

where E represents the molar absorptivity (extinction coefficient) of the photosensitizer where I_0 is the light intensity incident on the photosensitizer.

$I_{\leftarrow} = E I_0 [I]$ which represents the intensity of absorbed light in moles (called einsteins in photochemistry) of light quanta per litre second.

The rate of polymerization may be expressed as

$$R_p = k_p [M] \left(\frac{\phi E I_0 [I]}{k_t} \right)^{0.5}$$

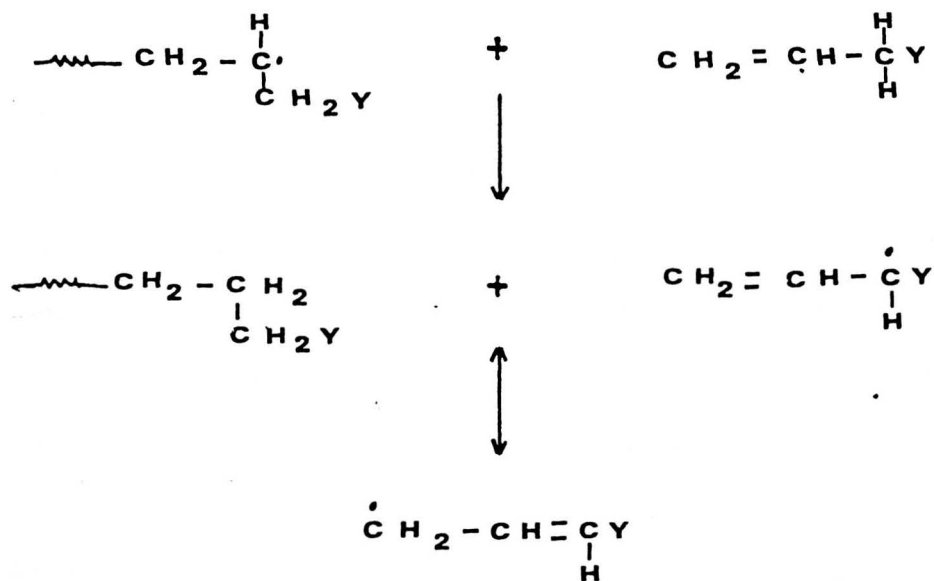
and may be expressed by the general equation of R_p depending on the particular case.

There may be a dependence of R_p on $[M]$ in the photosensitized polymerization at low monomer concentrations or low quantum yields. This would lead to different dependence of R_p on $[M]$ than the usually free radical polymerization case.

According to Beer's law, $I = I_0 e^{-E[M]b}$, I_0 and I_x will vary with thickness (b) which means the quantum yield will be affected with thickness. The value b , will either be the thickness of the polymer film, in the case of cross linking of polyethylene or the value will represent the diameter of the reaction vessel containing the solution. This will lead to the phenomenon called skin effect which means that light will be absorbed mainly on the surface of the solution or the film, forming higher quantum yield of free radical on the surface. This causes non-uniform photopolymerization or photo crosslinking. The skin effect will be very obvious in our system as it will be shown in the following chapters.

1.4.1 Polymerization of Allyl Acetate

Allyl Acetate polymerizes at abnormally low rates with unexpected dependence of the rate on the first power of the initiator concentration (28,29). The propagation radical in such a polymerization is very reactive while the allylic C-H (the CH bond alpha to the double bond) in the monomer is quite weak resulting in facile chain transfer to monomer (36).



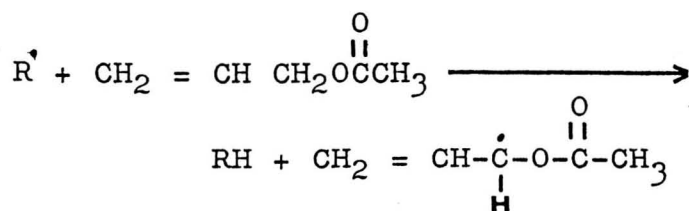
The weakness of the allylic CH bond arises from the high resonance stability of the allylic radical which is formed and is consequently less active, i.e. it has less tendency to initiate a new polymer chain. Therefore this chain transfer is essentially a termination reaction. This is known as degradative chain transfer. The chain transfer reaction competes exceptionally well with normal propagation. This will lead to the formation of low molecular weight polymer chains which were terminated by transfer after the addition of only a very few monomer units. When the allyl acetate was replaced with deuterated allyl acetate (30) $\text{CH}_2 = \text{CH} - \text{CD}_2\text{OCOCH}_3$, it was found that the acetate polymerizes 1.9 - 2.9 times as fast as normal allyl acetate and has a degree of polymerization 2.4 times as large under the same conditions.

This is to be expected as the allylic C-D bond is stronger than the CH bond and chain transfer reactions would therefore be decreased in the deuterated monomer. Bartlett and Altschul in their studies (28), of the five radical initiated polymerization of allyl acetate found that after 48 hours, which was the period to complete the reaction and to decompose all of the Benzoyl peroxide 6% B.P., only about half of the initial allyl acetate had polymerized. Bartlett and Altschul found that oxygen was capable of retarding the polymerization of allyl acetate. However, the effect of brief exposure to air was not great. With several evacuations and flushings with nitrogen, the rate of polymerization was increased 10% over that observed under air.

It was found by Bartlett and Altschul that the decomposition of benzoyl peroxide in allyl acetate is nearly unimolecular at 80°C over a tenfold range of initial concentration. The ratio of the remaining monomer to the remaining peroxide (dM/dP) was fairly constant throughout.

The degradative chain transfer reaction is generally known to give a large decrease in both R_p and X_n which is the number average degree of polymerization.

The termination reaction in allyl acetate polymerization may be represented as follows;



where R is the growing polymer chain radical RH represents a terminated Polymer molecule. Only a fraction of the monomer radicals are able to continue polymerization.

Polymerization of allyl acetate with azo-bis-isobutyro-nitrile (32) [AIBN] as initiator behaved similarly.

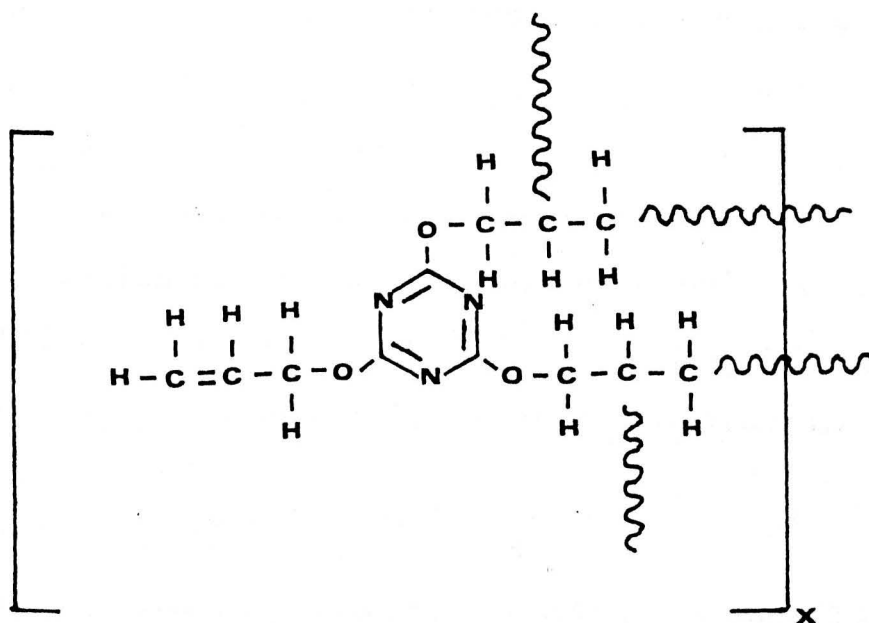
Bartlett and his workers found that separate homopolymerization of both allyl acetate and maleic anhydride was slow and gave low molecular weights but the copolymerization occurred with remarkable speed (33). Low molecular weight copolymers of 1-Octene with 10% allyl acetate (M.W. 350-750) was the only reported copolymer formed with hydrocarbon (34).

Part of this programme will be concentrated on the polymerization of allyl acetate in the presence of hydrocarbons as it models the behaviour of one allyl group of triallyl cyanurate.

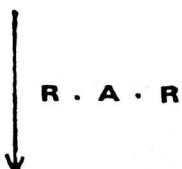
To summarize, allyl acetate does not form homopolymer of high molecular weight by radical polymerization. Moreover, allyl acetate and other monoallyl compounds retard radical polymerization of most vinyl and acrylic polymerizations on heating with peroxide catalysts.

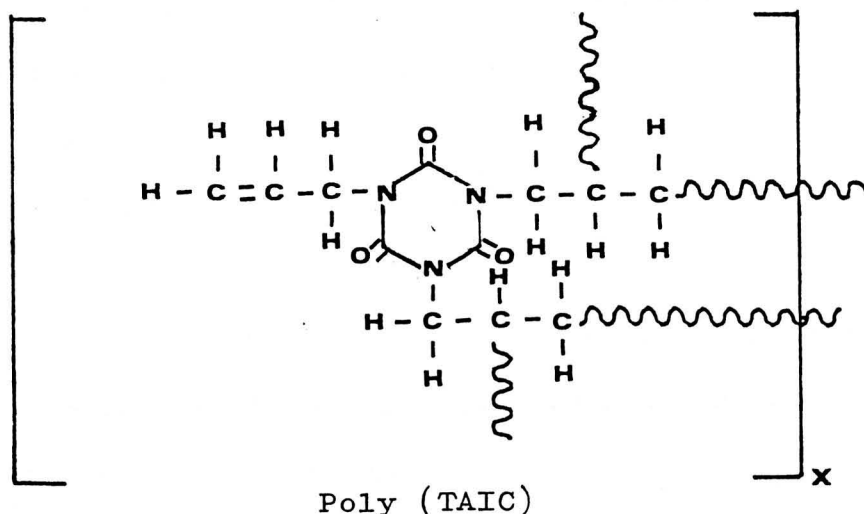
Allyl acetate forms oils or viscous liquid low polymers of degree of polymerization (DP) up to about 20 (28).

Clampitt (37) has used a combination of differential thermal analysis and infra-red analysis to study the Polymerization of TAC. It was found that the total polymerization of the two allyl groups was followed by isomerisation as shown below.

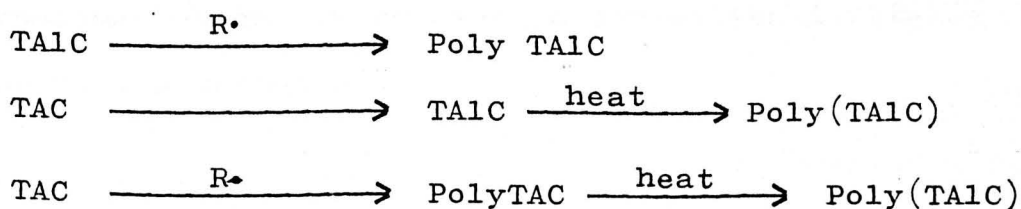


Poly (TAC)





Gillham and his workers (38) found that thermal initiated polymerization of TAC will take two steps. In the absence of air, TAC isomerises and TAC polymerizes in one thermal event. In the presence of air some of the TAC prepolymerizes to Poly(TAC) in a first step, which is followed by a second step which includes the isomerization of TAC to TA1C and Poly(TAC) to poly(TA1C) and the polymerization of TA1C. i.e. the Polymerization of TAC will produce a polymer of the isomers as shown below.



The large extents of reaction observed during polymerization of TAC and TA1C are attributed to the

formation of intramolecular rings. The higher conversions obtained with TAC are attributed to the extra length and flexibility of its allyl group.

The Poly(TAC) and poly(TAIC) are insoluble polymers, since crosslinking is involved because of the polyfunctional character of the TAC.

The heat of complete polymerization of Triallyl cyanurate is high. As measured by differential thermal analysis, two distinct exotherms can be observed, an initial release of 39 kCal/mole corresponding to the reaction of two allyl groups and a later exotherm believed to represent reaction of the third allyl group together with rearrangement to the more stable isocyanurate (38).

The homopolymerization of TAC has found to be of little use because of cost and difficulty in controlling the polymerization, as well as the brittleness of the homopolymer cast sheets produced. The changes in density and the high degree of crosslinking occurring, during the homopolymerization will tend to cause cracking and lack of uniformity through polymer cast sheets. Solution homopolymerization was used to partially prepare a prepolymer which can be used in conventional wet-lay up laminating techniques.

TAC monomer in solution with little or no catalyst will have a slow rate of polymerization and may give viscous solutions initially because of the soluble prepolymer (microgel). These soluble prepolymers can be cured slowly to a uniform polymer.

The TAC monomer was polymerized in bulk in the presence of 2% Benzoyl peroxide and by heating (40). The resulting polymer sheet was a clear, light yellow and hard. The polymerization of TAC could be promoted by Nickel, manganese and mercury. Polymers ranging in properties from viscous oils to rubbery solids were obtained and reviewed by Kropa in the American Cyanamide Patent (41).

Radiation polymerization of TAC using $^{60}\text{Co} - \gamma$ irradiation was found to avoid rearrangement and formation of the polymer of the isomer (42) but conversion was incomplete. However by increasing the temperature to above 200°C , isomerization of the polymer was inevitable.

A solid polymer was formed when TAC containing 5% B.P., was irradiated for 17 hours at 1 foot from mercury lamp (43).

The copolymerization of TAC and its isomers with e.g. methylmethacrylate, styrene and vinyl acetate (44) has attracted more interest than homopolymerization.

TAC is readily compatible and copolymerizes with highly unsaturated polyester (alkyd type) (45). Kropa in

his American Cyannide patent copolymerized TAC with polyester along with glass fibre. Kropa copolymerized 5% and 95% styrene containing 2.5% benzoyl peroxide by heating for 48 hours at 100°C. An example was also given of copolymerization of an unsaturated viscous liquid ester polymer obtained from a mixture of equal parts of TAC and Methyl Methacrylate.

On initiation with peroxides, heating or with higher energy radiation it was found that the polyfunctional allyl monomer TAC was effective in small concentrations as a crosslinking agent for preformed polymers. Such a compatible crosslinking agent can promote curing and improvement in physical properties in many plastics and synthetic rubbers. Earlier it was assumed that the base polymer needed unsaturation for crosslinking (48). Hewson added TAC to cellulose acetate sorbate and cast films, which were cured for 6 minutes at 160°C. Pinner (12) reported that vinyl chloride polymers were particularly responsive to crosslinking by triallyl cyanurate. In Germany, Bonin (47) found that crosslinking and grafting occurred when cellulose acetates containing TAC and peroxides were heated at 120°C for 30 minutes.

Triallyl cyanurate has been added to ethylene-propylene copolymer rubbers and cured (48, 53, 54). The efficiency of crosslinking by peroxides could be improved by TAC, which means the reduction of peroxide requirements goes down to 2.5% or less.

TAC with dicumyl peroxide has been suggested as a coupling agent in glass cloth laminates (49). Polyethylene fine powder, TAC, dicumyl peroxide was formulated as an adhesive for bonding to copper (50).

As reported earlier in this chapter, Logans (15) and Pinner (17) found that there was an improvement in efficiency of high energy radiation crosslinking of polymers, by adding TAC. The increase in curing effects could be due to the grafting reactions. Estimates of the crosslinking efficiency of TAC in polyethylene indicated that at concentrations of 0.5% to 5% each monomer molecule crosslinks about 3 polymer molecules (51). Polypropylene cured by low doses of radiation using TAC was also reported (52). Polyolefins were high energy radiation cured using 2 to 5% TAC, in order to obtain heat-shrinkable and self-soldering insulators (55, 56).

Extended network polymers were made by polymerizing TAC in polyvinyl chloride and in polyethylene (57).

The work which was carried out in the copolymerization of TAC, showed that in general there is a lot of interest as far as enhancement of crosslinking processes and improvements of certain properties are concerned. Apart from the studies already reported no other fundamental work has been carried out. The system which this thesis will deal with, has not been dealt with specifically before.

In the following chapters, some fundamentals of the crosslinking process of TAC with polyethylene using the

photosensitizer, xanthone, will be established from the results, which in turn will be obtained from the model systems and the polyethylene network.

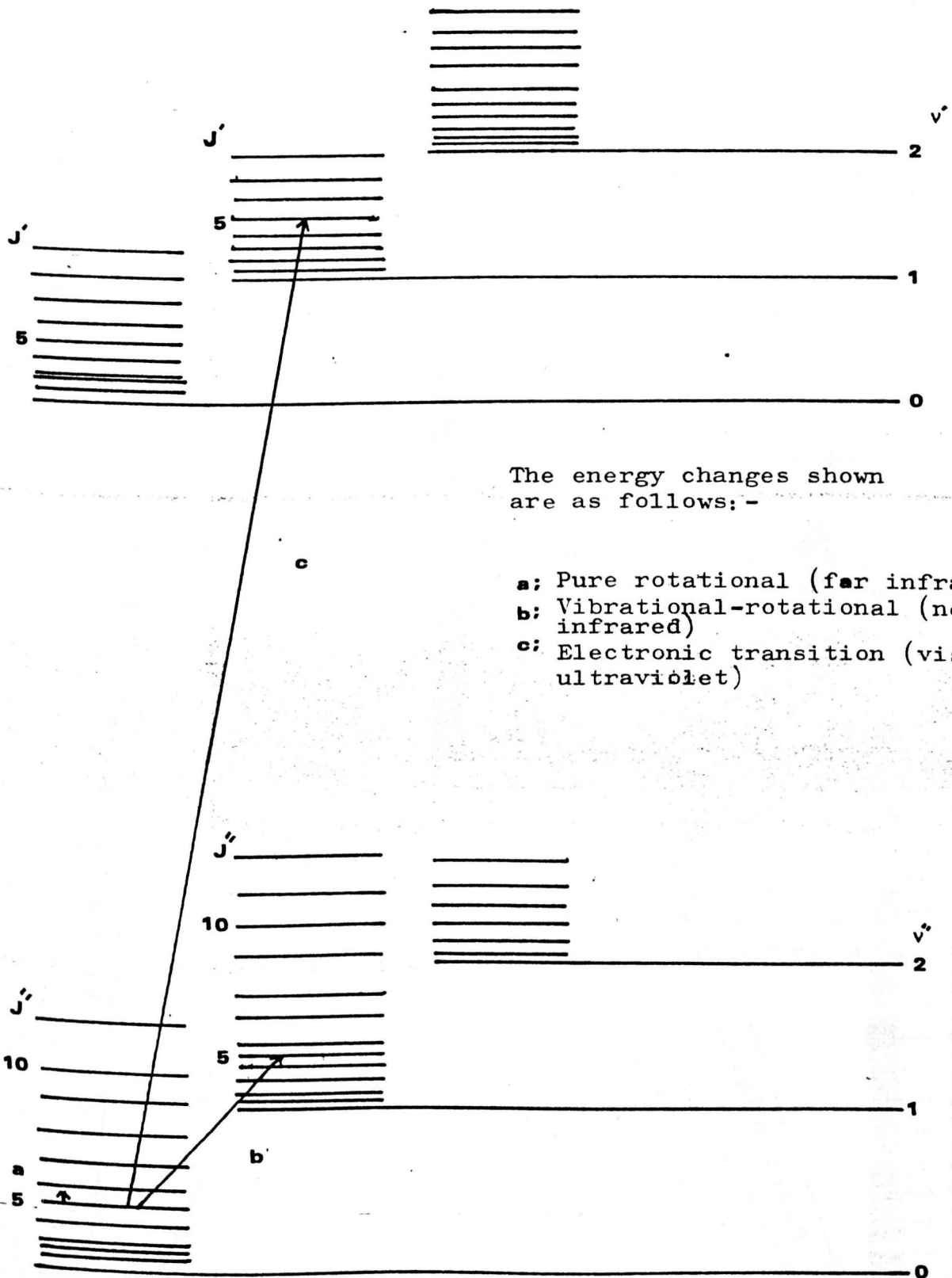
References

1. Charlesby, A., Hancock, N.H., Proc. Roy. Soc. (London) A218 245 1953.
2. Charlesby, A., Ross, M., Proc. Roy. Soc. (London) A217 122 1953.
3. Wilson, J.E. Radiation Chemistry of Monomers, Polymers & Plastics, Dekker 1974.
4. Oster, G., Proc. Conf. Radial Sources Ind. Warsaw 1959, 321.
5. Charlesby, A., Radiation Effects in Materials, Pergamon Press 1960.
6. Chapiro, A., Radiation Chemistry of Polymeric Systems Interscience 1962.
7. Bonotto, S., J. of Applied Polymer Science 9, 3819 1965.
8. Dannenberg, E.M., et al., J. of Polymer Science 31, 127, 1958.
9. Odian, G., Bernstein, B.S., J. Poly. Science P & A 2, 2835, 1964.
10. Technical Report, General Electric Company, Vulkene 107E, Vulcanized Reinforced Polyethylene.
11. Miller, A.A., Ind. Eng. Chem., 51, 1271 (1959). J. Applied Polymer Science 5, 388 1961.
12. Pinner, S.H., Nature 183, 1108 (1959).
13. Pinner, S.H., Nature 184, 1303 (1959).
14. Pinner, S.H., Wycherly, V., J. Applied Poly. Sci., 3, 388 (1960).
15. Lyons, B.J., Nature 185, 604, (1960).
16. Kevan, L., Libby, W.F., J. of Chemical Physics, 39, 1288, (1963).

17. Salovey, R., et al., J. of Physical Chem., 66 (7) 2345, 1965.
18. Salovey, R., et al., J. of Chemical Phys., 44 (9) 3151, 1966.
19. Salovey, R., et al., J. of Physical Chem., 70 (10) 3203, (1966).
20. Calvert, J.G., Pitts, Jr., J.N. Photochemistry, Wiley (1966).
21. Ledwith Paper Photoinitiation of Vinyl Polymerization.
22. Cohen, S.G., et al., Chemical Reviews 73 (2) 149 (1973).
23. Bartholomew, R.F., et al., J. Chem. Soc., C 2804 (1971).
24. Bachman, W.E., J. Amer. Chem. Soc., 55, 391 (1933).
25. Zanker, V., et al., Bull. Chem. Soc. Jap., 39, 1694 (1966).
26. Davidson, R.S., et al., Chem. Commua., 1265 (1967).
27. Rodriguez, F., Principles of Polymer Systems, McGraw-Hill 1970.
28. Bartlett, P.D., et al., J. Amer. Chem. Soc., 67, 812 1945.
29. Bartlett, P.D., et al., U.S. 2,512,410 (Shell).
30. Bartlett, P.D., et al., J. Amer. Chem. Soc., 75, 91 1953.
31. Bartlett, P.D., J. Amer. Chem. Soc., 67, 816 1945.
32. Sakurada, I., Takahashi, G., CA51 3255 (1957), CA52 1670 (1958), CA50, 601 (1956).
33. Bartlett, P.D., et al., J. Amer. Chem. Soc., 68, 1495, 1946.
34. Dierick, G.F.E.M., et al., U.S. 2,784,136 (Shell).
35. Laible, R.C., Chem. Rev., 58 (5) 807 1958.
36. Allyl Polymers Ency. Polymer Sci. and Tech. Vol 1, 750.
37. Clampitt, B.H., et al., J. Polymer Sci., 62 172, 15-21 (1962).

38. Gillham, J.K., J. of Applied Polymer Sci., 17, 1143 1973.
39. Clampitt, B.H., et al., J. Polymer Sci., 27 515 1958,
38, 344 1959.
40. Kropa, E.L., U.S. 2,510,503 (American Cyanamide).
41. Kropan, E.L., U.S. 2,557,667 (American Cyanamide).
42. Wuckel, L. and Wagner, H., Makromol. Chem., 66 212 (1963).
43. Unpublished work.
44. Roth, R.W. Church, R.F., J. Polymer Sci., 55 41 (1961).
45. Kropa, E.L. U.S. 2,510,503 (American Cyanamide).
46. Hewson, W.B., U.S. 2,749,319 (Hercules).
47. Hammond, G.S., et al., I.U.P.A.C. XXIIIrd Congress,
Boston 1971 Vol. 4 p257, London Butterworth 1971.
48. Robinson, A.E., et al., Ind. Eng. Chem. RRD 1, 78 (1962).
49. Brit. 895, 971 (Esso)
50. Lybeck, A.H., U.S. 3,523,862 (Am. Enka.).
51. Lyons, B.J., et al., Trans. Faraday Soc. 59 2350 (1963).
52. Odian, G.G., et al., (U.S. AEC, NYU 2481 1961), CA55,
25345.
53. Loan, L.D., J. Polymer Sci., A2 3053 (1964).
54. Smith, W.C., et al., Rubber World 153 79 (1966).
55. Cook, P.M., Belg. 638274.
56. Brit. 1,047,053 (Raychem.)
57. Pinner, S.H., et al., U.S. 3,125,546, Brit. 948,302
(Bs. Plastics), Brit. 905,711.

Fig. 1 - 1 Energy levels and transition in a typical diatomic molecule

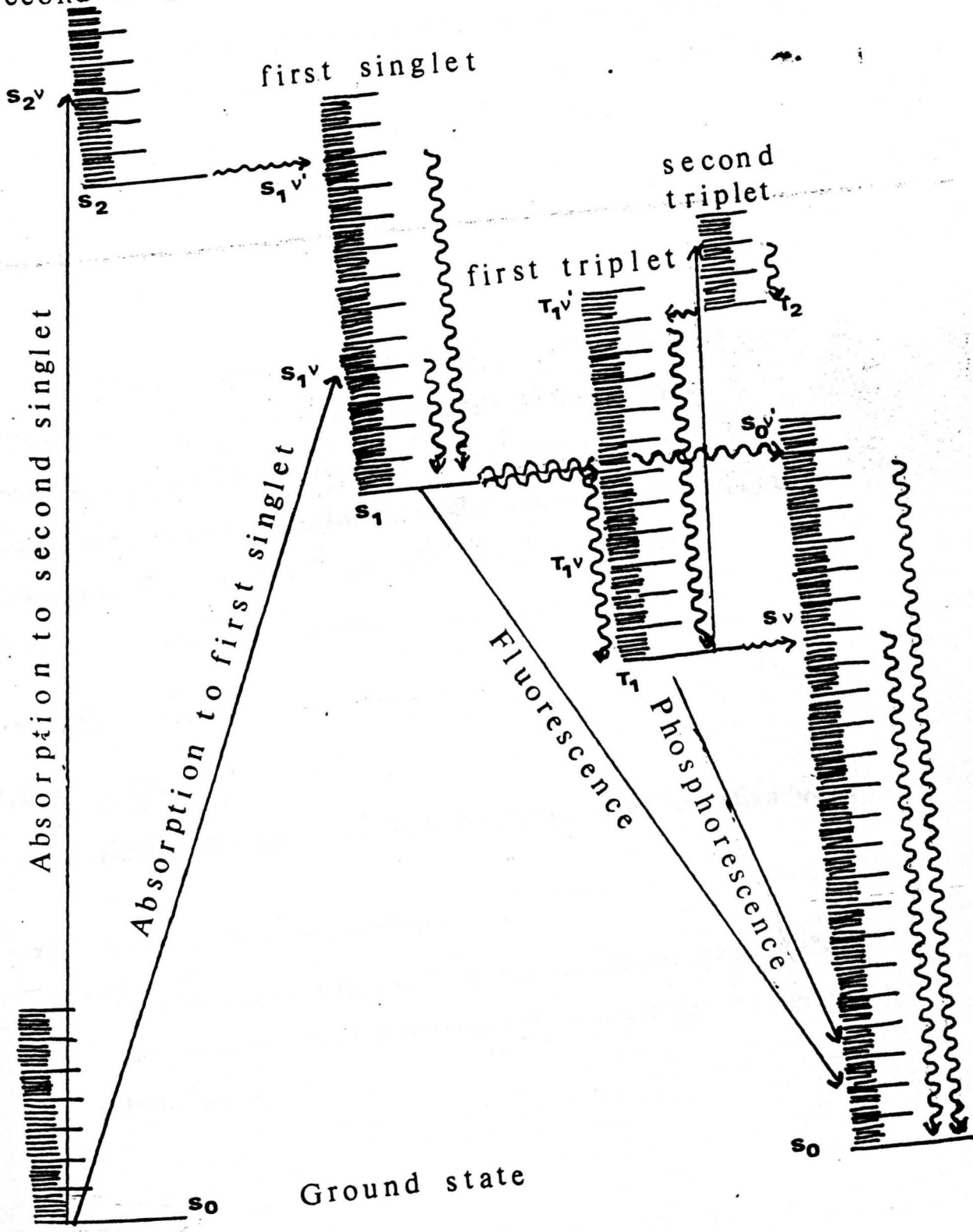


The energy changes shown are as follows: -

- a; Pure rotational (far infrared)
- b; Vibrational-rotational (near infrared)
- c; Electronic transition (visible ultraviolet)

Fig. 1-2 Excited states and photo physical transitions between these states in a typical organic molecule

second singlet



Ground state

CHAPTER 2

MODEL SYSTEMS I 'TRIALLYL CYANURATE AND XANTHONE IN HYDROCARBONS'

2.1 Introduction

This chapter describes model studies on the photoinitiation of various hydrocarbons in the presence and absence of triallyl cyanurate and xanthone, made to throw light on the analogous process occurring in polyethylene. Model saturated and unsaturated hydrocarbons containing primary, secondary and tertiary carbon atoms were studied.

The liquid products from both photoinitiation and ^{60}Co γ -irradiation were analysed by gas-liquid chromatography and compared. The solid polymeric crosslinked powder obtained in the presence of triallyl cyanurate was highly insoluble which limited the analysis to which it could be usefully subjected.

2.2 Experimental

2.2.1 Materials

Hydrocarbons: The hydrocarbons used in this work were:-

i) saturated hydrocarbons

Octane S.L. (supplied by Fison) (B.P. 125-127°C)

was firstly distilled and then used in the photo-induced reactions.

3-ethyl pentane and tetracosane (C₂₄) (supplied by Aldrich) was used without any further purification.

ii) Unsaturated hydrocarbons

1-Octene 97% (B.P. 122-123°C) trans-2-Octene 98% (B.P. 123°C) and 2-methyl-1-hexene 98% (B.P. 92°C).

These were supplied by Aldrich and were also used without any further purification.

Also n. Hexadecane (special grade for GLC) supplied by BDH was used for the Gas liquid chromatograph analysis.

The monomer triallyl cyanurate was used after recrystallization from hexane (M.P. 31°C, B.P. 140°C at 0.5mm).

Photoinitiator xanthone was used after having been recrystallized in chloroform (M.P. 174°C, B.P. 349 - 358°C).

2.2.2 Apparatus

- i) Reaction vessels: the photoinitiation of the hydrocarbon was carried out in a dilatometer which was constructed from pyrex glass as shown in Fig.2.1.
- ii) Vacuum line: Most of the photoinitiation reactions were carried out under high vacuum and degassed conditions using a vacuum line with a double stage vacuum pump as shown in Fig. 2.2.
- iii) Temperature controller: All the reactions described

in this chapter were carried out at 60°C which was maintained by using a water bath.

- iv) U.V. lamp: The ultraviolet lamp used for the photoinitiation is described in chapter 4.
- v) Gas liquid chromatography, Perkin Elmer F11.
- vi) U.V. spectrophotometer, Perkin Elmer 402.
- vii) I.R. spectrophotometer, Perkin Elmer 397.
- viii) Mass spectrometer, AEI MS9.
- ix) NMR spectrometer, Perkin Elmer R14.

2.2.3 Photoinitiation of different hydrocarbons in the presence of xanthone and triallyl cyanurate (TAC)

2.2.3.1 Preparation of solutions

Solutions of xanthone and TAC in five different hydrocarbons were prepared. Also, solution of (a) xanthone with Octane and (b) TAC with Octane were prepared individually.

The low solubility of xanthone and TAC in the hydrocarbons restricted the concentrations studied. Heat was often required to achieve dissolution. The solution compositions are given in table 2.1.

TABLE 2.1: Hydrocarbon Solutions used for the
Photoinitiation Process

<u>Solution Ref. No.</u>	<u>Type of hydrocarbon</u>	<u>Conc. of Xanthone Moles/litres</u>	<u>Conc. of TAC Moles/litres</u>
1	n-Octane	2.6×10^{-6}	4.0×10^{-6}
2	1-Octene	2.6×10^{-6}	4.0×10^{-6}
3	2-methyl 1-hexene	2.6×10^{-6}	4.0×10^{-6}
4	3-ethyl pentane	2.6×10^{-6}	4.0×10^{-6}
5	Trans 2-Octene	2.6×10^{-6}	4.0×10^{-6}
6	n-Octane	5.1×10^{-6}	-
7	n-Octane	-	8.0×10^{-6}
8	n-Octane	5.1×10^{-8}	2.4×10^{-6}
9	1-Octene	5.1×10^{-8}	2.4×10^{-6}

2.2.3.2 Reaction of the hydrocarbons

A series of experiments were run using a series of dilatometers containing identical solutions which were to be exposed to U.V. light for varying periods of time. After filling each dilatometer the system was degassed then sealed.

Exposure to radiation took place by having the dilatometer vertically at a distance of 30 cm (1ft) from the ultra-violet lamp in water bath thermostatted at 60°C. Throughout the exposure the dilatometers were occasionally shaken. The physical state of the solution did not change. A fine powder separated from certain solutions after a given exposure time. Tables (2.2,

2.3, 2.4, 2.5 and 2.6) show the xanthone and TAC concentrations throughout the irradiation process in the individual solutions.

2.2.3.3 Physical observations during U.V. radiation

Solution 1, containing octane, xanthone and triallyl cyanurate, showed an insoluble fine powder which started to separate from the solution after three hours of irradiation. The powder was uniformly dispersed in the solution. It was also similarly observed in the case of solution 4, which contains 3-ethyl pentane, xanthone and triallyl cyanurate. The powder in solution 4 began to appear after three hours of irradiation.

The fine, light yellow insoluble powder was filtered, washed and dried. The fine powder did not appear from solutions 2, 3, 5 or 9.

In solution 1 and to a smaller extent in 2, 3, 4 and 5 some fine crystals, thought to be the dimer of xanthone, began to appear after one hour of irradiation. Quite significant quantities formed in the octane/xanthone solution 6 and they were filtered off for analysis.

In the case of solution 7, containing only octane and triallyl cyanurate, the mixture was initially clear. However, after six hours of radiation a very fine, highly insoluble white powder appeared dispersed in the solution. The amount of the powder, although minute was still enough for its analysis.

2.2.3.4 Analysis of Hydrocarbon Solutions after Irradiation by U.V. Light

(i) Quantitative Analysis by Gas-Liquid Chromatography

For quantitative analysis, a calibration curve was obtained for both, triallyl cyanurate and xanthone, by preparing a series of standard solutions in chloroform (special grade for spectroscopy).

The GLC analysis was carried out at 160°C using 5% Apiezon, a 2 metre column and a flow of 6. The retention times for TAC and xanthone under the above conditions were as follows,

TAC	20 minutes
xanthone	40 minutes

By measuring the area under the curve of the TAC peak in the GLC chromatograph, with the aid of the calibration curve, the TAC concentrations in the different solutions, before and after irradiation, were calculated.

Tables 2.3, 2.3, 2.4, 2.5 and 2.6 show the TAC concentrations after irradiation for different solutions.

As seen from the tables, the TAC concentration did not change in the case of the solutions containing 1-Octene 2-Octene and Methyl hexene. Reduction of the TAC content occurred in those solutions where saturated hydrocarbons were incorporated, e.g. Octane and Ethyl pentane. Fig. 2.3 shows the rate of conversion of TAC in these two solutions.

(ii) Quantitative Analysis by Ultra Violet Spectrometry

A U.V. spectrometer was used to measure the concentration of xanthone in the irradiated solutions. In order to do this the extinction coefficient of xanthone was determined first by using xanthone solutions (in Chloroform) of known concentrations.

Using a 1 ml cell, the U.V. spectra of the different irradiated samples were measured and the concentration of xanthone was determined in each individual case.

Tables 2.2, 2.3, 2.4, 2.5 and 2.6 show the xanthone concentration in the different solutions after irradiating them for differing lengths of time. Fig. 2.4 shows the drop in the concentration of xanthone with respect to irradiation time in the different solutions.

TABLE 2.2: Xanthone and TAC concentrations at different
U.V. Irradiation time for Solution 1
[n-Octane + TAC + Xanthone]

<u>U.V.irradiation</u> <u>time(minutes)</u>	<u>Conc. of TAC left</u> <u>in the solution</u> <u>moles/litres</u>	<u>Conc. of Xanthone</u> <u>left in the</u> <u>solution moles/litres</u>
0	4.0×10^{-6}	2.5×10^{-6}
15	4.0×10^{-6}	2.2×10^{-6}
30	3.6×10^{-6}	5.7×10^{-7}
60	3.2×10^{-6}	1.8×10^{-7}
90	2.4×10^{-6}	4.6×10^{-8}
120	2.2×10^{-6}	4.6×10^{-8}
180	2.2×10^{-6}	0
240	2.0×10^{-6}	0
300	2.0×10^{-6}	0

TABLE 2.3: Xanthone and TAC concentrations at different
U.V. Irradiation time for Solution 2
[1-Octene + TAC + Xanthone]

<u>U.V.irradiation</u> <u>time(minutes)</u>	<u>Conc. of TAC in</u> <u>solution moles/litres</u>	<u>Conc. of Xanthone</u> <u>in solution</u> <u>moles/litres</u>
0	4.0×10^{-6}	2.5×10^{-6}
15	 No Change in Concentration Observed 	2.2×10^{-6}
30		2.2×10^{-6}
60		1.9×10^{-6}
90		1.5×10^{-6}
120		8.2×10^{-7}
180	2.2×10^{-7}	
240	4.6×10^{-8}	
300	4.6×10^{-8}	
510	2.6×10^{-8}	

TABLE 2.4: Xanthone and TAC Concentrations at different
U.V. Irradiation time for Solution 3
[2-methyl 1-hexene + TAC + Xanthone]

<u>U.V. irradiation</u> <u>time (minutes)</u>	<u>Conc. of TAC in</u> <u>solution moles/litres</u>	<u>Conc. of Xanthone</u> <u>in solution</u> <u>moles/litres</u>
0	4.0×10^{-6}	2.5×10^{-6}
30	↑ No Change in Concentration Observed ↓	2.5×10^{-6}
60		2.5×10^{-6}
90		2.5×10^{-6}
120		2.5×10^{-6}
240		2.2×10^{-6}
350		1.6×10^{-6}
420		1.4×10^{-6}
480		1.3×10^{-6}

TABLE 2.5: Xanthone and TAC Concentrations at different
U.V. Irradiation time for Solution 4
[3-ethyl pentane + TAC + Xanthone]

<u>U.V. irradiation</u> <u>time (minutes)</u>	<u>Conc. of TAC in</u> <u>solution moles/litres</u>	<u>Conc. of Xanthone</u> <u>in solution</u> <u>moles/litres</u>
0	4.0×10^{-6}	2.5×10^{-6}
15	4.0×10^{-6}	2.5×10^{-6}
30	4.0×10^{-6}	2.5×10^{-6}
60	3.8×10^{-6}	8.7×10^{-7}
90	3.6×10^{-6}	2.0×10^{-7}
180	3.4×10^{-6}	4.6×10^{-8}
300	3.3×10^{-6}	4.6×10^{-8}

TABLE 2.6: Xanthone and TAC Concentrations at different
U.V. Irradiation time for Solution 5
[Trans 2-Octene + TAC + Xanthone]

<u>U.V.irradiation</u> <u>time(minutes)</u>	<u>Conc. of TAC in</u> <u>solution moles/litres</u>	<u>Conc. of Xanthone</u> <u>in solution</u> <u>moles/litres</u>
0	4.0×10^{-6}	2.5×10^{-6}
60	↑	2.5×10^{-6}
120	No Change	2.2×10^{-6}
180	in	1.7×10^{-6}
300	Concentration	1.1×10^{-6}
420	Observed	1.0×10^{-6}
480	↓	8.7×10^{-7}

In solution 8, which contains Octane with a lower concentration of TAC and Xanthone, the Xanthone concentration became zero after five minutes of irradiation. The insoluble product was observed in the solution after two hours of irradiation.

In solution 9, containing 1-Octene with a lower concentration of TAC, the Xanthone concentration after one hour irradiation was $1.62 \times 10^{-8} \text{M}$. After exposure for a further hour the xanthone concentration became zero.

iii) Qualitative Analysis by Gas Liquid Chromatograph (GLC)

During GLC quantitative analysis of the irradiated solution, it was found that new peaks were appearing in the chromatogram. These were due to the new compounds. The area of these peaks differed according to the solution irradiated and depending on the concentration of the additives present.

The peaks which are close to each other were thought to be due to the isomers of C_8 dimer hydrocarbons. Under the same operating conditions used for the GLC analysis of TAC, a series of four peaks was obtained. By reducing the temperature and changing the column, it was found that the peaks comprised of at least seven compounds.

N-hexadecane hydrocarbon (BDH special grade for GLC) was analysed using GLC under the same conditions. It was found that the retention time was within that of the other peaks which appeared after irradiating the different hydrocarbon solutions.

The GLC mass spectrometer set up at ICI Corporate Laboratories was used to identify these compounds. The only information obtained from the GLC mass spectrometer was that these peaks were due to a series of hydrocarbons which may either be saturated or unsaturated hydrocarbons or a mixture of both.

Figs. 2.5, 2.6, 2.7, 2.8, 2.9, 2.10 and 2.11 show the appearance of these series of peaks and how

the area under the peaks differ between solutions and the other changes due to the different radiation times.

The synthesis of the expected isomer of C₈ dimer will be outside the scope of this thesis. However, to obtain more information about these peaks, some ⁶⁰Co γ -radiation of octane should be carried out. As a full investigation of this type of radiation has already taken place and the number of products analysed by different workers. By comparing the γ -irradiated solutions with the photoirradiated solutions a clearer picture of the peaks formed will be found.

iv) Qualitative Analysis of the insoluble product formed during the U.V. radiation

The insoluble fine pale-yellow powder which appeared after certain irradiation times in solutions containing saturated hydrocarbons, was separated by filtration, washed with methylene chloride and then dried. The amount of product was small, i.e. a few milligrams and was found to be insoluble in any solvents tried. Therefore the evaluation was limited to I.R. and elemental analysis. KBr discs of the insoluble, product were made and the I.R. spectra taken as shown in Fig. 2.13).

Elemental analysis for this insoluble product was as follows:-

<u>Sample</u>	<u>Element %</u> <u>Nitrogen</u>	present in the powder		
		<u>Carbon</u>	<u>Hydrogen</u>	<u>Oxygen</u>
1	11.40	64.52	7.42	16.66
2	11.41	63.56	7.27	17.76
3	11.02	66.57	7.28	15.13
4	11.05	64.88	7.50	16.57

Powder taken from Octane/TAC/Xanthone solutions was filtered, washed with methylene chloride and dried in a vacuum oven before analysis.

2.2.4 Octane, Xanthone and TAC solutions for U.V. and γ -irradiation

As xanthone reacted faster in octane solution, new fresh solutions of octane containing a higher amount of xanthone and TAC were prepared to further investigate the products.

These solutions were prepared as follows:-

Table 2.7: Composition of Octane solution with the additives

<u>Solution Ref.No.</u>	<u>Conc. of Xanthone</u> <u>moles/litres</u>	<u>TAC Conc.</u> <u>moles/litres</u>
10	$\left. \begin{array}{c} 1.27 \times 10^{-5} \\ - \\ 1.27 \times 10^{-5} \end{array} \right\}$	2.0×10^{-5}
11		2.0×10^{-5}
12		-
13	only octane	

These solutions were irradiated by U.V. using exactly the same procedure for preparation and analysis as in section 2.2.3. The results are shown in table 2.8 and in Fig. 2.14 and 2.15.

Table 2.8 shows the concentrations of TAC and xanthone in solution 10 after U.V. irradiation. The concentration of TAC was measured by GLC, and the concentration of xanthone by U.V.

From Fig. 2.14, the ratio of % TAC reacted % xanthone reacted is approximately constant throughout the reaction, which would indicate a first order relationship between the two in whatever reaction is occurring.

TABLE 2.8: Xanthone and TAC concentrations at different U.V. irradiation time for Solution 10

<u>Sample Ref.No.</u>	<u>U.V. irradiation time/minutes</u>	<u>Conc. of TAC moles/litres</u>	<u>Conc. of xanthone moles/litres</u>
S10-0	0	4.38×10^{-5}	9.8×10^{-6}
S10-1	30	2.93×10^{-5}	4.8×10^{-6}
S10-2	60	2.37×10^{-5}	3.29×10^{-6}
S10-3	90	2.29×10^{-5}	3.06×10^{-6}
S10-4	120	1.85×10^{-5}	2.1×10^{-6}
S10-5	420	1.16×10^{-5}	8.16×10^{-8}
S10-6	720	1.16×10^{-5}	8.16×10^{-8}
S10-7	24 hours	1.16×10^{-5}	8.16×10^{-8}

Table 2.9 and Fig. 2.16 show the concentration of xanthone in solution 12 after various periods of U.V. irradiation.

TABLE 2.9: Xanthone concentration at different U.V. irradiation time for Octane/Xanthone Solution

<u>Sample Ref No.</u>	<u>Irradiation time</u> (mins)	<u>Conc. of Xanthone</u> (moles/litres)
S12-0	0	1.27×10^{-5}
S12-2	30	1.07×10^{-5}
S12-3	60	7.96×10^{-6}
S12-4	120	6.28×10^{-6}
S12-5	180	4.08×10^{-6}

Figs. 2.17 and 2.18 show the U.V. spectra of the irradiated solutions at different times.

During the U.V. irradiation of solution 10 and solution 12, some fine crystals began to appear in the solution, in addition to the insoluble, yellowish product.

In solution 12, the formation of these crystals was clearer and they were separated by filtration, washed with acetone and then dried.

The crystals formed from solution 12 were analysed by mass spectrometry Fig. (2.25) and also by elemental analysis which was found (C: 79.02%, H 4.84) theoretical (C: 79.16%, H: 4.60%).

For comparison, solutions 11 and 13 were also irradiated by ^{60}Co - γ -radiation[†]. Two sets of dilatometers were

prepared. Set one consisted of eight dilatometers each containing 10 ml of solution 13. The other set of four dilatometers each contained 10 ml of solution 11.

Four dilatometers of set two were all sealed after degassing. The twelve dilatometers were irradiated by ^{60}Co gamma-radiation at room temperature at the following doses as shown in table 2.10.

TABLE 2.10: Octane solutions irradiated by ^{60}Co γ -radiation

<u>Solution 13</u> <u>degassed</u>	<u>Solution 13</u> <u>undegassed</u>	<u>Solution 11</u> <u>degassed</u>	<u>Dose M rad</u>
A1	B1	C1	5.54
A2	B2	C2	16.3
A3	B3	C3	23.4
A4	B4	C4	32.9

(+) ^{60}Co Source facilities at Scottish Universities research and reactor center in East Kilbride.

2.2.4.1 Analysis of the γ -irradiated solutions

The physical state of the octane solution did not change prior to irradiation nor did any solid product form. In the case of the octane with TAC (solution 11), a solid product appeared after irradiation.

The solid product formed during the irradiation of solution 11 was separated, washed by octane dried and then analysed by Infra red and elemental analysis. The I.R. spectra are shown in Fig.(2.19) and the elemental analysis shown in Table 2.11.

The irradiated samples were analysed qualitatively by GLC, applying the same conditions used for the previous work. The chromatogram obtained from these solutions is shown in Fig. 2.20.

The peaks formed after irradiation have the same pattern as that of the one obtained with the U.V. irradiation of octane and additives

The GLC analysis of the γ -irradiated solutions C₁, C₂, C₃, and C₄ did not show any TAC peak in the chromatogram i.e. all the TAC in solution 11 has reacted in the case of γ -irradiation.

TABLE 2.11

<u>Powder (insoluble product)</u> <u>from</u>	<u>Nitrogen</u>	<u>Element %</u>	
		<u>Carbon</u>	<u>Hydrogen</u>
C1	14.76	58.93	7.11
C2	14.02	59.06	7.06
C3	14.26	59.11	7.33
C4	14.58	51.61	11.81

2.2.5 Tetracosane (C₂₄ hydrocarbon), Xanthone, TAC, mixture. Irradiation and analysis

Hydrocarbons with higher molecular weight such as C₂₄ (tetracosane), would be helpful for the qualitative interpretation as will be shown further in the discussion. A mixture of C₂₄ containing xanthone and TAC was prepared in Toluene. The solutions were prepared as shown below. Since Tetracosane is a solid at room temperature, its introduction into the dilatometer was facilitated by making up a solution in 50 ml of Toluene.

<u>Solution No.</u>	<u>C₂₄ Content</u>	<u>Xanthone</u>	<u>TAC</u>
14	10 gram	0.075 gram	0.15 gram
15	10 gram	0.225 gram	0.45 gram

In two sets of dilatometers, each set comprising two dilatometers, the first contained 5 ml each of solution 14 and the second contained 5 ml each of solution 15. The dilatometers were connected to the vacuum line and degassed about fifteen times then the toluene was dried by the freeze and dry method. The dilatometers were kept

under vacuum using the freeze and dry method for 48 hours, to ensure that all the toluene has evaporated. The dilatometers were then sealed and were ready for UV irradiation.

The degassed mixtures were irradiated at 60°C for different time intervals as shown below.

<u>Solution Ref. No.</u>	<u>Irradiation time (hrs.)</u>
14-1	4
14-2	12
15-1	4
15-2	12

Each of the four irradiated dilatometers were broken from both sides and left in the extraction apparatus. The extraction was carried out for 24 hours. The contents of the dilatometer were transferred to a flask with the toluene during the extraction process. The contents of these dilatometers contained an insoluble product which was dispersed in the toluene solution in the flask. This insoluble product was in the form of a fine powder which was separated from the solution by filtration and several washings with toluene to ensure that the powder is free of any unreacted hydrocarbon C_{24} . Having been dried, the powder was analysed by elemental analysis and I.R.

Analysis for Dimer formation was carried out by GPC. Fig. 2.21 gives a GPC⁺ chromatogram for irradiated C₂₄ which shows that the shape of the peak has change. This could be due to the presence of some higher hydrocarbon. The GPC column available was not accurate enough for such analysis of low molecular weight material. However, the following data were obtained.*

	<u>Standard C₂₄</u>	<u>Soluble product after U.V. irradiation</u>
M _n	451	1779
M _w	460	2091
M _z	469	2557
M _w /M _n	1.02	1.17

GLC analysis for the product in toluene was not successful, simply because the GLC instrument column was limited with temperature which could be achieved.

However, the main reason for irradiation for the C₂₄ mixture was to analyse the insoluble part.

⁺(GPC chromatogram obtained from ICI Corporate Laboratories GPC unit analysis.

* GPC data shown above obtained from GPC unit analysis, Pure & Applied Chemistry Department.

2.3 Discussion

From the results shown in the previous section, it seems that the photoinitiator had reacted and was rapidly consumed in the case of the saturated hydrocarbon, whereas the process of photolysis was much slower in the case of the unsaturated hydrocarbon. It was also found that in the case of the U.V. irradiated unsaturated hydrocarbon (plus additives), the insoluble product and fine crystallites were not observed, whereas both were observed in the case of the saturated hydrocarbons, especially the octane solution.

In unsaturated hydrocarbon solutions, the main sensitization process of xanthone was different from that which was observed by Zanker with the saturated hydrocarbon.⁽¹⁾ Because of the decrease in concentration of xanthone, one could only think of the non-radiative deactivation processes of its singlet or triplet excited states to the ground state.

It has been noted that the excited states may be deactivated by energy transfer in the form of vibrational energy to the surrounding solvent or to the molecules of the same species, by processes that must involve collision⁽²⁾, which in turn will be utilized to excite another species electronically, provided that some conditions are satisfied.

It is a desirable characteristic that the sensitizer absorption is at longer wavelengths than those at which the solvent absorbs. It also requires that its triplet

excitation energy be higher than that of the solvent.

Such characteristics are present in xanthone

$[E_{T_1} = 74.2 \text{ kcal}]^3$ i.e. its singlet and triplet excited states are deactivated by energy transfer to the solvent molecule by collision processes. Since the triplet state is much longer lived, the triplet sensitizer state is ^{more} much/prone to encounter a solvent molecule.

However, the energies of the triplet states of the related unsaturated hydrocarbons are not available. The efficiencies of unsaturated hydrocarbon in the quenching of excitation states of the sensitizer increase with the number of alkyl groups substituted about the carbon double bond (4). The efficiencies of quenching increases with the decrease of energies of the triplet state of the respective unsaturated hydrocarbon. It was found (5) that the $S_0 \rightarrow T_1$ transition ^{of ethylene} has an E_{T_1} value of 82 kcal. Therefore the unsaturated hydrocarbons used in our experiments have E_{T_1} values well below the 82 kcal. Hence it is below the E_{T_1} of xanthone, which included increases in the quenching efficiencies of the unsaturated hydrocarbon in photolysis.

The formation of the unsaturated hydrocarbon excited state will lead mainly to isomerization of the respective hydrocarbon (2). However, since the disappearance of xanthone was taking place slowly during irradiation, it seems that the xanthone excited state did abstract hydrogen from the solvent and formed the respective

hydrocarbon free radical followed by the formation of the respective dimer.

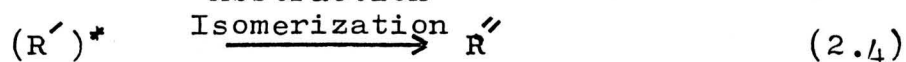
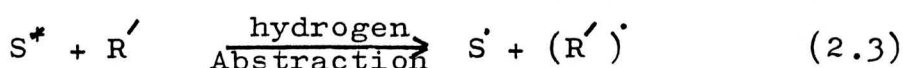
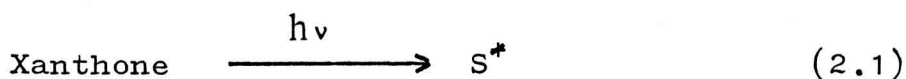
Fig. 2.4 will verify the above statement by the fact that the xanthone disappearance was slow in the unsaturated hydrocarbon and the order of disappearance was in the following order according to the solvent media.

1-Octene > 2-Octene > 2 methyl hexene. .

The quenching efficiency will be higher in 2-methyl hexene.

The fact that the U.V. spectra Fig. (2.22), for the reacted xanthone in the unsaturated hydrocarbon, shows the formation of a new peak which according to Zanker (1) is due to the formation of soluble xanthidrols with corresponding solvent fragment in 9-C position or the dimer of xanthone (9,9'dihydroxy dixanthene). The spectrum of the two are almost similar. However in the 9,9' dihydroxy dixanthene formed during the photolysis, part of it will separate from solution in the form of crystals (1). The latter phenomenon was observed in our experiments only in the case of octane and 2-ethyl pentane solutions. This means that the slow processes of xanthone decomposition in unsaturated hydrocarbon will lead mainly to the formation of branched hydrocarbon dimers of different isomers together with the soluble xanthidrols with the corresponding solvent fragmented in the 9-C position.

The analysis showed that there was no consumption of TAC content in the solutions, where unsaturated hydrocarbons were present. It appears that the energy transfer from xanthone excitation was only taking place to solvent molecules since the collision probability will be higher. Adding to the fact that no insoluble part was observed in the case of irradiation of unsaturated hydrocarbon solutions, means that the consumption of xanthone is due to the slow process of abstracting hydrogen from the solvent and not from the TAC. So the following representation for U.V. irradiation of xanthone/TAC unsaturated solutions could be sketched as follows.



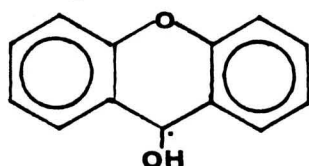
S^* Xanthone excited state

R' Unsaturated hydrocarbon

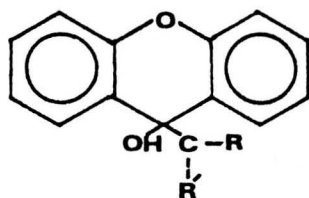
$(\text{R}')^*$ Excited hydrocarbon species

R'' Isomer of unsaturated hydrocarbon

S' Xanthyl free radical



- (R') Hydrocarbon free radical
 R'-R' Dimers of different isomers (Branched)
 S-R' Xanthydrols where hydrocarbon fragment
 in 9c position.



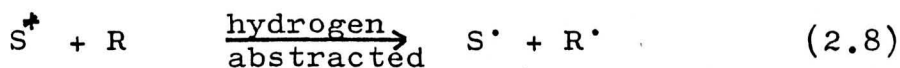
As mentioned in Chapter 1, Zanker and Ehrhardt proved that the photolysis of xanthone in the presence of saturated hydrocarbon leads to the formation of a xanthone dimer, and this was due to the formation of xanthone triplet state which will abstract hydrogen from saturated hydrocarbons.

The analysis of the crystallites formed in the irradiation of Octane/xanthone and Octane/xanthone and TAC solutions correspond to the dimer of xanthone (9,9' dihydroxy-dixanthene). This again agrees with the Zanker paper (1).

The GLC analysis of the Octane/xanthone irradiated solution, cf Fig. 2.11, showed the formation of new compounds. The peaks of these compounds are the finger print of the peaks drawn in Fig. 2.20 which are due to different isomers of the C₈ dimer. Fig. 2.20 shows that these peaks, after ⁶⁰C-γ-irradiation, were proved to be the isomers of the hydrocarbon dimer, as mentioned in Chapter 1, which were mainly branched hydrocarbons.

Also from section 2.2.5, it seems clear that the C₄₈ hydrocarbon did indeed form, although definite proof could not be submitted due to the limitation of analysis with the instruments available.

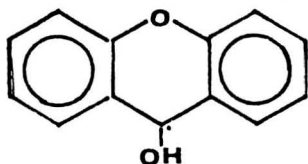
Therefore by irradiating Octane/xanthone solution with U.V. light, one would obtain the dimer of C₈ and the dimer of xanthone. The following reaction schedule may be drawn according to 1.



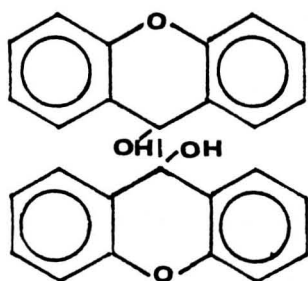
R saturated hydrocarbon

R[·] hydrocarbon free radical

S[·] xanthyl radical



- R -R : Branched hydrocarbon dimer of different isomers.
 S-S: 9,9' dihydroxy dixanthene



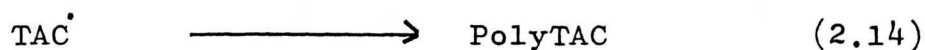
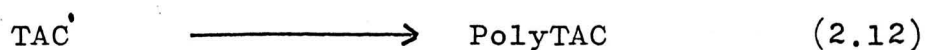
However, by irradiating Octane/xanthone + TAC solution, the amplitude of the hydrocarbon peaks are very much reduced (as shown in Fig. 2.5 and Fig. 2.6). This could be explained by suggesting, that some of the octane free radicals are involved in the chain growth and in the addition polymerization of TAC rather than dimerization. Such a process will indeed reduce the formation of the C_8 dimer. In the case of the saturated hydrocarbon namely octane and ethyl pentane, the insoluble

product is some kind of TAC polymer. This TAC polymer was also analysed by I.R. (Fig.2.13) and its spectrum still shows the TAC, S-Triazine 815 cm^{-1} and ether, 1130 cm^{-1} bands, together with the reduction of the allyl 925 and 990 cm^{-1} bands. These facts indicate that the polymer is Poly(TAC) rather than the polymer of TAC isomer i.e. TALC. The latter fact was supported by the non-appearance of a $\text{C}=\text{O}$ 1700 cm^{-1} band. Because of its lack of solubility and the fact that TAC is a highly functional monomer, the polymer formed was gelled, and gel formation appeared at low conversion. It was reported (6) that 9% conversion of TAC will result in the appearance of the insoluble polymer. In our system, the insoluble polymer appeared in Octane and ethyl pentane solutions, after about 45% and 15% conversion respectively, as shown in Fig. 2.3. This indicates, that, the formation of gelled polymer after 9% conversion, may well take place and that, instead of forming this insoluble product, it will form a microgel dispersed in the hydrocarbon solution up to the 45% or 15% conversion, where the gelled polymer will separate from the respective solution.

The polymerization of TAC is due to the allyl radical formation which took place either by a direct initiation process from xanthone, or indirect initiation processes due to the presence of octane radical in solution. Since the direct initiation process did not appear to take place in the case of unsaturated hydrocarbon/

xanthone/TAC solutions, then it is more likely that with such low TAC concentration present in the mixture, the chain growth and gelation of TAC was due to radical transfer from octane free radical, although direct initiation polymerization has not been ruled out. The indirect initiation process assumptions are supported by the fact that the allyl group has very strong chain transfer ability providing it will cause the formation of some effective chain transfer in addition to the degradative chain transfer (7). The following reaction schedule could be put forward as steps for the saturated hydrocarbon/xanthone/TAC photoinitiation.

In addition to reaction 2.7, 2.8, 2.9 and 2.10, the following are also included in the schedule.

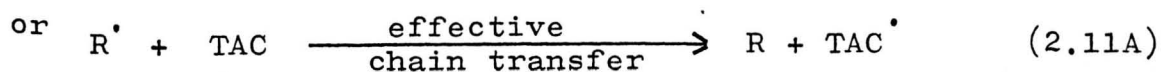
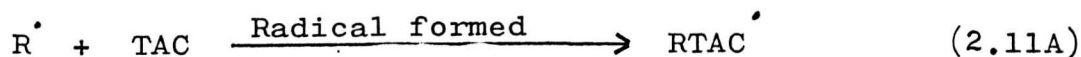


Also according to Zanker, the following two steps may be possible

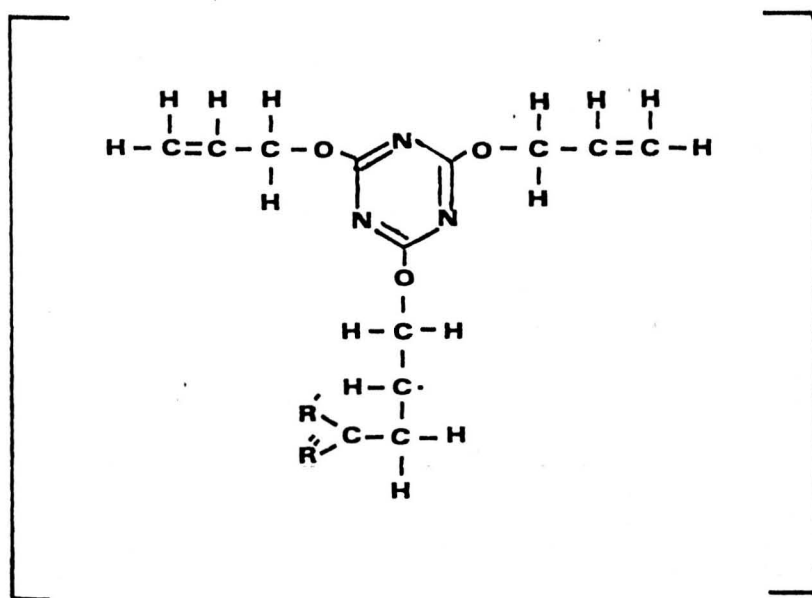


$\left. \begin{array}{l} S - R \\ S - TAC \end{array} \right\}$ Xanthydrols where, hydrocarbon or TAC
 fragments in the 9-C position of xanthone
 molecule.

The formation of PolyTAC grafted with hydrocarbon, due to steps 2.11 and 2.12, could be possible but cannot be certain at this stage. However, the initiation step 2.11 could be classified in either of the following.

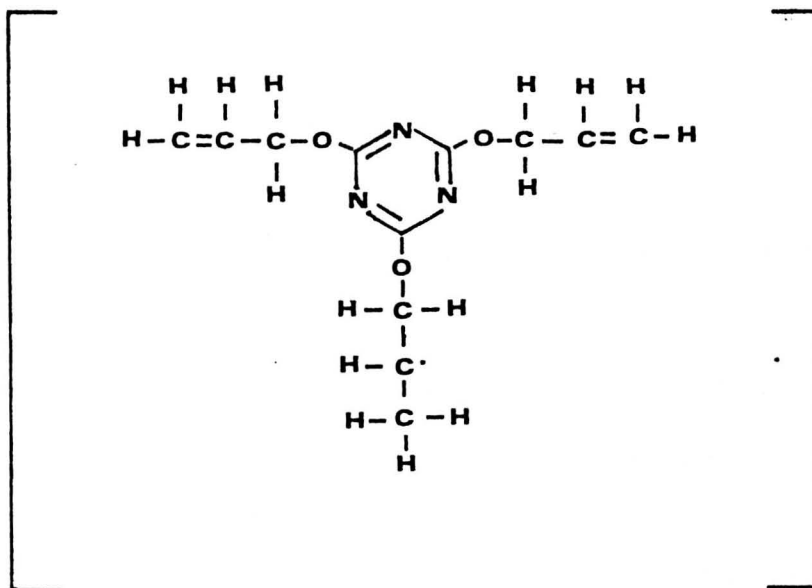


where $RTAC^{\cdot}$ could have the following chemical structure



Where $R'-C-R''$ represents the hydrocarbon molecule

and TAC' would have the following chemical structure



If RTAC' is indeed forming then the PolyTAC obtained due to step 2-11A will be grafted with hydrocarbon. This was studied by utilizing allyl acetate to replace TAC and is reported in the next chapter.

References

1. Zanker, V., et al. Bull Chem. Soc. Jap., 39, 1694 (1966).
2. Robert, O.K. Organic Photochemistry, McGraw-Hill Book 1966.
3. Hammond, G.S., et al. J. of Amer. Chem. Soc., 86, 4537 1964.
4. Robert, R.E., Ansloos, P. J. of Amer. Chem. Soc., 87, 5569 1965.
5. Evans, D.F., J. Chem. Soc. 1351 (1957), 1753 (1960).
6. Gillham, J.K., Mentzer, C.C., J. Applied Polymer Sci., 17, 1143, (1973).
7. Gaylord, N.G., J. of Polymer Sci., 22, 71 (1956).

Fig. 2-1

The dilatometer used for degassing and irradiation

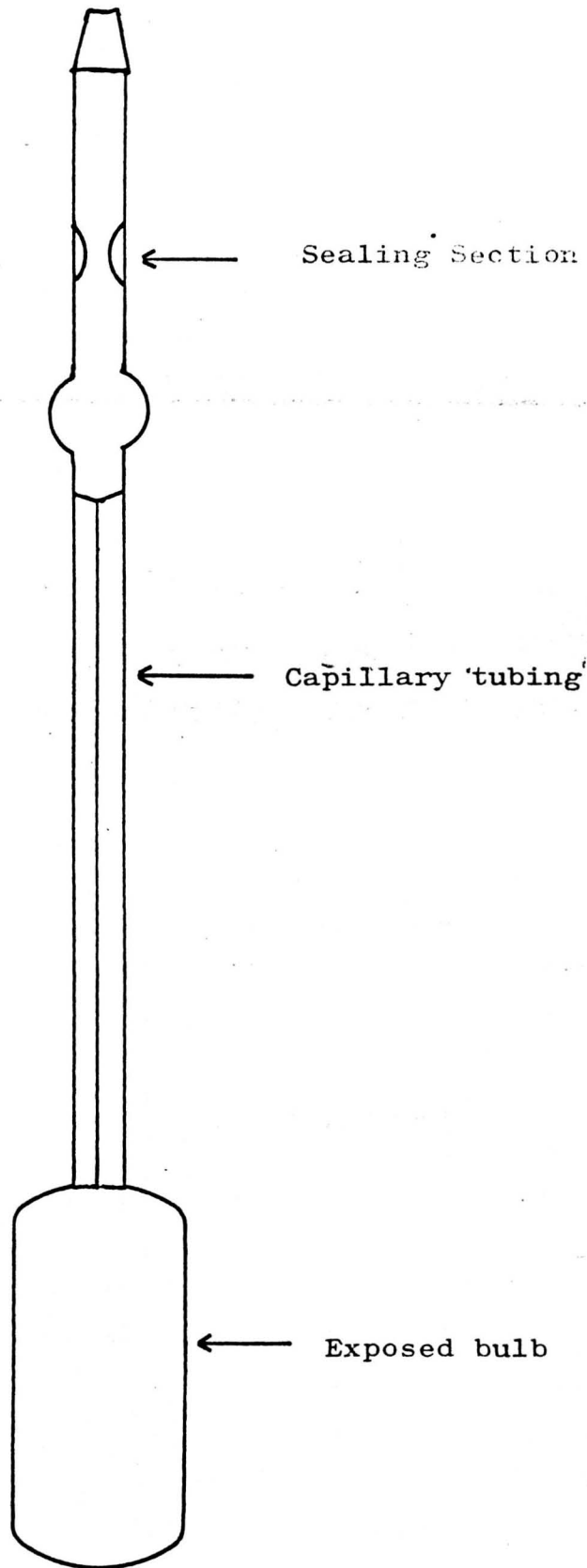


Fig. 2-2 The vacuum line which was used throughout the project

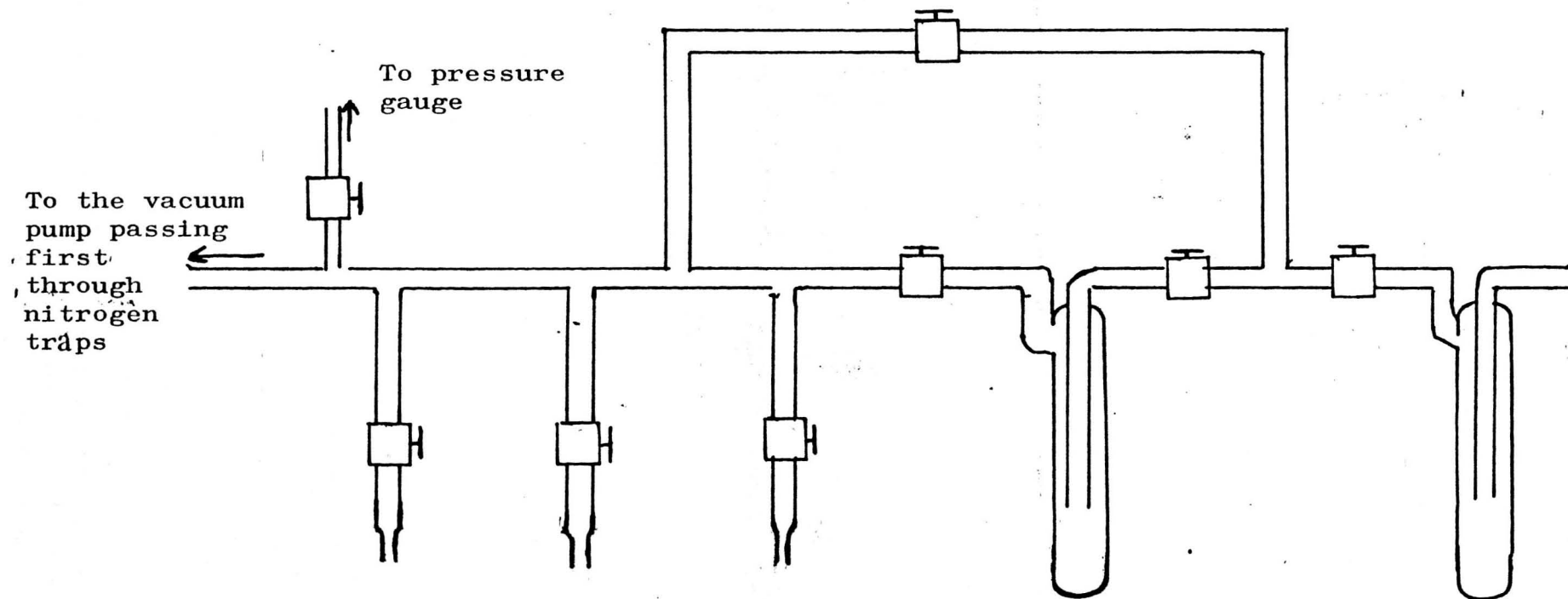


Fig. 2_3 TAC Rate of conversion during the UV radiation in hydrocarbon

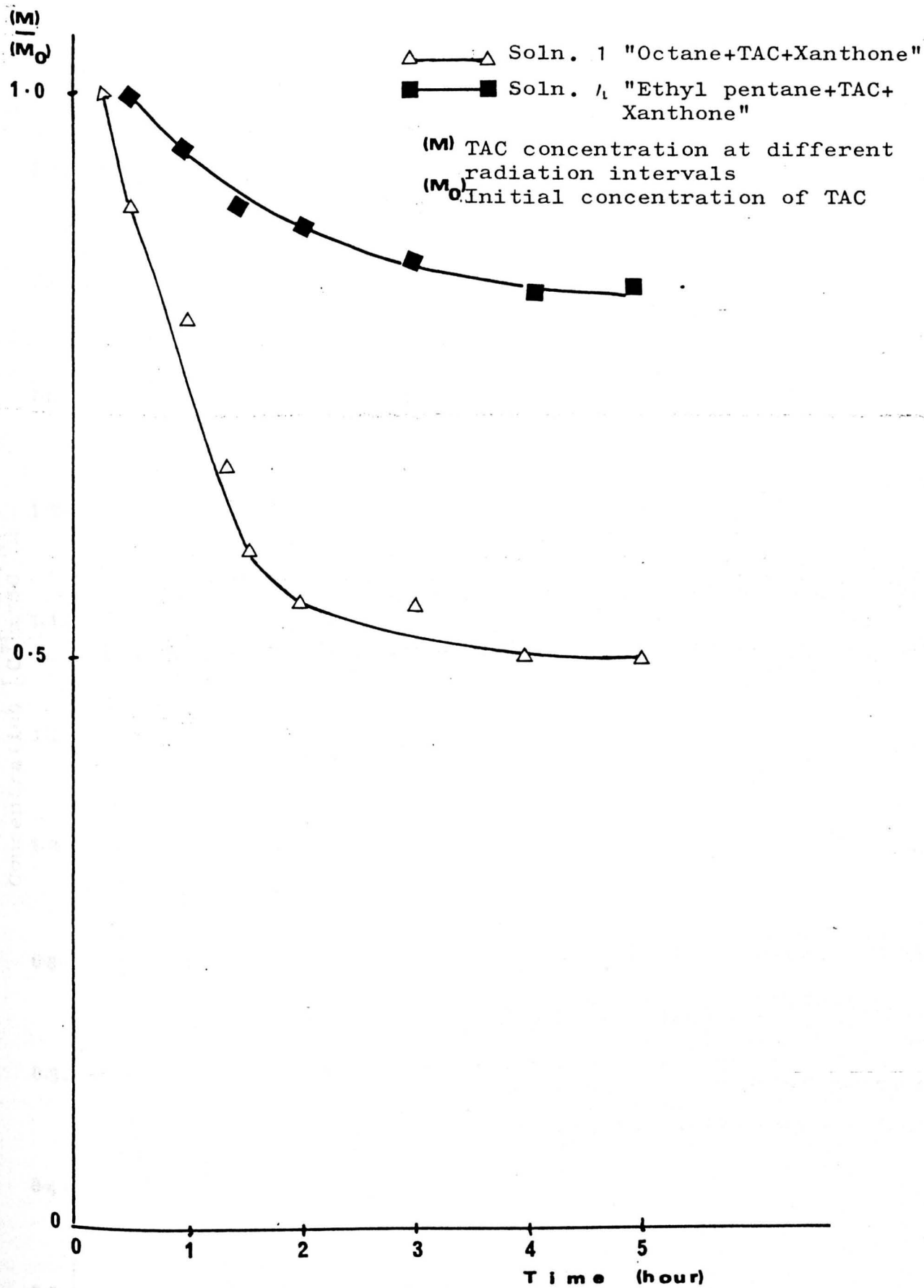
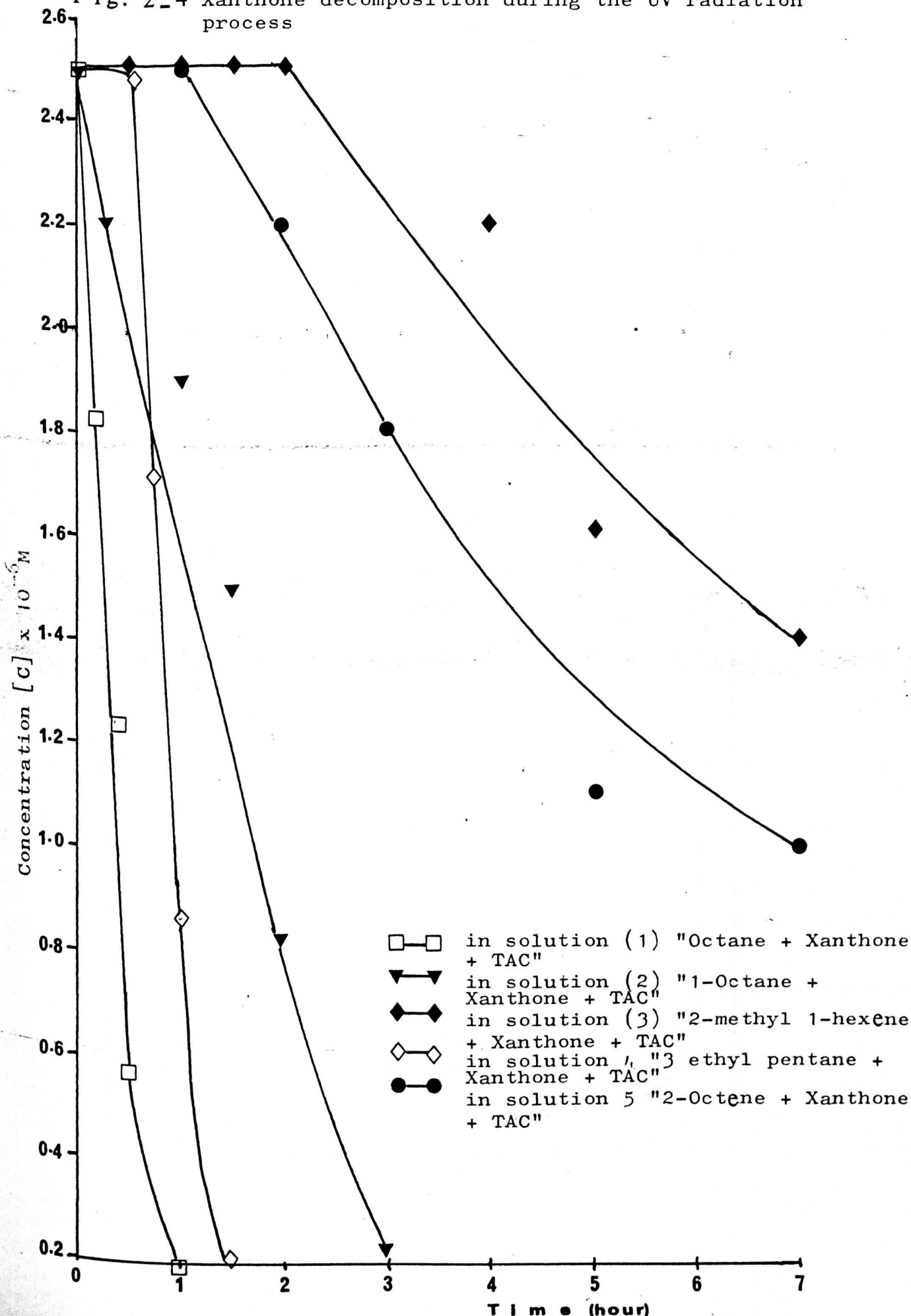
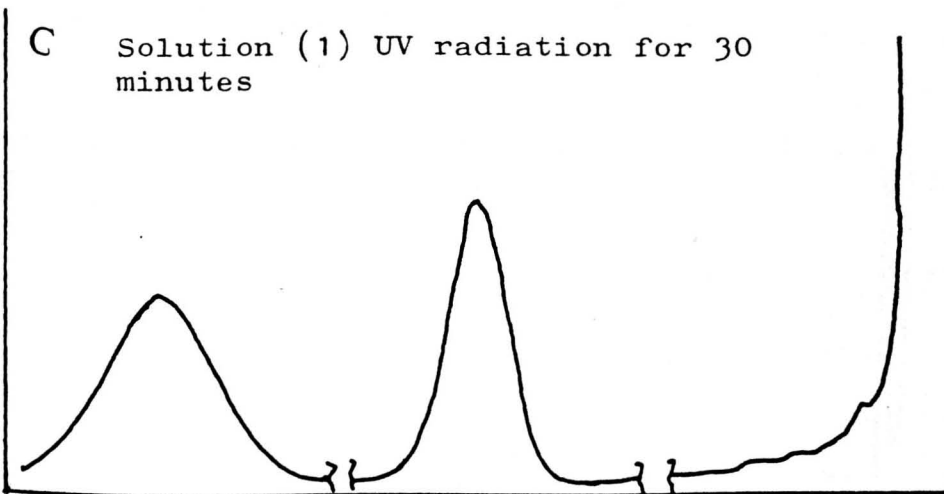
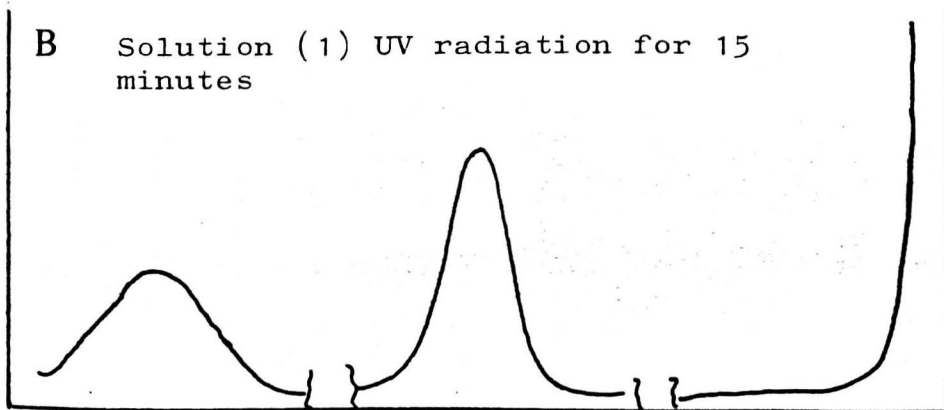
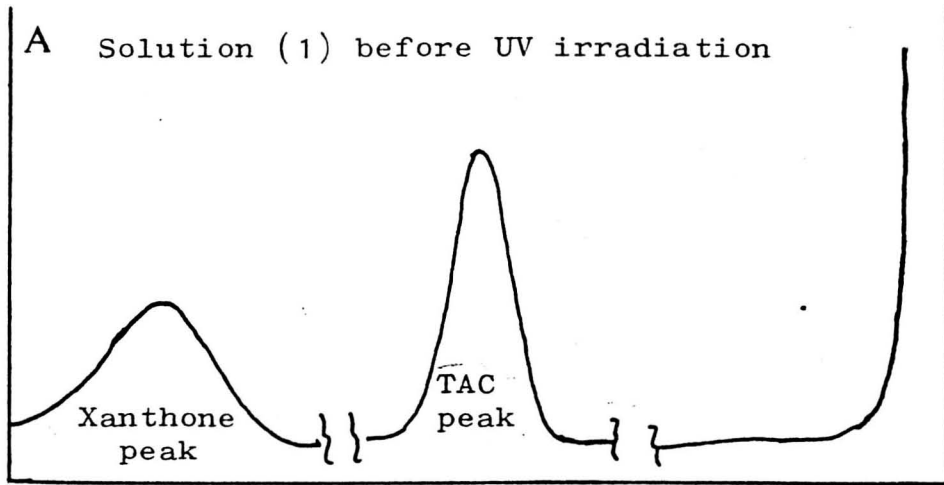


Fig. 2_4 Xanthone decomposition during the UV radiation process



- in solution (1) "Octane + Xanthone + TAC"
- ▼—▼ in solution (2) "1-Octane + Xanthone + TAC"
- ◆—◆ in solution (3) "2-methyl 1-hexene + Xanthone + TAC"
- ◇—◇ in solution (4) "3 ethyl pentane + Xanthone + TAC"
- in solution (5) "2-Octene + Xanthone + TAC"

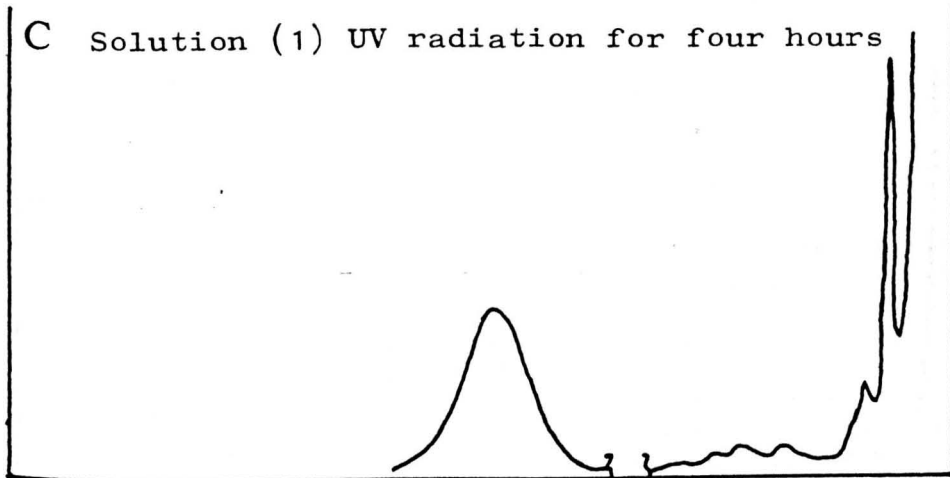
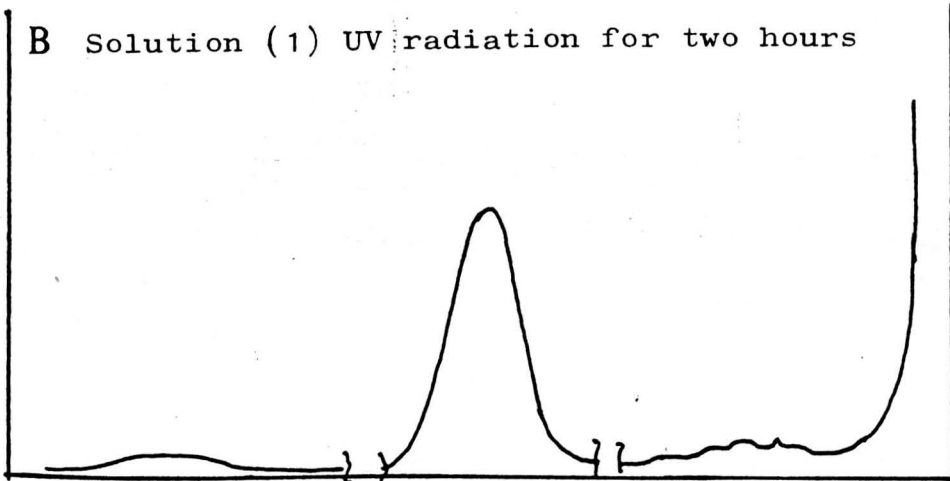
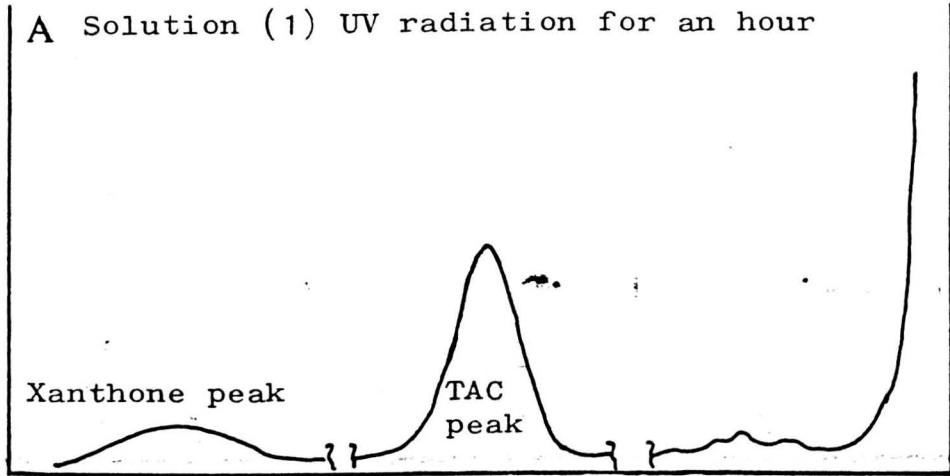
Fig. 2-5 GLC chromatogram



Retention time

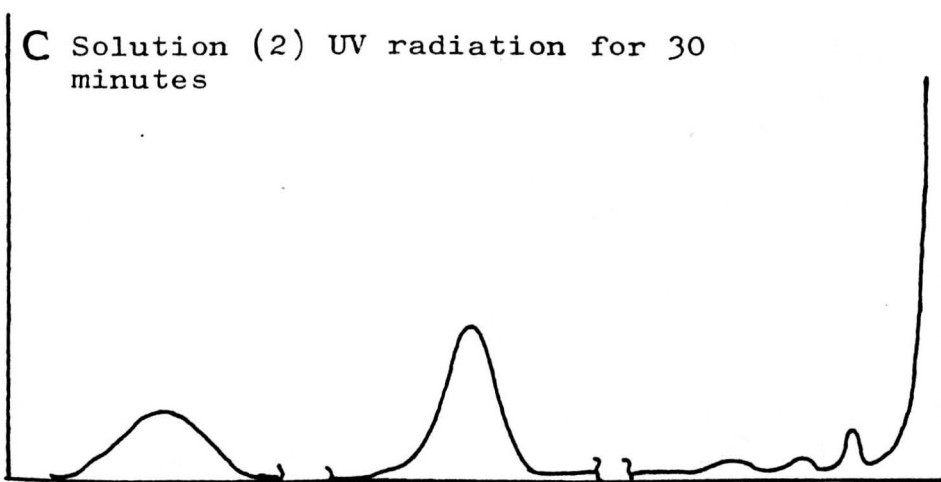
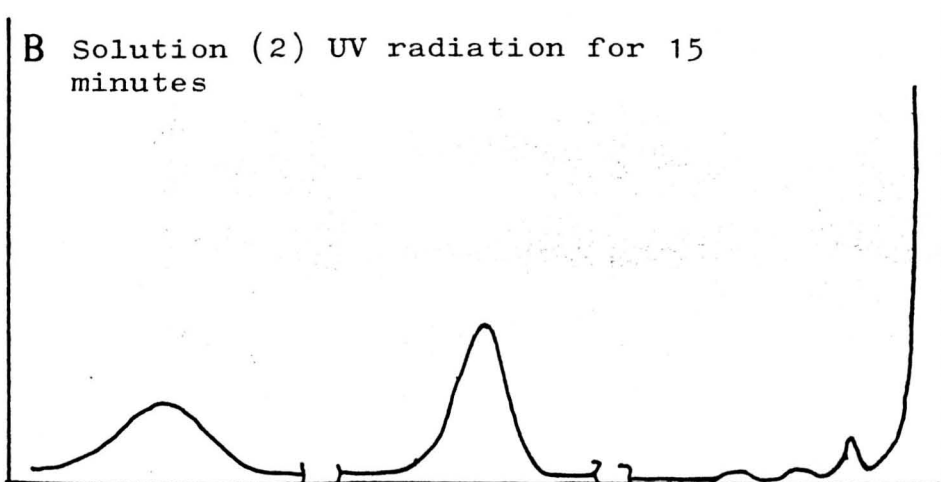
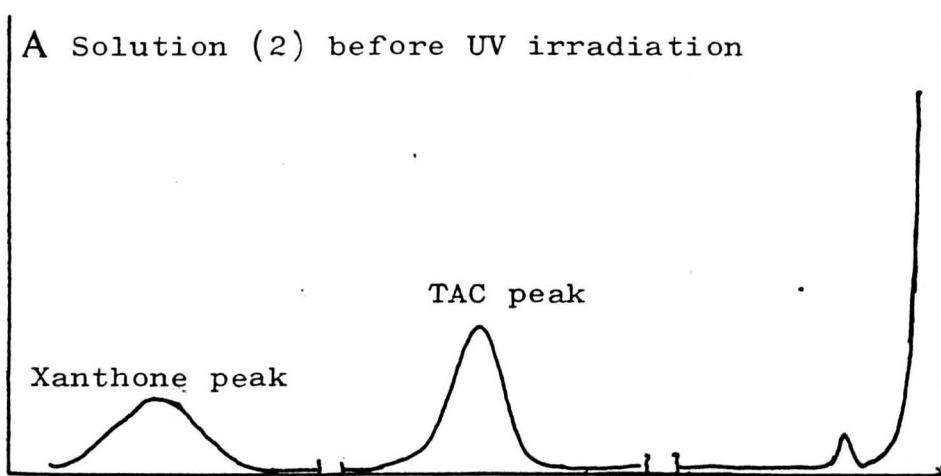


Fig. 2-6 GLC chromatogram



Retention time ←

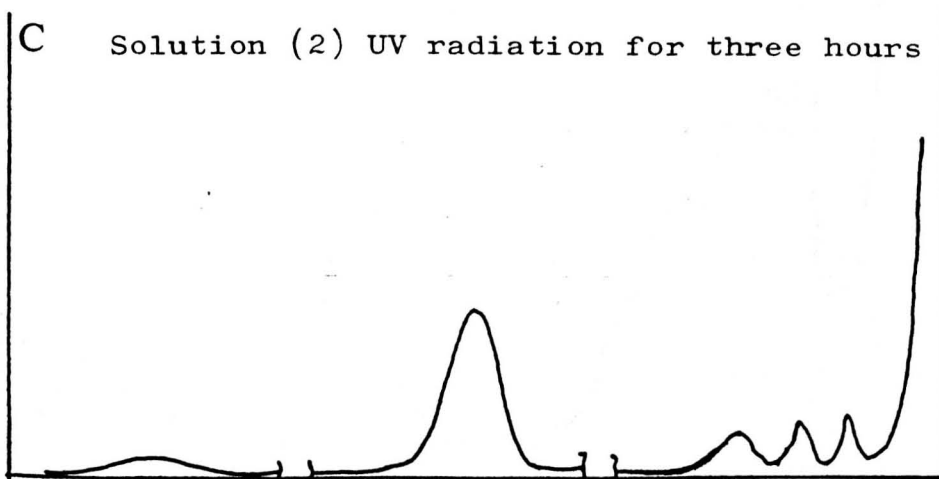
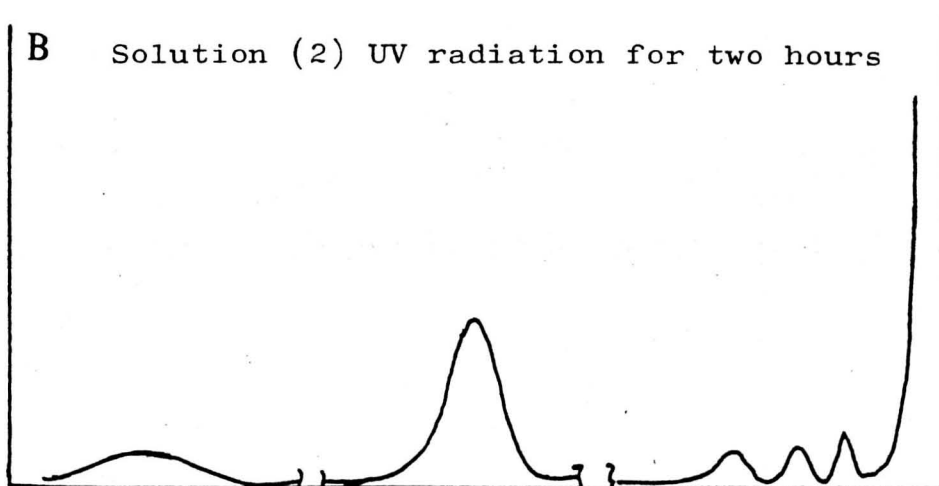
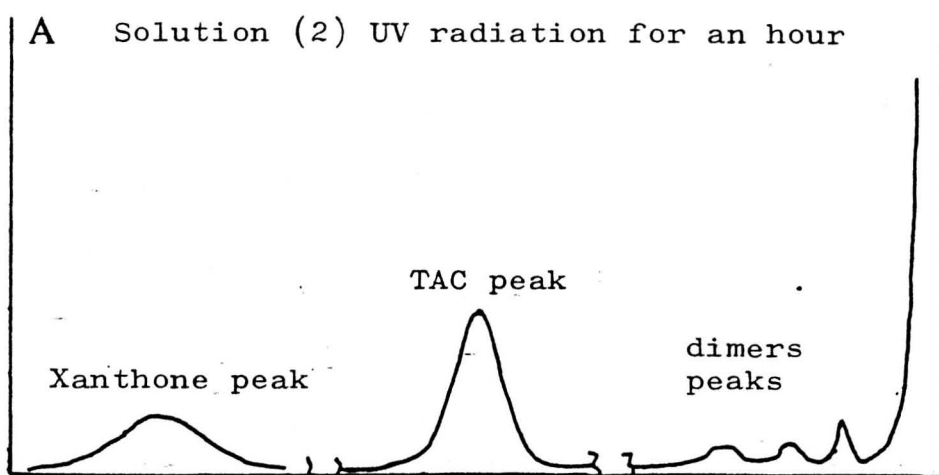
Fig. 2_7 GLC chromatogram



Retention time

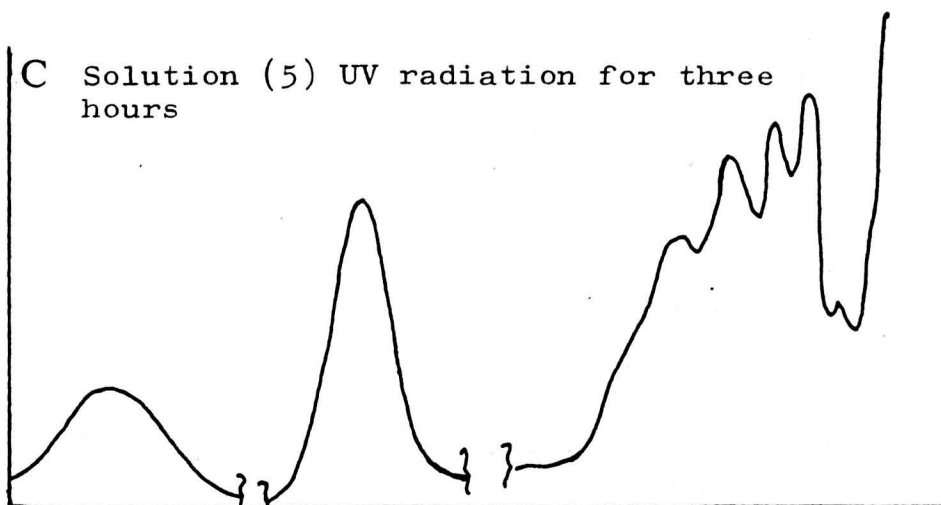
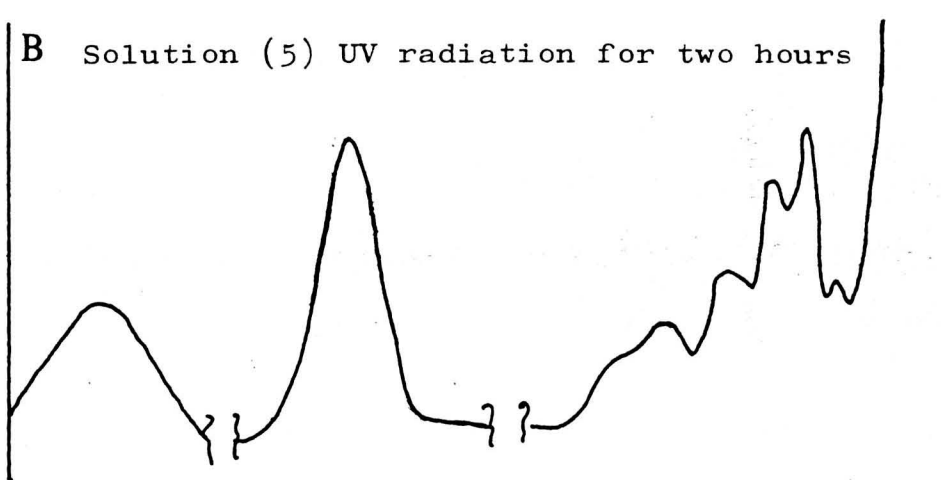
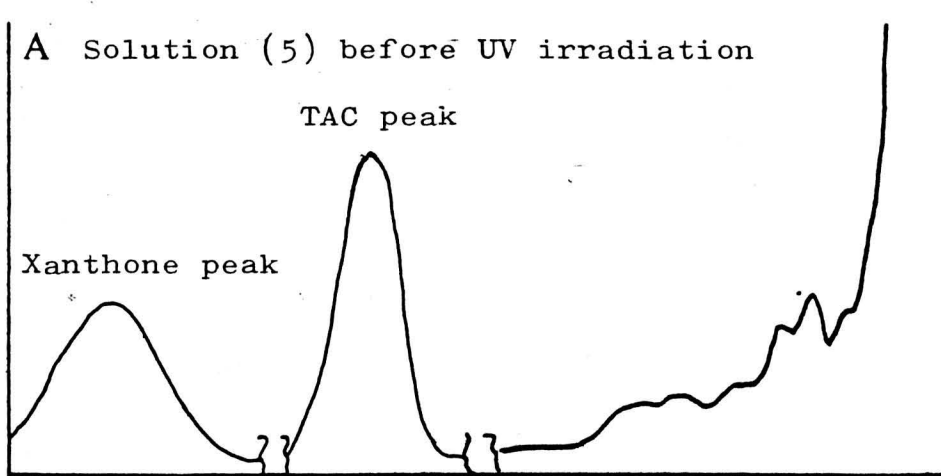


Fig. 2-8 GLC chromatogram



Retention time

Fig. 2-9 GLC chromatogram



Retention time



Fig. 2-10 GLC chromatogram

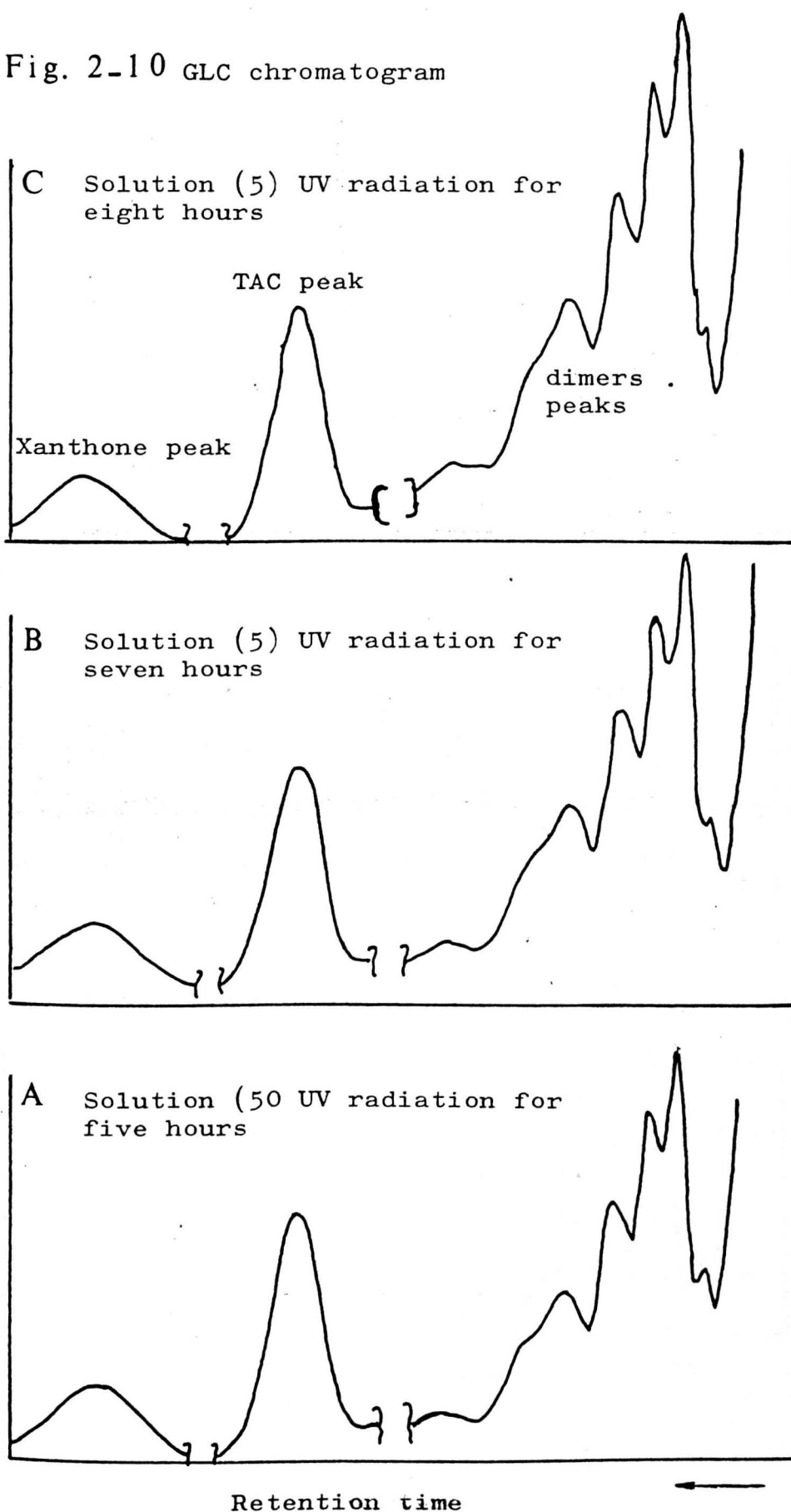
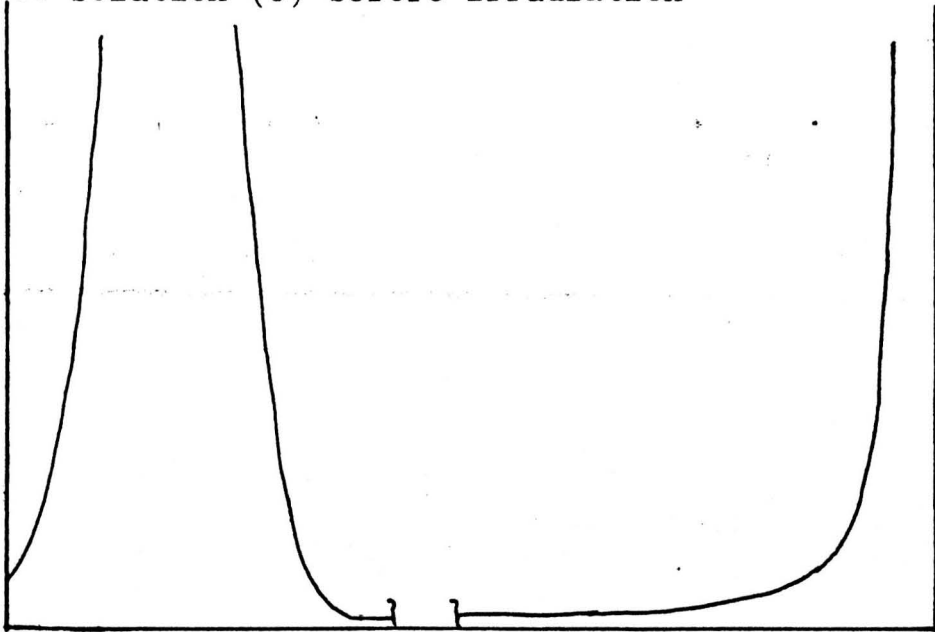
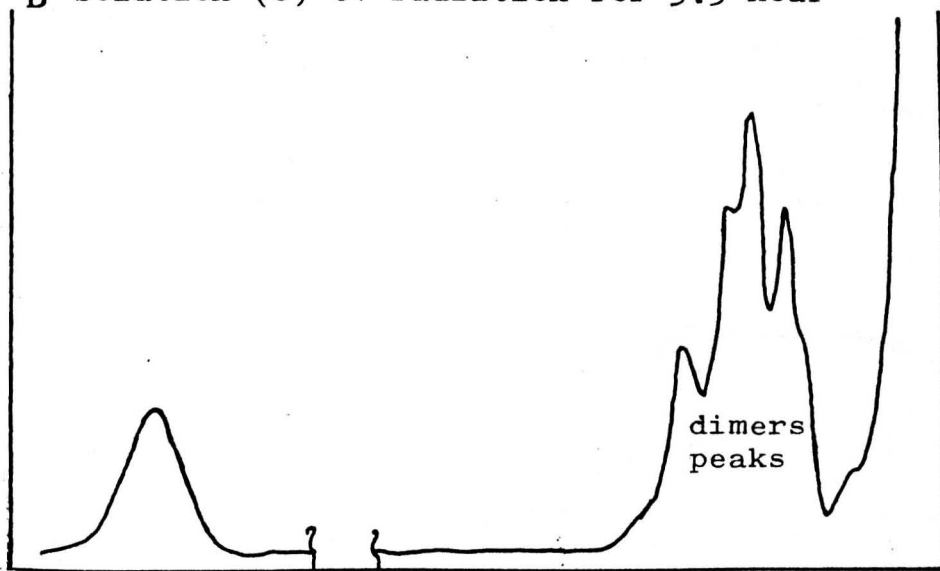


Fig. 2-11 GLC chromatogram

A Solution (6) before irradiation



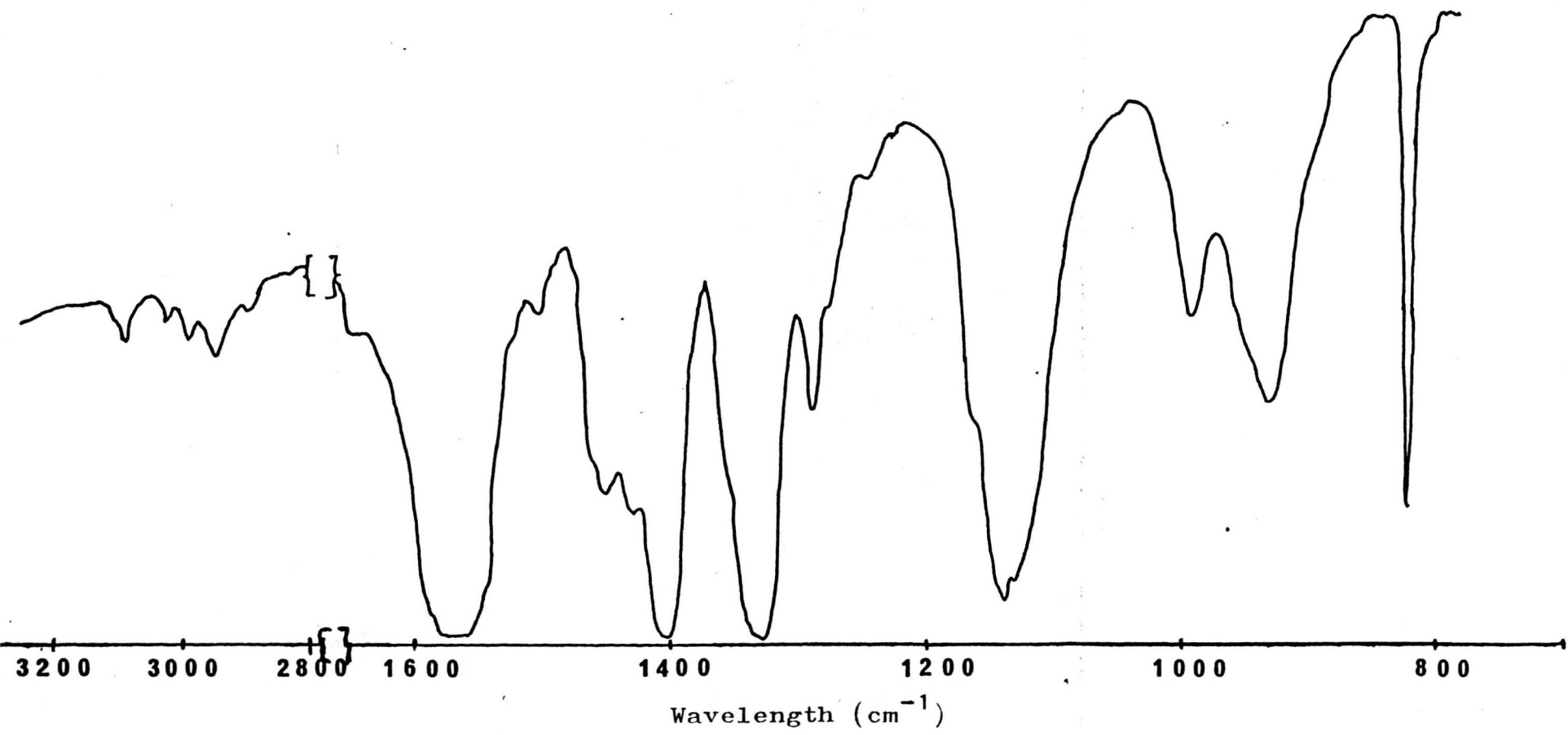
B Solution (6) UV radiation for 3.5 hour



Retention time .

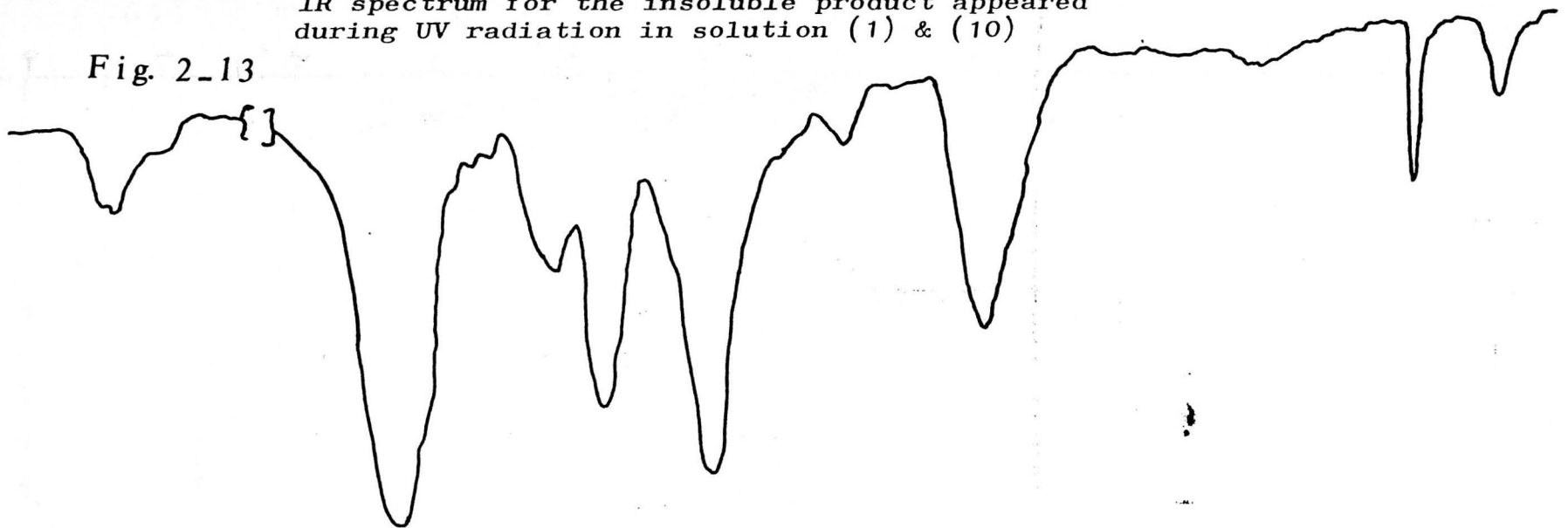


Fig. 2_12 TAC, IR spectrum using KBr disc



IR spectrum for the insoluble product appeared during UV radiation in solution (1) & (10)

Fig. 2-13



3200 3000 2800 1600 1400 1200 1000 800
Wavelength (cm^{-1})

Fig. 2-14 TAC and Xanthone concentration throughout the UV radiation process in solution 10 "Octane + Xanthone + TAC"

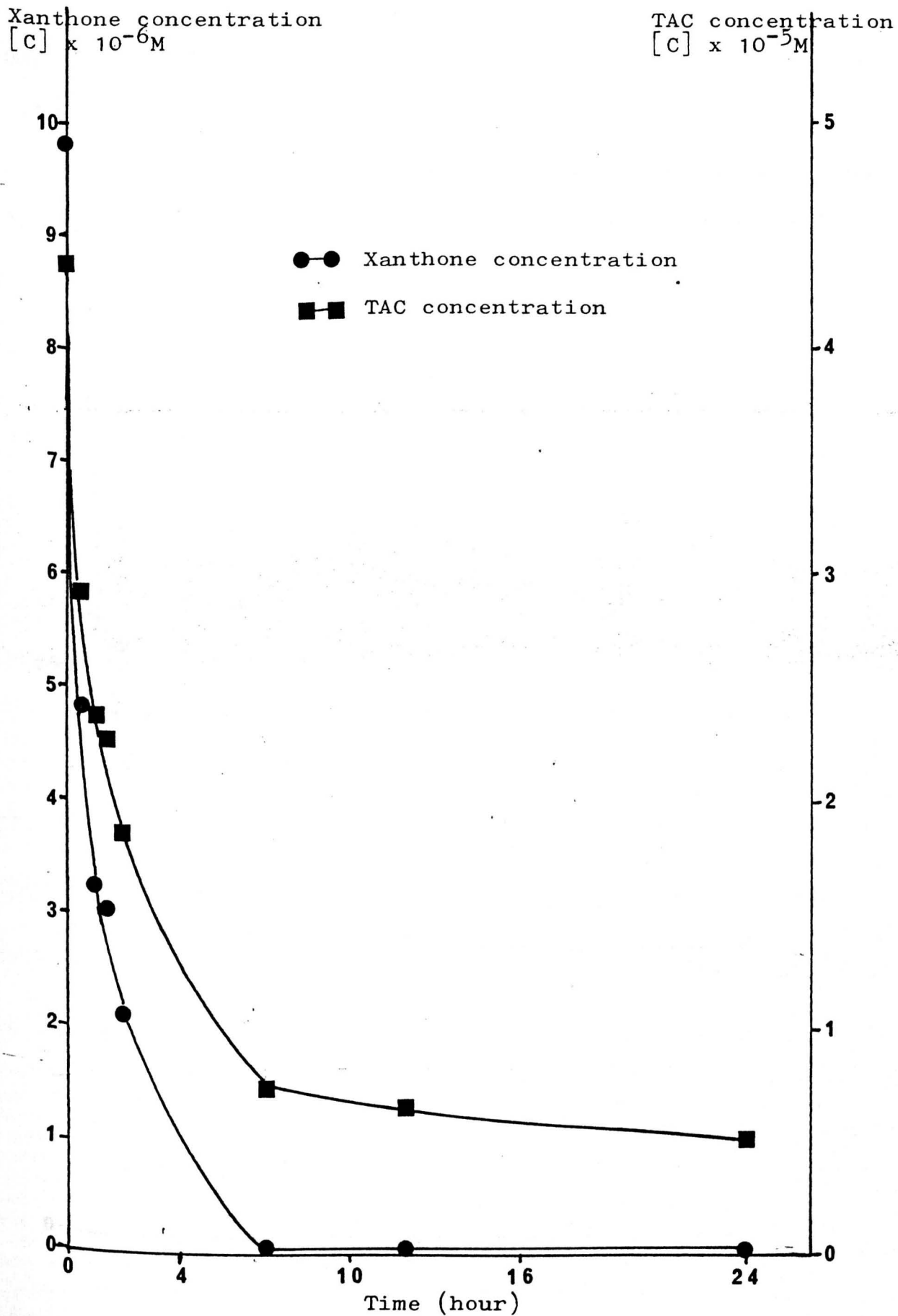


Fig. 2_15 TAC rate of conversion during the UV radiation of solution 10 "Octane + Xanthone + TAC"

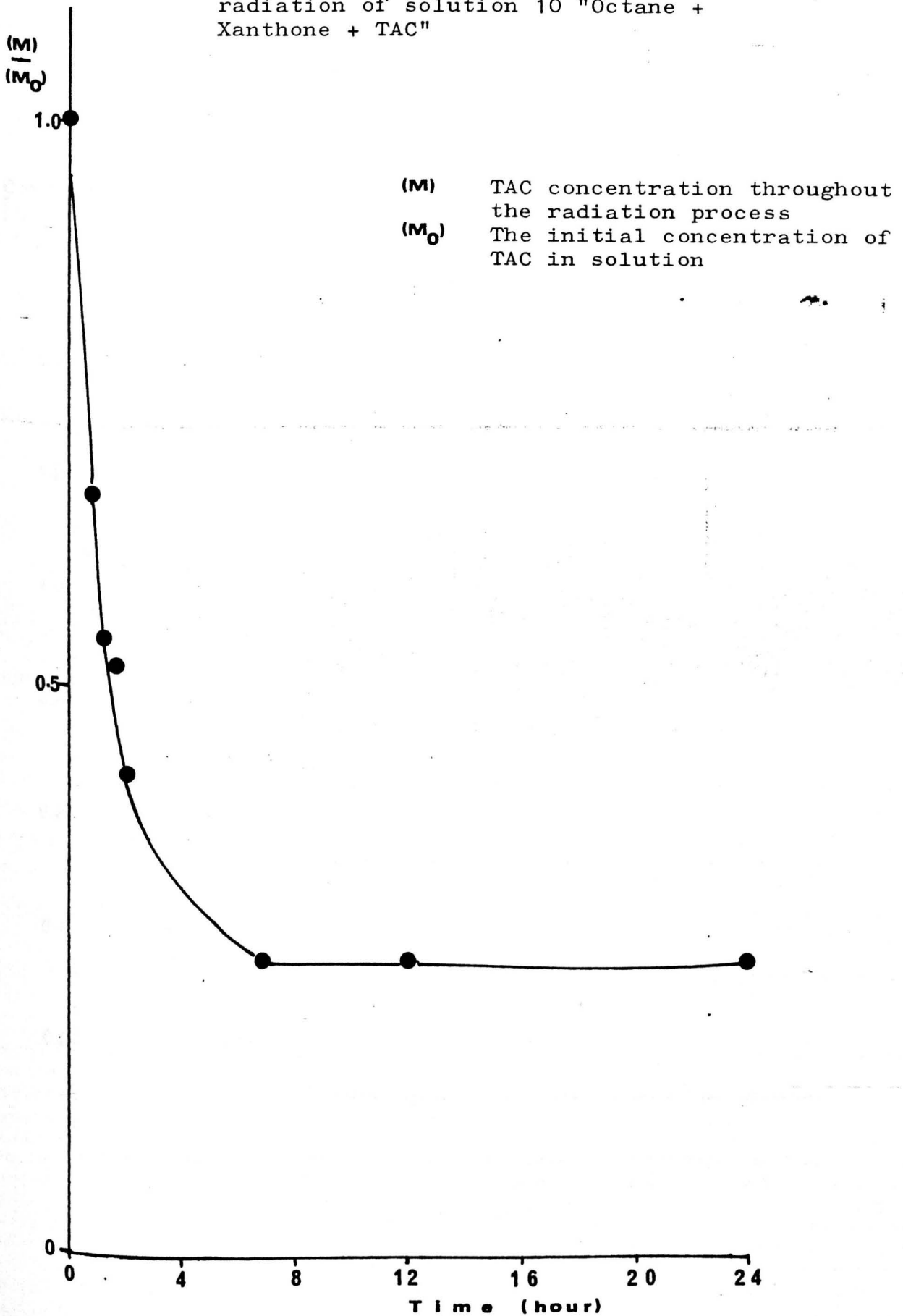


Fig. 2_16 Decomposition Xanthone throughout the UV radiation of solution 12 "Octane + Xanthone"

Concentration of Xanthone
[C] x 10⁻⁵M (moles/litre)

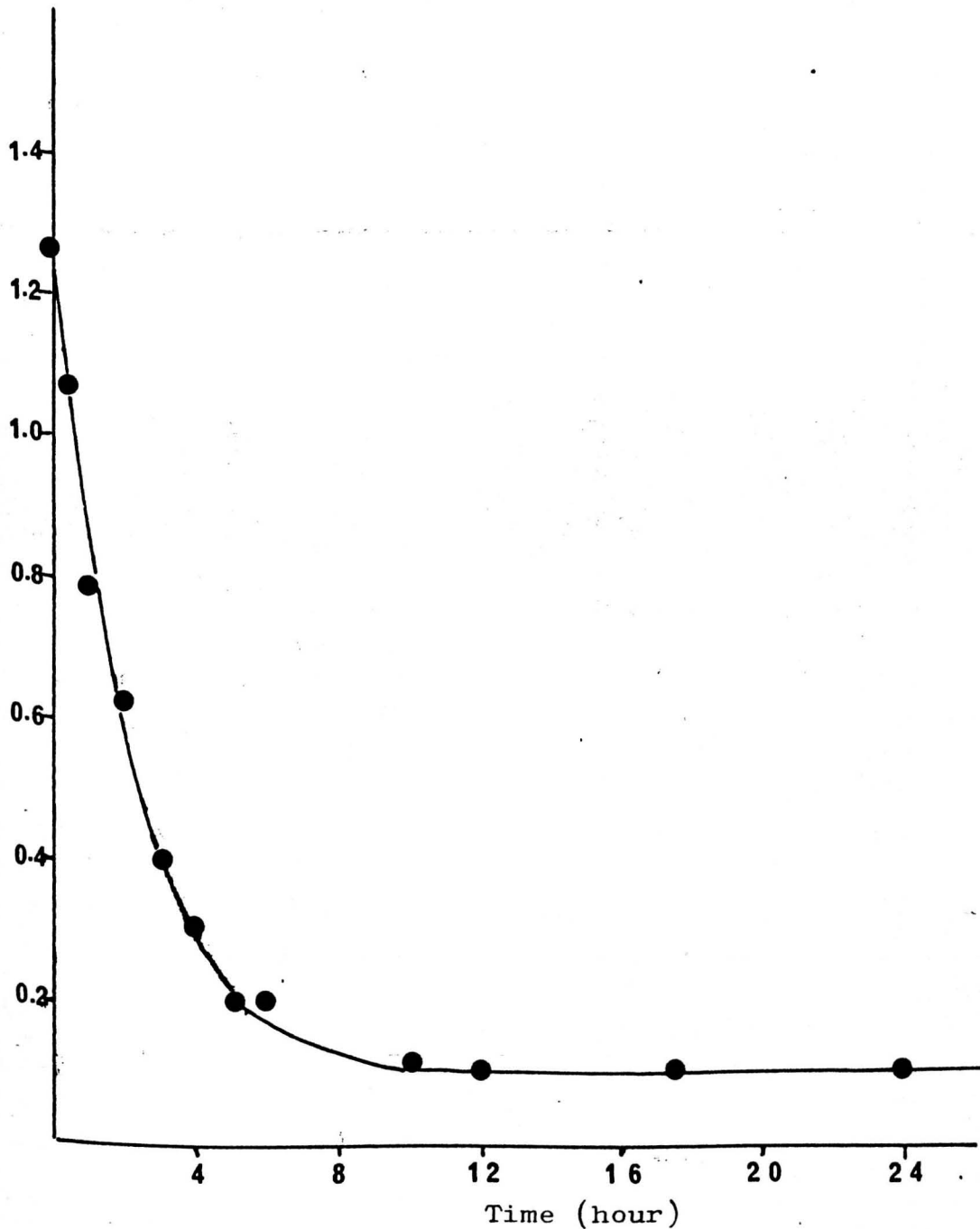


Fig. 2-17 UV spectrum of the Octane solution before, during and after UV radiation process.
(The spectrum is for Xanthone present in solution)

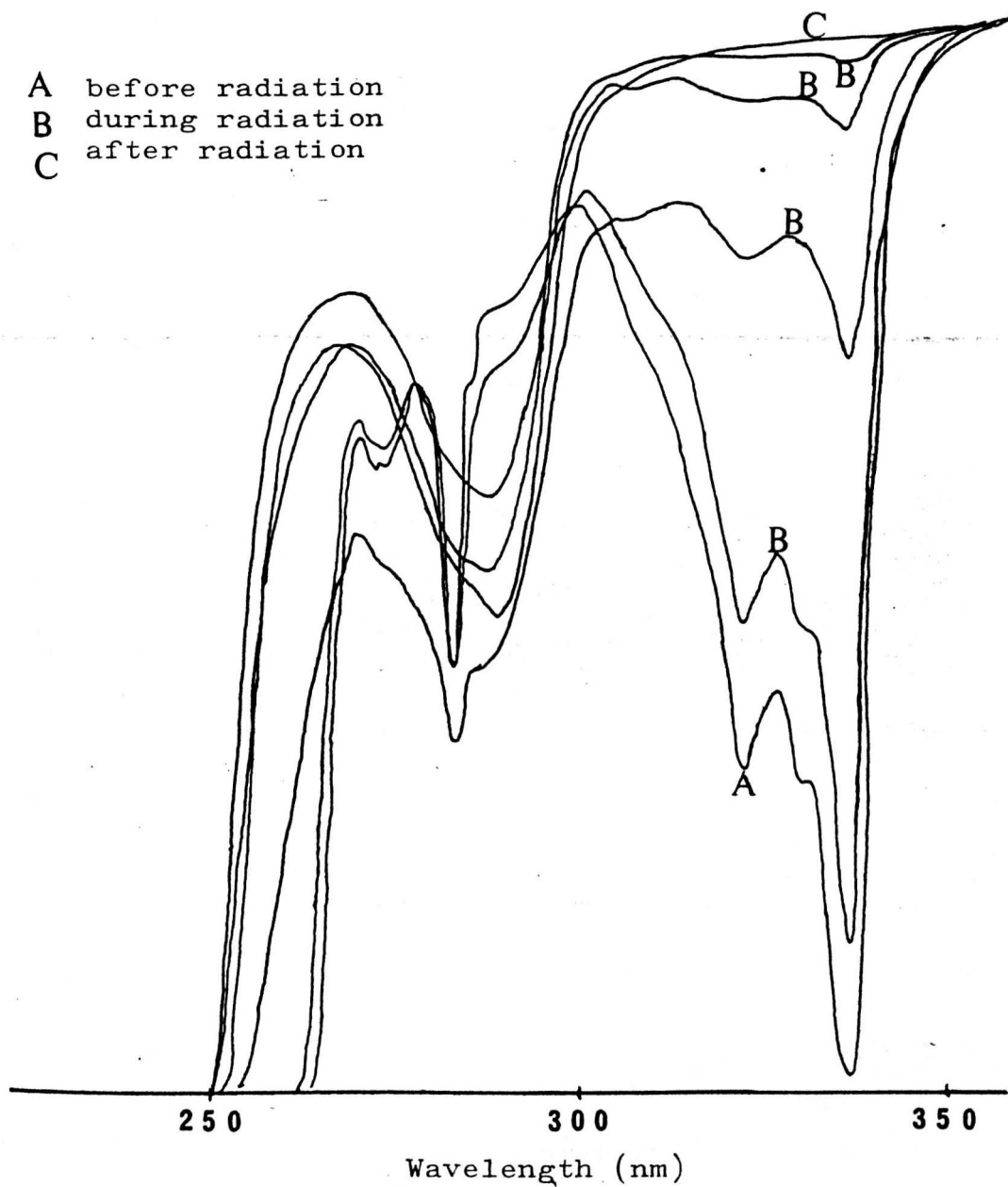


Fig. 2-18

Xanthone UV spectrum in Octane solution
(10) before and after the UV radiation

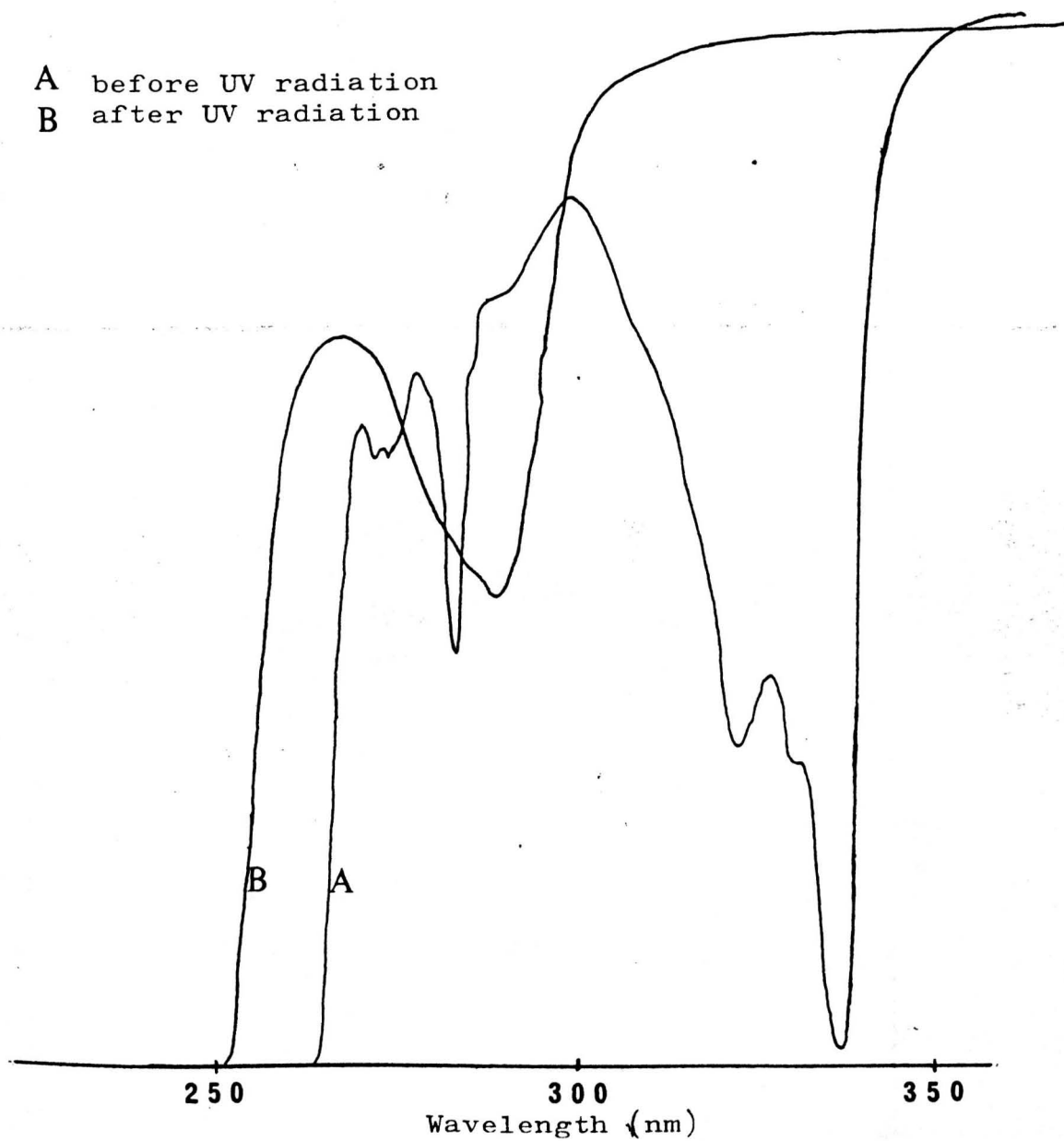


Fig. 2-19 IR spectrum of γ -irradiated TAC in Octane solution (C series) using KBr disc

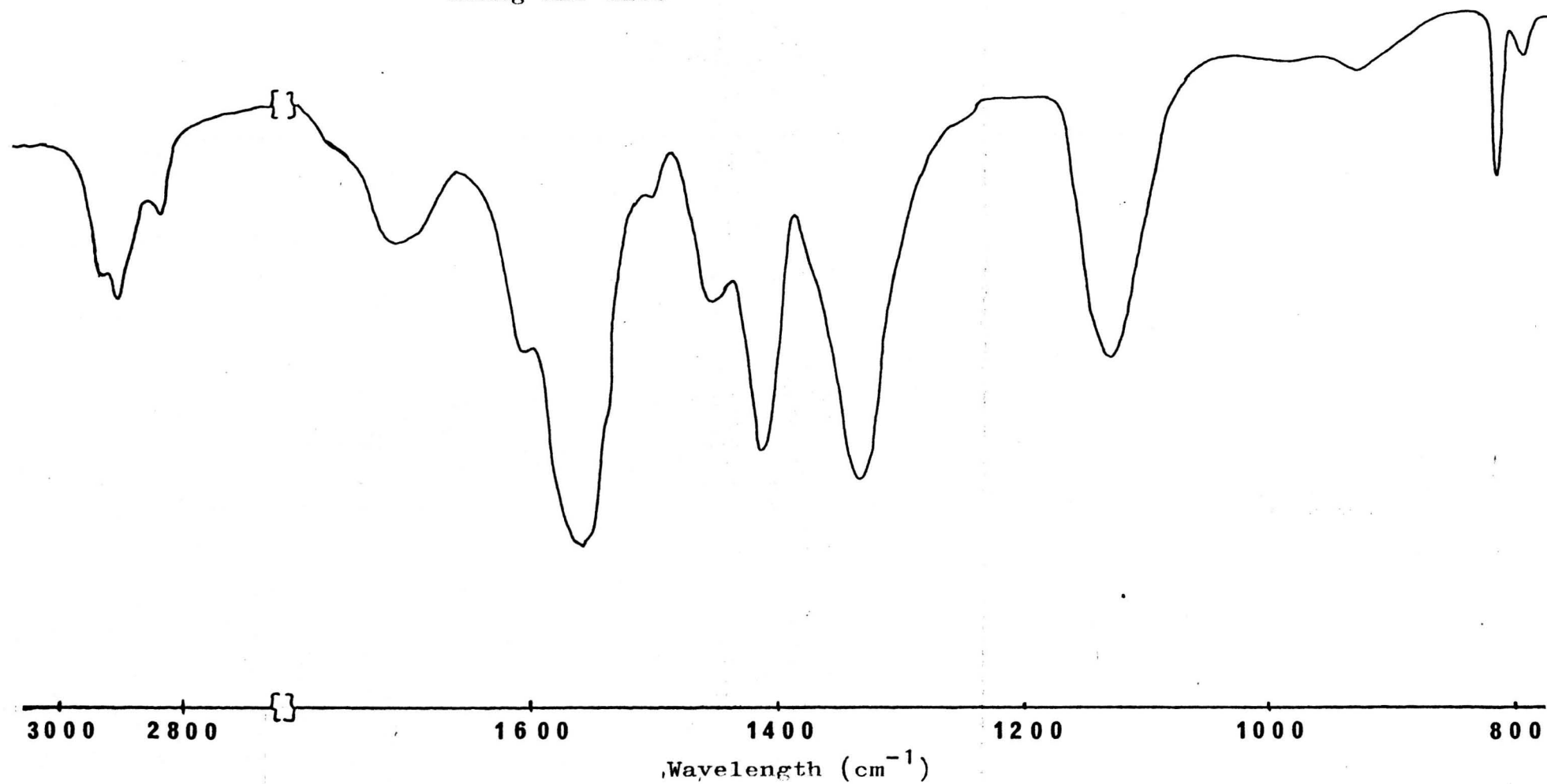
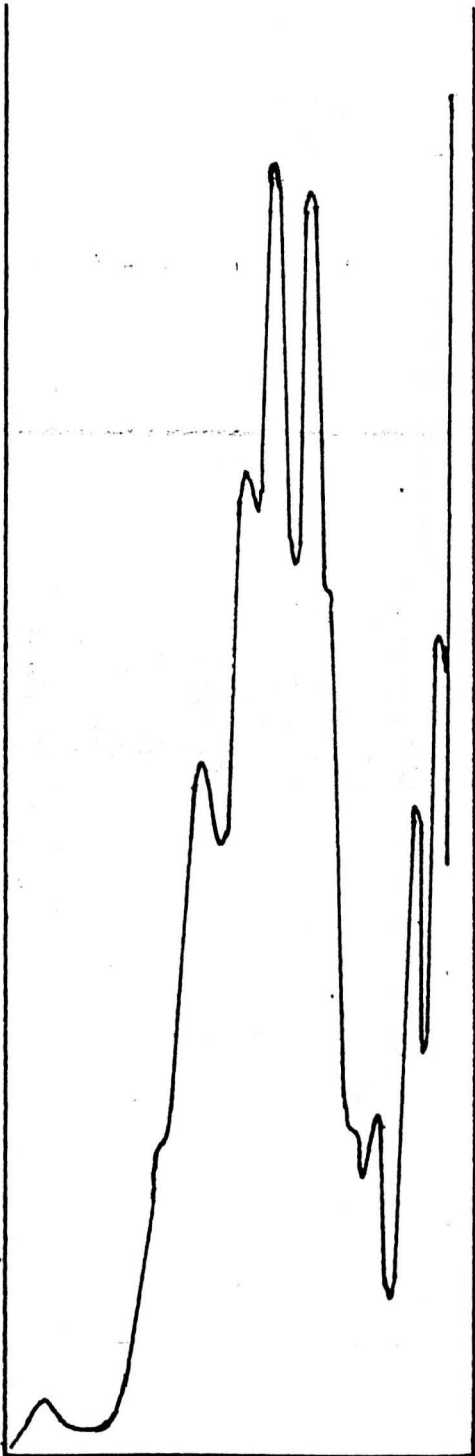
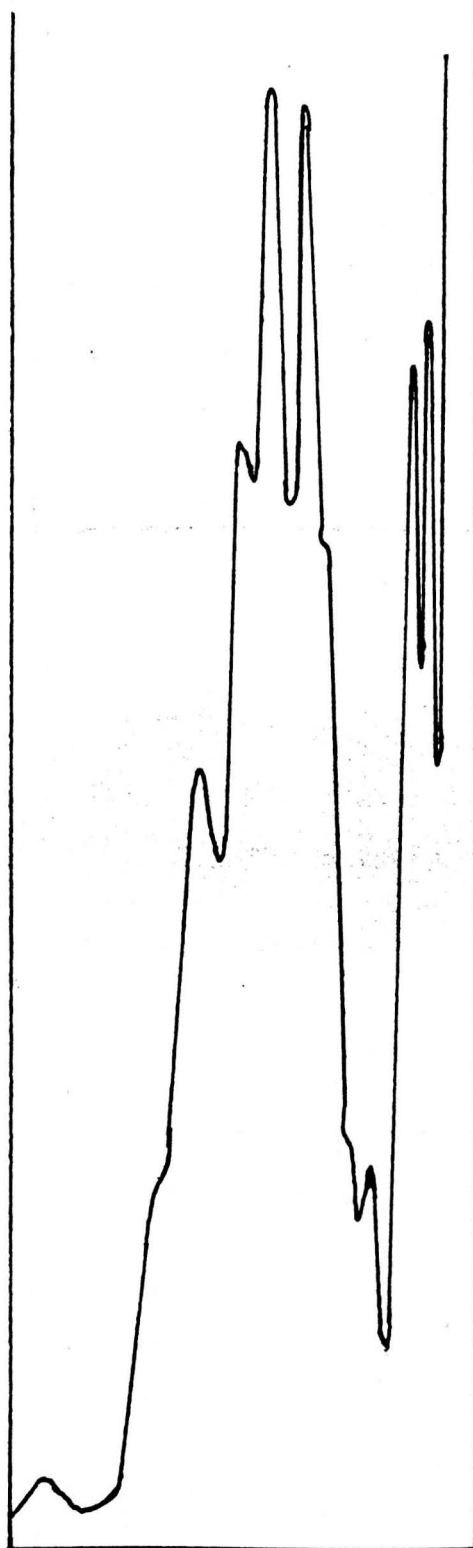


Fig. 2_20A GLC chromatogram γ -irradiated A4 solution



Retention time ←

Fig. 2_20B GLC chromatogram γ -irradiated B4 solution



Retention time ←

Fig. 2-20 C GLC chromatogram γ -irradiated C4 solution

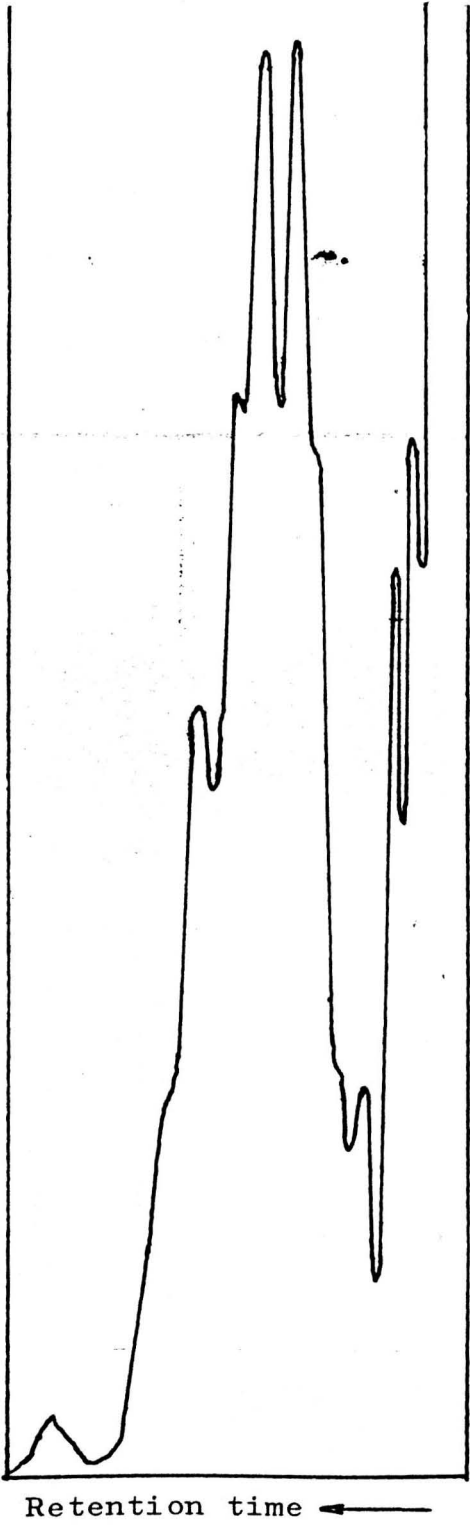


Fig. 2-21 GPC chromatogram for tetracosane before and after UV radiation

Normalised deflection

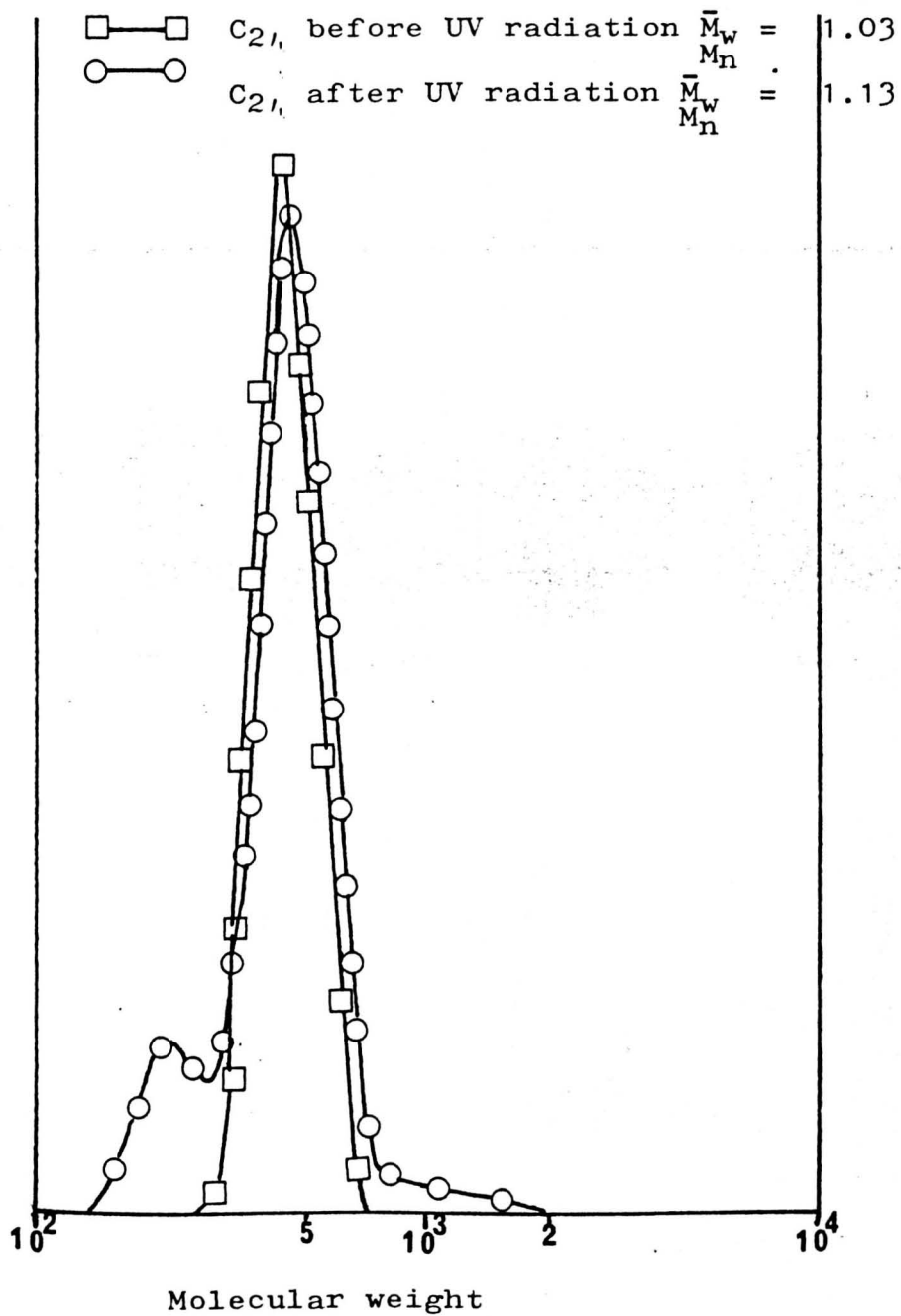


Fig. 2-22 Xanthone UV spectrum in 1-Octene solution

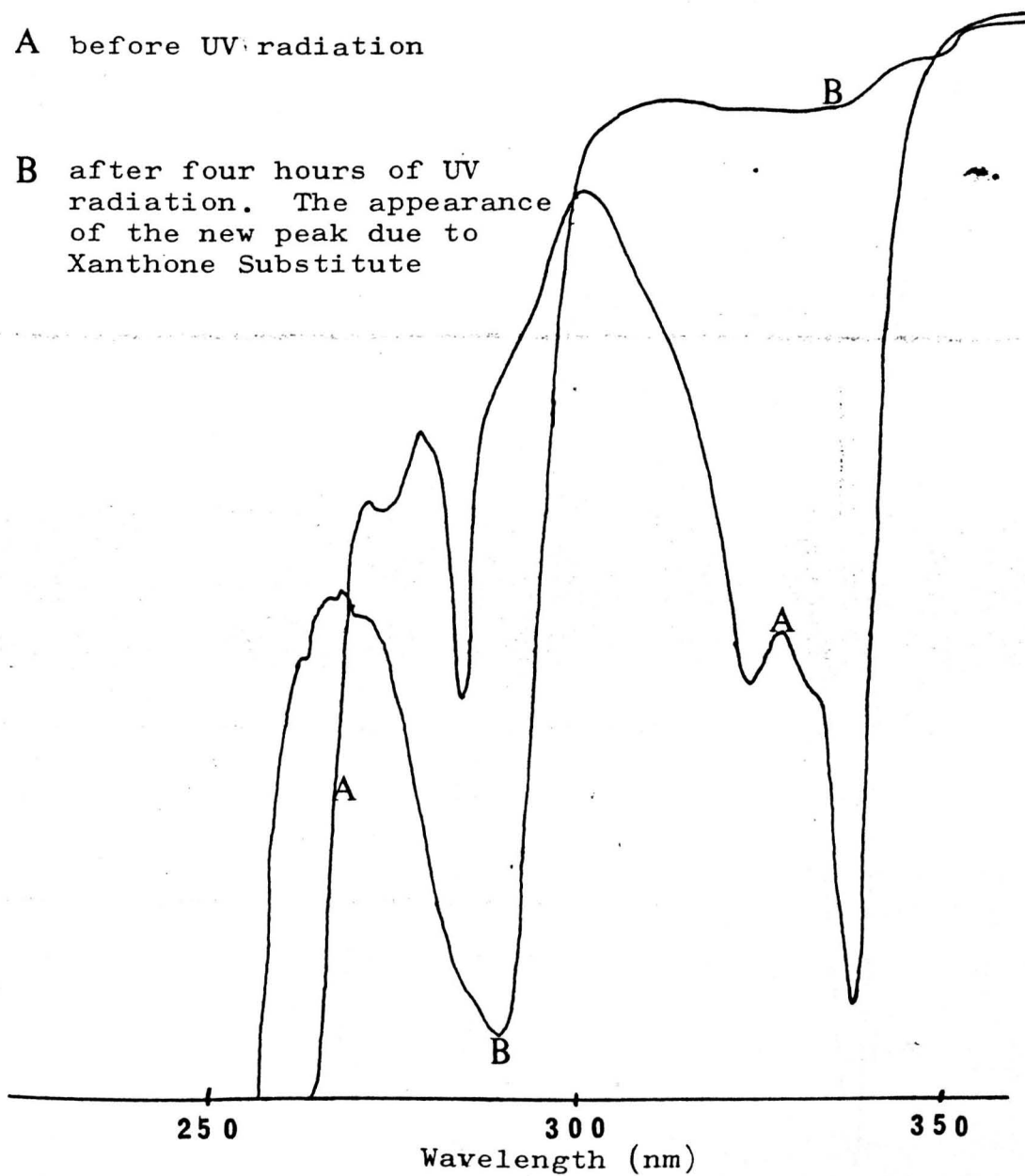


Fig. 2-23

Xanthone: UV spectrum in 2-methylhexene solution

A before UV radiation

B after eight hours of UV radiation

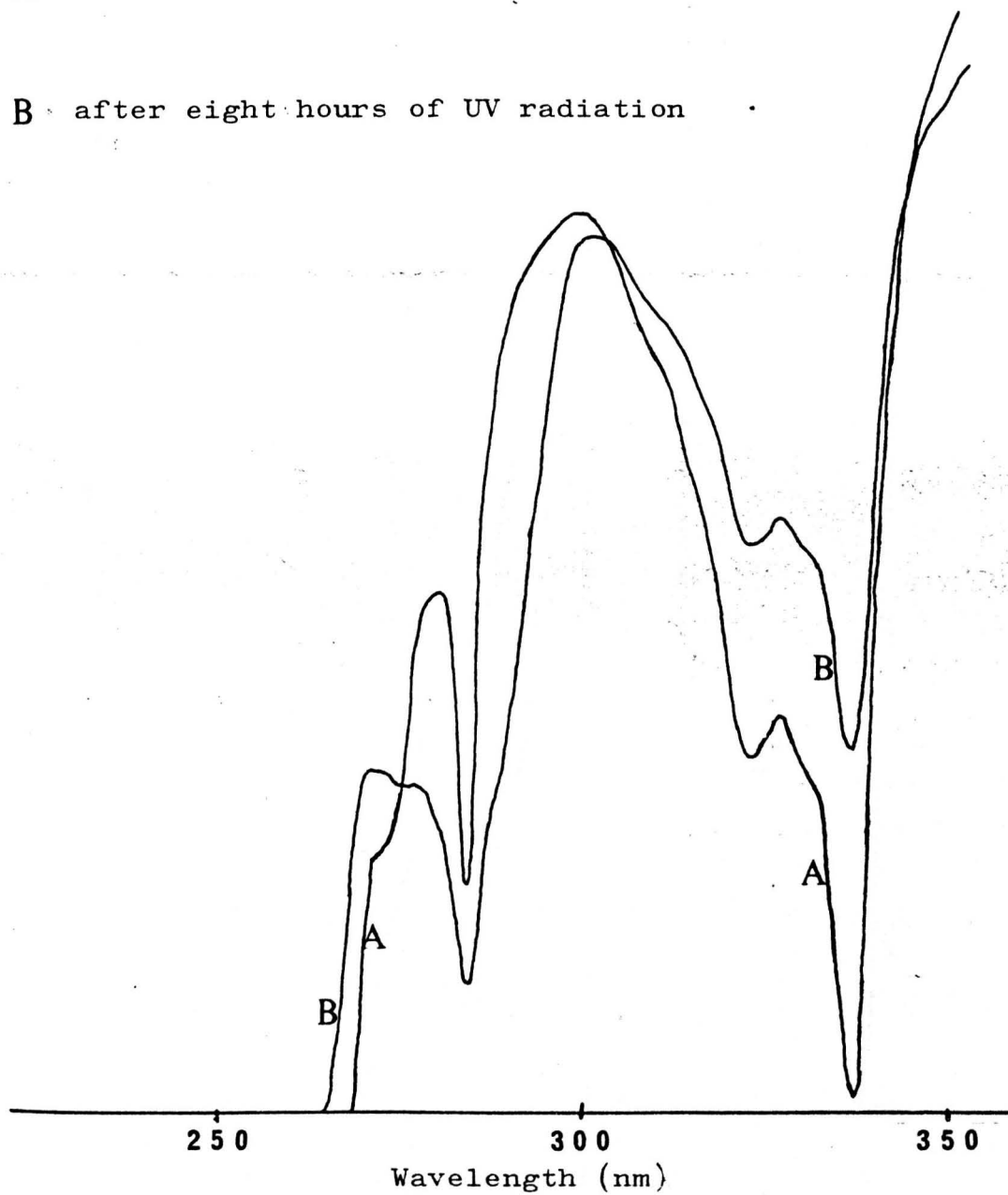
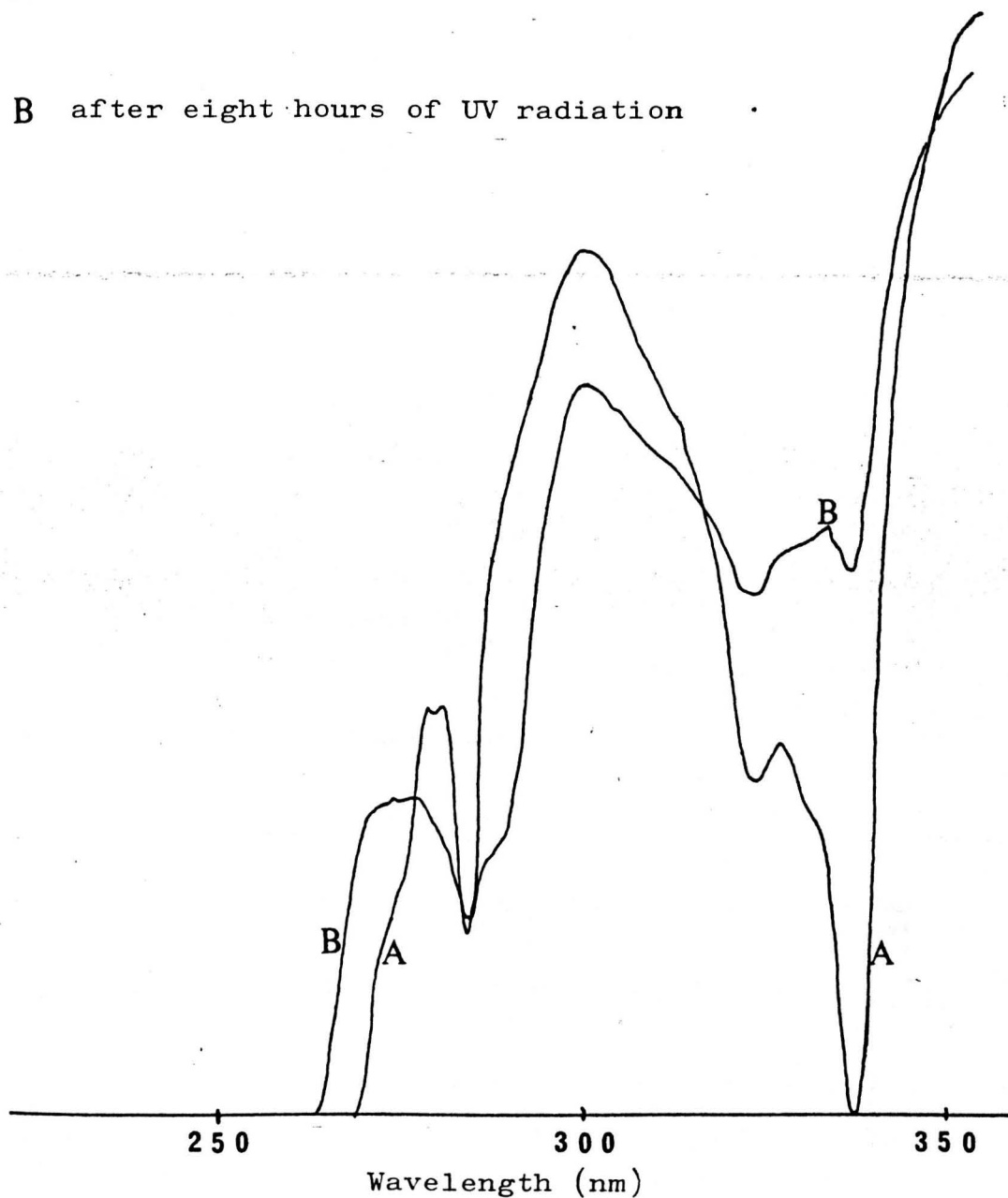


Fig. 2-24 Xanthone UV spectrum in trans 2-Octene

A before UV radiation

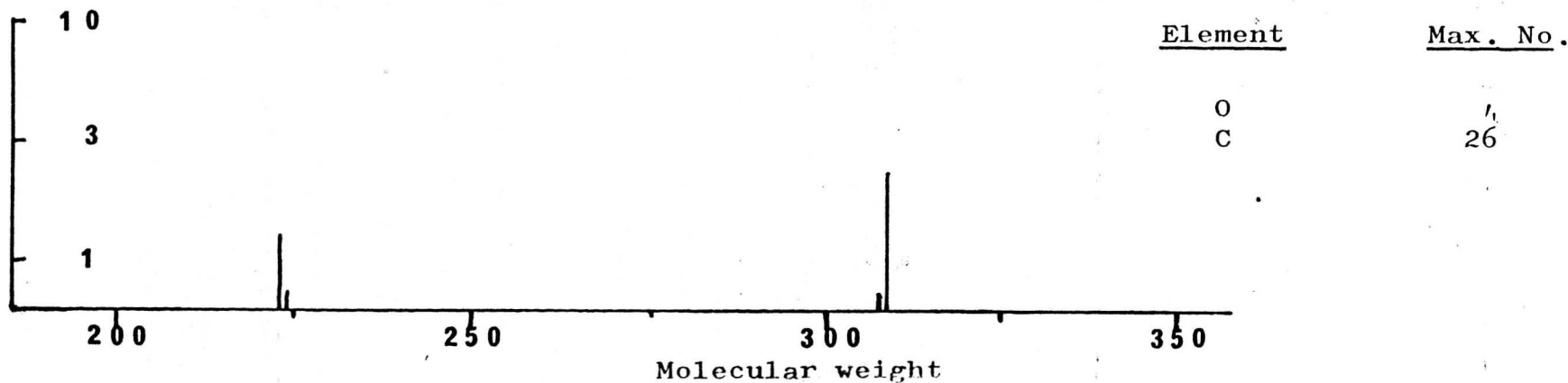
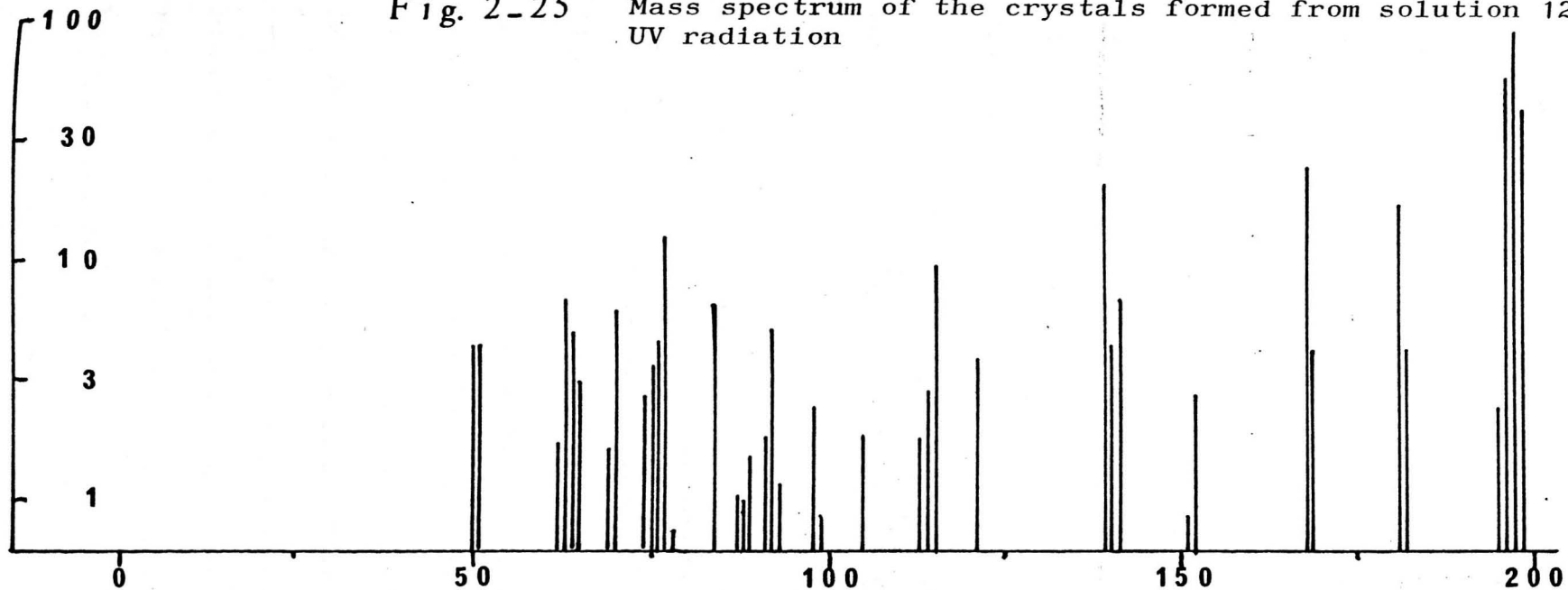
B after eight hours of UV radiation



Intensity

Fig. 2-25

Mass spectrum of the crystals formed from solution 12
UV radiation



CHAPTER 3

MODEL SYSTEM II, ALLYL ACETATE, XANTHONE AND HYDROCARBONS

3.1 Introduction

In the previous chapter, it has been shown that the C₈ dimer forms together with Poly(TAC). Due to the limitation of the analysis of Poly(TAC) using I.R. and elemental analysis, the nature of the grafting of hydrocarbon to the Poly(TAC) is still not very clear. It was thought however, to use a simple monomer with a monofunctional group which would be expected to have similar behaviour with any of the three allylic groups in the TAC.

Allyl acetate (AA) was used instead of TAC in the model system, in which crosslinking was not possible, since the product obtained would be easy to analyse. However, with AA, only low molecular weight polymer is formed as the polymerization tends to be terminated by reductive chain transfer which has been mentioned in Chapter 1.

AA was irradiated in the presence and in the absence of hydrocarbons using xanthone as the photoinitiator. The photoinitiation was also carried out in the presence and absence of air.

The order of the polymerization of AA in the presence of octane was meant to be established by irradiation at different concentrations of photoinitiator, hydrocarbon and AA.

The effect of polymerization at different temperatures was also studied.

3.2 Experimental

3.2.1 Materials

Octane and 1-Octene: These were the same as those used in chapter 2.

Allyl Acetate: This was supplied by Aldrich and it was used without any further purification.

Xanthone: This was used as photoinitiator, it was used after having been recrystallized in Chloroform.

Apparatus

A vacuum line was used for degassing in addition to another attachment which was used for the freeze and drying process as shown in Fig.3.1.

Two different dilatometers were used in this part of the work. The first type was as shown in Fig. 2.1. The second type was one which was modified to a different shape and then connected to a U.V. cell (0.1 cm path) to enable the measurements of U.V. spectrum throughout the irradiation process. Fig. 3.2 shows the modified dilatometer.

Two different water thermostat baths were used. One of these baths has already been mentioned in Chapter 2 and was used for vertical irradiation. The other water bath was placed in a glass container covered with a metal jacket. The samples were irradiated through a window in the side of the jacket. The second bath was used for horizontal irradiation where the modified dilatometer was used.

3.2.2 The irradiation of allyl acetate, xanthone and hydrocarbon for qualitative analysis

Five solutions were prepared using different concentrations of xanthone and by using octane and 1-octane. Two of these solutions were comprised of allyl acetate and xanthone alone in order that the comparison of Polyallyl acetate could be made with the products in which the hydrocarbons are incorporated.

TABLE 3.1

<u>Solution Ref. No.</u>	<u>Composition</u>	<u>Ratio of Composit.</u>	<u>Conc. of xanthone moles/litres</u>
16	Allyl acetate	-	$5.1 \times 10^{-5}M$
17	Allyl acetate: octane	1:1	$5.1 \times 10^{-5}M$
18	Allyl acetate	-	$1.3 \times 10^{-5}M$
19	Allyl acetate: octane	1:1	$1.3 \times 10^{-5}M$
20	Allyl acetate: 1-octene	1:1	$1.3 \times 10^{-5}M$

The above five solutions were UV irradiated for different times at 60°C. The distance between the UV lamp and the samples was 30 cm (1ft). Ten millilitres of sample were transferred to the dilatometers. The dilatometers were then connected to the vacuum line for degassing by freezing, degassing and heating up process, which was carried out in each case at least five times. The dilatometers were sealed after the degassing process and used for the irradiation experiment. The following table indicates the different radiation times for each of the five solutions.

TABLE 3.2

<u>Solution Ref. No.</u>	<u>Radiation Time (hrs)</u>
16.1	12
16.2	2 $\frac{1}{4}$
16.3	$\frac{1}{4}$ 8
17.1	12
17.2	2 $\frac{1}{4}$
17.3	$\frac{1}{4}$ 8
18.1	12
18.2	2 $\frac{1}{4}$
18.3	$\frac{1}{4}$ 8
19.1	12
19.2	2 $\frac{1}{4}$
19.3	$\frac{1}{4}$ 8
20.1	12
20.2	2 $\frac{1}{4}$
20.3	36
20.4	$\frac{1}{4}$ 8

As has been reported previously, allylacetate does not form a high molecular weight polymer. During the radiation, there was no change in the physical state of the solution. Even if there was a small change in the viscosity, there was no attempt to study the dilatometer measurements since the purpose for the above practice was purely qualitative. However, an attempt to separate the polymer formed was successful using the freeze and dry technique. The polymers formed from the above sample were separated by transferring 5 ml of the irradiated solution to a Q.F. round bottomed flask connected to the freeze and dry attachment in the vacuum line which was kept at liquid nitrogen temperature for five minutes. The line was then left under vacuum and allowed to warm to room temperature, while the unreacted allyl acetate and octane was collected in the trap. The polymer which remained in the round bottomed flask was washed several times with n-hexane, dried in a vacuum oven for 18 hours, and then analysed by N.M.R. Fig. (3.3-3.10) show the NMR spectra of the polymers formed in these cases.

A GPC analysis did not show any result as the polymers were of low molecular weight and out with the range of the column available.

The irradiated solutions 16 and 17 were analysed by GLC applying the same operating conditions mentioned

in section 2.2.3.4. The chromatograms for the bare solutions shown in Fig. 3.12, 3.13 and 3.14. Also by changing some of the above operating conditions, there was an attempt to calculate the amount of AA reacted in each case by measuring the concentration of unreacted AA using GLC quantitative technique. This attempt did not succeed because of the changes in concentration of allyl acetate was so minute. The allyl acetate GLC peak did not change significantly and consequently no concentration changes could be detected.

The concentration of the unreacted xanthone was measured for solution 18,19 and 20 by UV analysis as shown in table 3.3. A full quantitative analysis for this system will be studied in the following section.

TABLE 3.3

<u>Solution Ref. No.</u>	<u>Conc. of unreacted Xanthone Mole/Litre</u>
18	1.3×10^{-5}
18.1	7.33×10^{-6}
18.2	5.0×10^{-6}
18.3	2.1×10^{-6}
19	1.3×10^{-5}
19.1	2.9×10^{-6}
19.2	2.96×10^{-7}
19.3	1.77×10^{-7}
20	1.3×10^{-5}
20.1	3.66×10^{-6}
20.2	4.13×10^{-7}
20.3	4.13×10^{-7}
20.4	4.13×10^{-7}

3.2.3 Irradiation of Allyl Acetate, Xanthone and Octane for Quantitative Analysis

Photoinitiated polymerization of allyl acetate was studied quantitatively in the presence of octane and xanthone. The polymerization was studied by varying the concentration of allyl acetate, octane and xanthone in the solution. Eighteen solutions were prepared and polymerized in the modified dilatometer which allowed determination of the changes in concentration of the xanthone during irradiation. These changes were detected by measuring the UV spectra at different intervals of the photo-induced polymerization process in each individual solution. Solutions 21-38 were irradiated horizontally in the water bath through the window in the water bath.

Each of the 18 samples were irradiated in the water bath at 60°C after having been degassed on the vacuum line. During the irradiation process, U.V. spectra were obtained at certain intervals of the polymerization process. In the U.V. spectra measurements, the same relevant mole ratio of Allyl acetate and Octane was used in the reference cell.

Solution 28 was also degassed and irradiated at a lower temperature of 30°C.

Solution 27 was degassed and irradiated at a higher temperature of 90°C. Solution 27 was also irradiated on one occasion with the dilatometer sealed, without

degassing and the irradiation carried out at 60°C.

In all the above polymerization cases, the distance between the lamp and the dilatometer was 30 cm (1 ft). The following table shows the solutions with the conditions in which the irradiation was carried out.

TABLE 3.4: Conditions applied to the Individual U.V. irradiation processes

<u>Run No.</u>	<u>Solution No.</u>	<u>Allyl acetate/octane ratio in mole</u>	<u>Irradiation temp °C</u>	<u>Condition before sealing</u>
1	21	1:3	60	degassed
2	22	2:2	60	⋮
3	23	3:1	60	⋮
4	25	4:0	60	⋮
5	24	0:4	60	⋮
6	26	1:3	60	⋮
7	27	1:3	60	⋮
8	28	1:3	60	⋮
9	28	1:3	30	⋮
10	30	1:1	60	⋮
11	31	1:2	60	⋮
12	32	1:4	60	⋮
13	29	1:3	60	⋮
14	33	1:5	60	⋮
15	34	2:3	60	⋮
16	35	3:3	60	⋮
17	36	4:3	60	⋮
18	37	5:3	60	⋮
19	27	1:3	60	⋮
20	38	6:3	60	⋮
21	27	1:3	60	not degassed
22	27	1:3	90	degassed

TABLE 3.5: Xanthone Concentration throughout irradiation process (Run 1) for Solution 21.

<u>U.V.irradiation time (mins).</u>	<u>Conc. of Xanthone left in solution moles/litres</u>
0	2.26×10^{-6}
1	2.26×10^{-6}
2	2.25×10^{-6}
3	2.17×10^{-6}
4	2.16×10^{-6}
5	2.15×10^{-6}
7	2.08×10^{-6}
10	1.94×10^{-6}
15	1.68×10^{-6}
20	1.35×10^{-6}
25	1.09×10^{-6}
30	8.75×10^{-7}
40	4.61×10^{-7}
50	1.89×10^{-7}
60	7.09×10^{-8}
90	1.18×10^{-8}

TABLE 3.6: Xanthone concentration throughout irradiation process (Run 2) for Solution 22.

<u>U.V.irradiation time (mins).</u>	<u>Conc. of Xanthone left in solution moles/litres</u>
0	2.12×10^{-6}
1	2.12×10^{-6}
2	2.1×10^{-6}
3	2.1×10^{-6}
4	2.1×10^{-6}
5	2.09×10^{-6}
7	2.07×10^{-6}
10	2.01×10^{-6}
15	1.94×10^{-6}
20	1.82×10^{-6}
25	1.78×10^{-6}
30	1.68×10^{-6}
40	1.44×10^{-6}
50	1.2×10^{-6}
60	1.00×10^{-6}
75	7.21×10^{-7}
90	4.73×10^{-7}

TABLE 3.7: Xanthone Concentration throughout irradiation process (Run 3) for Solution 23.

<u>U.V. irradiation time (mins).</u>	<u>Conc. of Xanthone left in solution (moles/litres)</u>
0	2.22×10^{-6}
5	2.19×10^{-6}
10	2.15×10^{-6}
15	2.13×10^{-6}
20	2.08×10^{-6}
25	2.03×10^{-6}
30	1.99×10^{-6}
35	1.91×10^{-6}
40	1.88×10^{-6}
45	1.82×10^{-6}
50	1.76×10^{-6}
55	1.70×10^{-6}
60	1.63×10^{-6}
75	1.44×10^{-6}
90	1.28×10^{-6}
105	1.11×10^{-6}
120	9.57×10^{-7}
150	6.86×10^{-7}
180	4.73×10^{-7}
210	3.07×10^{-7}
270	1.42×10^{-7}
330	9.46×10^{-8}

TABLE 3.8: Xanthone concentration throughout irradiation process (Run 4) for solution 25.

<u>U.V. irradiation time (mins)</u>	<u>Conc. of Xanthone left in solution Moles/litres</u>
0	2.17×10^{-6}
5	2.17×10^{-6}
10	2.15×10^{-6}
15	2.15×10^{-6}
20	2.14×10^{-6}
25	2.13×10^{-6}
30	2.08×10^{-6}
35	2.08×10^{-6}
40	2.06×10^{-6}
45	2.03×10^{-6}
50	2.01×10^{-6}
55	1.99×10^{-6}
60	1.96×10^{-6}
75	1.91×10^{-6}
90	1.87×10^{-6}
120	1.73×10^{-6}
180	1.38×10^{-6}
240	1.15×10^{-6}
300	8.63×10^{-7}
360	6.86×10^{-7}
480	4.26×10^{-7}
600	2.72×10^{-7}

TABLE 3.9: Xanthone concentration throughout irradiation process (Run 5) for solution 24

<u>U.V. irradiation time (mins)</u>	<u>Conc. of Xanthone left in solution moles/litres</u>
0	2.26×10^{-6}
5	2.01×10^{-6}
10	1.56×10^{-6}
15	1.16×10^{-6}
20	7.68×10^{-7}
25	4.61×10^{-7}
30	2.36×10^{-7}
35	1.18×10^{-7}
40	2.36×10^{-8}
45	5.91×10^{-9}

TABLE 3.10: Xanthone concentration throughout irradiation process (Run 6) for solution 26

<u>U.V. irradiation time (mins)</u>	<u>Conc. of Xanthone left in solution moles/litres</u>
0	5.3×10^{-7}
5	4.26×10^{-7}
10	3.42×10^{-7}
15	2.48×10^{-7}
20	1.77×10^{-7}
25	1.3×10^{-7}
30	8.27×10^{-8}
45	3.55×10^{-8}
65	3.55×10^{-8}

TABLE 3.11: Xanthone concentration throughout irradiation process (Run 7) for solution 27.

<u>U.V. irradiation time (mins)</u>	<u>Conc. of xanthone left in solution moles/litres</u>
0	4.02×10^{-7}
5	2.96×10^{-7}
10	2.25×10^{-7}
15	1.65×10^{-7}
20	1.06×10^{-7}
25	5.9×10^{-8}
30	3.55×10^{-8}
40	1.18×10^{-8}

TABLE 3.12: Xanthone concentration throughout irradiation process (Run 8) for solution 28.

<u>U.V. irradiation time (mins)</u>	<u>Conc. of xanthone left in solution moles/litres</u>
0	2.48×10^{-7}
5	1.89×10^{-7}
10	1.42×10^{-7}
15	8.27×10^{-8}
20	4.73×10^{-8}
25	2.36×10^{-8}

TABLE 3.13: Xanthone concentration throughout irradiation process (Run 9) for solution 28.

0	2.60×10^{-7}
5	2.19×10^{-7}
10	1.54×10^{-7}
15	1.06×10^{-7}
20	7.09×10^{-8}
25	4.73×10^{-8}
30	3.55×10^{-8}

TABLE 3.14: Xanthone concentration throughout irradiation process (Run 10) for solution 30.

<u>time (mins)</u>	<u>Conc. (moles/litres)</u>
0	3.9×10^{-7}
5	3.66×10^{-7}
10	3.19×10^{-7}
15	2.84×10^{-7}
20	2.6×10^{-7}
25	2.25×10^{-7}
30	2.01×10^{-7}
35	1.66×10^{-7}

TABLE 3.15: Xanthone concentration throughout irradiation process (Run 11) for solution 31.

<u>time (mins)</u>	<u>Conc. (moles/litres)</u>
0	4.10×10^{-7}
5	3.61×10^{-7}
10	3.07×10^{-7}
15	2.48×10^{-7}
20	2.01×10^{-7}
25	1.54×10^{-7}
30	1.18×10^{-7}
35	8.27×10^{-8}

TABLE 3.16: Xanthone concentration throughout irradiation process (Run 12) for solution 32.

<u>time (mins)</u>	<u>Conc. (moles/litres)</u>
0	4.10×10^{-7}
5	3.19×10^{-7}
10	2.36×10^{-7}
15	1.6×10^{-7}
20	8.87×10^{-8}
25	4.73×10^{-8}

TABLE 3.17: Xanthone concentration throughout irradiation process (Run 14) for solution 33.

<u>time (mins)</u>	<u>Conc. (moles/litres)</u>
0	4.0×10^{-7}
5	2.72×10^{-7}
10	1.54×10^{-7}
15	7.09×10^{-8}
20	2.96×10^{-8}
25	1.18×10^{-8}

TABLE 3.18: Xanthone concentration throughout irradiation process (Run 15) for solution 34.

<u>time (mins)</u>	<u>Conc. (moles/litres)</u>
0	4.0×10^{-7}
5	3.45×10^{-7}
10	3.01×10^{-7}
15	2.6×10^{-7}
20	2.13×10^{-7}
25	1.65×10^{-7}
30	1.3×10^{-7}
35	1.0×10^{-7}
40	8.27×10^{-8}
45	5.9×10^{-8}

TABLE 3.19: Xanthone concentration throughout irradiation process (Run 16) for solution 35

<u>time (mins)</u>	<u>Conc. (moles/litres)</u>
0	4.1×10^{-7}
5	3.96×10^{-7}
10	3.6×10^{-7}
15	3.31×10^{-7}
20	2.96×10^{-7}
25	2.6×10^{-7}
30	2.25×10^{-7}
35	2.01×10^{-7}
40	1.65×10^{-7}
45	1.48×10^{-7}

TABLE 3.20: Xanthone concentration throughout irradiation process (Run 17) for solution 36

<u>time (mins)</u>	<u>Conc. (moles/litres)</u>
0	3.9×10^{-7}
5	3.55×10^{-7}
10	3.25×10^{-7}
15	3.01×10^{-7}
20	2.6×10^{-7}
25	2.36×10^{-7}
30	2.13×10^{-7}
35	1.89×10^{-7}
40	1.65×10^{-7}
45	1.42×10^{-7}

TABLE 3.21: Xanthone concentration throughout irradiation process (Run 18) for solution 37

<u>time (mins)</u>	<u>Conc. (moles/litres)</u>
0	3.9×10^{-7}
5	3.55×10^{-7}
10	3.43×10^{-7}
15	3.07×10^{-7}
20	2.72×10^{-7}
25	2.48×10^{-7}
30	2.25×10^{-7}
35	2.01×10^{-7}
40	1.77×10^{-7}
45	1.6×10^{-7}
50	1.48×10^{-7}

TABLE 3.22: Xanthone concentration throughout irradiation process (Run 19) for solution 27)

<u>time (mins)</u>	<u>Conc. (moles/litres)</u>
0	4.2×10^{-7}
5	3.31×10^{-7}
10	2.36×10^{-7}
15	1.65×10^{-7}
20	1.18×10^{-7}
25	8.27×10^{-8}

TABLE 3.23: Xanthone concentration throughout irradiation process (Run 20) for solution 38

<u>time (mins)</u>	<u>conc. (moles/litres)</u>
0	3.9×10^{-7}
5	3.55×10^{-7}
10	3.37×10^{-7}
15	3.19×10^{-7}
20	3.07×10^{-7}
25	2.9×10^{-7}
30	2.78×10^{-7}
35	2.6×10^{-7}
40	2.36×10^{-7}
45	2.25×10^{-7}
50	2.13×10^{-7}
55	2.01×10^{-7}
60	1.89×10^{-7}

TABLE 3.24: Xanthone concentration throughout irradiation process (Run 21) for solution 27

<u>time (mins)</u>	<u>conc. (moles/litres)</u>
0	4.2×10^{-7}
5	4.08×10^{-7}
10	3.91×10^{-7}
15	3.66×10^{-7}
20	3.43×10^{-7}
25	3.25×10^{-7}
30	3.08×10^{-7}
35	2.78×10^{-7}
40	2.60×10^{-7}
50	1.95×10^{-7}
55	1.65×10^{-7}
60	1.54×10^{-7}

TABLE 3.25: Xanthone concentration throughout irradiation process (Run 22) Solution 27

<u>time (mins)</u>	<u>Conc. (moles/litres)</u>
0	4.2×10^{-7}
5	2.84×10^{-7}
10	2.13×10^{-7}
15	1.77×10^{-7}
20	1.30×10^{-7}
25	1.18×10^{-7}
30	9.47×10^{-8}

3.3 Discussion

3.3.1 Discussion based on the N.M.R. qualitative results

The spectrum of NMR analysis for solutions 18, 19 and 20 together with allyl acetate spectrum are shown in (3.3 - 3.10).

The NMR peaks shown in Fig. 3.4 and Fig. 3.5 are due to the polyallyl acetates formed from irradiating solution 18. The individual peaks may be illustrated as follows.

Peak (i)	6.1 T	Proton resonances due to	O-CH ₂
Peak (ii)	7.9 T	'	CH ₃ -C(=O)-
Peak (iii)	8.7 T	'	-C-CH ₂ -C-

The NMR peaks shown in Fig. 3.5 have an additional peak at 8.2 T. This peak may be due to the proton resonance of $\left(\begin{array}{c} \text{H} \\ | \\ \text{C} - \text{C} \\ | \quad | \\ \text{R} \quad \text{H} \end{array} \right)_n$.

The NMR peaks shown in Fig. 3.6 and 3.7 are due to the poly allyl acetate formed from irradiating solution 19, which contains octane in addition to allyl acetate. The individual peaks could be due to the following.

Peak (i)	6.1 T	Proton resonances due to	$-O-CH_2$
Peak (ii)	7.9 T	'	$\begin{array}{c} O \\ \\ CH_3-C- \\ \\ H \end{array}$
Peak (iii)	8.2 T	'	$\begin{array}{c} (C-C)_n \\ \quad \\ R \quad \end{array}$
Peak (iv)	8.7 T	'	$\begin{array}{c} -C-CH_2-C- \\ \quad \quad \\ CH_3 \quad \quad \end{array}$
Peak (v)	9.1 T	'	$\begin{array}{c} CH_3-C-C- \\ \quad \quad \end{array}$

Fig. 3.8, 3.9 and 3.10 shows the NMR spectrum of poly allyl acetate formed from irradiating solution 20, which also contains 1-octene in addition to the allyl acetate. The peaks appeared to be the same as those shown in Fig. 3.6 and 3.7 with the exception of a slight shift of peak (iii), and higher intensity of peak (iv).

In all of the NMR spectra, discussed above, there were a series of peaks which appeared in the region of 2.1 T. These are possibly due to the aromatic hydrogen resonances, which are due to some traces of the unreacted xanthone. However, the NMR spectrum of the xanthone, which is shown in Fig 3.11 has its main peaks in the region of 2.4 T.

From the spectra it is shown that there are traces of unreacted xanthone even in the polymer. However this will not interfere with our analysis since the peaks

representing the polymer will be based mainly in a different part of the spectrum. Even if these peaks are due to xanthone derivatives, then the NMR peaks will still be outside the region in which our interpretation is based.

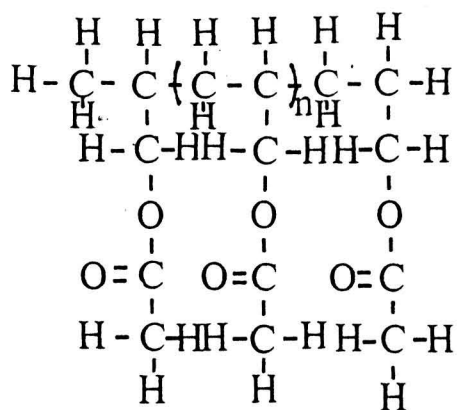
The obvious difference between the NMR spectrum discussed is the appearance of peak (v) in the spectra shown in 3.6, 3.7, 3.8, 3.9 and 3.10. These spectra are due to the product formed from the polymerization of allylacetate in the presence of either octane and 1-octene and that of the photoinitiator.

Peak (v) in the above mentioned spectrum is possibly due to the protons from the methyl groups attached at the end of the hydrocarbon chains, i.e. $(\text{CH}_3 - \underset{\text{|}}{\overset{\text{|}}{\text{C}}} - \text{R})$.

This means, that in the polymers formed in the case of polymerizing solutions 19 and 20, a hydrocarbon chain is attached to the main chain of the allyl acetate polymer, since no such chain could be formed if only the allyl acetate is polymerized.

As no other explanation could be given as to the presence of such a peak at 9.1T, therefore, the following structures of the polymers formed in the individual cases maybe sketched.

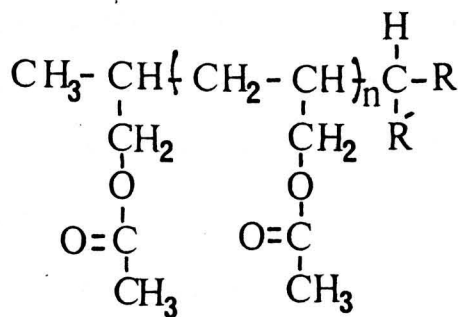
The formation of poly allyl acetate by irradiating solution 18, which was predicted, will have the following structure (I).



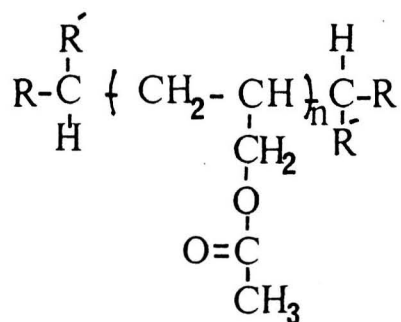
(I)

n : will have a very low value which will be discussed later in this section.

Poly allyl acetate copolymer with hydrocarbon, formed from solution 19 and 20, has been concluded from the above discussion and will possibly have the following structures (II) and (III)



(II)



(III)

R'-C-R Octane molecule where [C] could be in any position between carbon No.2 - Carbon No.7. The above three structures will fit, individually, to the N.M.R. spectrum obtained.

The mechanism for the above polymerization and copolymerisation will be sketched at the end of this section.

3.3.2 Discussion based on the GLC qualitative results

The GLC chromatograms obtained for solutions 16 and 17 before and after irradiation, are shown in Fig. 3.12 3.13 and 3.14.

Fig. 3.13, which is the GLC chromatogram for allyl acetate solution after irradiation in the presence of xanthone, shows that even after 12 and 24 hours irradiation, there was no change or no appearance of significant new peaks. This, however, does not mean that no polymer was formed. After 48 hours a new peak

was observed at a retention time of about 15 minutes. There was an attempt to separate this compound by GLC but nothing was achieved from it. Fig. 3.14 shows the GLC chromatogram for allyl acetate/octane solution after irradiation in the presence of xanthone.

Small numbers of dimer peaks were observed in the GLC chromatogram. The peaks were of the same nature as in the case of Octane/TAC/xanthone and also Octane/xanthone solutions (Fig. 2.6 and 2.11). This indicates that most of the hydrocarbon free radicals formed during the irradiation were either terminated or reacted with the allyl acetate rather than dimerised. Also in Fig. 3.14, it shows that after 2 $\frac{1}{2}$ and 1 $\frac{1}{8}$ hours of irradiation the polymer formed, presumably with low molecular weight and significantly the peaks are observed due to the formation.

3.3.3 Discussion based on the U.V. quantitative results

It was desirable, however, to study the kinetics of polymerization of allyl acetate and allyl acetate/octane solutions in the presence of xanthone. To achieve this task, a few complications may be involved, these factors are due to the formation of degradative chain transfer which will cause the low conversion of polymer throughout the polymerization process, as has previously been reported. The chain transfer was also expected due to the presence of solvent.

This low conversion of polymer will cause difficulties in following the rate of polymerization by a common method such as the change in volume which may be followed by the dilatometer technique. However, our aim is to study the effect of allyl acetate in the photoinitiation process, which in turn will give us a picture of what the process would be in the presence of triallyl cyanurate. Although it is not possible to say that the allyl acetate will act exactly as one of the allyl groups in the TAC, both allylic groups will have some common features, such as the weak allylic hydrogen.

To follow the photoinitiation process, the decomposition of xanthone will be studied quantitatively by UV. As has been discussed in the previous chapter, the efficiency of xanthone to initiate a reaction in the presence of unsaturated hydrocarbon was low, as the energy transfer from xanthone excited states was quite clear.

From fig. 3.15 and 3.16, the rate of xanthone decomposition was different in the allyl acetate and octane solutions which were irradiated in the presence of xanthone of initial concentrations about 2.2×10^{-6} moles/litres. It appears that the decomposition of xanthone was low (4.5×10^{-9} moles/litre⁻¹mins⁻¹) in the case of allyl acetate solution. Whereas in the case of the octane solution, the xanthone rate of decomposition was 6.67×10^{-8} moles l⁻¹min⁻¹. In the former, it means

that most of the xanthone will be activated by UV light and form its excited state which will eventually reform. This will be the main process, whereas the secondary, slower one will be the decomposition which will be due to the hydrogen abstraction from the media by the activated state of xanthone. The hydrogen abstraction process from the media (allyl acetate) will lead to the formation of allyl acetate free radicals which will be followed by the reduction of xanthone to one of xanthone derivatives, in addition to the polymerization of the allyl acetate.

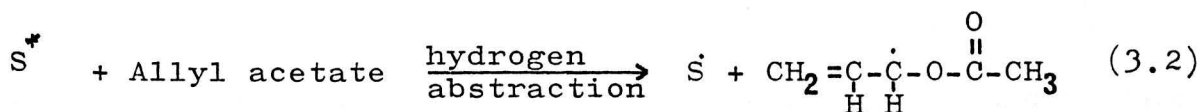
The most obvious xanthone derivatives will be either the formation of dihydroxy dixanthene, due to the dimerization of xanthinol free radical, or the formation of xanthinol with the corresponding solvent molecules (in this case allyl acetate) fragment in the 9-C position due to the combination of xanthinol radical and allyl acetate radical.

The former possibility will be overruled in this case since no dixanthene crystals appeared in the irradiated solutions. This indicates that most of the xanthinol radicals will form the corresponding xanthene with allyl acetate.

This postulation is supported by Figs. 3.17 and 3.18 which show the UV spectra of allyl acetate solutions during different periods of UV irradiation. New UV peaks at 290 nm and 320 nm will gradually appear during the

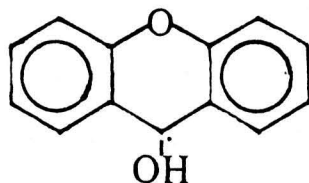
course of irradiation, which are due to xanthene derivatives (1).

The hydrogen abstraction by xanthone in the activated state will probably cause the formation of the stable degradative free radical monomer. It will be most probable to abstract the weakest hydrogen present, i.e. the allylic hydrogen. To put the photoinitiation process (the slow process) in the case of allyl acetate solution, in terms of a chemical equation, the following scheme maybe drawn out.



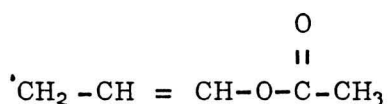
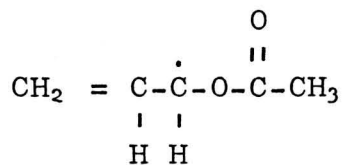
here S^* is the xanthone excited state

$S\dot{}$ xanthinol free radical (IV)



(IV)

The allyl acetate free radical formed in equation 3.2 is the degradative type free radical (2,3,4), which is a stable radical due to the resonances.

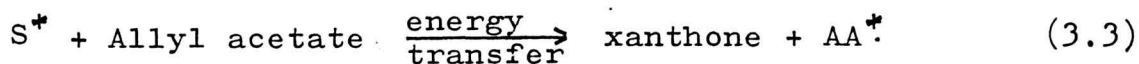


The formation of such a free radical centre will obviously not lead to a high conversion of monomer. However, the main process in this case which causes the reformation of xanthone may well be the process which will cause further polymerization. The reformation of xanthone may be due to two different processes:-

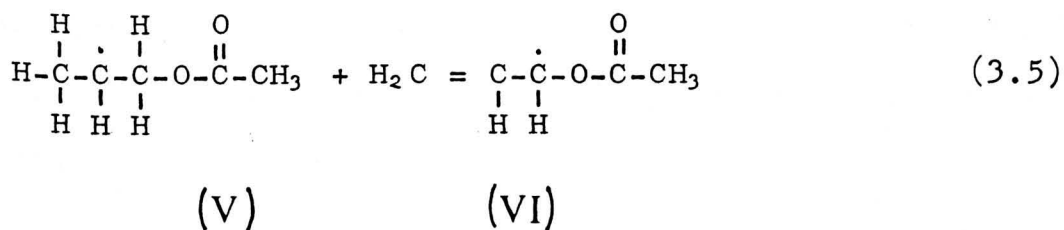
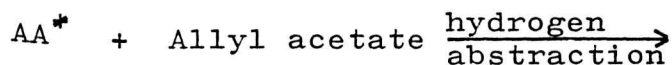
1. The energy transfer from xanthone excited state to the media molecule, i.e. Allyl acetate, caused by the collision between the two, which is similar to what has been suggested in section 2.3.
2. The xanthinol free radical IV which was formed from the reaction 3.2 will possibly initiate due to the transfer of a hydrogen atom from the xanthinol free radical to allyl acetate monomer. Such an assumption has been put forward by Braun (5) in the case of semipinacol radicals and has not been completely excluded as a possibility by Hutchinson (6).

Looking at the first possibility, the xanthone will act as a photosensitizer rather than that of a photoinitiator. The initiation could be drawn out as follows:-

followed by step 3.1

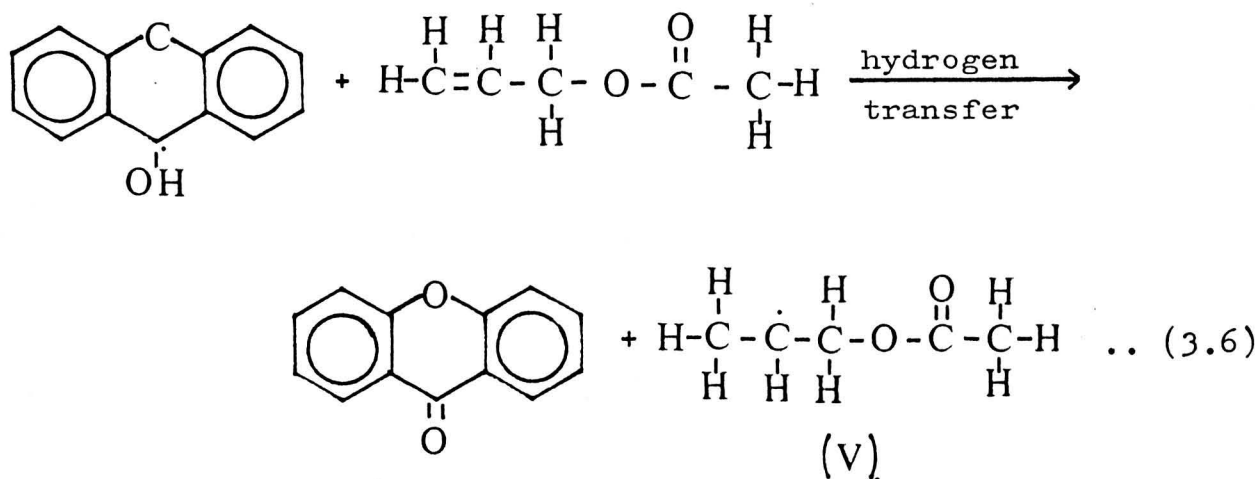


or



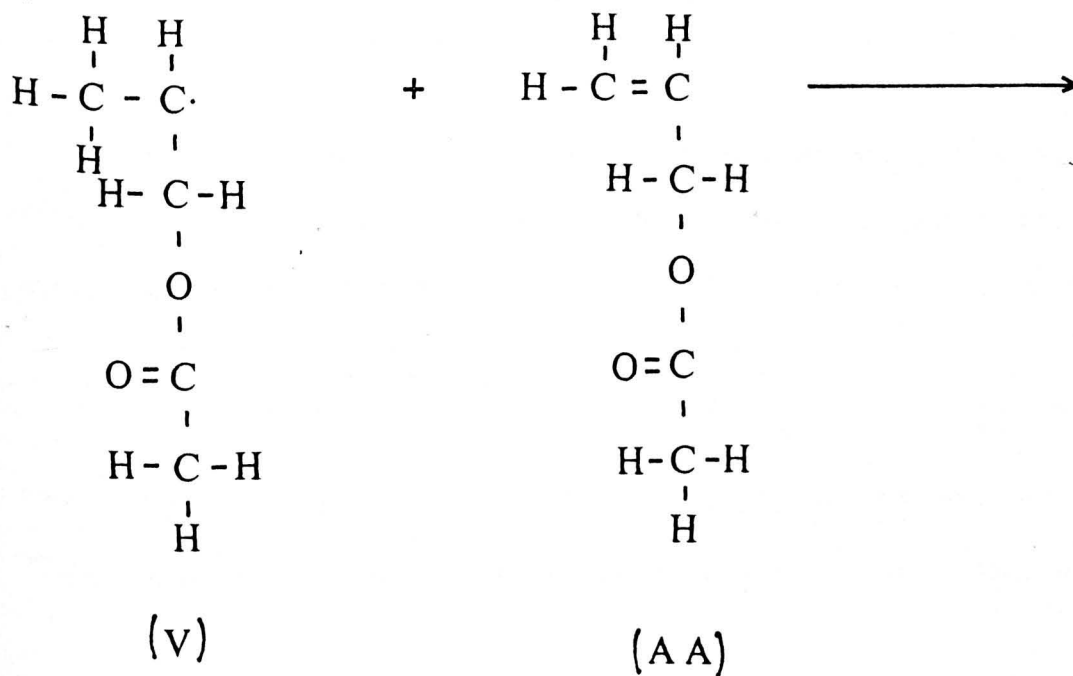
AA* is allyl acetate activated state.

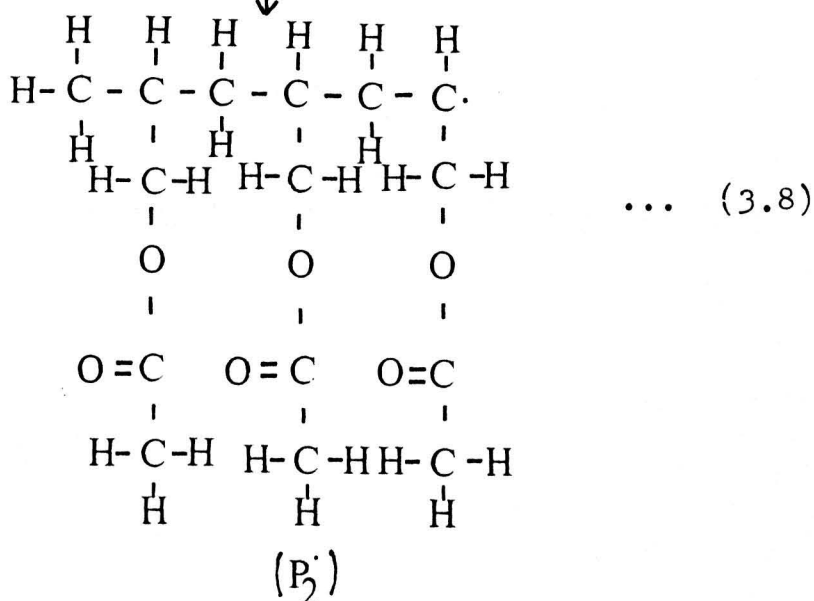
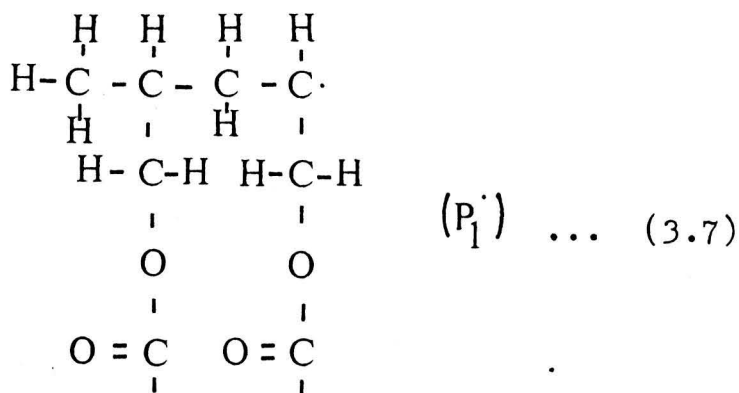
Where the first free radical (V) from step 3.5 will propagate to form a polymer chain, as the second free radical (VI) is the degradative type. The initiation process due to assumption No.2 may drawn as follows:-



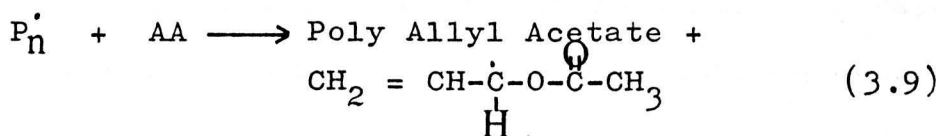
The allyl free radical formed from step 3.6 could propagate and form the polymer chain.

From our experimental data, it seems possible that the propagation could be followed after either step 3.5 or 3.6, whereas the xanthene derivatives formation will be followed after step 3.2. This will be a slow process since the rate of decomposition of xanthone in the case of allyl acetate is very slow. Propagation steps could be drawn out as follows:-



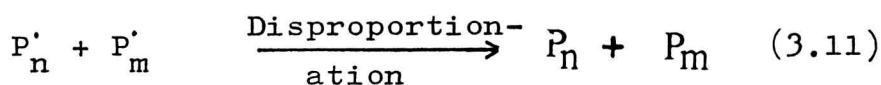
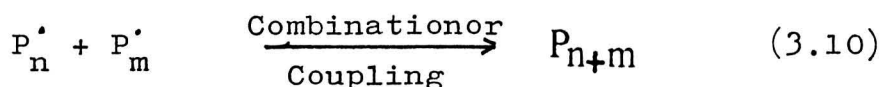


The propagation process will not go very far to form high molecular weight polymers, due to the chain transfer process (2, 3, 4)



The polymer formed may possibly contain as little as three monomer units. (7) The termination process, which is

probably due to the combination of the two chain radicals or to the disproportionation, may be drawn out as follows:-



where P_{n+m} , P_n and P_m are poly allyl acetate of different molecular weight.

In the case of the allyl acetate solution mixed with octane, the rate of the xanthone decomposition was as follows (values obtained from Fig. 3.15-3.16).

TABLE: 3.26 Xanthone Rate of Decomposition

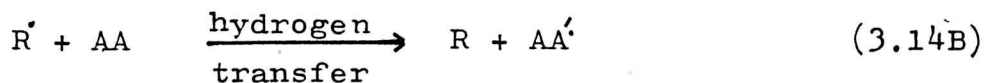
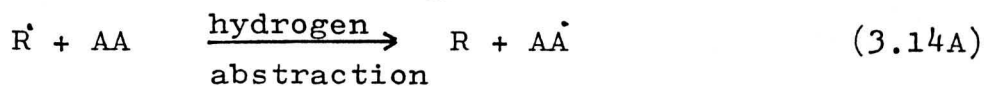
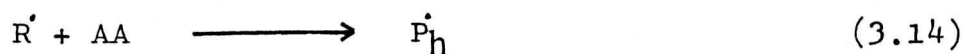
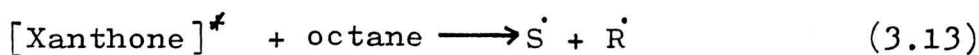
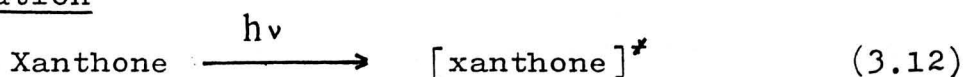
<u>Allyl acetate: Octane</u> <u>ratio in moles</u>	<u>Rate of decomposition</u> <u>moles/litres⁻¹ min⁻¹</u>
0:4	6.67 x 10 ⁻⁸
1:3	5.0 x 10 ⁻⁸
2:2	2.0 x 10 ⁻⁸
3:1	1.08 x 10 ⁻⁸
4:0	4.5 x 10 ⁻⁹

It is quite clear that the higher the octane ratio, the faster the rate of decomposition. This indicates that the xanthone activated state will abstract hydrogen from the octane and form an octane free radical. The reaction steps for the above reaction were written in section 2.3.

This observation obviously indicates that the xanthone, which is available to initiate allyl acetate directly will be less and therefore more of the octane free radical will react with the allyl acetate .

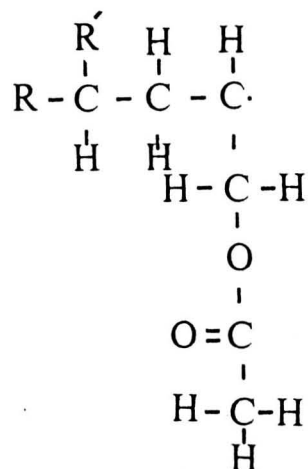
The higher the content of octane present, the more chance of xanthone's activated states molecules colliding and interacting with octane, which will then form xanthinol radicals and octane radicals. The octane radical will then initiate the allyl acetate and form a polymer chain radical. This is in turn followed by propagation, chain transfer and termination steps. The following scheme for allyl acetate/octane solution in the presence of xanthone may be drawn out. This will be consistent with the experimental observations and also with previous, similar work done with benzo phenone ([1]).

Initiation



where

P_h^\cdot represent



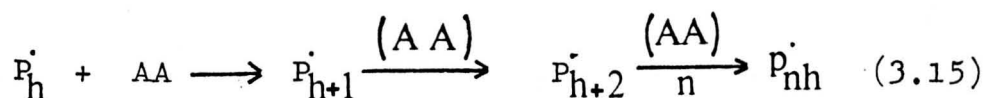
S^\cdot : xanthinol radical as (IV)

R^\cdot : octane free radical [Carbon No.2]
will be the possible location for the free radical centre]

AA^\cdot : from step 3.14A represent the allyl acetate degradative radical as (VI).

AA^\cdot : from step 3.14B represent the allyl acetate free radical as (V).

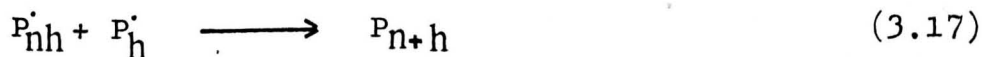
Propagation



degradative chain transfer



termination



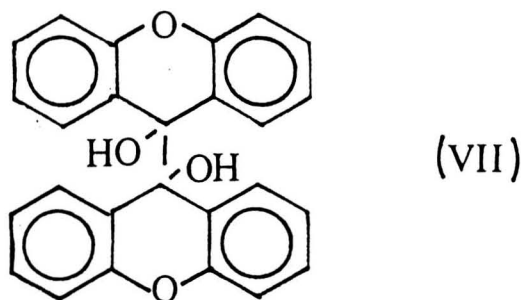
where P_{nh} represents poly allyl acetate copolymer

as (II)

P_{n+h} represents poly allyl acetate copolymer

as (III)

S-S : dihydroxy dixanthene



R-R: branched hydrocarbon dimer (C_{16})

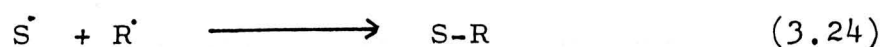
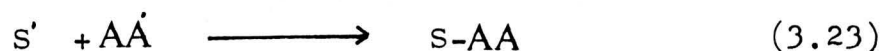
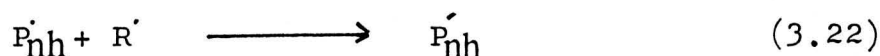
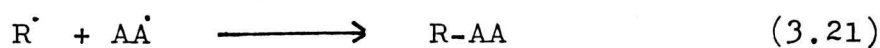
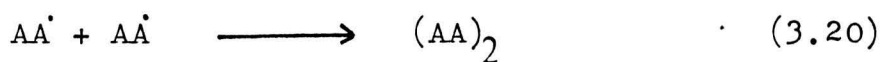
The initiation step 3.14 will be considered to be the main one. The initiation step 3.14A will cause the formation of the degradative type of free radical. The initiation step 3.14B will be possible. However, if we consider step 3.14B to be the main step of initiation, the polymer chain will not be the type of copolymer with hydrocarbon and hence will contradict our conclusions from section 3.3.1 which are based on the N.M.R. results. From the conclusions drawn from section 3.3.1, the polymers formed from allyl acetate/octane solutions contain a hydrocarbon chain.

However, our suggestion that the hydrocarbon will be added to the allyl acetate and initiate the polymer chain, is supported by other work done by Lewis and Mayo⁽⁸⁾, in which case the allylic monomers are initiated

by chloroform and carbon tetrachloride addition.

In addition to the termination steps 3.17, 3.18 and 3.19, other termination steps may possibly take place in which polymer chains and hydrocarbon radicals are involved.

The degradative allyl radical can react with another degradative allyl radical, with a hydrocarbon radical or with xanthinol radical. The other termination steps may be drawn out as follows:-

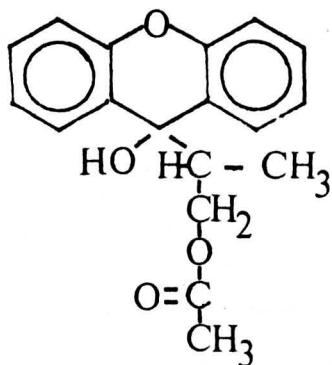


where $(AA)_2$ is allyl acetate dimer

R-AA: Octane/allyl acetate molecules combined together.

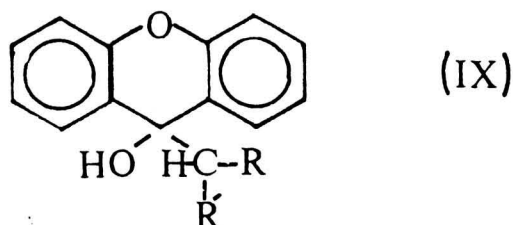
P_{nh} : polymer with a structure similar to III

S-AA: Xanthene derivative



(VIII)

S-R: Xanthene derivative with octane molecule
in 9-C position.



The xanthene product from step 3.23 and dixanthene from step 3.18 will be the main xanthene derivatives in the case of allyl acetate/octane irradiation.

Dihydroxy dixanthene, which usually separates and appears in the solution as fine crystals, was not observed in the allyl acetate/octane solutions of even ratios or with higher allyl acetate content. However, dixanthene was observed with irradiated solutions which contain much higher concentration of octane than allyl acetate e.g. solutions 32, 33.

In the case of the allyl acetate/1-octene solutions, no crystals were observed which means that the xanthene was mainly the xanthidrol fragment with monomer solvent molecules in the 9-C position. The xanthene derivatives formed in allyl acetate/octane and allyl acetate/1-octene solutions are shown in the U.V. spectrum in Fig. 3.19, 3.20 and 3.21 in which the original 280 nm peak shifts to 290 nm due to the xanthene product.

From Fig. 3.22, it appeared that even in the allyl acetate/1-octene solution, xanthone will decompose at a faster rate than in allyl acetate solution.

Therefore one would expect that in the case of allyl acetate/1-octene solution, the initiation of allyl acetate will take place indirectly through the addition of 1-octene radicals. This will cause the formation of poly allyl acetate with hydrocarbon incorporated in the structure.

This above statement is consistent with conclusions drawn in section 3.3.1. However, there are other factors which may effect the polymerization, e.g. the weak allylic hydrogen in 1-octene as well as allyl acetate together with the possible energy transfer which will take place from xanthone-excited state to 1-octene.

Fig. 3.23 and 3.24 show the effect of rate of xanthone decomposition with different ratios of allyl acetate and octane in solution:

It is obvious that the rate of decomposition increases as the octane ratio increases in the solution.

As shown from Fig. 3.26, the rate of decomposition of xanthone has an index of [0.6] in reference to the octane present in the irradiated solution, whereas the decomposition rate has a negative index of [0.38] in reference to allyl acetate present in the irradiated solution as shown in Fig. 3.27. This in fact will

verify the assumption that with higher octane present in the solution, there will be a higher probability of hydrogen abstraction from octane by the xanthone activated state. Therefore, in turn the octane free radical will form and initiate the allyl acetate polymerization.

Fig. 3.25 shows that the higher the initial xanthone concentration present, the faster the rate of decomposition with an index of [1.29] depending on the xanthone, as shown in Fig. 3.28. This in fact indicates that with a high amount of xanthone present there will be more of the photoinitiator free radical present in the solution, which means that even a lower molecular weight polymer is produced. In addition, the high amount of xanthone concentration will not be a favourable thing to work with, since it will cause a skin effect because of its high extinction coefficient.

From Fig. 3.29, it appears that the rate of xanthone decomposition is hardly effected when the temperature of the media changes from 30-60°C. The value of decomposition could be the same allowing for experimental error. The same is shown in Fig. 3.30 where the rate of decomposition has not been affected by changing the media temperature from 60 to 90°C. Again the rate of decomposition values are almost the same considering the experimental error.

Runs 19 and 21 are shown from table 3.4 were different due to the fact that one run was degassed, the other run was not degassed before UV irradiation.

It appears that the rate of decomposition will slow down from 1.6×10^{-8} moles liter $^{-1}$ min $^{-1}$ to 2.0×10^{-9} moles $^{-1}$ min as shown in Fig. 3.31. This is due to the fact that in the case of the undegassed sample, the oxygen will act as quencher with energy values for the excited states of [$E_S = 22.5$ kcal/mole and $E_T = 102$ kcal/mole]⁽⁹⁾.

Different mechanisms were suggested for the quenching process by oxygen⁽¹⁰⁾ in which they all agree that the oxygen acts as a quencher and forms peroxides and hydroperoxides and due to this process the photosensitizer will reform.

Finally in the case of the octane solution, irradiated in the presence of xanthone by U.V. light, Fig. 3.32 shows the U.V. spectrum of the xanthone present in solution during the course of irradiation. This gives a clearer picture of the formation of the new peak at 290 nm and the disappearance of the 280 nm peak. As mentioned in section 2.3, this is due to the fact the xanthone will be reduced to a xanthene derivative; which in the case of the octane solution, the dihydroxy dixanthene will be formed which in turn will be separated from the solution in the form of fine crystals.

The crystals were identified in section 2.3 and their N.M.R. spectrum shown in Fig. 3.33. This agrees with the Zanker conclusion (1) as stated in section 2.3. This

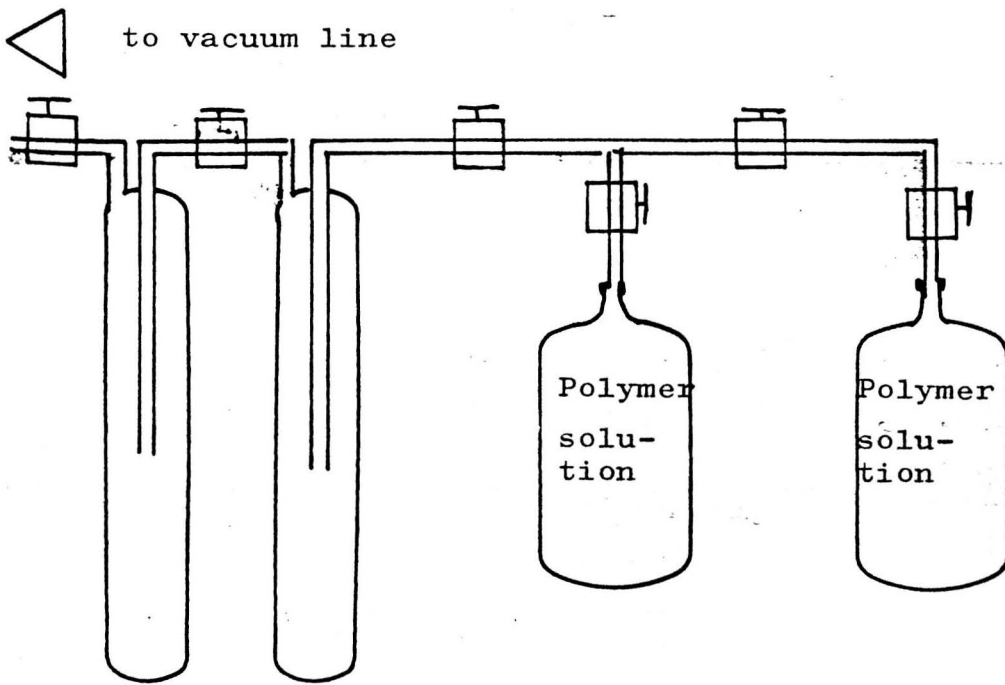
also agrees with the Hammond ⁽¹¹⁾ et al. conclusion, which was based on the semipinacol radicals. These were found to recombine and form the dimer in the presence of purely alkane solvents. The product differs in different solvents used, as the process seems to be controlled by diffusion in the different media.

The discussion in section 2.3 and 3.3 will be used in the following chapter to get an improved understanding of the crosslinking mechanism for low density polyethylene by U.V. light in the presence of xanthone and TAC.

References

1. Zanker, V., Ehrhardt, E., Bull of Chem. Soc. Japan 1694, (1966).
2. Bartlett, P.D., et al. J. Amer. Chem. Soc. 67, 812, 816 (1945).
3. Litt, M., Eirich, F.R., J. of Pol. Sci., pp379-396 (1960).
4. Gaylord, N.G. J. Poly. Sci., 22, 71, (1956).
5. Braun, D., et al. Makromol. Chem. 6, 186 (1969).
6. Hutchison, J., et al. Polymer 14, 250 (1973).
7. Ham, G.E. Vinyl Polymerization Vol. I Part 1, Marcel Dekker Inc., (1967).
8. Mayo, F.R., Lewis, M. J. Amer. Chem. Soc. 76, 457, (1954).
9. Murov, S.L. Handbook of Photochemistry, Marcel Dekker (1973).
10. Kan, R.O. Organic Photochemistry, McGraw-Hill (1966).
11. Hammond, G.S., et al. IUPAC XXIIrd Congress, Boston (1971) Vol 4, p257. Butterworth, London (1971).
12. Cookson, R.C. Quant. Rew., 22, 423, (1968).

Fig. 3-1 Freeze and drying process attachment to the vacuum line



Nitrogen Traps

Fig. 3-2 The modified dilatometer with UV cell attachment

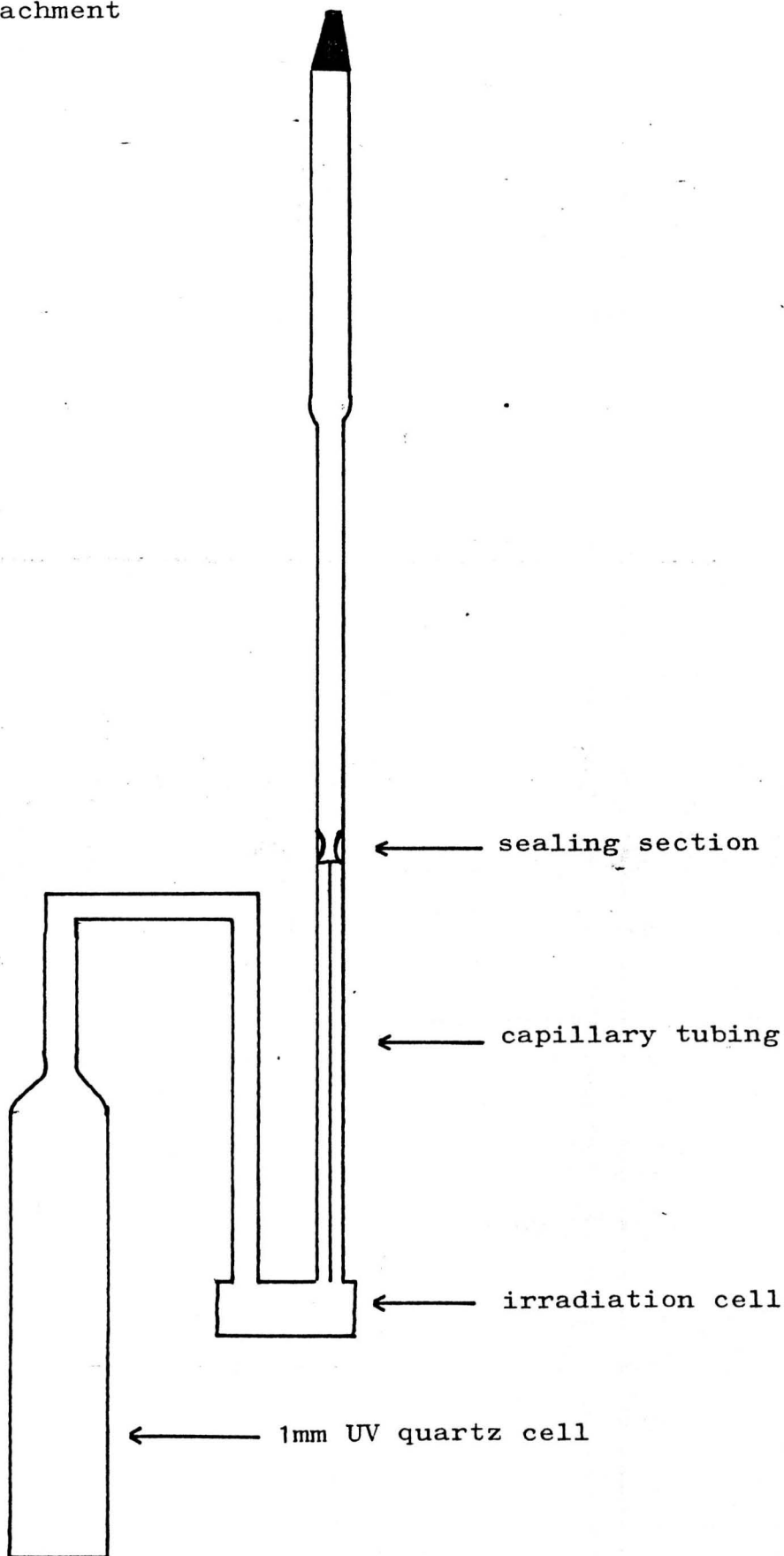
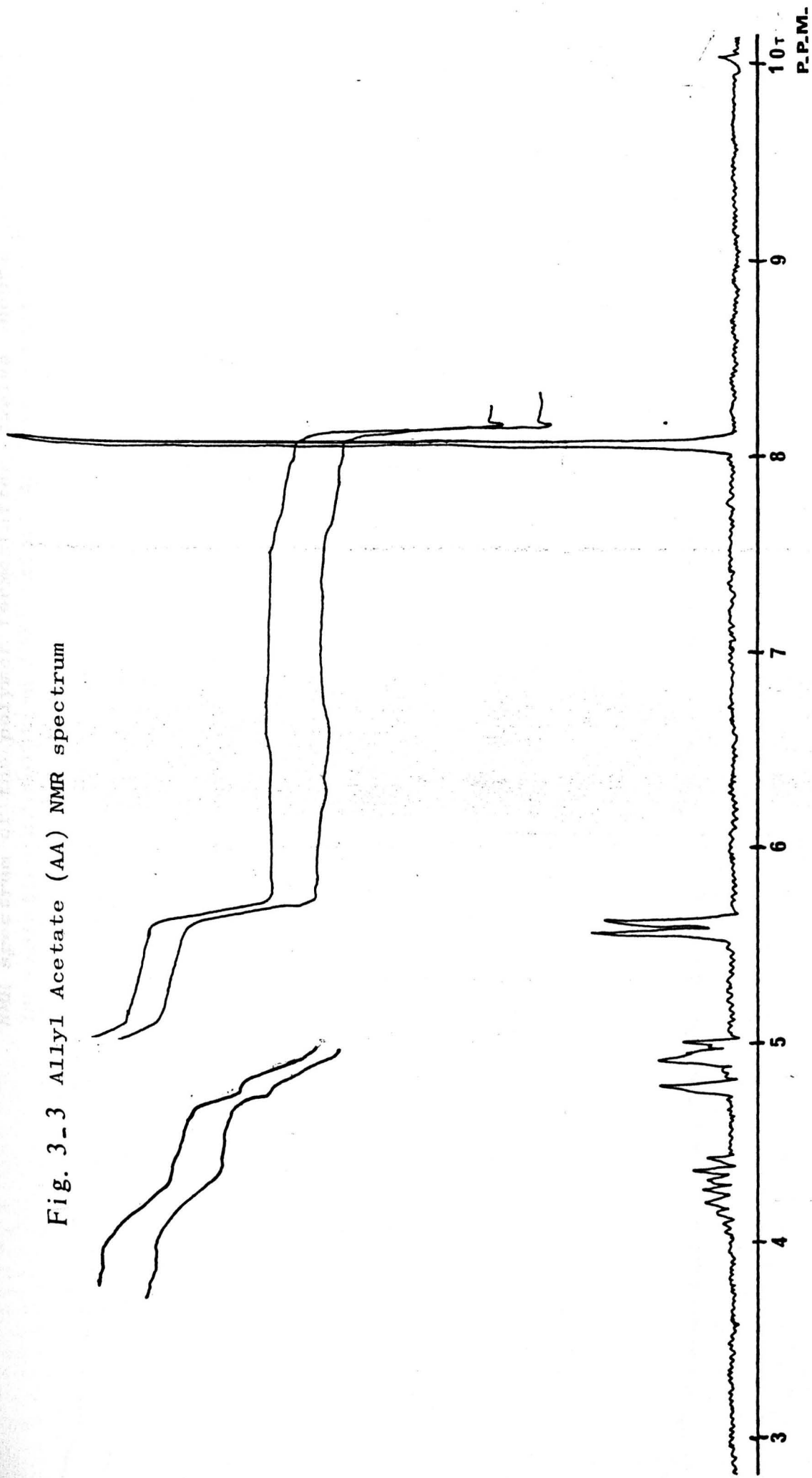


Fig. 3-3 Allyl Acetate (AA) NMR spectrum



NMR spectrum of the polymer formed after twelve hours
UV radiation of solution (18) "Allyl Acetate + Xanthone"

Fig. 3-4

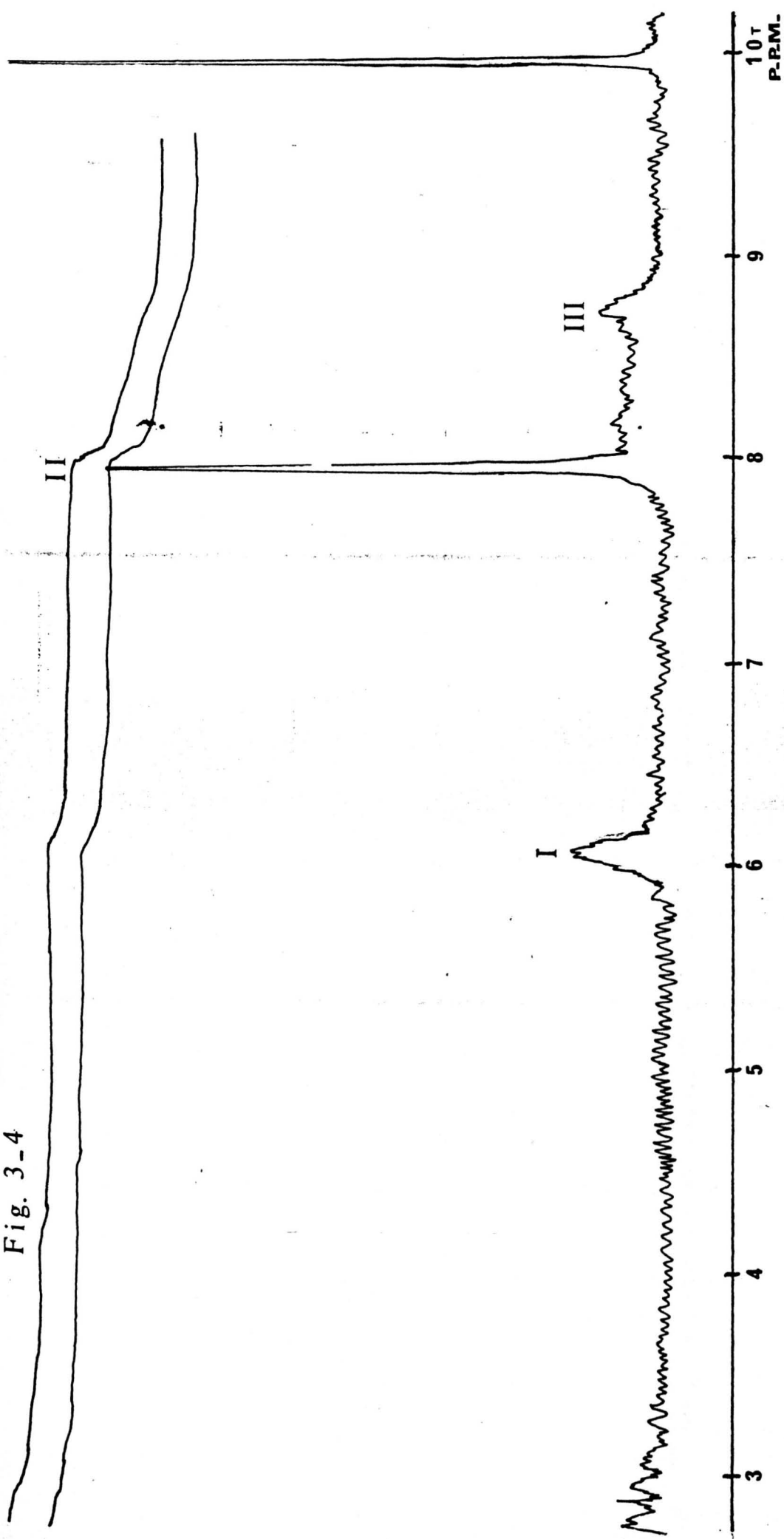


Fig. 3-5 NMR spectrum of the polymer formed after fortyeight hours UV radiation of solution (18) "Allyl Acetate + Xanthone"

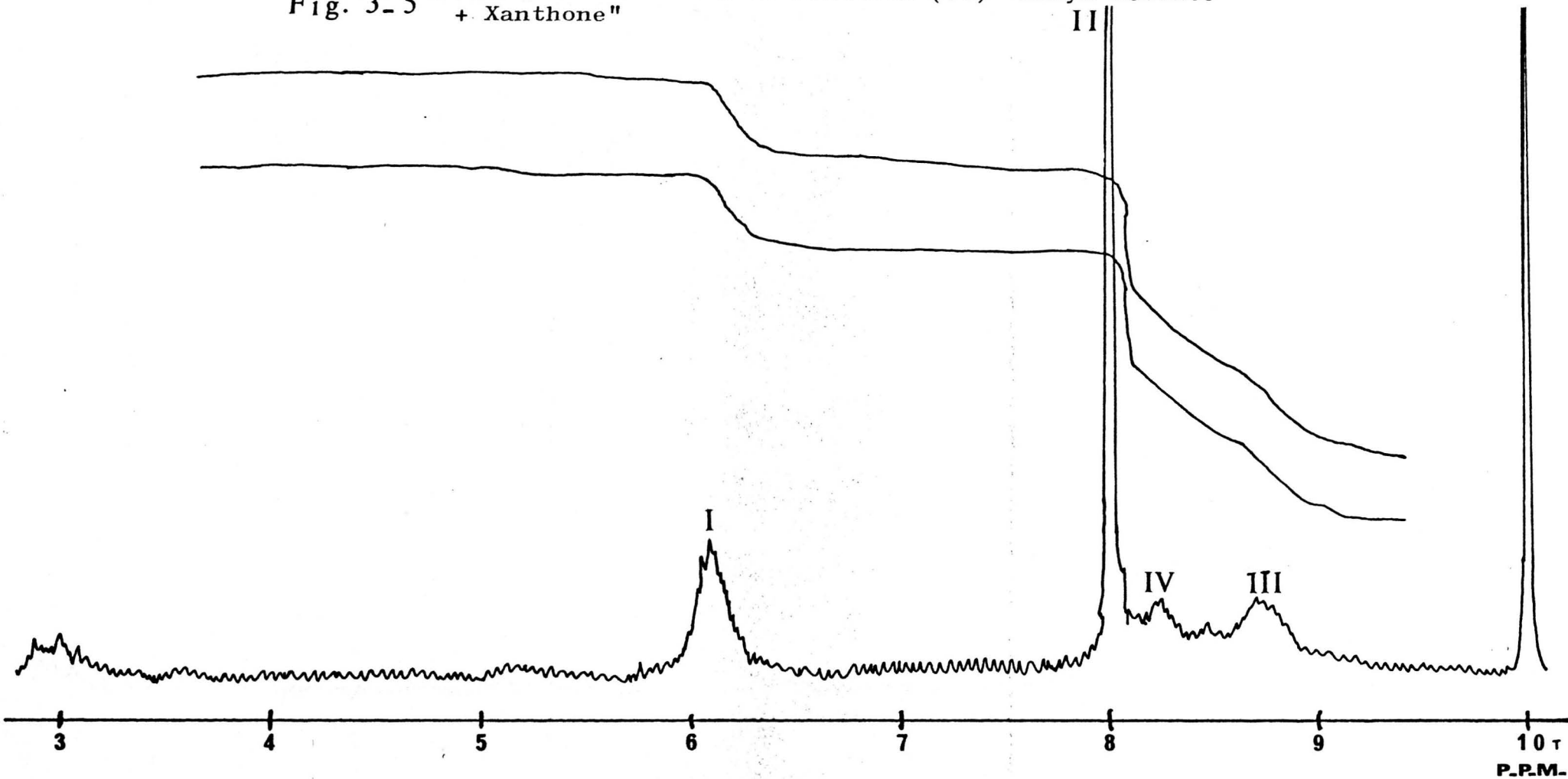
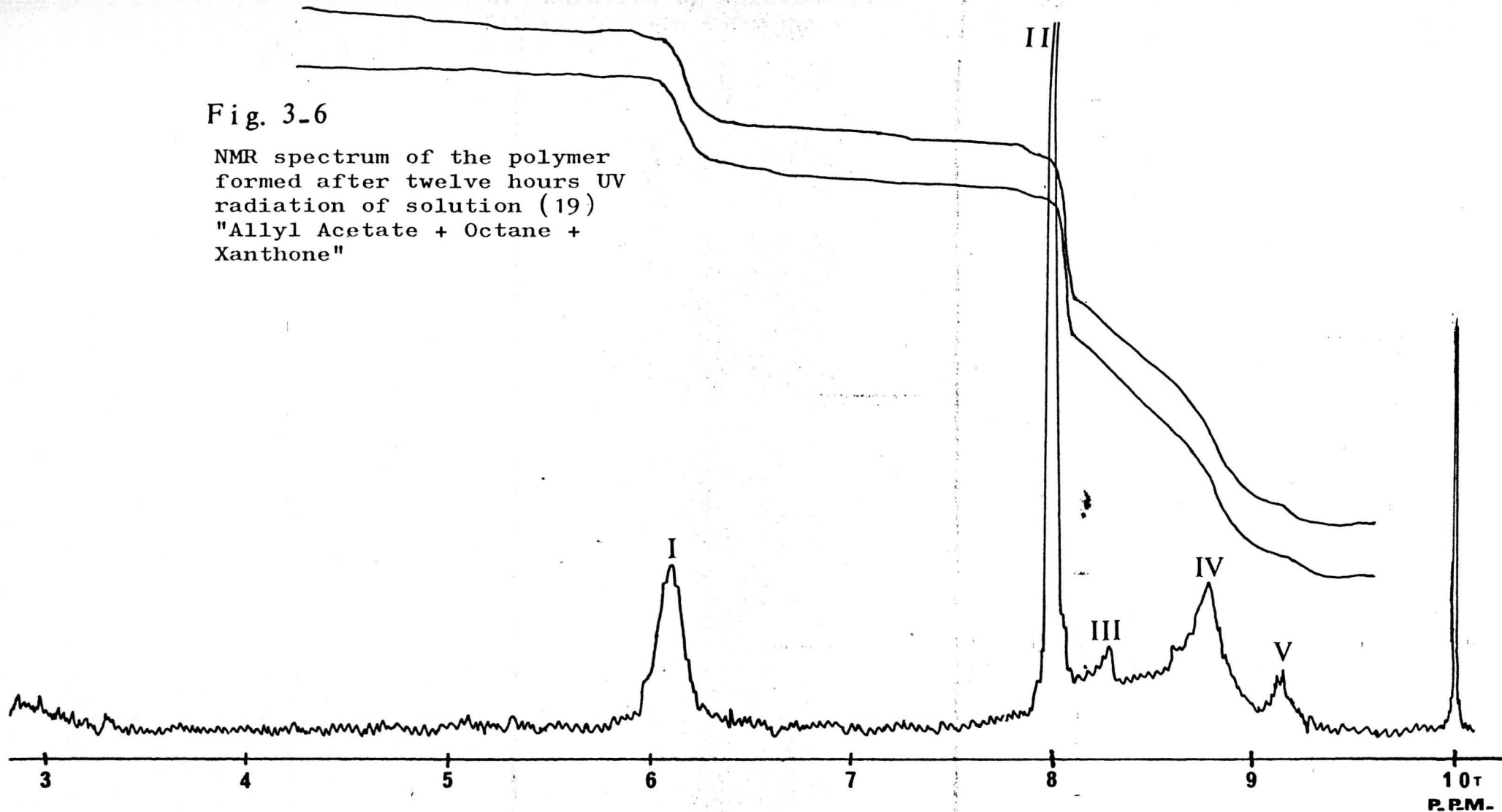


Fig. 3-6

NMR spectrum of the polymer
formed after twelve hours UV
radiation of solution (19)
"Allyl Acetate + Octane +
Xanthone"



NMR spectrum of the polymer
formed after fortyeight hours
UV radiation of solution (19)
"Allyl Acetate + Octane +
Xanthone"

Fig. 3-7

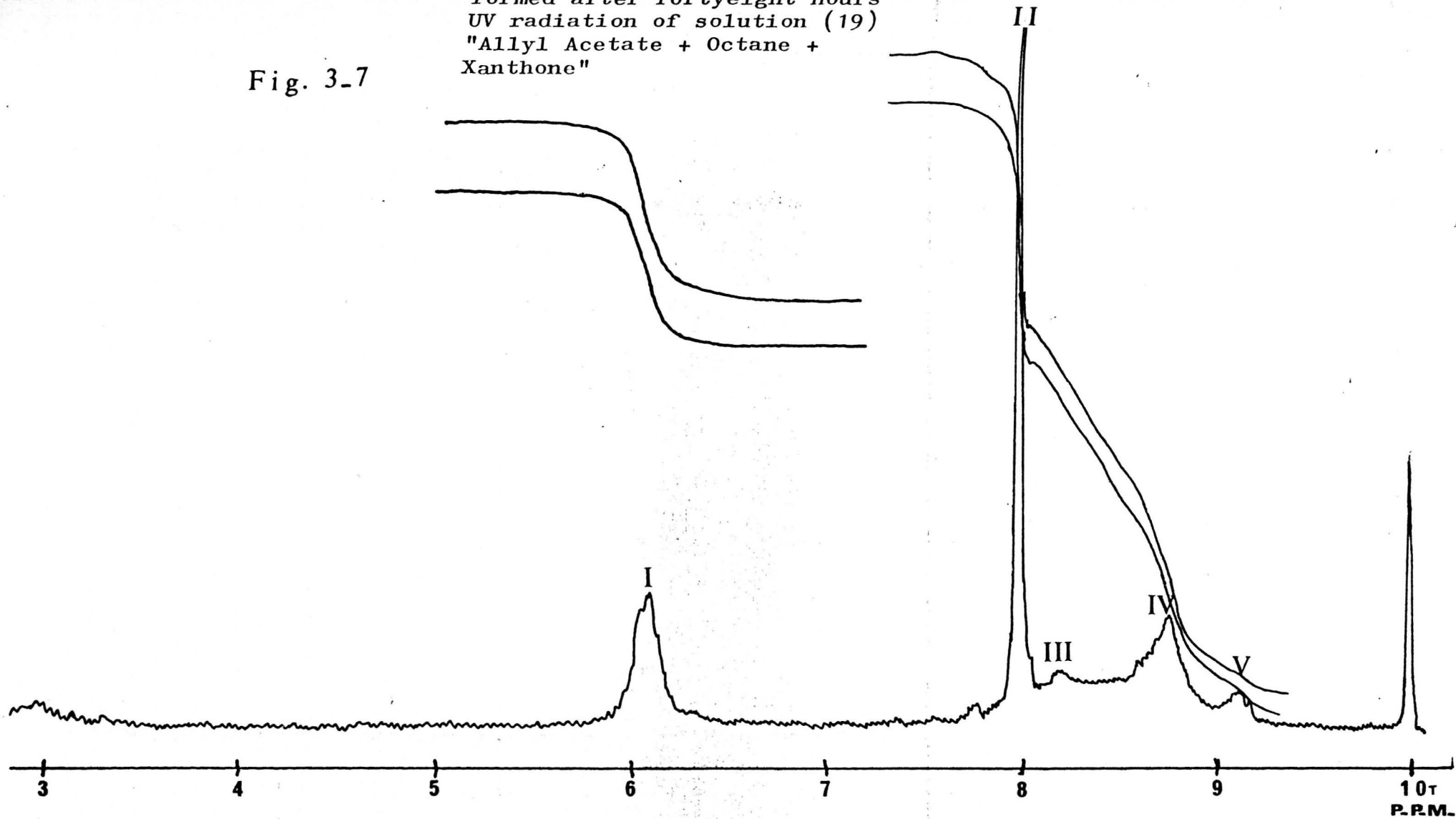


Fig. 3-8

NMR spectrum of the polymer which
was formed after twelve hours UV
radiation of solution (20)
"Allyl acetate + 1-Octene +
Xanthone"

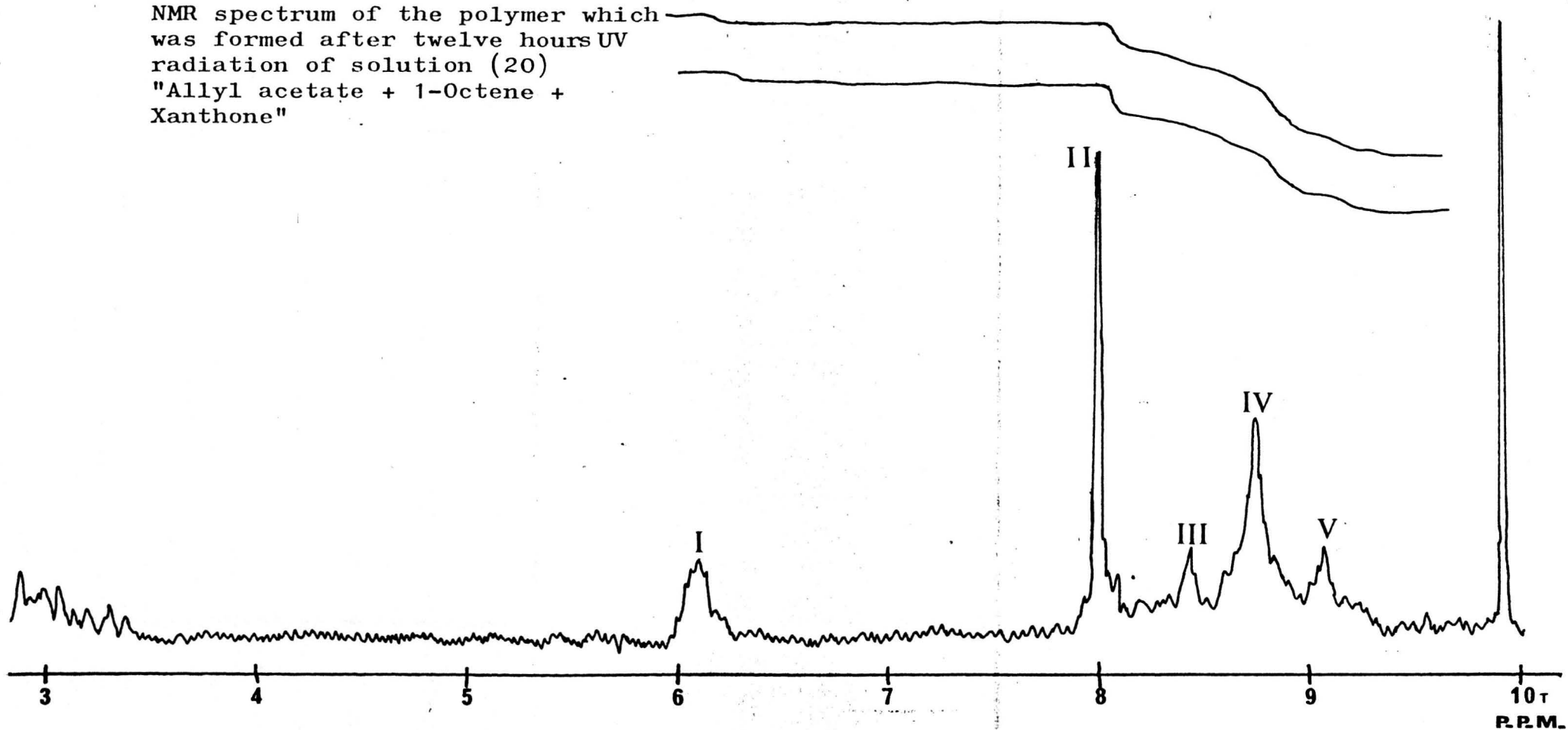


Fig. 3-9

NMR spectrum of the polymer
which was formed after twenty
four hours UV radiation of
solution (20) "Allyl acetate
+ 1-Octene + Xanthone"

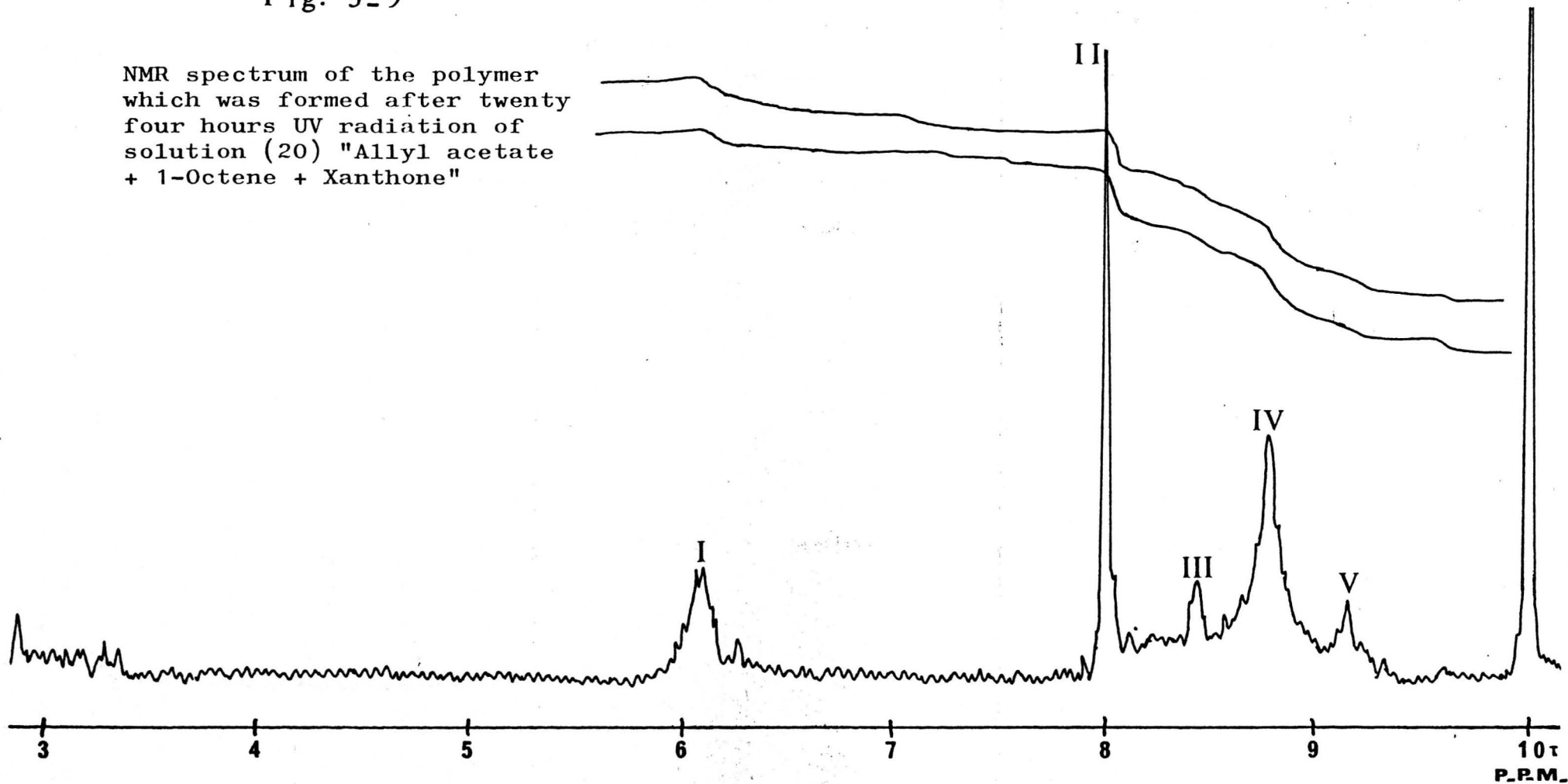


Fig. 3-10

NMR spectrum of the polymer which
was formed after fortyeight hours
UV radiation of solution (20)
"Allyl Acetate + 1-Octene + Xanthone"

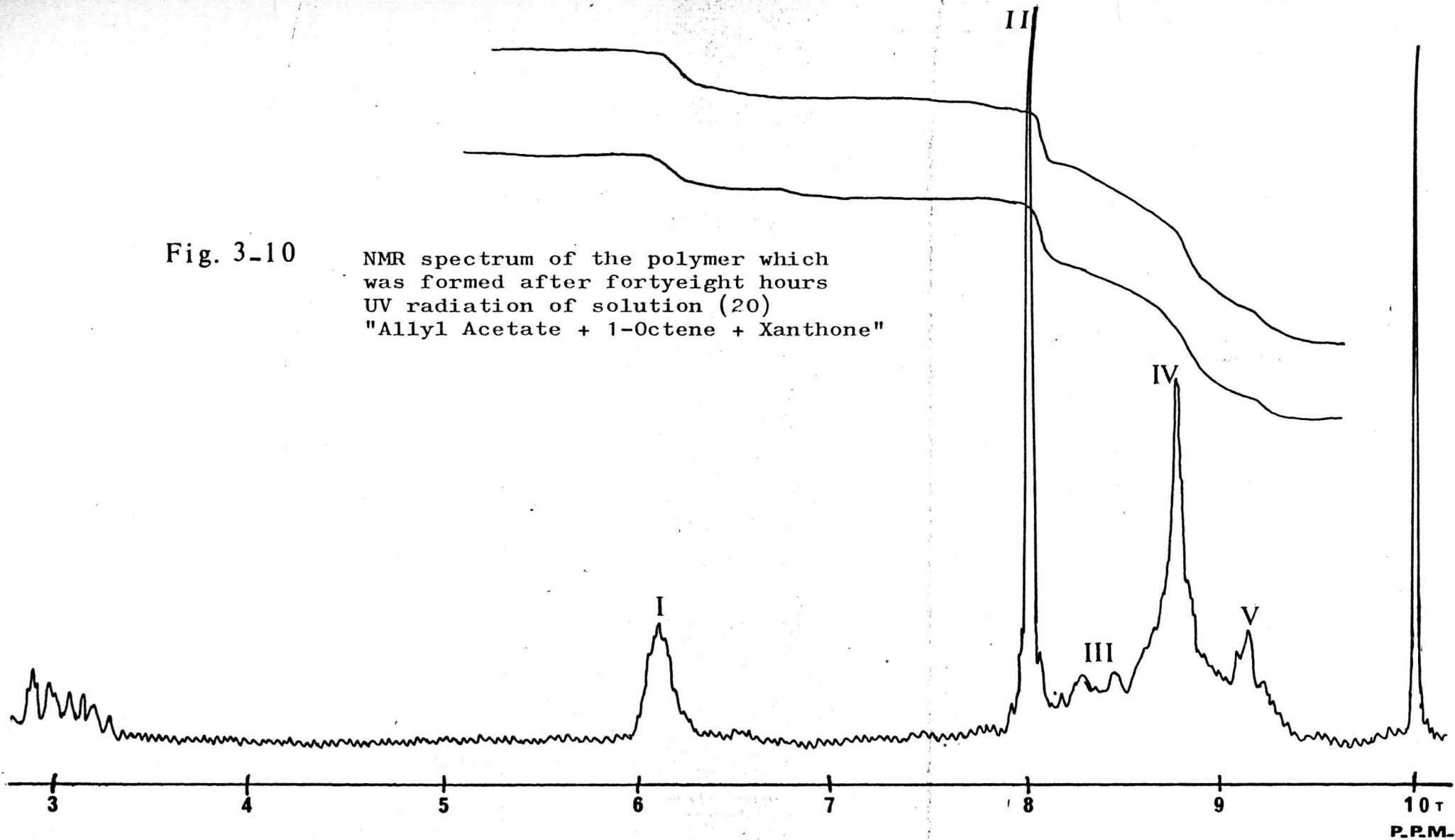


Fig. 3-11 TAC and Xanthone NMR spectra

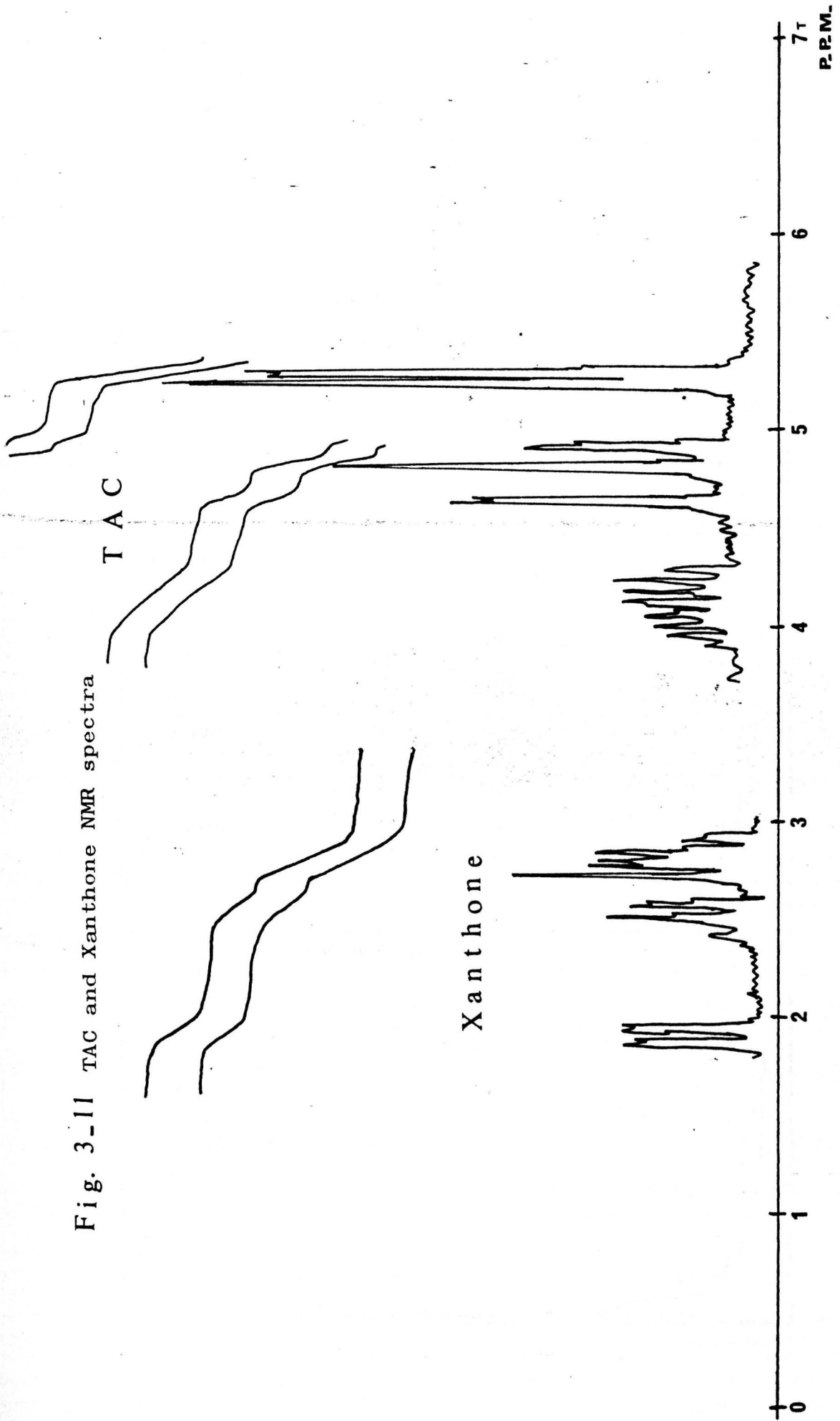
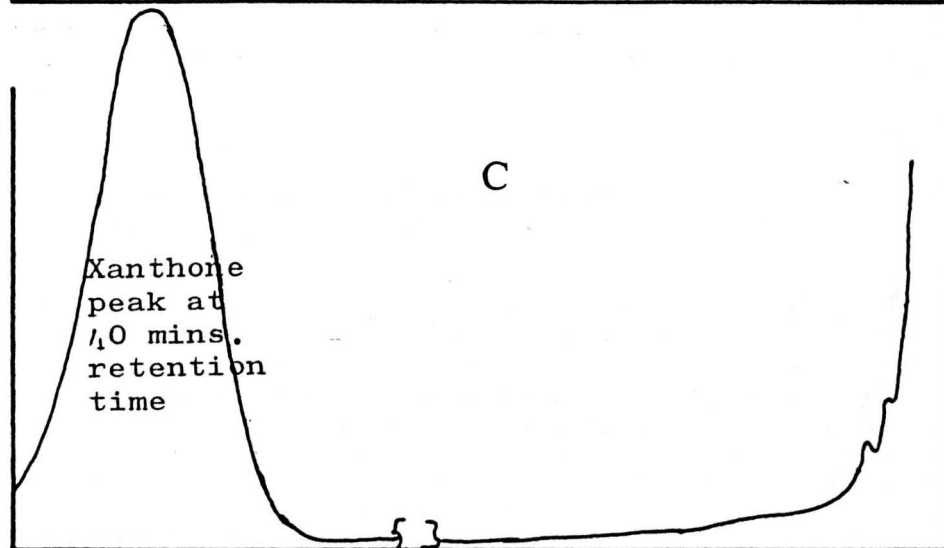
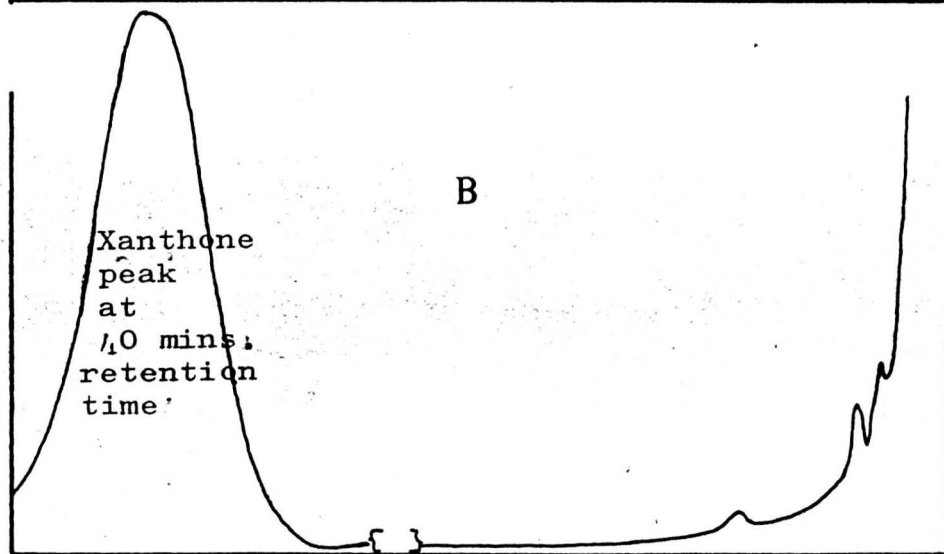
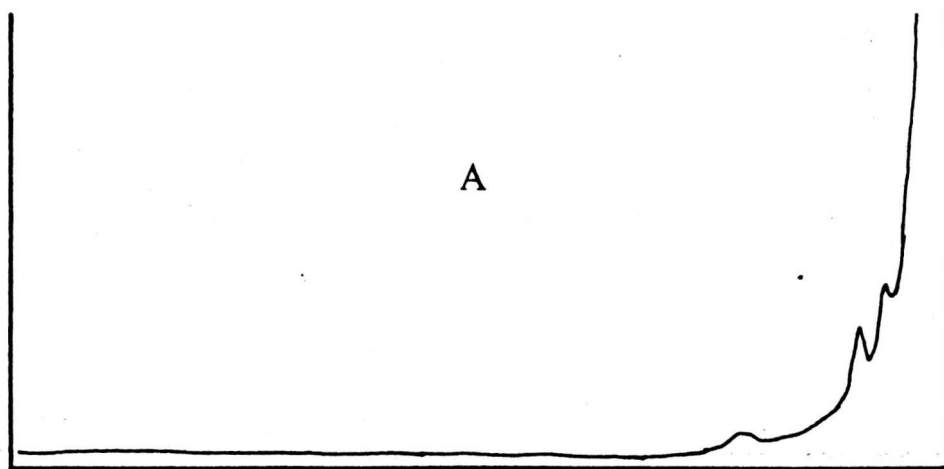


Fig. 3-12 GLC chromatogram of

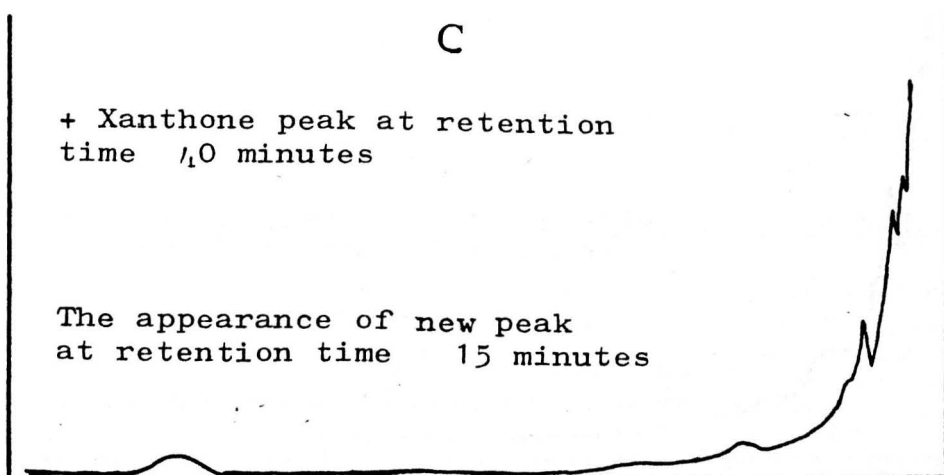
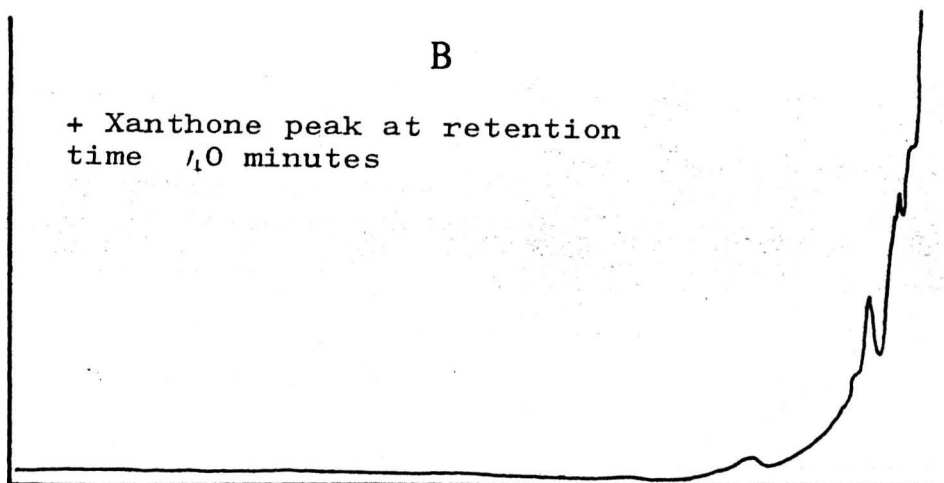
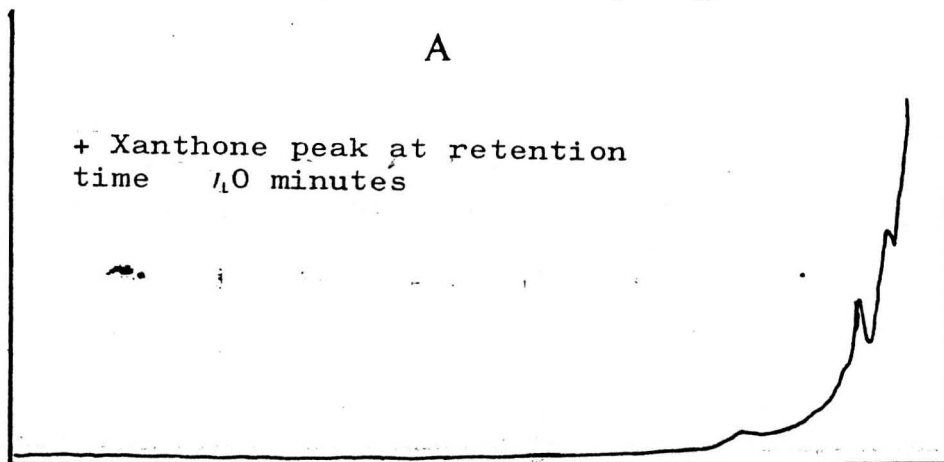
- A Allyl Acetate
- B Solution 16 "Allyl acetate + Xanthone"
- C Solution 17 "Allyl acetate + Octane + Xanthone"



Retention time ←

Fig. 3-13 GLC analysis of solution 16 "Allyl acetate + Xanthone" after UV radiation.

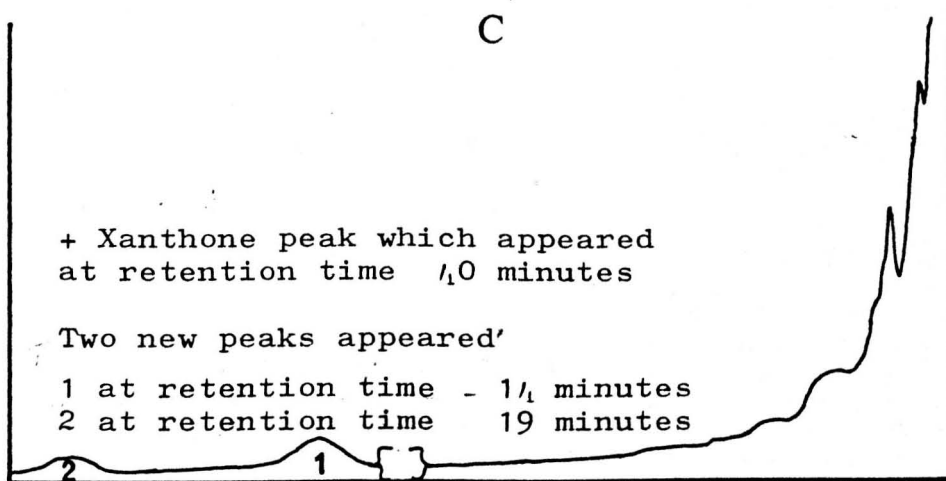
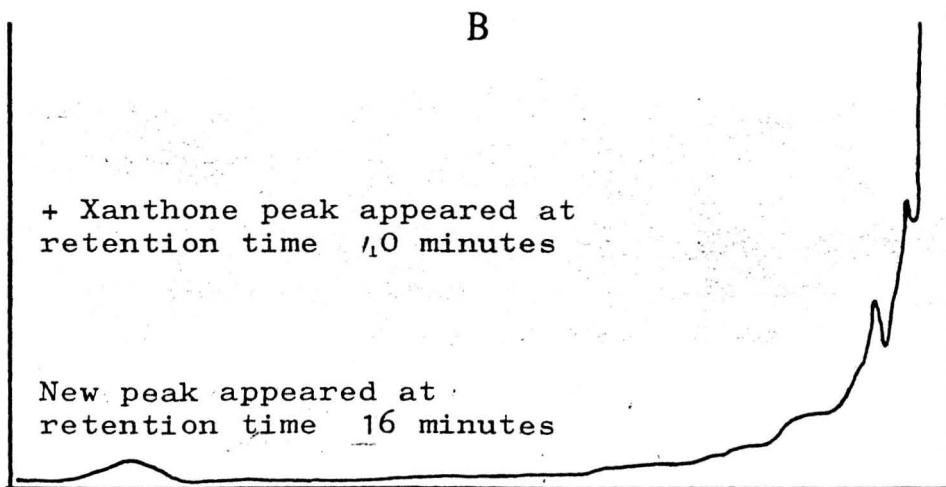
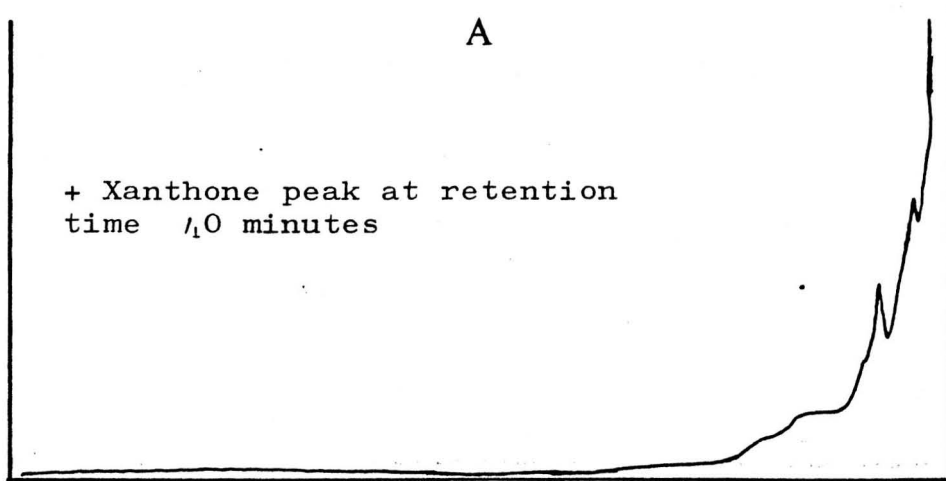
- A Chromatogram after twelve hours radiation
- B Chromatogram after twenty four hours radiation
- C Chromatogram after forty eight hours radiation



Retention time ←

Fig. 3-14 GLC analysis of solution 17 "Allyl acetate + Octane + Xanthone" after UV radiation

- A Chromatogram after 12 hours radiation
- B Chromatogram after $2\frac{1}{2}$ hours radiation
- C Chromatogram after $\frac{1}{8}$ hours radiation



Retention time ←

Fig. 3_15

Xanthone Rate of decomposition in Octane/
Allyl acetate UV irradiated solutions

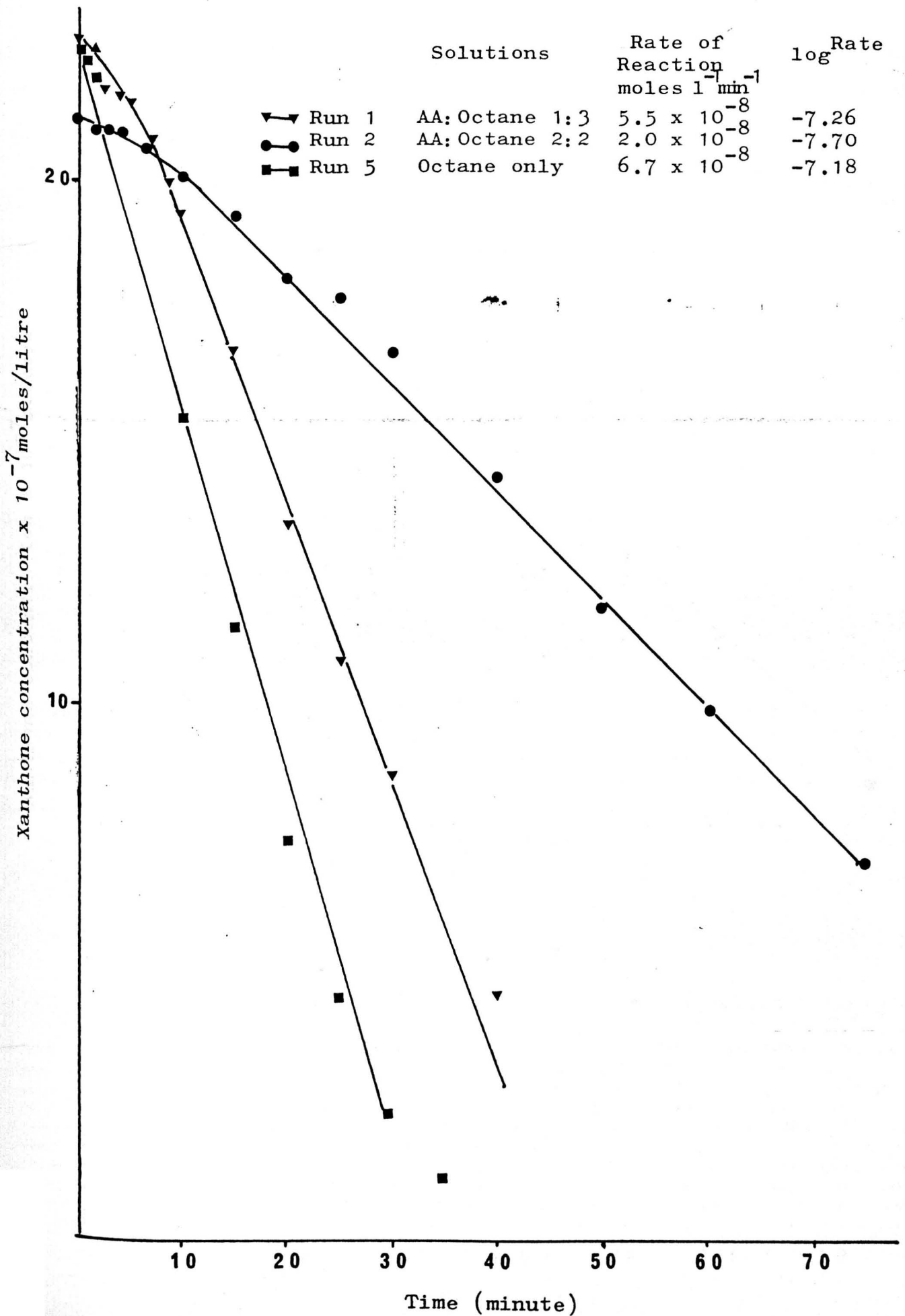


Fig. 3-16 Xanthone rate of decomposition in Octane/allyl acetate UV irradiated solutions

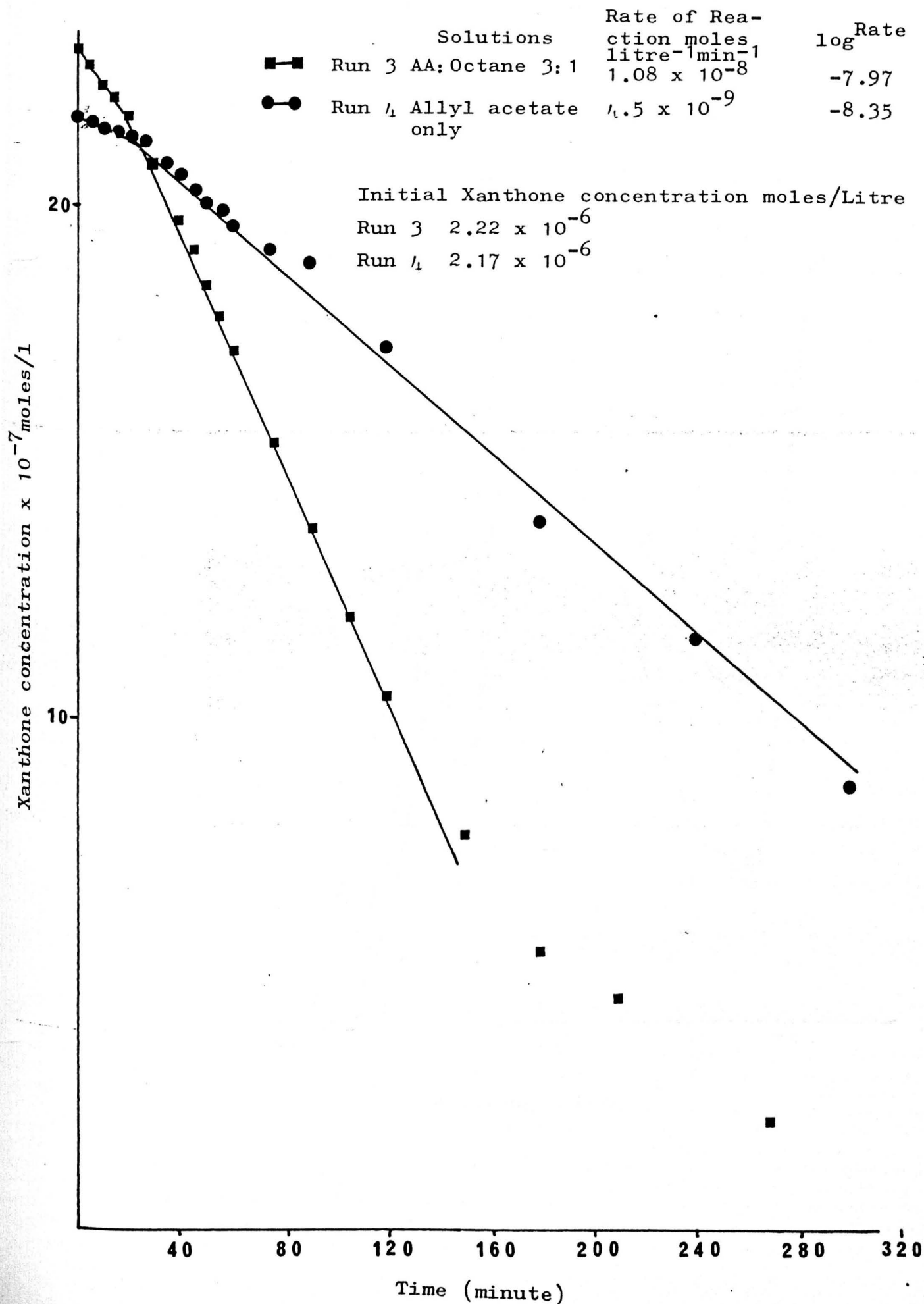


Fig. 3-17 UV spectra of solution 18 "Allyl acetate + Xanthone"

- A Before UV radiation (5% dilution)
- B After 12 hours radiation (10% dilution)
- C After 2 $\frac{1}{2}$ hours radiation (10% dilution)
- D After 1 $\frac{1}{8}$ hours radiation (10% dilution)
cell path 2 mm

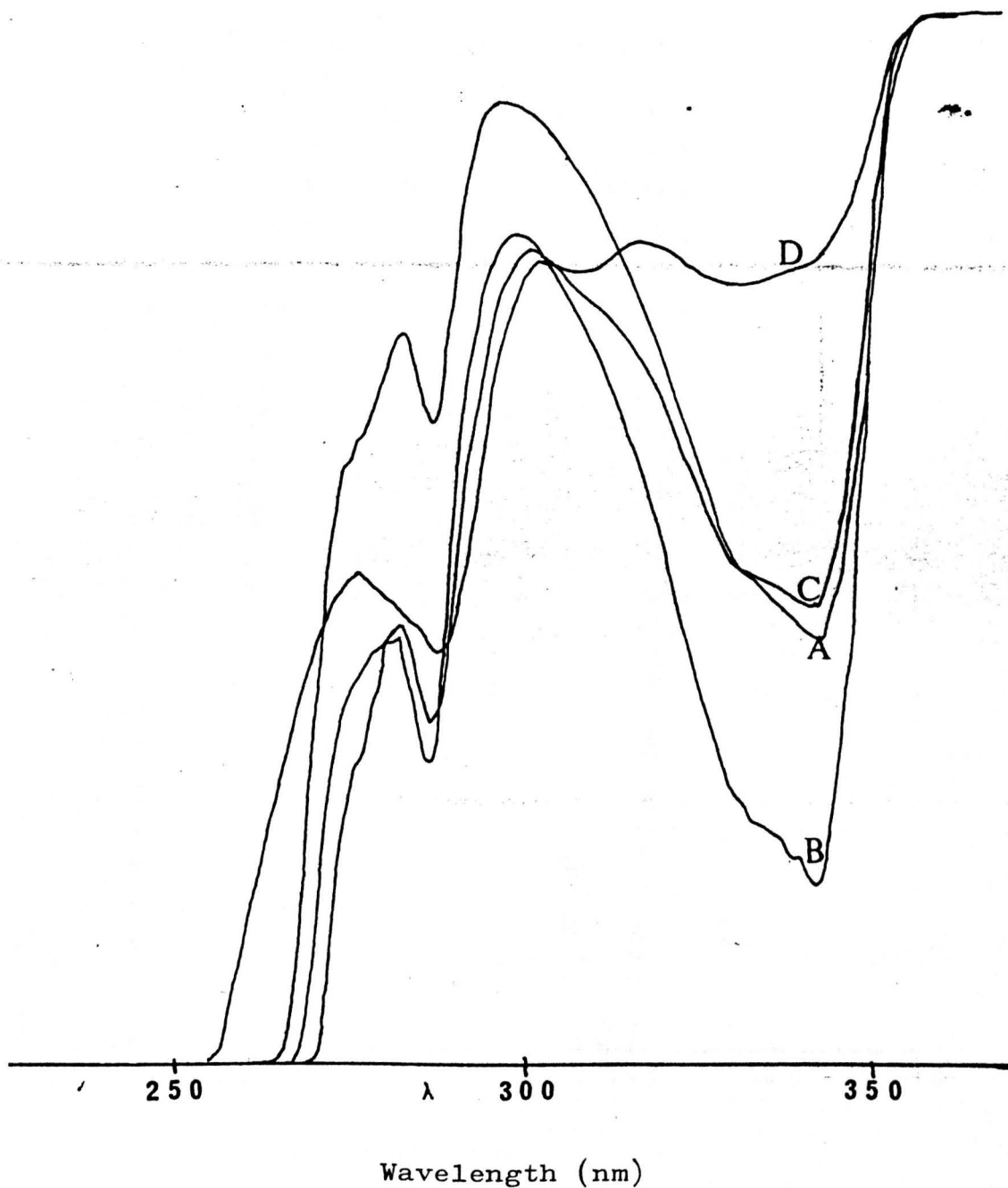


Fig. 3-18 Xanthone UV spectra at different stages in Run (1) "Allyl acetate + Xanthone solution"

- A Before UV radiation
- B After 30 minutes radiation
- C After 55 minutes radiation
- D After 210 minutes radiation
- E After 300 minutes radiation
- F After 360 minutes radiation
- G After 180 minutes radiation
- H After 600 minutes radiation
cell path 1 mm

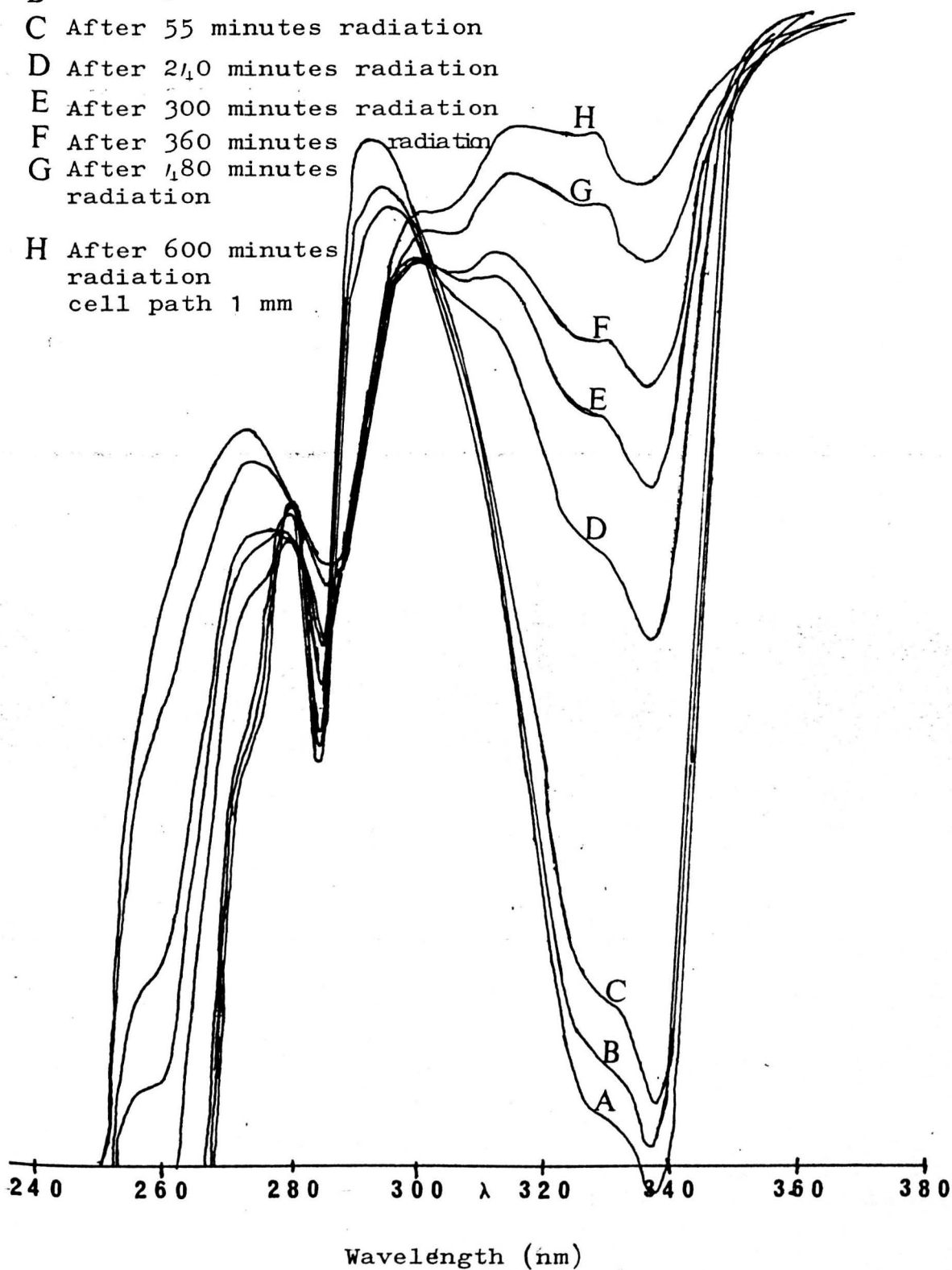


Fig. 3-19 UV spectrum of solution 19 "Allyl acetate + Octane + Xanthone"

- A Before UV radiation (5% dilution)
- B After 12 hours radiation (10% dilution)
- C After 2 $\frac{1}{2}$ hours radiation (10% dilution) cell path 2 mm

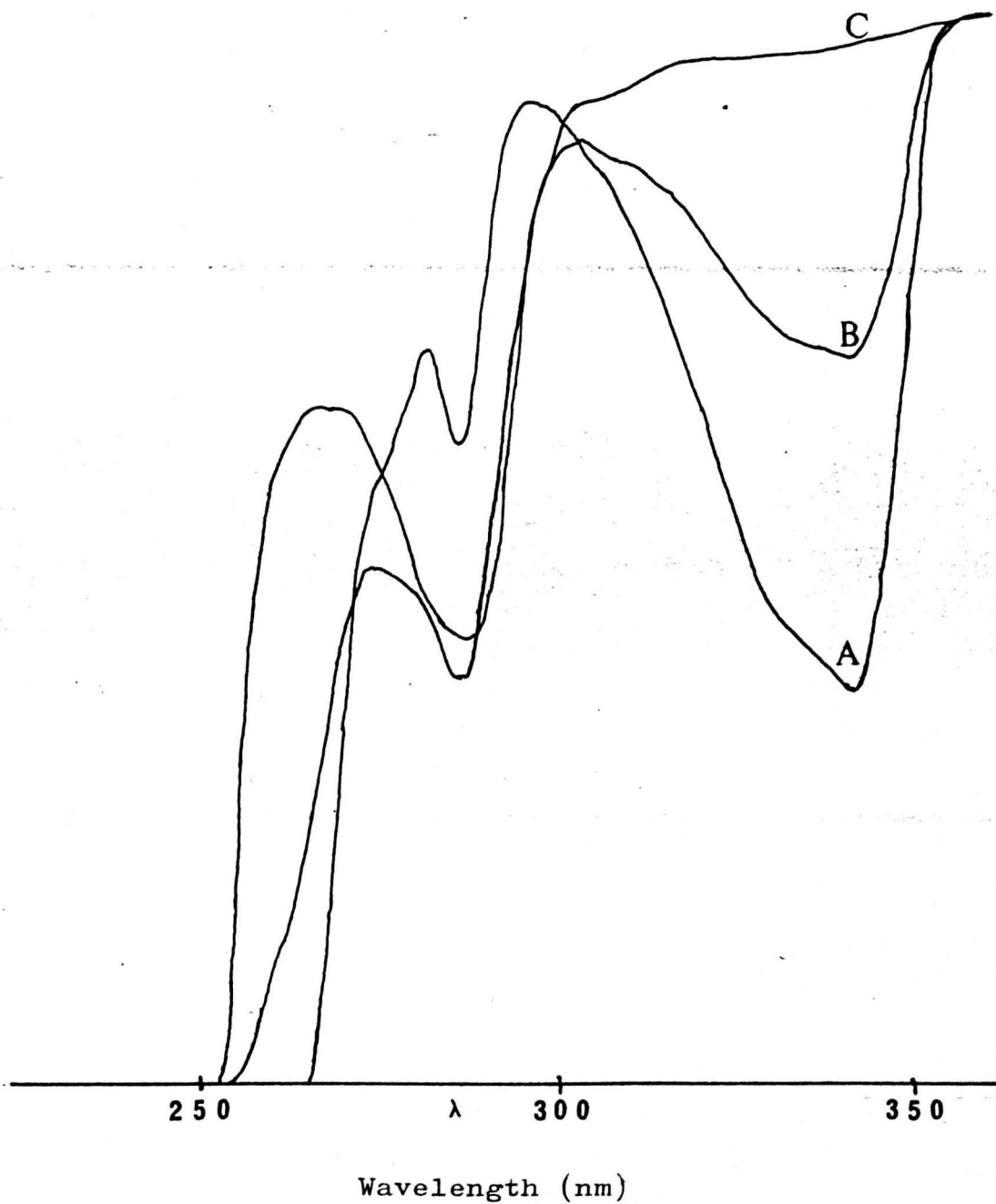


Fig. 3-20 UV spectra of solution 20 "Allyl acetate + 1-Octene + Xanthone"

- A Before UV radiation (5% dilution)
- B After 12 hours radiation (10% dilution)
- C After 2 $\frac{1}{2}$ hours radiation (10% dilution) cell path 2 mm

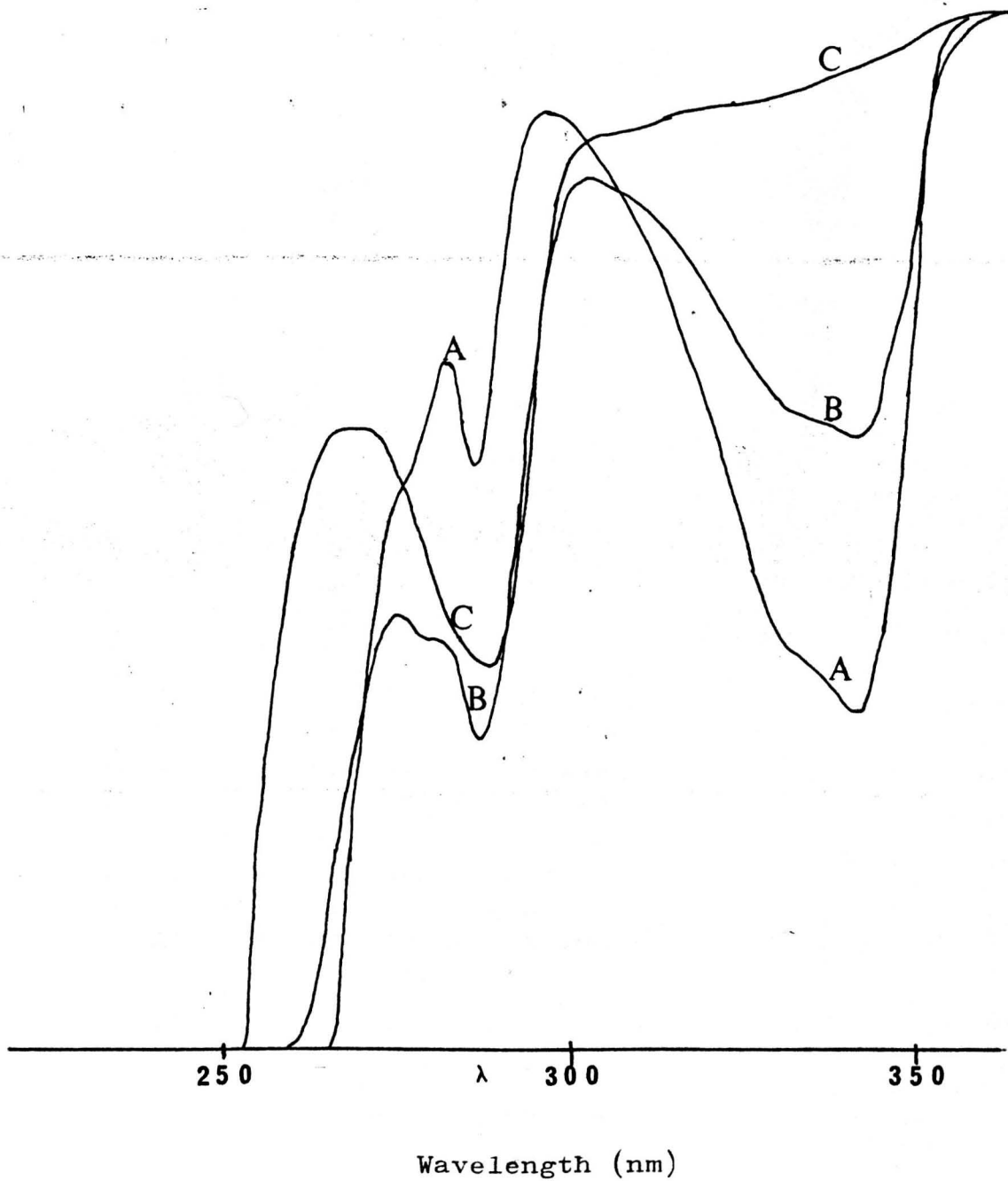


Fig. 3-21

Xanthone spectra at different stages throughout Run (16)
"Allyl acetate:Octane 3:3 + Xanthone"

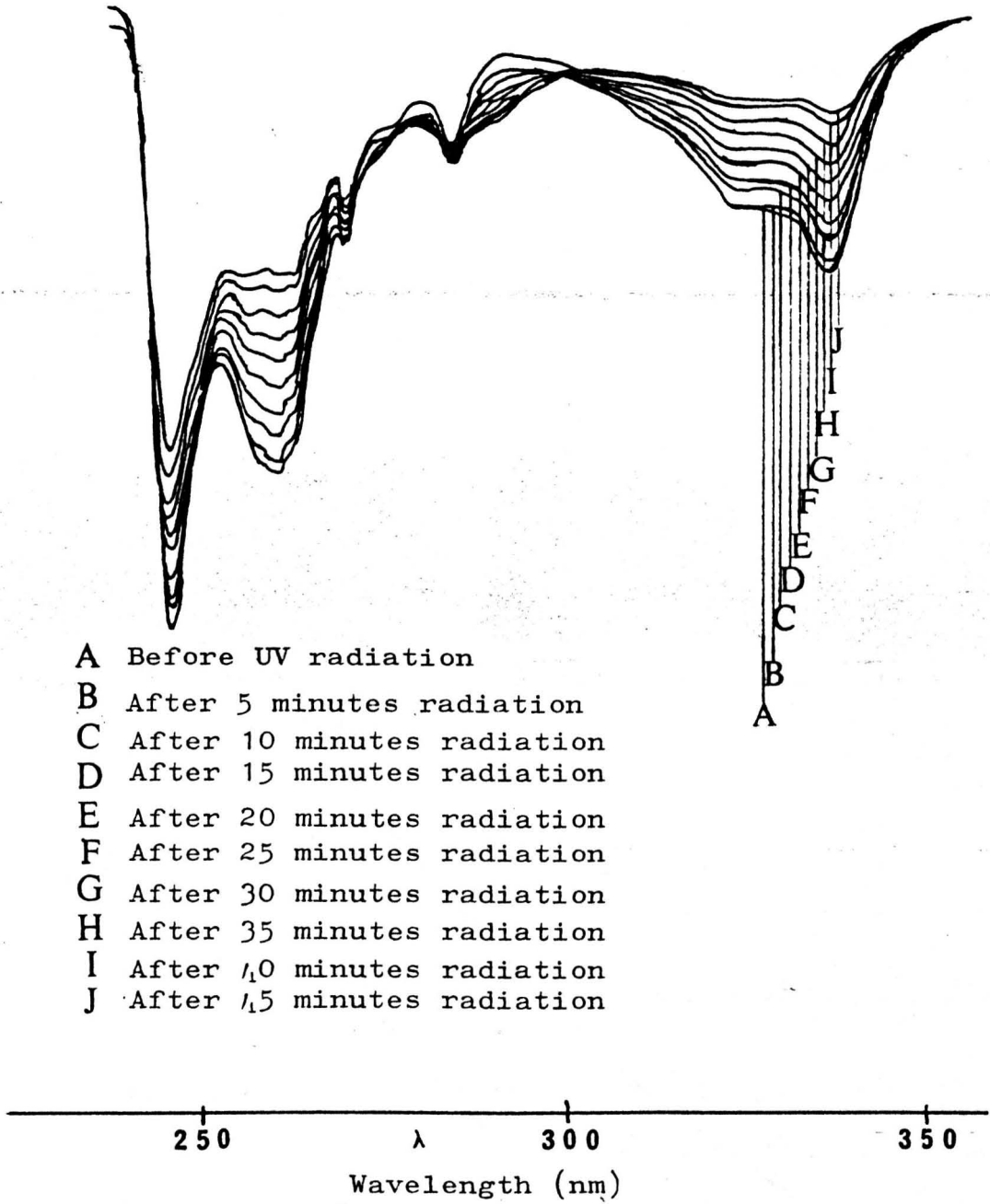


Fig. 3-22 Xanthone rate of decomposition during the UV radiation process in

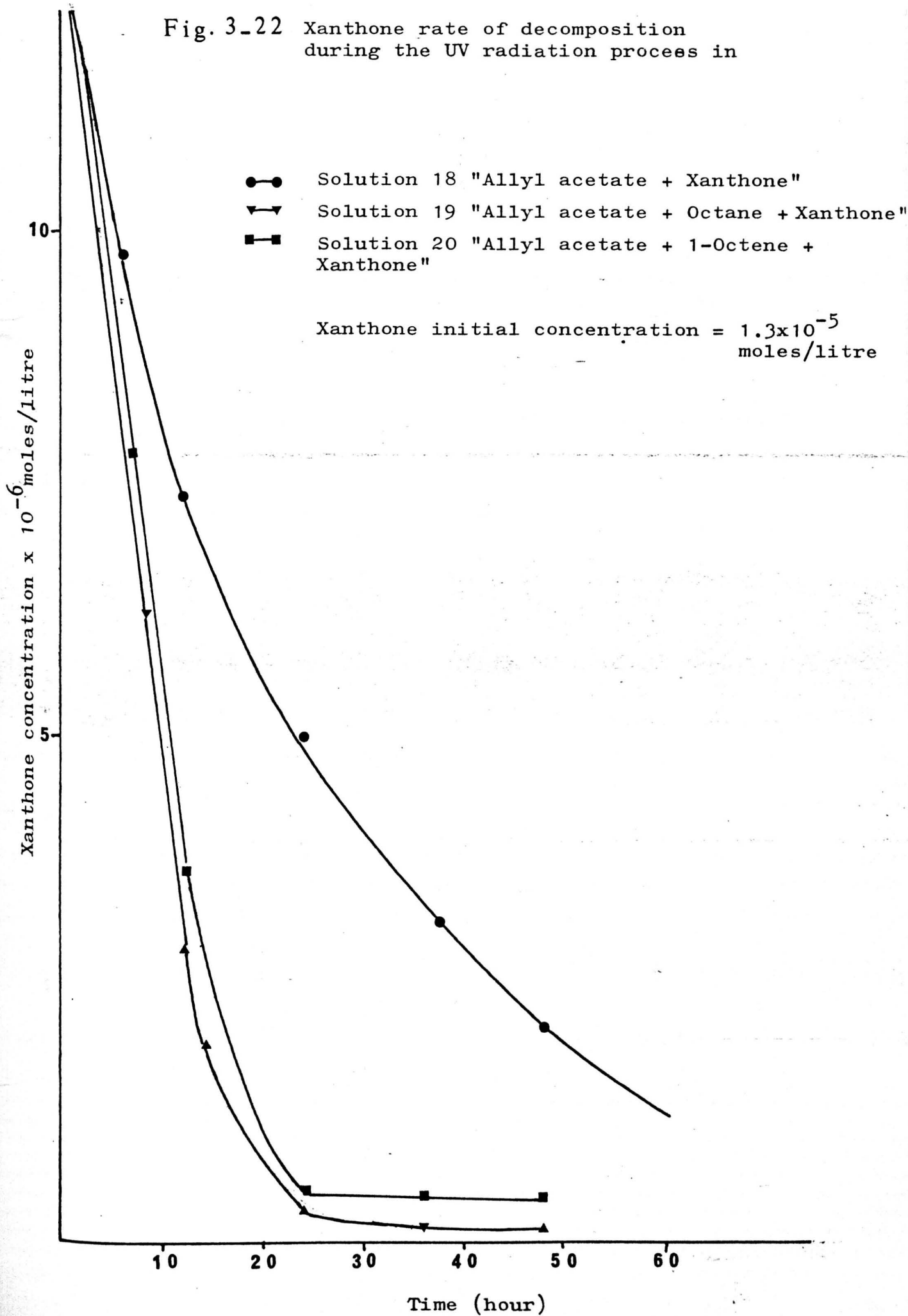


Fig. 3-23 Xanthone rate of decomposition throughout the UV radiation process in different ratios of Octane/allyl acetate mixtures.

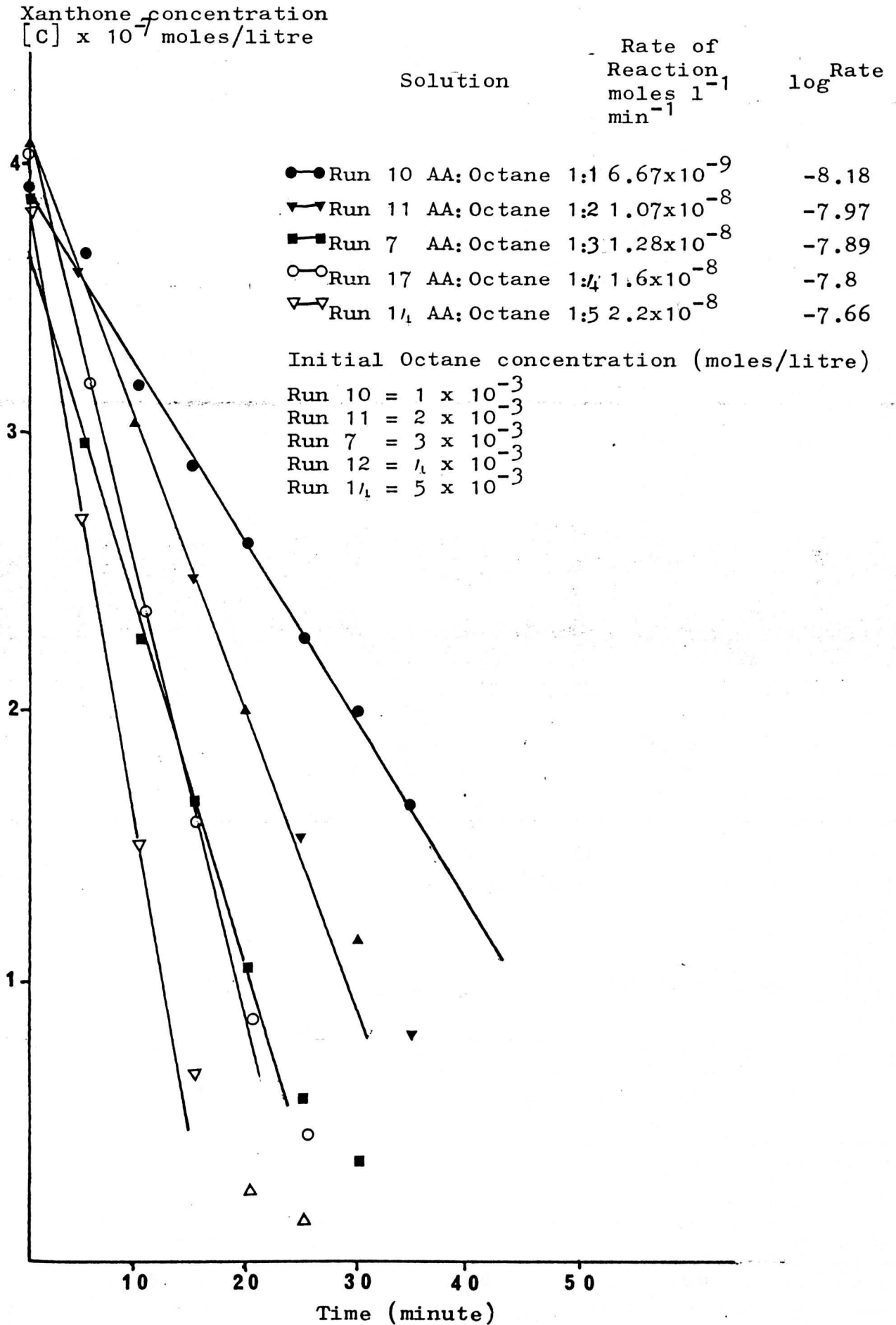


Fig. 3_24 Xanthone rate of decomposition throughout the UV radiation process in different ratios of Octane/allyl acetate mixtures

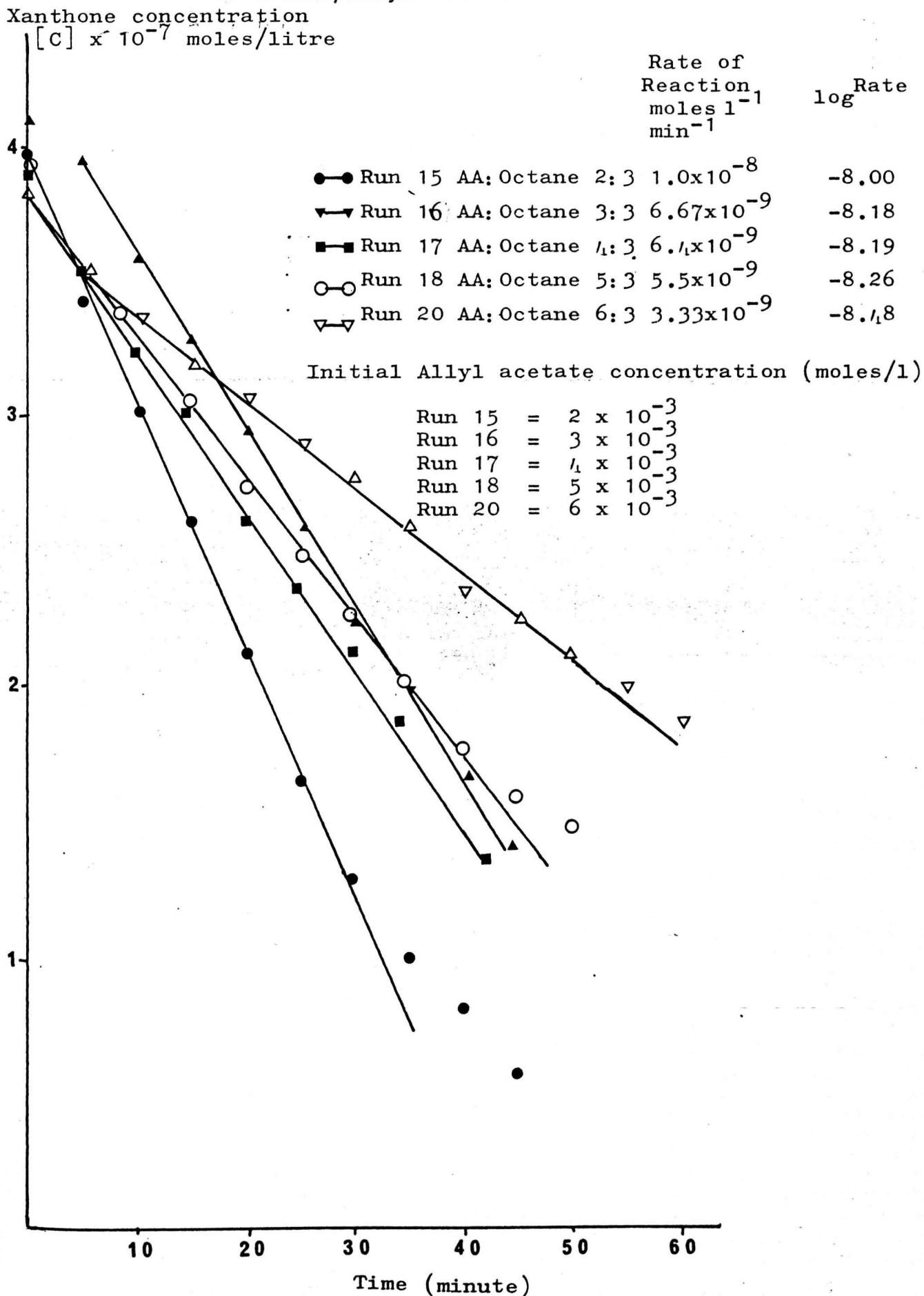


Fig. 3-25 Xanthone rate of decomposition throughout the UV radiation process in allyl acetate/Octane (1:3) solution

Xanthone concentration
 $[C] \times 10^{-7}$ moles/litre

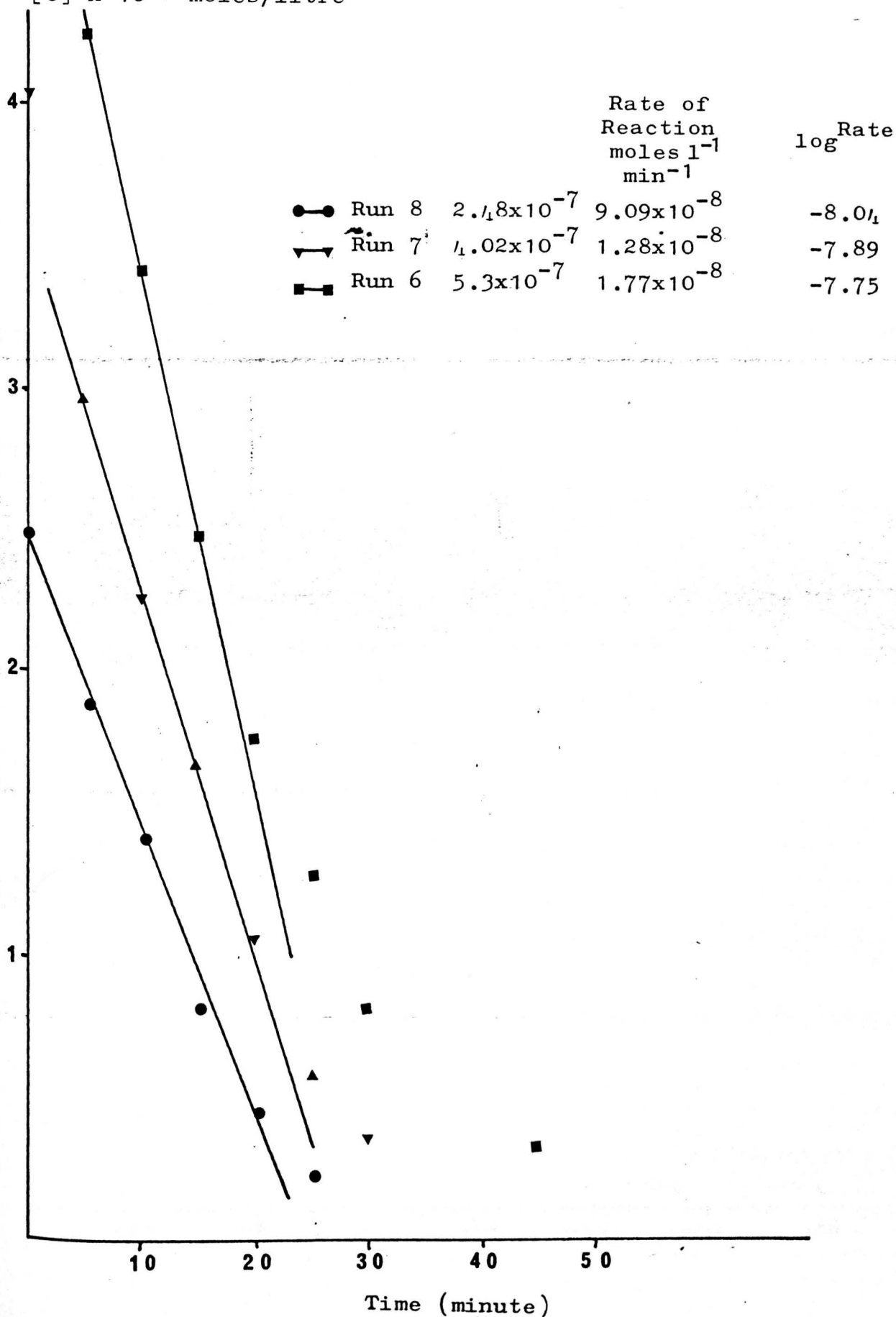


Fig. 3-26 Order of Xanthone decomposition in reference to the Octane concentration (Allyl acetate and Xanthone concentrations are constant in different Octane solutions)

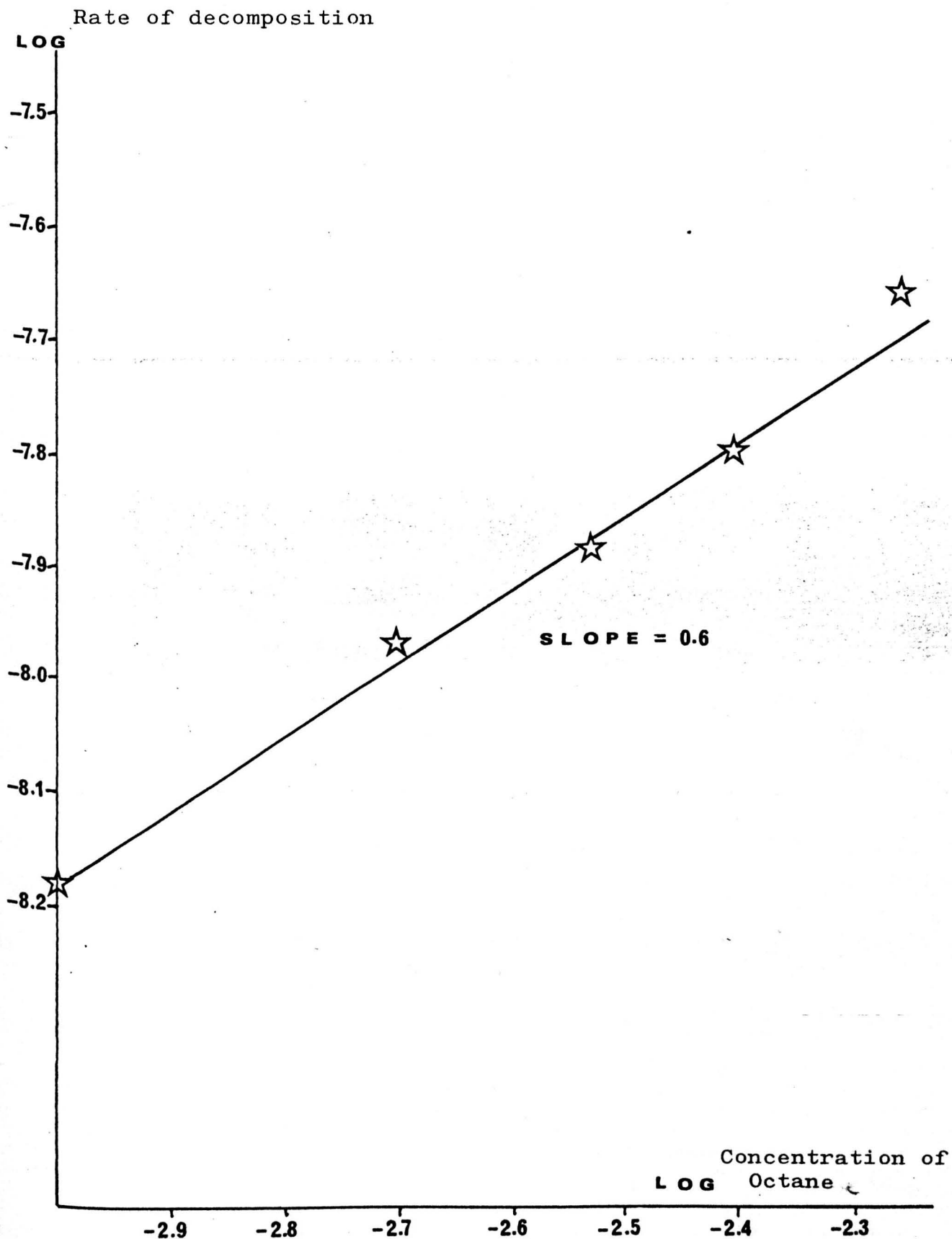
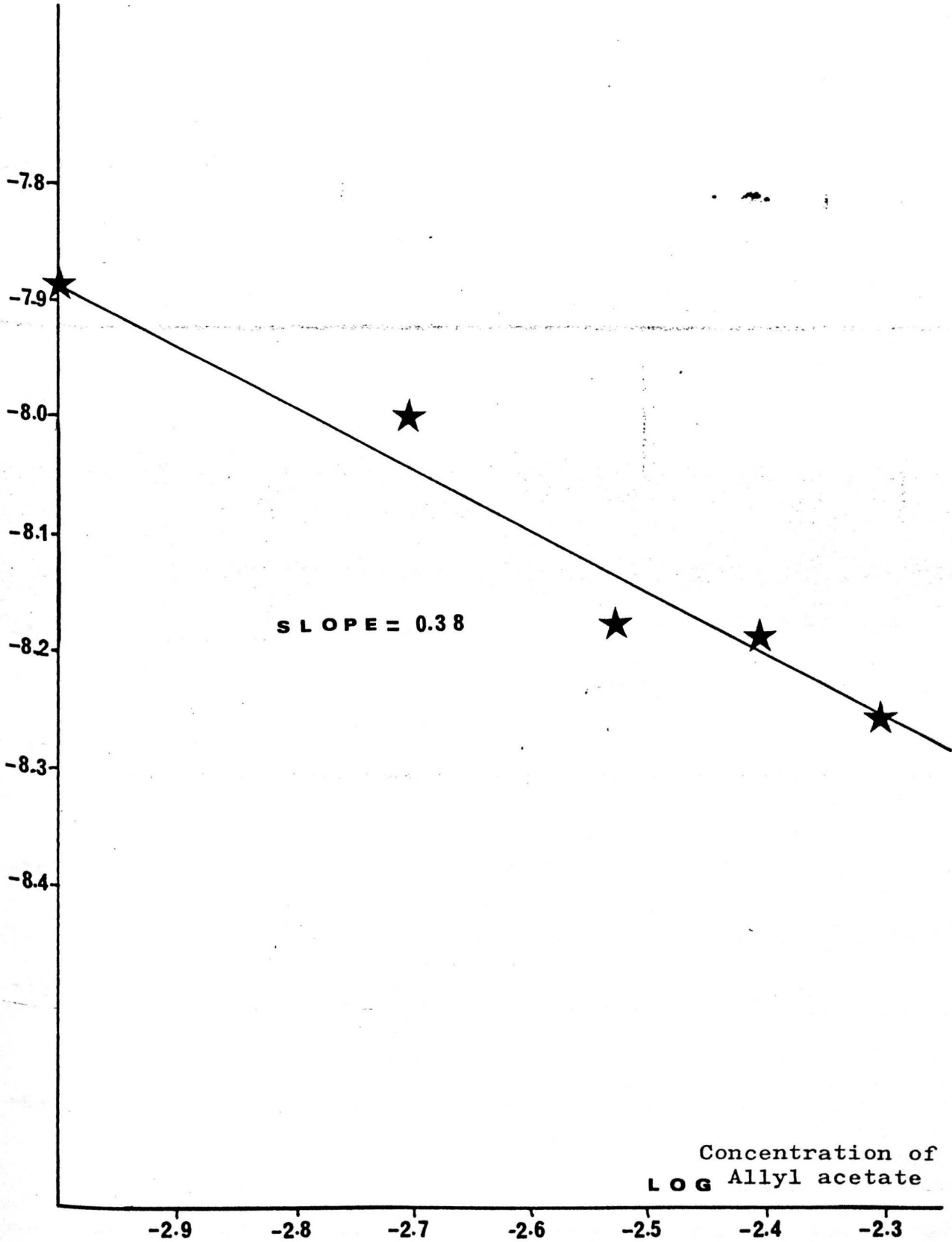


Fig. 3-27

Order of Xanthone decomposition in reference to the Allyl acetate concentration (Octane and Xanthone concentrations are constant in different Allyl acetate solutions)

Rate of decomposition

LOG



Concentration of
LOG Allyl acetate

Fig. 3-28 Order of Xanthone decomposition in reference to its concentration (Allyl acetate/Octane ration is 1:3)

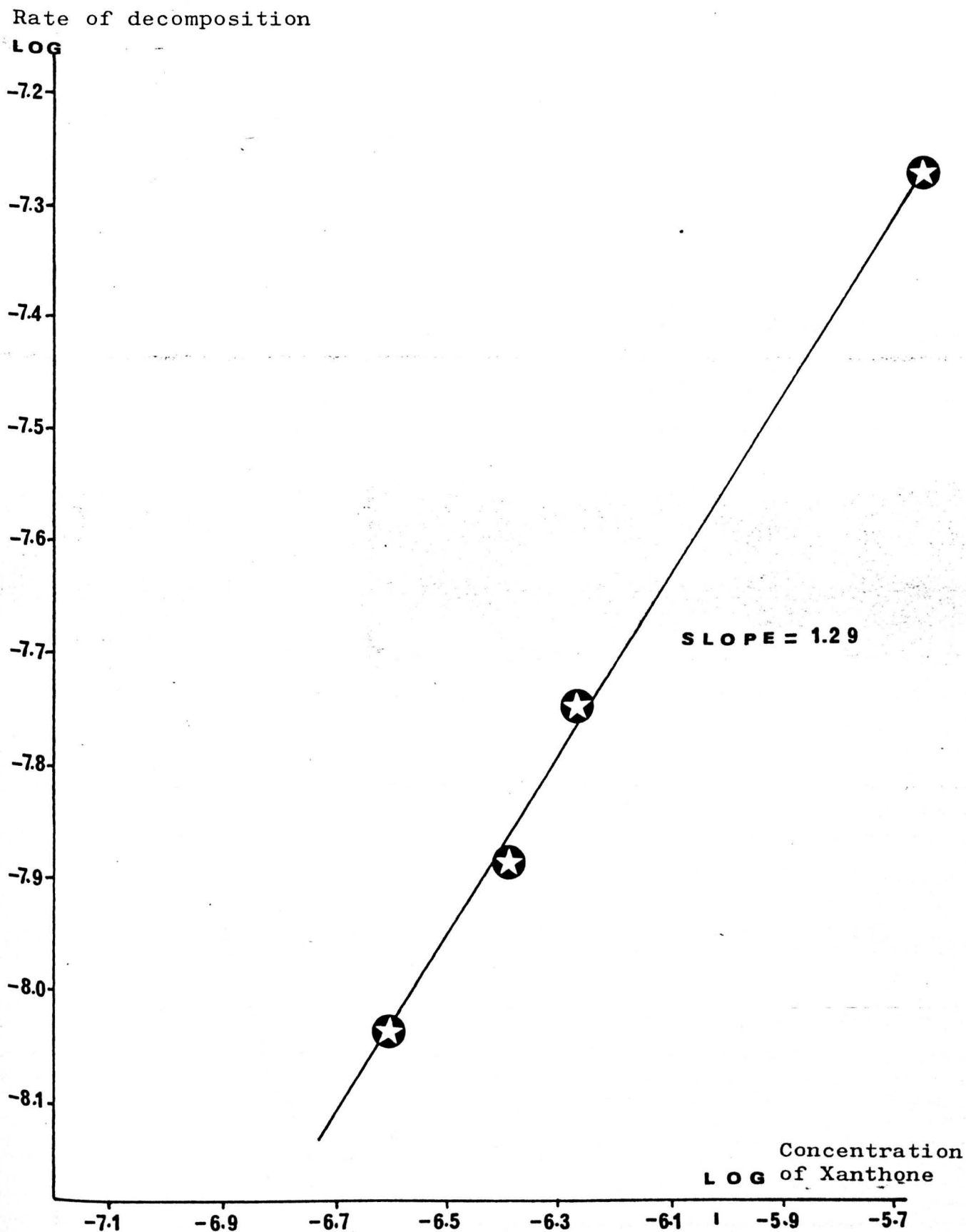


Fig. 3-29 Effect of temperature on the Xanthone rate of decomposition during the UV radiation process in Allyl acetate/Octane 1:3 solution.

Xanthone concentration
 $[C] \times 10^{-7}$ moles/litre

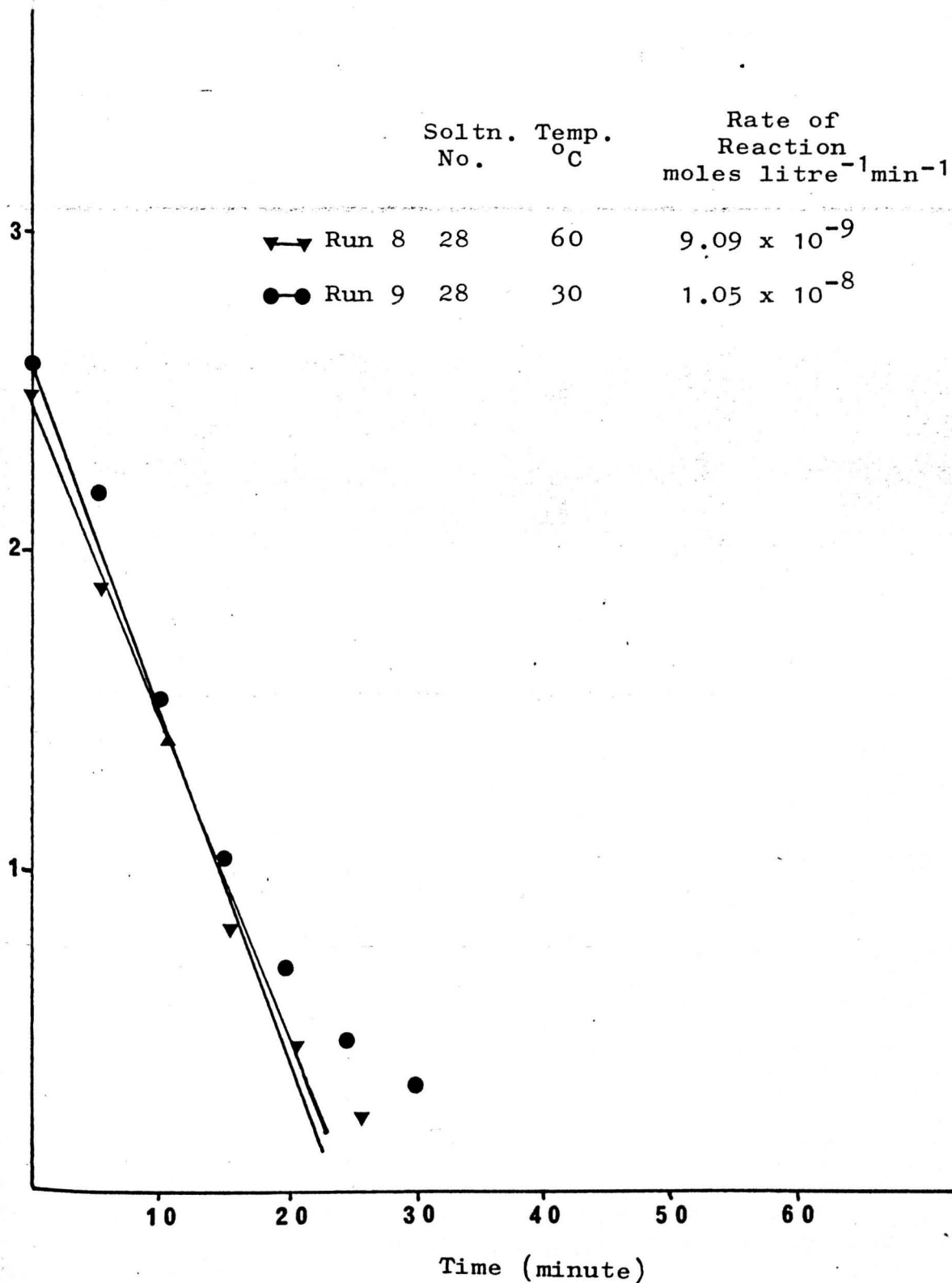


Fig. 3-30

Effect of temperature on the Xanthone rate of decomposition during the UV radiation process in Allyl acetate/Octane 1:3 solution.

Xanthone concentration
 $[C] \times 10^{-7}$ moles/litre

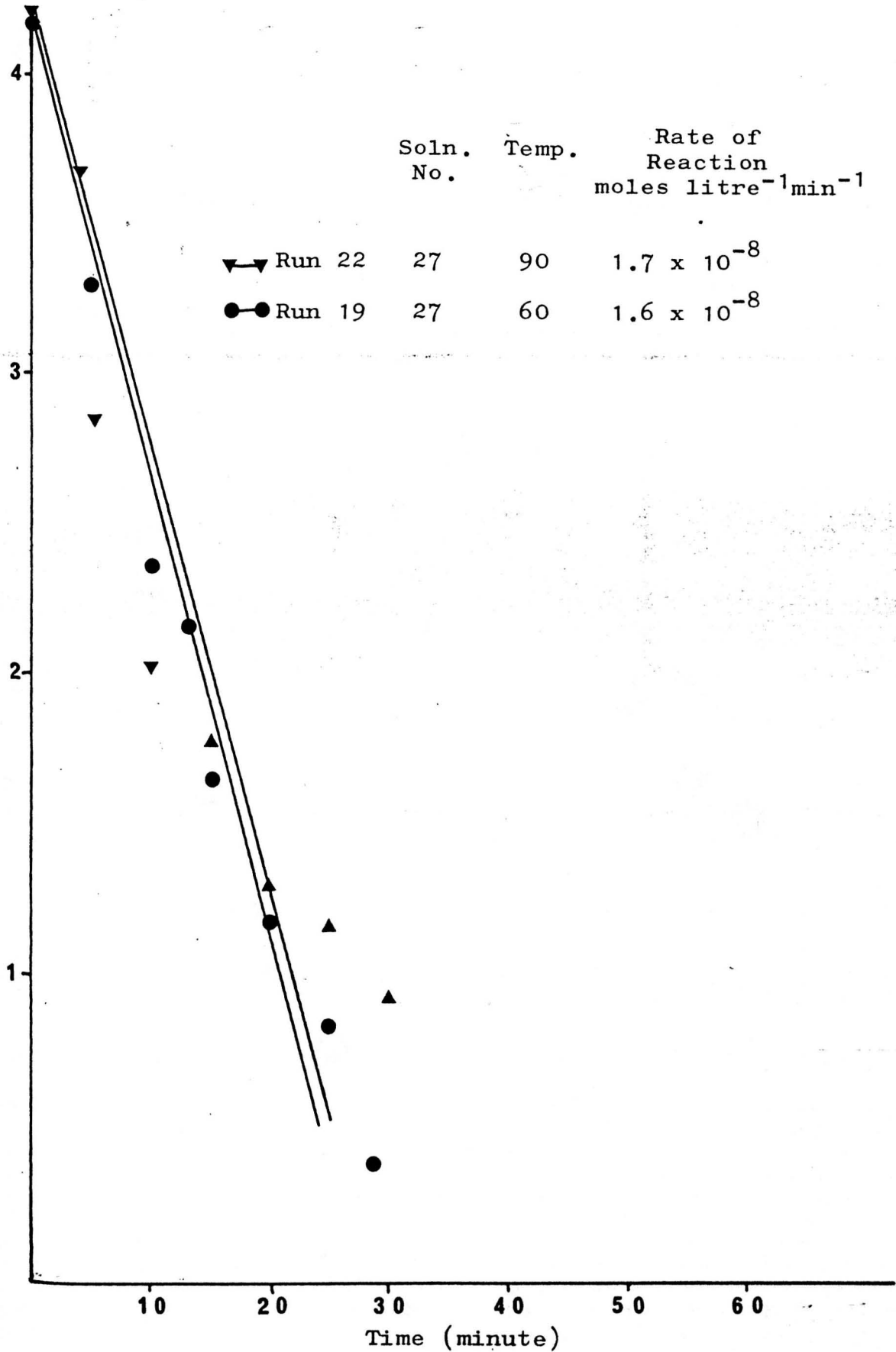
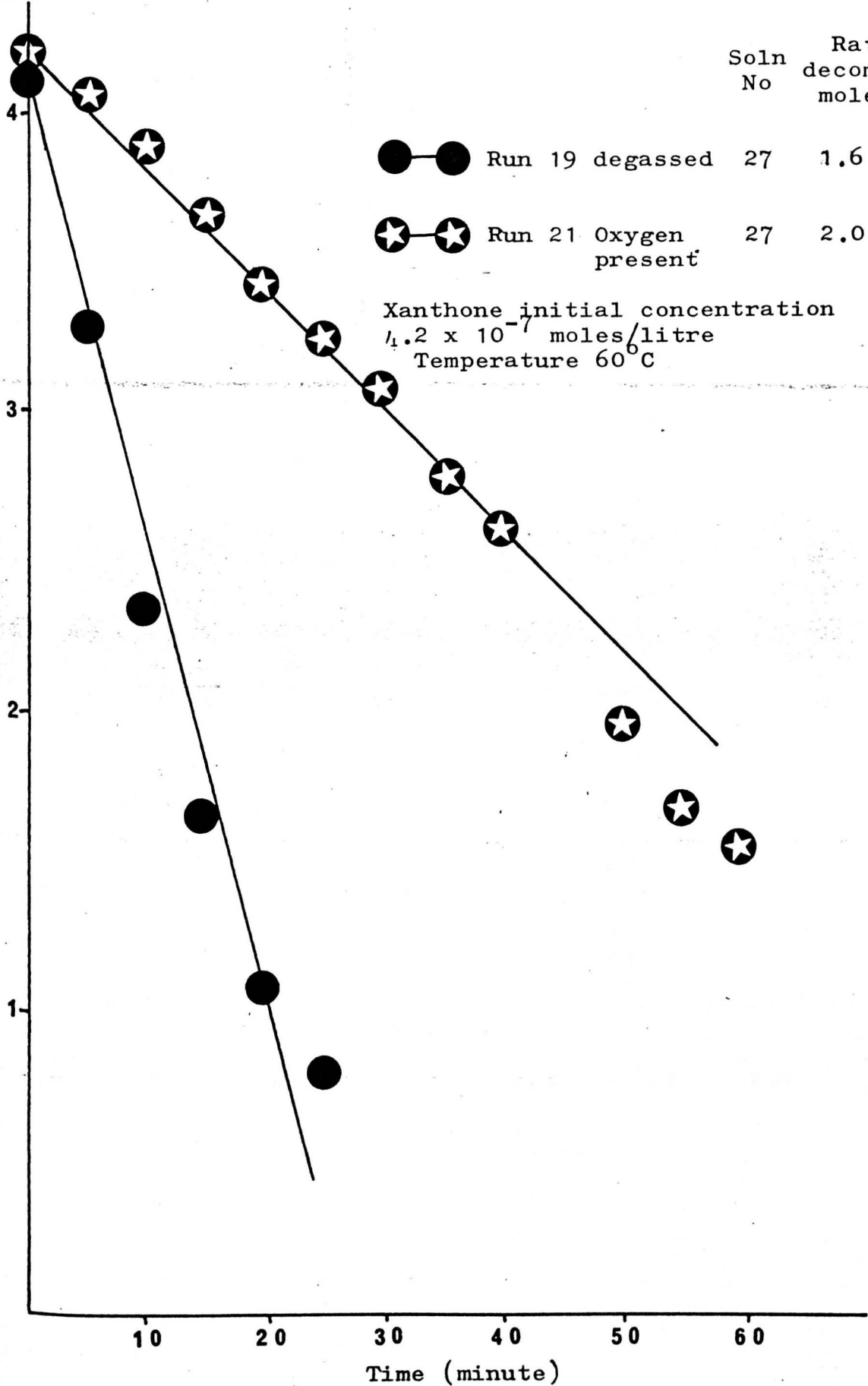


Fig. 3-31 Effect of oxygen on the Xanthone rate of decomposition during the UV radiation process in Allyl acetate/Octane 1:3 solution.

Xanthone concentration
 $[C] \times 10^{-7}$ moles/litre



Soln No Rate of decomposition, moles $\text{l}^{-1}\text{min}^{-1}$

●—● Run 19 degassed 27 1.6×10^{-8}

★—★ Run 21 Oxygen present 27 2.0×10^{-9}

Fig. 3_32 Xanthone UV spectra at different stages of UV radiation process of Octane solution "Run 5 solution Ref. No. 21"

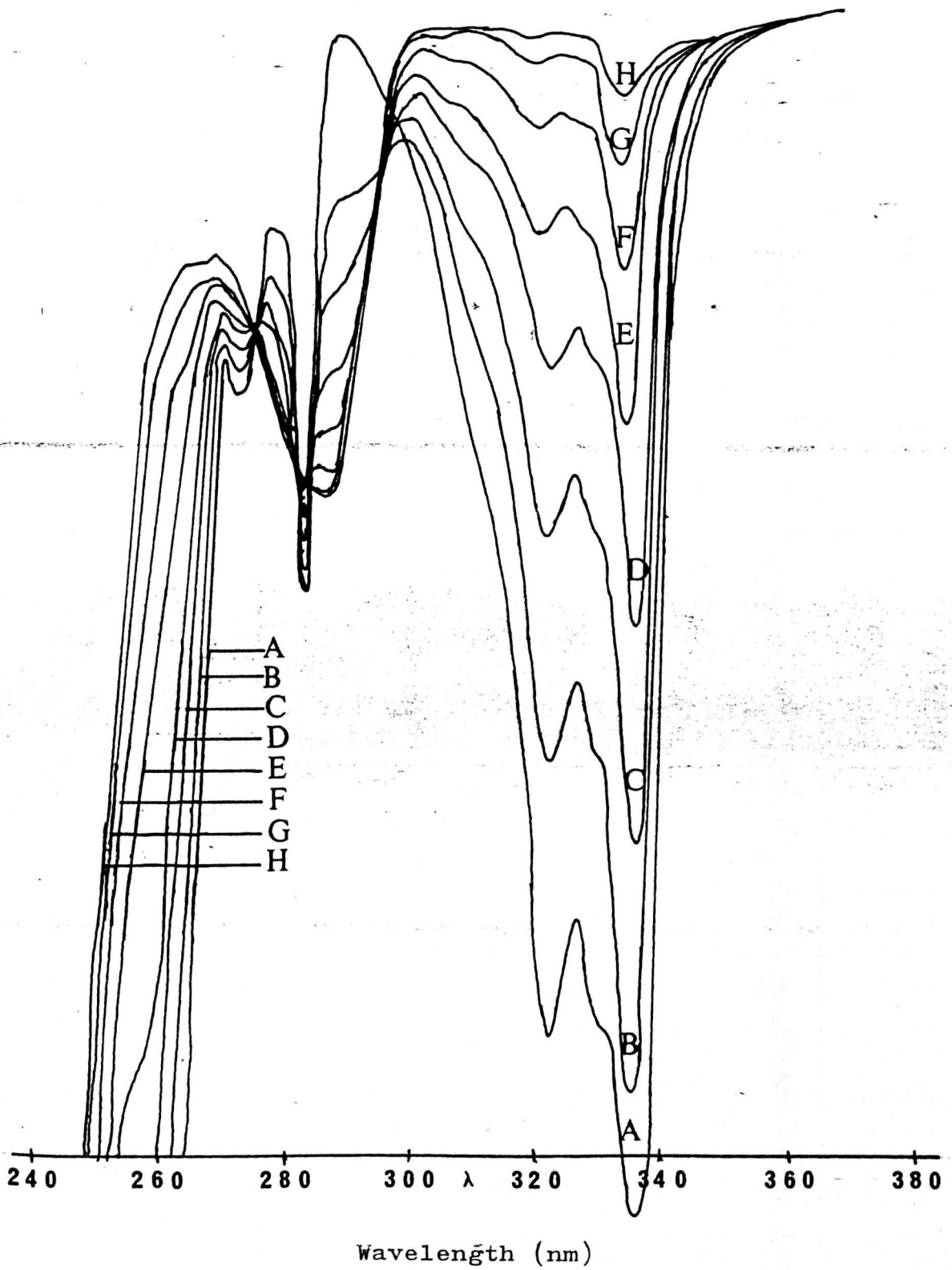
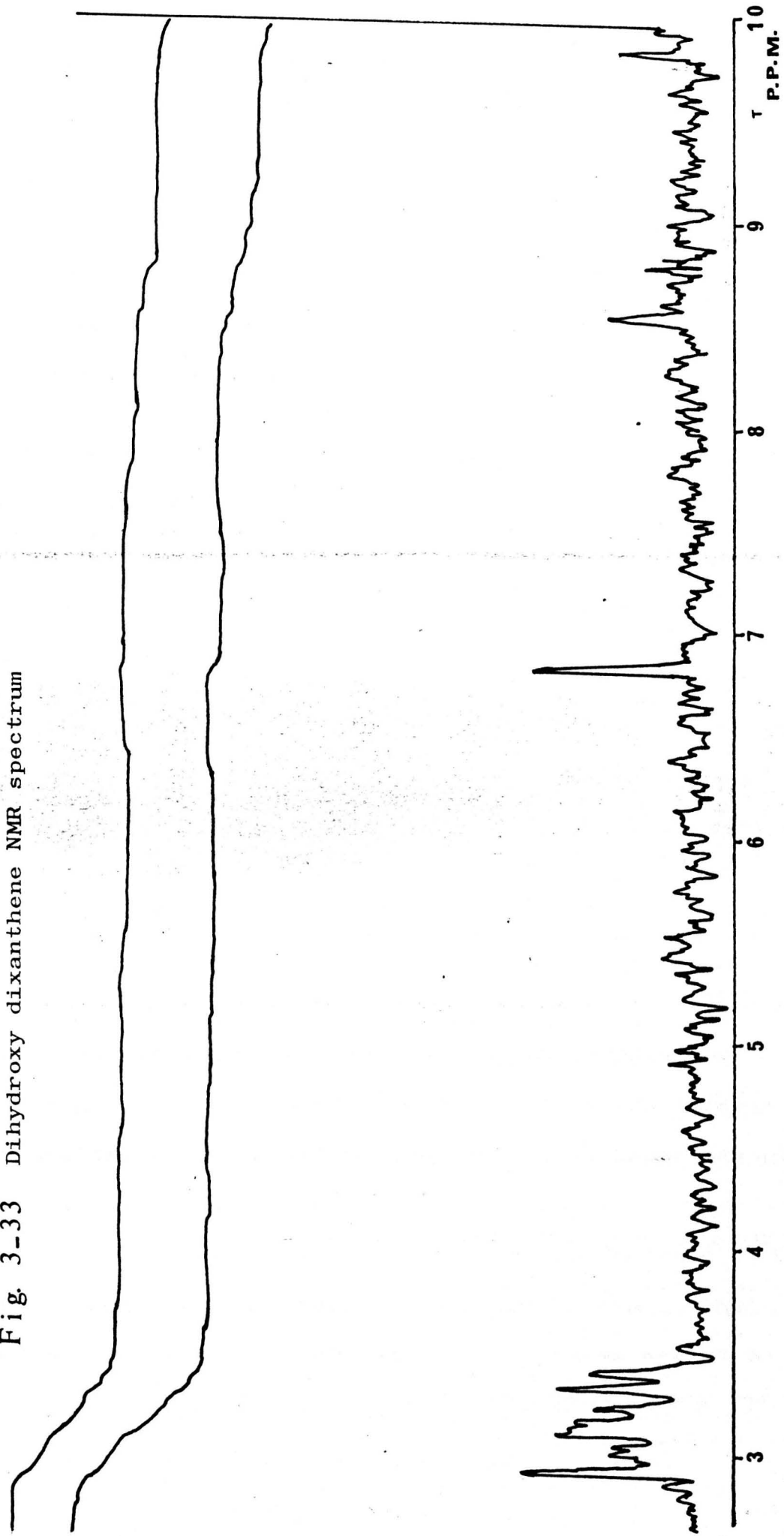


Fig. 3-33 Dihydroxy dioxanthene NMR spectrum



CHAPTER 4CROSSLINKING OF POLYETHYLENE4.1 Introduction

Low density polyethylene (Melt flow index =7) has been crosslinked by the author with ultraviolet light using xanthone as the photoinitiator and triallyl cyanurate (monomer) as the crosslinking agent.

For comparison, the low density polyethylene was also crosslinked by ^{60}CO γ -irradiation with and without the crosslinking agent (TAC) as this type of polyethylene crosslinking has already been extensively studied by different people.

The ultraviolet light curing was carried out under the following conditions; in the presence of air and also in its absence, crosslinking at low temperatures, below the crystalline melting temperature ' T_m ' and above T_m .

The effect of photoinitiator and the crosslinking agent on the degree of crosslinking was studied by varying their concentration during the curing process. In addition, the effect of penetration of light was also studied by crosslinking films of polyethylene which were four layers thick. The degree of crosslinking was followed by means of gel content measurements. Gel permeation chromatography and melt flow index measurements also served as a guide for the effect of crosslinking on the flow

properties. The Weissenberg Rheometer was used to study, in more detail, the effect of crosslinking on the flow properties of the polyethylene. (This topic will be dealt with in the next chapter). Also some spectral analyses for the gel part were carried out to calculate quantitatively the amount of TAC incorporated in the network. A brief study of the mechanical properties will also be reported in this chapter.

4.2 Structure of Polyethylene

Before looking into the crosslinking of polyethylene, a brief look at the polyethylene structure would be considered a useful guide.

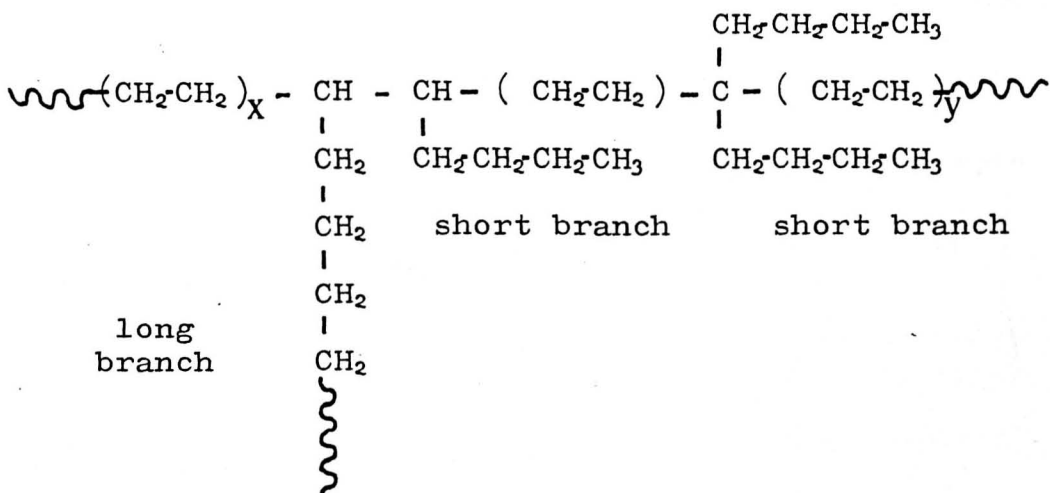
Polyethylene may be considered as being a long chain molecule composed exclusively of methylene groups, (CH_2) . The polymer prepared by free radical polymerization under high pressure is known as low density polyethylene. It contains a large number of short chain branches together with a limited number of longer branches (15, 16, 17, 18).

The degree of branching and the type of branching mainly depends on the polymerization conditions and in particular the reaction temperature.

The polymer is partly crystalline, the degree of which depends upon the chemical structure of the polymer and particularly upon the extent of branching. As the temperature is raised, these crystalline regions progressively melt and the polymer becomes softer and more flexible until at the temperature at which all the crystals have completely melted it is transformed into a viscous fluid. Practically no crystallites remain in the low density polyethylene above $110^{\circ} - 115^{\circ}\text{C}$.

In highly branched polyethylene, individual crystals tend to be small and possibly distorted and consequently have a low melting point. The density will be reduced with a higher proportion of non-crystalline material.

The polyethylene chain may contain some or all of the following structures in varying proportions.

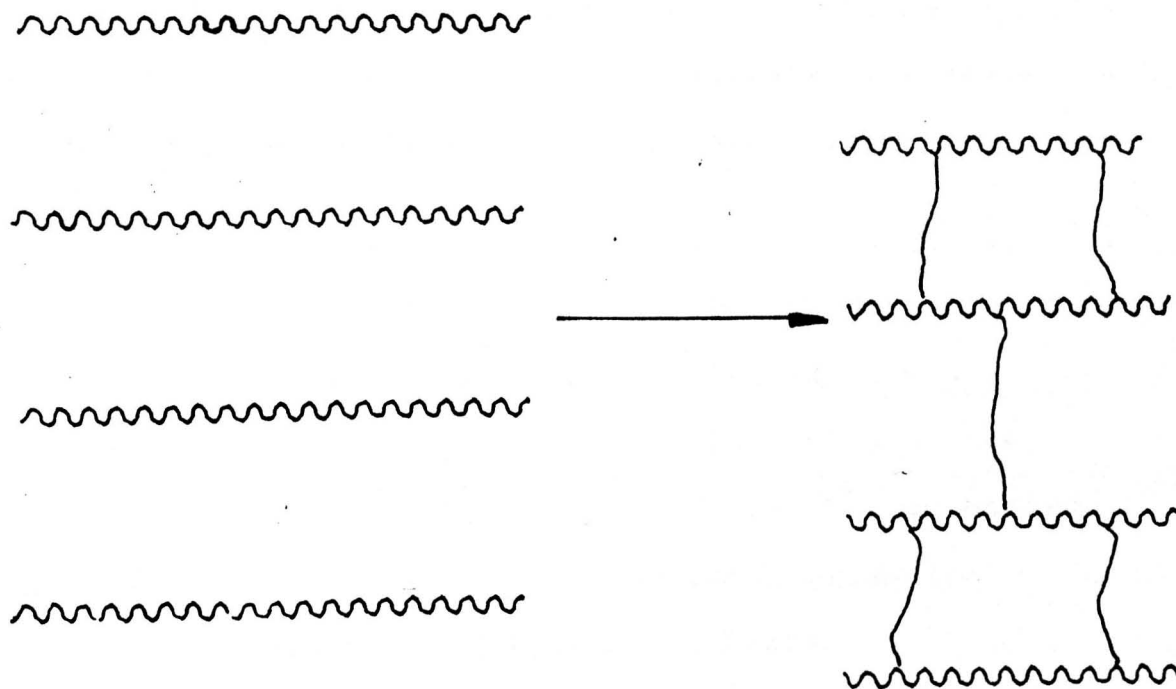


4.3 General Aspects of Crosslinking in Polyethylene

4.3.1 Radiation effect in polyethylene

In general the irradiation of linear polymers either crosslinks or degrades the polymer (1,2,3), depending on its chemical structure. Polyethylene was found to be crosslinked under high energy electron beams or when subjected to γ -irradiation (4,5) from ^{60}Co source.

Branching and higher molecular weights will follow when crosslinking takes place until ultimately a tridimensional network is formed, where on average each polymer chain is linked to one or two chains. This may be represented in the following simple diagram.



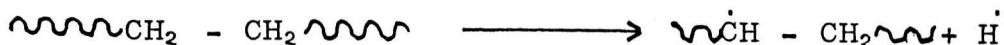
The polymer network produced from such chain crosslinking will no longer dissolve nor melt to a fluid (4). Some solvent extractable material usually remains unattached to the main network.

Although crosslinking is the main process in polyethylene under radiation, some chain scission process takes place but is not predominant (6).

Gas evolution has been observed in the case of polyethylene which is mainly composed of hydrogen, accounting for 85-95% of the gas (7-10). Also during the radiolysis of polyethylene and many other polymers, unsaturation increases (8). Dole found that the vinyl and vinylidene unsaturation initially present in the polyethylene disappeared while transvinylene unsaturation steadily increased. The amount of double bonds could be determined by using Infra-red analysis or chemical methods e.g. by bromine or iodine absorption.

Different workers found (11,12) that oxygen will influence the progress of the radiolysis of polyethylene which normally crosslinks when irradiated in the absence of oxygen. Much larger radiation doses are required in the presence of air. A possible mechanism for this reaction based on conventional oxidative degradation is outlined below.

Primary radiation step



Reaction with oxygen



Decomposition and rearrangement

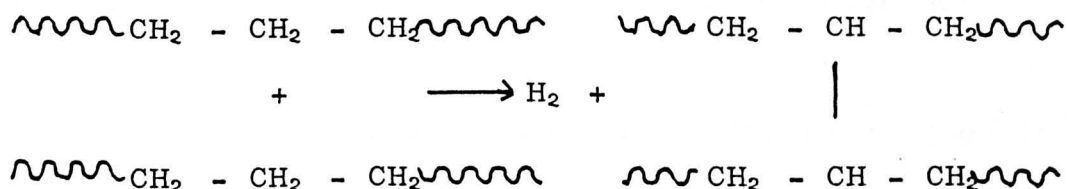


The free radical formation in the irradiated polyethylene is a main step in the crosslinking process, and one which is readily observed by E.S.R. (13). These free radicals which are formed could be trapped firm within the crystalline region of the irradiated polyethylene.

It was also found that the free radicals which are formed in the amorphous regions can be utilized readily in a crosslinking process (14), where as those radicals which are located within the crystalline areas only react at elevated temperatures, when most of the crystalline regions have melted. Oxygen can however;

diffuse into the crystalline regions and react with the trapped radicals (14).

The earliest description of chemical changes produced by radiation in polyethylene was given by Dole (5). It was followed by a detailed study of the effects by Charlesby (4) in which he conclusively demonstrated that polyethylene became crosslinked after irradiation in the reactor at Harwell. Charlesby assumed in his paper that all hydrogen gas originated from the crosslinking process accounting to an overall scheme such as



Little (19) and Lawton (20) reported that polyethylene could be crosslinked by irradiation with fast electrons. Numerous other related investigations have appeared since 1953. The major chemical effects of the irradiation of polyethylene can be summarised as follows:-

a) Formation of crosslinking

This accounts for many of the observed changes in physical properties. These include changes in elastic modulus, density, transparency,

melting behaviour and changes in crystallinity.

b) Evolution of gas

This is mainly hydrogen with a small percentage of hydrocarbon. The hydrocarbon fraction contains mainly C_2 , C_3 and C_4 compounds (7) which may explain the 'breaking-off' of the side chains.

c) Decay of vinyl and vinylidene unsaturation.

d) Formation of transvinyl (t-V₁) unsaturation

The concentration of t-V₁ may continue to rise or fall for some time after the irradiation has ceased, probably as a result of reactions of the radicals trapped in the polymer.

e) Formation of radicals and other reactive Intermediates

Dole and his associates (13,20,21) have worked extensively on the identification and reactions of such reactive intermediates using U.V. and I.R. spectroscopy and E.S.R. in order to study the reactive intermediate formed. The evidence indicates that irradiation of polyethylene leads to the formation of a host of reactive species, including positive ions, trapped electrons, electronically excited groups, alkyl and alkyl free radicals and atomic hydrogen.

The work of Odian and Bernstein (22) relates closely to the subject of this thesis. They crosslinked polyethylene in the presence of allylmethylacrylate (AMA) using ^{60}Co . Odian also used other polyfunctional monomers such as allyl acrylate and diallylmaleate.

It was found that in the presence of different polyfunctional monomers the radiation crosslinking was greatly enhanced but difunctional monomers such as styrene and methyl methacrylate did not increase the crosslinking of polyethylene. Charlesby (23) however, incorporated acrylic acid with the irradiated polyethylene which tends to enhance crosslinking with doses far below these needed for conventional crosslinking.

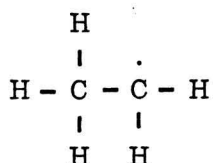
4.3.2 Photochemically Cured Polyethylene

The effects of ultraviolet light on polymers are of practical importance. These effects have been extensively studied by experiments following the degradation, crosslinking, gas evolution and E.S.R.

The wavelengths of typical ultraviolet lines from a mercury lamp are 253, 313 and 365 nm, which correspond to 4.88, 3.95 and 3.39 eV respectively. Common chemical bonds in polyethylene i.e. C-H and C-C have bond strengths of 4.28 and 3.44 e.v. respectively (24). It is therefore expected that ultraviolet light quanta will break chemical bonds somewhat selectively, giving free radicals, where as ionizing radiation with

much higher energy per particle may break the bonds more or less at random.

Maas and Volman (25) suggested the possibility that C-C bonds are broken by ultraviolet light. Free radicals from U.V. irradiation of polyethylene were observed by Ranby (26,27), using E.S.R. Polyethylene irradiated by U.V. light at 77 K gives free radicals



Later it was found out by E.S.R. studies that $\dot{\text{C}}\text{H}_2 - \dot{\text{C}}\text{H} - \text{C}\text{H}_2$ and $-\text{C}\text{H}_2 - \dot{\text{C}}\text{H}_2$ free radicals will be produced when polyethylene is irradiated by ultraviolet light (28). Further, it is reported by Tsuji⁽²⁸⁾ that $-\text{C}\text{H}_2 - \dot{\text{C}}\text{H} - \text{C}\text{H}_2$ is the main free radicals formed with U.V. irradiation. However, when U.V. irradiation is carried out with wavelengths longer than 300 nm, the radical formation was sensitized by addition of an aromatic compound (29). Since the incident light with longer wavelengths > 300 , only is absorbed by the aromatic molecules, it was suggested that the radical formation is related to a bi-photon absorption of the incident photons by the aromatic molecules, followed by energy transfer mainly to C=C bonds in polyethylene, which causes allylic radical formation. Takeshita's⁽²⁹⁾ studies were again based on the E.S.R. analysis.

However, to obtain a crosslinked polyethylene by U.V. light (near U.V.), a sensitizer should be introduced. U.V. sensitizers such as benzophenone may be used or xanthone which has been used in this programme. Peroxides could be initiated thermally causing crosslinking.

It was found that ultraviolet crosslinking of polyethylene with peroxides and thermally crosslinked polyethylene affects the mechanical, physical and morphological properties Miltz (30), Dannenberg (31). This was also reported by Oster et al (32).

The ultraviolet method has a number of advantages over the ionizing radiation method. Oster introduced sensitizer into the polyethylene film prior to its fabrication. Alternatively, the film may be soaked for a few minutes in a solution of benzophenone.

It was also found by Bonotto (33) that the efficiency of the crosslinked product improved with the additions of coagents. Bonotto found that the coagent with multifunctional system is more efficient than the coagent with a linear molecule with shortest spacings; than the coagent with the maximum compatibility and intermediate spacing and also more efficient than the coagent with the maximum spacing between crosslinking sites.

In general, crosslinking of low density polyethylene by U.V. light increases its tensile strength and toughness, improves abrasion resistance and resistance to deformation at elevated temperatures, to other environmental conditions and to many chemicals. Researchers agreed that crosslinking of ethylene polymers occurs because the free radicals resulting from the decomposition of the organic peroxide abstract hydrogen from the polymer chains, replacing it with carbon atoms, which produce linkages between the chains.

The organic peroxide used must be one that will not decompose prematurely during the initial compounding and forming processes.

Dicumyl peroxide, $\text{C}_{10}\text{H}_{18}\text{O}_2$, bis (t-butyl peroxy)diisopropyl benzene and 2,5, - dimethyl - 2,5, - bis (2-ethyl hexanoyl peroxy)hexane are the leading peroxides used for crosslinking low density polyethylene. The system which has been used during the course of this work, has not been commonly used and the crosslinking agent (coagent, monomer) has not been used in such a mixture of these compounds together. Although much fundamental and extensive work has been carried out with the irradiated polyethylene using some model compounds, such as hydrocarbons, not many fundamental studies if any, have been carried out with a system involving photo-curing by sensitizer and in the presence of a coagent.

4.3.3 Methods for analysing and characterizing the crosslinked polyethylene

During the crosslinking process and the formation of the network, the polymer will form some insoluble fraction (Gel part) while uncrosslinked polymer will remain soluble (sol part). To evaluate the crosslinking process, the gel content may be determined. Analysis of the sol part by GPC will give a very useful piece of information. Characterization of gel by measuring the swelling ratio in the gel part may be used to determine the density of crosslinkages using the Flory equation (34).

The statistical theory of crosslinking was first proposed by Flory (35) who looked at the conditions required for the formation of an infinite three dimensional network (gel) when linking together molecular species of finite dimensions. The theory Flory has developed was, by his treatment to the gelation occurring in polycondensation reactions involving polyfunctional monomers and to the crosslinking of linear macromolecules originally having a uniform molecular weight distribution. He further developed his theory (34,36). Charlesby applied this theory to radiation crosslinking [37,38]. As a full review of the structure and elasticity of non-crystalline polymer network was published by Dusek [39] only a few highlights will be referred to in this thesis.

When a crosslinking process starts in a polymer, which is assumed to be composed initially of linear chains of uniform molecular weight M_1 , the reaction products formed in the early stages are branched macromolecules with increasing molecular weights $2M$, $3M$ XM in which they have the same probability of reacting with another molecule and then crosslinking proceeds step by step. Formally, such a reaction is equivalent to the polycondensation of a polyfunctional monomer, which also proceeds via successive steps of similar type. Thus a statistical treatment analogous to the theory developed for polycondensation reactions can be applied to the random crosslinking of macromolecules. If crosslinks are assumed to occur at random, the resultant change in molecular weight, solubility, elastic modulus, and swelling in solvents can be deduced theoretically from the number of crosslinks. The first two properties depend on the probability that an individual molecule is linked to its neighbour and the relevant variables to study the average number of crosslinks per molecule.

Elasticity and swelling on the other hand depend on the thermodynamic behaviour of flexible chains restrained at both ends. The equilibrium position is determined by the chain length between crosslinks, the average kinetic energy (i.e. temperature) and the applied stresses. The density of the crosslinks is a

relevant factor along the molecular chain or alternatively the average molecular weight between successive crosslinks, e.g. $\frac{\text{number of crosslinked units}}{\text{per number average molecule}}$ is referred to as the crosslinking index ' γ ' and per weight average molecule is referred to as the crosslinking coefficient ' δ '. The proportion of main chain units crosslinked is known as the crosslinking density ' Q '. ' M_c ' is the number average molecular weight between crosslinks. M_c is a fundamental quantity on which depends the elastic properties and the swelling behaviour of a fully crosslinked network.

$$M_c = W/Q \quad (1.1)$$

where W is the molecular weight of the polymer unit. The other two concepts used are crosslinking coefficient and crosslinking index, in which the relation between the two varies according to the polymer used.

For monodisperse polymers,

$$\begin{aligned} \bar{P}_w &= \bar{P}_n \\ \delta &= \gamma \end{aligned} \quad (1.2)$$

For polymers having the most probable distribution (random distribution),

$$\begin{aligned} \bar{P}_w &= 2 \bar{P}_n \\ \delta &= 2\gamma \end{aligned} \quad (1.3)$$

If the Polymer has a very broad molecular weight distribution i.e.,

$$\begin{aligned} \bar{P}_w &= x\bar{P}_n \\ \text{then } \delta &= x\gamma \end{aligned} \quad (1.4)$$

\bar{P}_w = weight average degree of polymerization of
the original polymer

\bar{P}_n = number average degree of polymerisation of
the original polymer

$$\text{where } \bar{P}_w = \frac{\bar{M}_w}{w} \text{ and } \bar{P}_n = \frac{\bar{M}_n}{w}$$

For irradiated crosslinked polyethylene γ and δ
will be represented in reference to \bar{P}_w and \bar{P}_n as
follows (24).

$$\gamma = q\bar{P}_n \quad (4.5)$$

$$\delta = q\bar{P}_w \quad (4.6)$$

When the polymer is irradiated and crosslinks,
the links formed between the molecules decreases the
number of separate molecules, and also increases their
average size (Flory 34).

The point at which an insoluble network first
begins to form is termed the gel point. The gel point
is determined by the simple condition $\delta = 1$
(Flory 34). The specimen first starts to become
insoluble when there is an average of one crosslinked
unit per weight average molecule. This is true

regardless of the initial molecular weight distribution. Up to the gel point, the polymer is still soluble and no network structure has been formed, where $\delta < 1$. The only radiation effect will be to increase the average molecular weight and the degree of branching. Each link decreases the number of separate molecules by one. Beyond the gel point the number average of the sol fraction falls. At the gel point the \bar{M}_w and \bar{M}_z of the gel will rise to infinity as shown in Fig. (4.1) below.

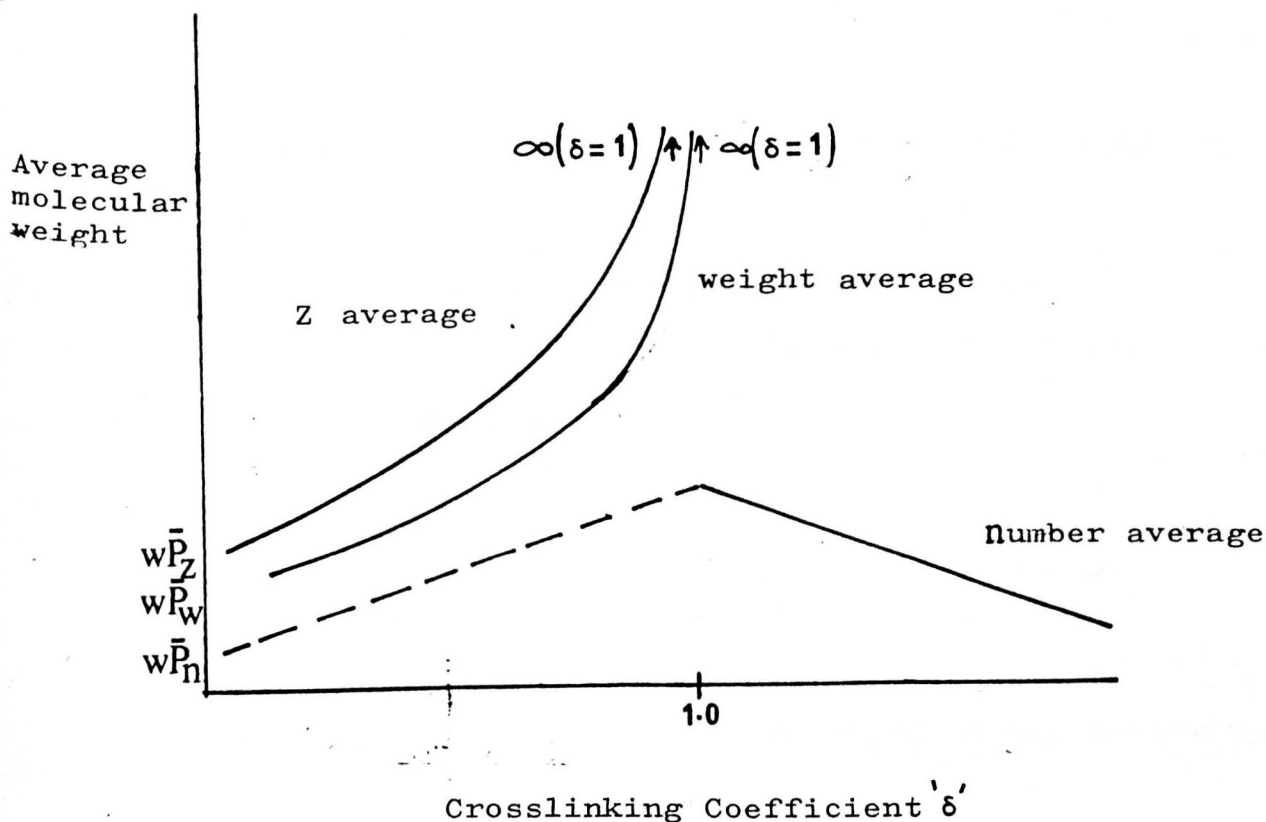


Fig. 4.1 Arbitrary initial distribution

Increase in number average, weight average and Z average up to the gel point. Beyond this point the number average of the sol fraction falls.

Whereas the weight average molecular weights of the polymer tends to infinity at the gel point as shown above, the number average molecular weight reaches a finite value when the crosslinking coefficient equals unity. Charlesby proposed (38) that the ratio of number average molecular weight at the gel point $(\bar{M}_n)_g$ to its initial value \bar{M}_n is directly related to the ratio of number average to weight average molecular weight in the original polymer. The equation will be

$$(\bar{M}_n)_g / \bar{M}_n = 1 - \frac{\bar{M}_n}{2\bar{M}_w} \quad (4.7)$$

The ratio of the weight average molecular weight of polymer, prior to gelation, to its original value does not depend on the initial molecular weight distribution. The following equation will be valid throughout the pre-gel range (38).

$$\frac{\bar{M}_w'}{\bar{M}_w} = \frac{1}{1 - \delta} \quad (4.8)$$

The above equation could be modified in the following form.

$$\frac{1}{\bar{M}_w'} = \frac{(1 - \delta)}{\bar{M}_w} \quad (4.9)$$

This shows that the reciprocal of the weight average molecular weight is a linear function of the crosslinking coefficient.

After the gel points the average molecular weight of the sol fraction steadily decreases. This is because of the assumption that the largest molecules will be linked first to the gel and the lowest molecular weight fraction will remain unattached and soluble.

A general expression is derived by Flory relating the gel fraction $[W_g = 1 - W_s]$, to the crosslinking coefficient ' δ ' in terms of the initial molecular weight distribution; where W_g is the gel weight fraction and W_s in the sol weight fraction.

If the initial distribution is uniform then the expression will be

$$W_g = 1 - \exp(-\delta / 1 - W_s) \quad (4.10)$$

and for sol fraction it will be

$$W_s = \exp(-\delta / 1 - W_s) \quad (4.11)$$

or,

$$W_s = 1 / (1 + \gamma - \gamma W_s)^2 \quad (4.12)$$

For random initial distribution

or could be written in the simpler form

$$W_s + \sqrt{W_s} = \frac{1}{Y} = \frac{2}{\delta} \quad (4.13)$$

For pseudo-random distribution the formula becomes

$$W_s = \frac{1}{\delta} \quad (4.14)$$

In all cases the formulae only apply if $\delta \gg 1$. Below this value $\delta=1$

Alternative methods of network formation are due to polycondensation or polyfunctional addition monomers. In polycondensation, Flory used the branching coefficient ' α_b ' as a function to calculate the weight fraction of the various species. The branching coefficient may be defined as the probability that a polymer branch of weight ' M ' connected to a branch point, selected at random in the molecule, causes another branch point. The gel point in the polycondensation is directly connected with the branching coefficient ' α_b '.

Infinite network formation becomes possible when the expected number of chains, which will succeed a certain number of chains through branching them, exceeds this number, i.e. if the product $\alpha_b (f-1)$ exceeds unity (f is the functionality of the branch points). The critical value of the branching coefficient is therefore.

$$(\alpha_b)_c = \frac{1}{f} - 1 \quad (4.15)$$

The branching coefficient may be calculated from the probabilities that functionalities have reacted. This could be calculated experimentally.

As the condensation reaction starts [Flory 34], the number of molecules is decreased and the number average degree of polymerisation becomes,

$$\bar{P}_n = 1 / (1 - \frac{1}{2} \alpha f) \quad (4.16)$$

at the gel point,

$$\bar{P}_n = 1 / (1 - \frac{1}{2} (\alpha_b)_c f) = 2(f-1)/(f-2) \quad (4.17)$$

where the weight average degree of polymerization will be

$$(4.18)$$

$$\bar{P}_w = (1 + \alpha) / [1 - \alpha(f-1)] \quad (4.18)$$

which will become infinite at the gel point.

In the system with which this thesis is involved, crosslinking formation is a mixture of the two networks since the polyethylene contains a crosslinking agent which is a hexafunctional group.

The network formation is influenced in possible structural imperfections, which may be introduced or fixed as a result of the crosslinking.

The type and extent of imperfections depend on the type of network formation.

- a) Crosslinking polymerization (e.g. radical or ionic copolymerization, polycondensation, or poly-addition).
- b) Crosslinking of existing polymer chains.
- c) Joining of active chain ends into crosslinks. (and linked networks).

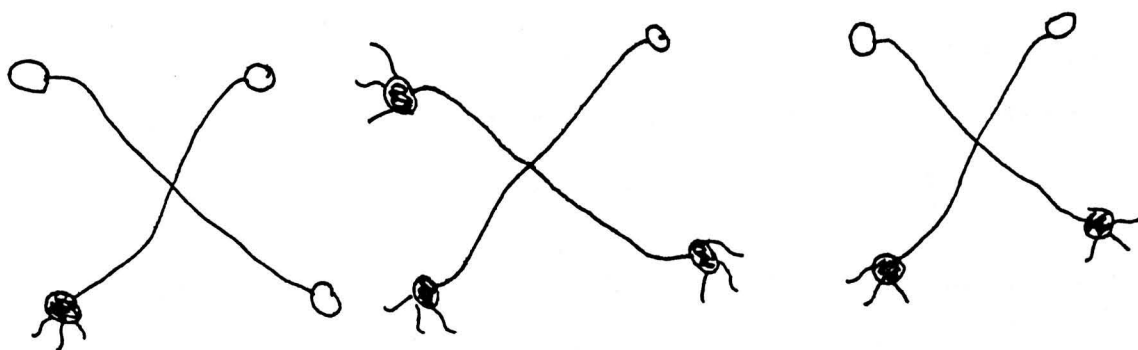
Other imperfections are developed in the process of crosslinking such as network defects, unreacted functionalities, intramolecular loops, chain entanglements, inhomogeneity in crosslink distribution or heterogeneity of the network due to phase separation. The latter possibility exists in crosslinking of polymer to itself by added monomer (e.g. as in the system used in this work).

The structure of the network is closely related to the network formation process, of which the general picture is well known. In the first stages the molecular weight increases through branching and its weight average reaches an infinite value at the gel point.

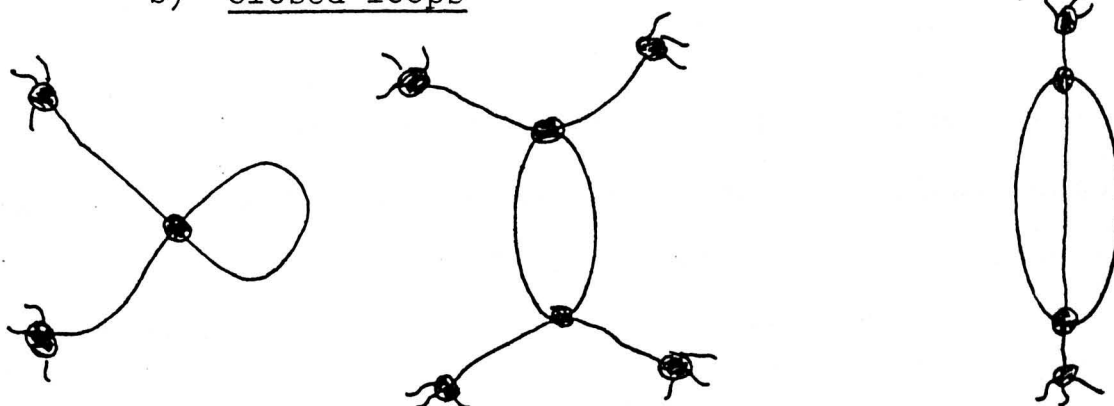
Even beyond the gel point, finite species (sol fraction) still coexist which is gradually attached to

the infinite network as the crosslinking reaction proceeds. Even if completely homogeneous and disordered in a relaxed state, a real network differs from the ideal network because of the networks defects. Three types of defects are commonly considered to be present in the polymer network.

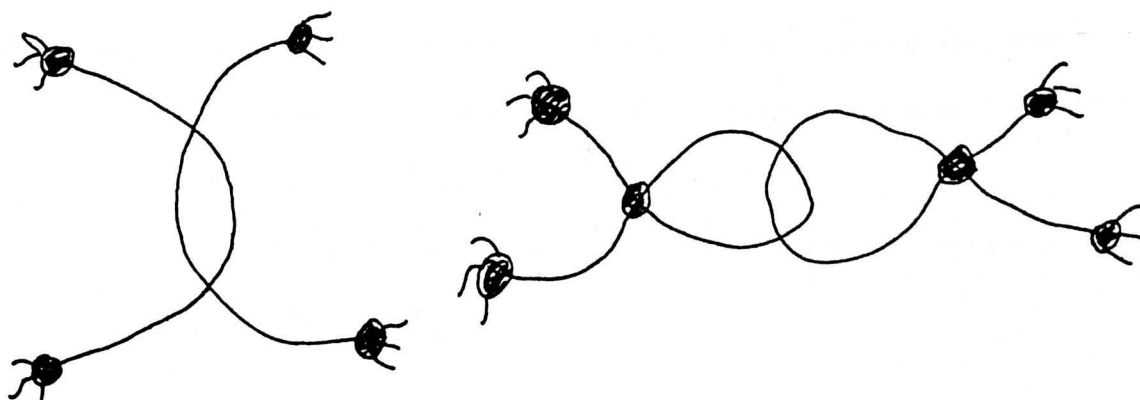
a) unreacted functionalities



b) Closed loops



c) Permanent chain entanglements



Within each group there are several possibilities dependent on the arrangement of chains; the effect of defects on the elastic properties of the network is thus by no means simple (40).

As mentioned earlier in this section, characterization of the network is possible by the thermodynamic behaviour of the network as a function of elasticity and swelling. The elastic properties of a crosslinked network arise from the entropy decrease which results when external constraints impose a less statistical probable arrangement on the units.

The number of network chains active in the elastic behaviour of networks, (elastically effective chains) can be obtained from the equilibrium behaviour of networks, subjected to various types of stress.

Charlesby summarised in his work (24) the calculation of the elastic modulus for the three dimensional network based on Kuhn, Wall, Treloar and Flory (43,44,45, 46, 34).

$$E = n \rho RT/M_c \quad (4.19)$$

where ρ : is the density of the crosslinked polymer
 n : constant which in the simplest case is 3
 R : Gas constant
 T : Temperature in K at which the modulus was measured.

M_c : number average molecular weight between links.

The above equation could be written in another form where $M_c = w/q$

$$E = nPRTQ/W \quad (4.20)$$

Owing to the considerable assumptions and simplifications made in deriving this theory, a note of caution must be sounded in applying it to quantitative measurements on crosslinked polymers.

This equation should be modified in the presence of network defects such as end effects or entanglements. Free chain ends (unreacted functionalities) reduce the number of active network chains in a network, compared with the network which is without the free ends.

In the case of entanglements, when the chain is sufficiently tangled together, it may cause considerable hindrance to the motion of the molecules passing each other without being crosslinked. Charlesby proposed (24), that the addition of parameter $g > 1$ because of the entanglements will cause an increase in the elastic modulus. So the elastic modulus equation will become,

$$E = nPRTg/M_c \quad (4.21)$$

Equation 4.21 which applies to amorphous polymers may be used normally for crystalline polymer (6) providing that modulus measurements were carried out above the T_m of the polymer.

Characterizing the gel content by swelling measurements will be valuable. Flory (34) developed the theory of the isotropic swelling of crosslinked amorphous polymers. The derivation of the equilibrium swelling of a gel in solvent was based on the entropy of mixing and the entropy of chain configuration. Swelling in the gel is determined by the density of crosslinks and the type of solvent used. Crystalline polymers which are not soluble in solvent are barely swollen unless the temperature is raised to a point at which some crystalline regions start to melt. So if the swelling equilibrium for the polymer network is measured, one should take into account the swelling due to the crystalline region or else the swelling will only be carried out in the gel portion.

When a polymer molecule is dissolved, there is a heat of mixing due to the interaction energy of polymer and solvent, also in addition there is a change in entropy of the system. In the case of a crosslinked polymer, the solvent molecules will have the tendency to enter the polymer network, in which swelling will take place in the form of a three dimensional stretching

of the individual chains. Flory (34) equation for the equilibrium swelling is

$$v_1 \left(\frac{v_e}{V_0} \right) \left(v_{2m}^{1/3} - v_{2m}/2 \right) + \ln^{1 - v_{2m}} + v_{2m} + \chi v_{2m}^2 = 0 \quad (4.22)$$

v_1 is the molar volume of the solvent

v_{2m} is the ratio of the volume of the unswollen polymer V_0 to the volume of the swollen polymer V at the swelling equilibrium.

$$\text{i.e.} \quad v_{2m} = V_0/V$$

v_{2m} could be replaced by the swelling ratio V which is the reciprocal of v_{2m}

$$\text{i.e.} \quad V = v_e/v_0$$

v_e/v_0 is the density of crosslinkages, where v_e is the effective number of chains connecting the crosslink points.

The characterization may be defined in terms of M_c , therefore the quantity v_e/v_0 will be replaced by the term ρ/M_c according to the terminology used in the Rubber Elasticity theory.

$$\ln^{1-\nu_{2m}} + \nu_{2m} + \chi \nu_{2m}^2 + \frac{\nu_1 P}{M_c} \left(\nu_{2m}^{1/3} - \nu_{2m}/2 \right) = 0 \quad (1.23)$$

where P is the polymer density

χ is the polymer solvent interaction, which is the heat of mixing term, arising from the heat of interaction between solvent and the network.

This parameter was introduced by Huggins (17) and Flory (18). Determination of the polymer - solvent interaction parameter may be carried out by osmotic pressure, gas liquid chromatography or freezing point depression of solvent. A review of these methods of determination and others are covered by Orwoll (19).

If the degree of swelling is large (ν_{2m} small), the equation may be simplified (Flory 31).

$$(0.5 - \chi) \nu_{2m}^2 = P \nu_1 \nu_{2m}^{1/3} / M_c \quad (1.24)$$

or by replacing ν_{2m} by $1/V$ then the equation becomes

$$V^{5/3} = (0.5 - \chi) M_c / P \nu_1 \quad (1.25)$$

It was observed by Flory (31) that at swelling equilibrium, the degree of swelling invariably decreases with increasing degree of crosslinking.

4.4 Characterisation of Polyethylene - TAC network cured by ultra violet light

The system in which this work is involved will be more complicated to understand since the polyethylene is crosslinked in the presence of a hexafunctional crosslinking agent. The polyethylene network prepared in this programme was characterized by measuring the gel content in reference to the time of crosslinking, concentration of the photosensitizer and the crosslinking agent. M_c was calculated by using swelling equilibrium equation and it will be compared by M_c calculated from the elastic modulus equation, which will be discussed in the next chapter.

The previous section covered the characterizing, which mainly covered a network which was a completely homogeneous structure. It should be taken into consideration, that since the system initially ^{is} not compatible, ^{this} could lead to a crosslinking process with aggregation of network elements. It was postulated by Odian (22), that when polyethylene was crosslinked in the presence of allyl methacrylate (AMA), using ^{60}Co γ - irradiation, the (AMA) will polymerize forming a low molecular weight grafted with polyethylene chains, which in turn will lead to the formation of three dimensional crosslinked network.

It was shown, in the previous Chapter, that by using a low molecular weight hydrocarbon the (TAC) will polymerize and form a fine crosslinked poly(TAC) separated from the hydrocarbon.

In the following sections, the presence of such separate phases within the network will be considered, especially when specimens of gel should be studied under the electron microscope.

4.5 Experimental

4.5.1 Materials Used

Low density Polyethylene:- The polymer used^{was}/supplied by I.C.I. Corporate Laboratories, grade 17/00/04 with melt flow index of 7.32 gm/10 min.

The polymer has the following molecular weight specification [$\bar{M}_n = 18,000$, $\bar{M}_w = 11,600$, $\bar{M}_w/\bar{M}_n = 6.11$]. From the X-ray analysis, the crystallinity of polymer was about 43% with density of 0.92 g/ml.

Xanthone:- The photoinitiator which was supplied^{was} by B.D.H./recrystallised by dissolving in acetone (Analar grade), then filtered, dried and kept in the dark.

Triallyl Cyanurate (TAC):- The crosslinking agent (monomer) was manufactured by Cyanamide of America. This polyfunctional monomer was recrystallised by dissolving in n-hexane, filtered and dried. The melting point of the monomer was 31°C. Under 0.5 mm Hg the monomer boiling point is 140°C. Density at 30°C is 1.1133 g/ml with refractive index $D^{25}_D = 1.5049$. The monomer was relatively stable under nitrogen even at 125°C for up to 24 hours.

4.5.2 Equipment Used

An ultra violet lamp was used for curing, which was made by Thorn lighting [400 W curing lamp. Metal halide sealed, beam lamp MB1 Par 64) is a high pressure metal halide quartz arc lamp, enclosed in a sealed beam envelope with internal reflector providing a radiation as shown in Fig.4.2, primarily in the 417 nm waveband. The overall width of the lamp is 205 mm. The recommended life time is about 1000 hours. The intensity of the lamp was followed regularly with UV intensimeter. The lamp unit is fitted with a spreader lens to give an elliptical light distribution, capable of giving reasonably uniform radiation over a 90 x 60 cm area at a distance of approximately 60 to 90 cm.

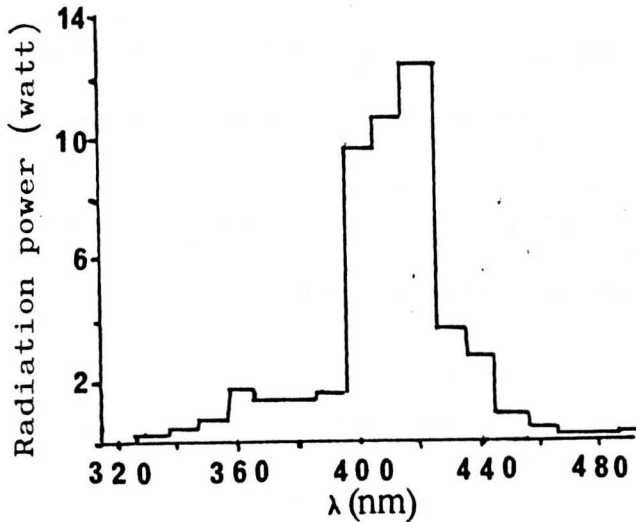


Fig.4.2: The spectral energy distribution curve of the ultraviolet lamp.

4.5.3 Preparation of polyethylene batches and films with the additives

A number of polymer, TAC, Xanthone batches were prepared by using different concentrations of the additives. Two batches were prepared by mixing the polyethylene with one of the additives. The following procedure was used in the preparation of the different batches.

The desirable amount of TAC and Xanthone were dissolved in 200 ml of toluene and added to low density polyethylene. This blend was sealed in glass and thermostatted at 60°C for 48 hours then under vacuum for five days to remove the toluene. The mixture so formed was finally roll-milled for five minutes while maintaining the roll temperature at 140 ± 5°C. The product sheet was cooled in liquid nitrogen and granulated.

The following table (4.1) shows the symbols used for each batch with the concentration of the additives.

Table 4.1

<u>Symbol Per Batch</u>	<u>TAC Concentration % w/w</u>	<u>Xanthone Concentration % w/w</u>
PE/1	0.5	0.1
PE/2	1.0	0.1
PE/3	3.0	0.1
PE/4	5.0	0.1
PE/6	0.5	0.25
PE/7	1.0	0.25
PE/X	-	0.1
PE/M	0.5	-

Sheets were made from three different batches, by pressing at 160°C in between Melinex sheets which were backed by stainless steel plates. This procedure was fast and efficient. The sheet thickness was controlled by putting a brass frame in between the two Melinex sheets. The two stainless steel plates were 12 x 12 cm². The brass frame was 0.25 mm thick and covered the stainless steel area. The press used had electrically heated upper and lower plates, controlled by a thermocouple. The pressure used was about 900 PSI. During pressing, the polyethylene was placed between the two plates at this pressure and 160°C for one minute then allowed to cool to room temperature. The thickness of polyethylene film made was 0.35 ± 0.05 mm

4.5.4 Curing of Polyethylene by Ultraviolet light

The curing was carried out inside a simple radiation vessel made in the department and shown in Fig.4.3, to allow the curing to be carried out in the presence or absence of oxygen. The ultra violet lamp used is described in Section 4.5.2. The radiation vessel was kept inside a box in which the temperature was controlled by means of a thermocouple and may be raised to the temperature required by means of heating the element surrounding the box.

The polyethylene samples of size 7 cm x 4 cm were usually placed in a sample holder and left inside

the vessel. The sample holder comprised two aluminium frames between which the polyethylene samples were placed.

The distance of 30 cm between the lamp and the polyethylene samples was kept constant at all times. When curing was carried out in the absence of air, a stream of nitrogen gas was passed through one side of the vessel and a water pump connected to the other side of the vessel. The nitrogen gas was normally passed through the vessel ten minutes before curing started and kept until the end of the curing time. No nitrogen gas was used when curing in the presence of air. After irradiation, the samples were analyzed for gel content, Gel permeation chromatography analysis (GPC) and for flow properties.

For other tests such as tensile and environmental stress cracking (ESC), the full polyethylene sheet was cured by leaving it inside the temperature control box without using the irradiation vessel. The distance between lamp and the samples was maintained at the same 30 cm. Some gel content measurements for the samples prepared by the latter method were carried out since the intensity of light penetration throughout the samples is different because of the radiation vessel. The radiation vessel which was made of pyrex glass was expected to absorb a limited amount of the light.

4.5.5 Measuring the Gel Content

The gel content was extracted by refluxing in a soxhlet apparatus for 72 hours using refluxing xylene (150 ml) containing antioxidant[†](0.5 g). The flask was covered with aluminium foil to prevent further light initiated changes from occurring.

Individual samples were weighed and kept inside the soxhlet thimble of known weight. The weight of the soxhlet was recorded after leaving under vacuum at 60°C to remove any moisture present both before and after extraction. The soluble polyethylene extract precipitated in the main solvent flask after cooling down the content of the flask. It was filtered and dried under vacuum, then analysed by gel permeation chromatography. The results are given in tables 4.2 to 4.14.

[†] Antioxidant used is 2,6Di-Tert-Butyl-4-methyl phenol 99%
m.w. = 220.36.

TABLE 4.2: Ultra Violet Curing of PE/1 Batch Film
Thickness of 0.9 ± 0.05 mm

<u>Sample Ref. No</u>	<u>Curing time mins</u>	<u>Curing temp. °C</u>	<u>Atmosphere</u>	<u>% Gel Content</u>
LP/1/9/60	60	60	Nitrogen	43.17
LP/1/8/60	30	60	'	35.04
LP/1/7/60	15	60	'	32.32
LP/1/6/60	10	60	'	21.66
LP/1/5/60	5	60	'	0.66
LP/1/4/60	4	60	'	No gel
LP/1/3/60	3	60	'	'
LP/1/2/60	2	60	'	'
LP/1/1/60	1	60	'	'
LP/1/9/120	60	120 ± 5	'	50.28
LP/1/8/120	30	120 ± 5	'	47.29
LP/1/7/120	15	120 ± 5	'	36.46
LP/1/6/120	10	120 ± 5	'	32.29
LP/1/5/120	5	120 ± 5	'	7.13
LP/1/4/120	4	120 ± 5	'	No gel
LP/1/3/120	3	120 ± 5	'	No gel
LP/1/2/120	2	120 ± 5	'	No gel
LP/1/1/120	1	120 ± 5	'	No gel
OLP/1/9/60	60	60	Oxygen	21.67
OLP/1/8/60	30	60	'	18.59
OLP/1/7/60	15	60	'	4.91
OLP/1/6/60	10	60	'	4.49
OLP/1/5/60	5	60	'	No gel
OLP/1/4/60	4	60	'	'
OLP/1/3/60	3	60	'	'
OLP/1/2/60	2	60	'	'
OLP/1/1/60	1	60	'	'

TABLE 4.3: Ultra violet Curing of PE/2 Batch Film
Thickness of 0.3 ± 0.05 mm

<u>Sample Ref No.</u>	<u>Curing time mins</u>	<u>Curing temp. °C</u>	<u>Atmosphere</u>	<u>% Gel Content</u>
LP/2/9/60	60	60	Nitrogen	46.52
LP/2/8/60	30	'	'	46.62
LP/2/7/60	15	'	'	29.53
LP/2/6/60	10	'	'	20.63
LP/2/5/60	5	'	'	No gel
LP/2/4/60	4	'	'	'
LP/2/3/60	3	'	'	'
LP/2/2/60	2	'	'	'
LP/2/1/60	1	'	'	'
LP/2/9/120	60	120 ± 5	'	51.71
LP/2/8/120	30	'	'	49.60
LP/2/7/120	15	'	'	43.61
LP/2/6/120	10	'	'	38.29
LP/2/5/120	5	'	'	1.76
LP/2/4/120	4	'	'	No gel
LP/2/3/120	3	'	'	No gel
LP/2/2/120	2	'	'	No gel
LP/2/1/120	1	'	'	No gel
OLP/2/9/60	60	60	oxygen	19.57
OLP/2/8/60	30	'	'	16.76
OLP/2/7/60	15	'	'	9.34
OLP/2/6/60	10	'	'	5.75
OLP/2/5/60	5	'	'	No gel
OLP/2/4/60	4	'	'	'
OLP/2/3/60	3	'	'	'
OLP/2/2/60	2	'	'	'
OLP/2/1/60	1	'	'	'

TABLE 4.4: Ultra Violet Curing of PE/6 Batch Film
Thickness of 0.3 ± 0.05 mm

<u>Sample Ref No.</u>	<u>Curing time mins</u>	<u>Curing temp. °C</u>	<u>Atmosphere</u>	<u>% Gel Content</u>
LP/6/9/60	60	60	Nitrogen	61.70
LP/6/8/60	30	'	'	56.46
LP/6/7/60	15	'	'	51.94
LP/6/6/60	10	'	'	46.91
LP/6/5/60	5	'	'	19.53
LP/6/4/60	4	'	'	23.12
LP/6/3/60	3	'	'	No gel
LP/6/2/60	2	'	'	'
LP/6/1/60	1	'	'	'
LP/6/9/120	60	120 ± 5	'	48.02
LP/6/8/120	30	'	'	52.56
LP/6/7/120	15	'	'	46.30
LP/6/6/120	10	'	'	40.45
LP/6/5/120	5	'	'	19.71
LP/6/4/120	4	'	'	10.07
LP/6/3/120	3	'	'	1.22
LP/6/2/120	2	'	'	No gel
LP/6/1/120	1	'	'	No gel

TABLE 4.5: Ultra Violet Curing of PE/7 Batch Film
Thickness of 0.3 ± 0.05 mm

<u>Sample Ref No.</u>	<u>Curing time mins</u>	<u>Curing temp. °C</u>	<u>Atmosphere</u>	<u>% Gel Content</u>
LP/7/9/120	60	120 ± 5	Nitrogen	65.21
8/120	30	'	'	60.31
7/120	15	'	'	57.52
6/120	10	'	'	47.61
5/120	5	'	'	36.46
4/120	4	'	'	1.45
3/120	3	'	'	No gel
2/120	2	'	'	'

The U.V. curing for the samples in tables 4.2, 4.3, 4.4 and 4.5 were carried out inside the reaction vessel. Samples were however, irradiated without using the radiation vessel and in these cases all samples were irradiated in the presence of oxygen. Also, some polyethylene sheets were cured by ^{60}Co γ -irradiation. This was carried out at S.U.R.R.C. The process was in the presence of oxygen and at room temperature. The following tables show the Gel content for samples which were cured by U.V. light without using the radiation vessel and also for those samples cured by γ -irradiation.

TABLE 4.6: Ultra Violet Curing of PE/1 Batch Film
Thickness of 0.3 ± 0.05 mm

<u>Sample Ref No</u>	<u>Curing time mins</u>	<u>Curing temp. °C</u>	<u>% Gel Content</u>
PE/1/10/60	12 hours	60	25.42
9/60	60 mins	'	21.61
8/60	30 '	'	20.95
7/60	15 '	'	25.41
6/60	10 '	'	20.33
5/60	5 '	'	12.48
4/60	4 '	'	5.43
3/60	3 '	'	No gel
2/60	2 '	'	No gel
1/60	1 '	'	No gel
9/120	60 '	120 ± 5	21.95
8/120	30 '	'	25.80

TABLE 4.7: Ultra Violet Curing of PE/2 Batch Film
Thickness of 0.3 ± 0.05 mm

PE/2/10/60	12 hours	60	29.43
9/60	60 mins	'	22.34
8/60	30 '	'	20.79
7/60	15 '	'	20.99
6/60	10 '	'	16.52
5/60	5 '	'	10.38
4/60	4 '	'	10.34
3/60	3 '	'	0.58
2/60	2 '	'	No gel
9/120	60 '	120 ± 5	31.36
8/120	30 '	'	40.67

TABLE 4.8: U.V. Curing of PE/3 Batch film thickness
of 0.3 ± 0.05 mm

PE/3/9/60	60	60	17.47
8/60	30	60	16.67
7/60	15	'	17.08
6/60	10	'	13.77
5/60	5	'	10.8
4/60	4	'	9.42
3/60	3	'	0.54
2/60	2	'	No gel
1/60	1	'	No gel
9/120	60	120 ± 5	31.36
8/120	30	'	13.85

TABLE 4.9: U.V. Curing of PE/4 Batch film thickness
of 0.3 ± 0.05 mm

PE/4/9/60	60	60	13.22
8/60	30	60	12.84
7/60	15	'	15.36
6/60	10	'	11.87
5/60	5	'	7.64
4/60	4	'	10.08
3/60	3	'	0.62
2/60	2	'	No gel
1/60	1	'	No gel
9/120	60	120 ± 5	42.57
8/120	30	'	42.41

TABLE 4.10: U.V. Curing of PE/6 Batch film thickness of
0.3 \pm 0.05 mm

PE/6/10/60	12 (hrs)		41.15
9/60	60 mins	60	34.98
8/60	30	60	35.23
7/60	15	60	13.83
6/60	10	60	19.75
5/60	5	'	8.08
4/60	4	'	6.93
3/60	3	'	3.84
2/60	2	'	No gel
1/60	1	'	No gel
9/120	60	120 \pm 5	50.15
8/120	30	'	41.22

TABLE 4.11: U.V. Curing of PE/7 Batch film thickness of
0.3 \pm 0.05 mm

PE/7/10/60	12 hrs	60	41.87
9/60	60 mins	'	36.36
8/60	30	'	30.24
7/60	15	'	28.36
6/60	10	'	16.99
5/60	5	'	11.07
4/60	4	'	5.24
3/60	3	'	No gel
2/60	2	'	No gel
1/60	1	'	No gel
9/120	60	120 \pm 5	42.52
8/120	30	'	41.79

TABLE 4.12: U.V. Curing of PE/X and PE/M batches films
thickness of 0.3 ± 0.05 mm

PE/X/8 /60	30	60	9.72
PE/M/9/60	60	60	No gel
PE/M/8/60	30	60	No gel

TABLE 4.13: Polyethylene film thickness 0.3 ± 0.05 mm
from Batch PE/M cured by ^{60}Co γ -irradiation
at 25°C.

<u>Sample Ref No.</u>	<u>Doses in Mrad</u>	<u>Gel Content %</u>
PE/M/D200	200	60.29
D100	100	67.58
D60	60	41.87
D40	40	15.43
D20	20	24.97
D12	12	19.81
D10	10	12.1
D6	6	3.13
D1	1	No gel

TABLE 4.14: Polyethylene film thickness of 0.3 ± 0.05 mm grade 17/00/04 with no additives, cured by ^{60}Co γ -irradiation at 25°C

<u>Sample Ref No.</u>	<u>Doses in Mrad</u>	<u>Gel Content %</u>
PE/D200	200	66.87
D100	100	65.73
D60	60	35.67
D40	40	21.97
D26	20	16.42
D12	12	20.12
D10	10	25.25
D8	8	18.62
D6	6	5.77
D2	2	No gel

4.5.6 Analysis of the Gel Part

The molecular weight of the crosslinks M_c was determined by the swelling measurements. The gel part of the irradiated samples was also analysed by I.R. for TAC content in the gel.

4.5.6.1 Swelling measurements

A known weight of the gel part of the different individual polyethylene samples was left in xylene (which was dried and distilled) for 48 hours at 85°C using a solid state bath. The polyethylene samples and

6 ml of xylene were left in a test tube and covered with rubber stoppers which were wrapped in aluminium foil. The time for the swelling equilibrium was determined to be about 30 hours. It was then decided to leave the individual samples for a further 18 hours to be marginally on the safe side. The polyethylene samples were left in a vacuum oven at 80°C for 24 hours and then having measured their weights, the swelling experiments were started.

After the 48 hours, each sample was dried by using filter paper and then weighed using the weighing bottle.

From the experimental data, the M_c was determined using equation 4.25.

From this equation 4.25

ρ : the polyethylene density considered to be 0.917 g/ml

v_1 = molar volume of the solvent was calculated by using the follow equation:-

$$v_1 = \frac{\text{molecular weight of xylene}}{\text{xylene density at } 85^\circ\text{C}} = \frac{106.17}{0.808} = 1.31 \times 10^2 \text{ mole volume}$$

The xylene density at 85°C was calculated according to the relation established by Johnson and T. Smith (52) which states,

$$\frac{d\rho}{dt} = -8 \times 10^{-4} \text{ g/ml}^\circ\text{C}$$

in which the xylene density at 20°C was considered to be 0.8600 g/ml.

χ = the interaction parameter was taken to be to be 0.27 using Orwall data (49).

V = which is the swelling ratio and equal to v/v_0

v_0 = the volume of the unswollen polymer
 = $\frac{\text{initial polymer weight}}{\text{polymer density}}$

and v = the volume of the swollen polymer at the swelling equilibrium
 = $\frac{\text{weight of the system (Polymer + solvent)}}{\text{density of the system } \rho_{\text{sys}}}$

The system density was determined using the following relationship.

$$\rho_{\text{sys}} = \rho_p W'_p + \rho_s W'_s$$

where ρ_p = Polymer density
 W'_p = Weight fraction of polymer in swollen network
 ρ_s = xylene density
 W'_s = weight fraction of xylene in swollen network.

The M_c data was calculated for the individual networks from the swelling measurements. This is shown in tables (4.15 - 4.21).

The crosslink density Q was determined using the simple relationship.

$$M_c = \frac{W}{Q}$$

where W is the molecular weight of the polyethylene unit i.e. ethylene unit which equals 28. Q values for the individual network determined from the swelling measurements are shown in tables (4.15 - 4.21). Also M_c and Q values are determined in reference to the crosslinking coefficient δ .

The determination of the latter was applied using the following relationship as mentioned in section 4.3.3.

The crosslinking coefficient ' δ ' was calculated from equation 4.14

$$W_s = 1/\delta$$

Where the W_s value was calculated from the gel content.

Using equation 4.6.1 the crosslinking density Q was determined.

$$\delta = Q \cdot \bar{P}_w$$

where \bar{P}_w = weight average degree of polymerization of the original polymer = $\frac{\bar{M}_w}{w}$

$$\bar{P}_w = \frac{110600}{28}$$

\bar{M}_w value measured by GPC as shown in section 4.5.10.

By determining Q the M_c values were also determined.

Tables (4.15 - 4.21) shows the M_c and Q values determined in reference to the crosslinking coefficient.

4.5.6.2 I.R. Analysis

I.R. quantitative analysis technique is a far from perfect tool for analysis especially when dealing with polymer films. However, it was noticed that two distinct peaks e.g. at 1560 cm^{-1} and 820 cm^{-1} characterise TAC in the I.R. spectrum of the polyethylene gel. For that reason, the I.R. analysis was used to determine roughly the amount of TAC present in the gel. Thin discs of the gel part were pressed at 190°C . The size of these discs were the same as the KBr discs which are commonly used in I.R. analysis. The profile thickness of the discs were considered to be the path length. The usual thickness obtained was around $0.09 \pm 0.02 \text{ mm}$.

By determining the extinction coefficient of TAC at 1500 cm^{-1} and 820 cm^{-1} , the concentration of TAC in

the individual gel was calculated from their spectra by applying Beer's law,

$$A = \log \frac{I_0}{I} = \epsilon lc$$

where A = absorption
l = path length in cm
C = percentage concentration
 ϵ = extinction coefficient

at 1560 cm^{-1} $\epsilon = 8000 \text{ ml g}^{-1} \text{ cm}^{-1}$

at 820 cm^{-1} $\epsilon = 1800 \text{ ml g}^{-1} \text{ cm}^{-1}$

Tables (4.22 - 4.26) show the % w/w TAC content of some selected gels in reference to one or both peaks.

TABLE 4.15

Sample Ref.No.	M_c Calculated from swelling measurements	Q	δ	Q calculated from δ	M_c calculated from δ
LP/L/9/60	2.303×10^5	1.24×10^{-4}	1.76	4.45×10^{-4}	6.29×10^4
LP/1/8/60	1.95×10^5	1.44×10^{-4}	1.54	3.9×10^{-4}	7.18×10^4
7/60	2.26×10^5	1.24×10^{-4}	1.48	3.7×10^{-4}	7.49×10^4
6/60	3.85×10^5	7.27×10^{-5}	1.28	3.23×10^{-4}	8.66×10^4
5/60	-	-	1.01	2.55×10^{-4}	1.10×10^5
9/120	8.49×10^4	3.3×10^{-4}	2.01	5.09×10^{-4}	5.49×10^4
8/120	-	-	1.90	4.8×10^{-4}	5.82×10^4
7/120	4.14×10^5	6.76×10^{-5}	1.57	3.98×10^{-4}	7.03×10^4
6/120	4.58×10^5	6.12×10^{-5}	1.48	3.74×10^{-4}	7.49×10^4
5/120	2.16×10^5	1.29×10^{-4}	1.08	2.73×10^{-4}	1.02×10^5
OLP/1/9/60	1.58×10^5	1.41×10^{-4}	1.28	3.23×10^{-4}	8.66×10^4
8/60	1.81×10^5	1.55×10^{-4}	1.23	3.11×10^{-4}	9.0×10^4
7/60	2.04×10^5	1.37×10^{-4}	1.05	2.66×10^{-4}	1.05×10^5
6/60	3.65×10^5	7.67×10^{-5}	1.04	2.65×10^{-4}	1.06×10^5

TABLE 4.16

Sample Ref.No.	M_c Calculated from swelling measurements	Q	δ	Q	M_c calculated from δ
LP/2/9/60	9.7×10^4	2.89×10^{-4}	1.87	4.73×10^{-4}	5.9×10^4
8/60	1.89×10^5	1.48×10^{-4}	1.87	4.74×10^{-4}	5.9×10^4
7/60	3.75×10^5	7.47×10^{-5}	1.42	3.59×10^{-4}	7.79×10^4
6/60	2.15×10^5	1.30×10^{-4}	1.26	3.19×10^{-4}	8.78×10^4
9/120	1.01×10^5	2.77×10^{-4}	2.07	5.24×10^{-4}	5.34×10^4
8/120	1.53×10^5	1.83×10^{-4}	1.98	5.02×10^{-4}	5.57×10^4
7/120	2.67×10^5	1.05×10^{-4}	1.77	4.49×10^{-4}	6.24×10^4
6/120	3.10×10^5	9.03×10^{-5}	1.62	4.10×10^{-4}	6.8×10^4
5/120	-	-	1.02	2.58×10^{-4}	1.09×10^4
OLP/2/9/60	1.08×10^5	2.59×10^{-4}	1.24	3.15×10^{-4}	8.9×10^4
8/60	1.32×10^5	2.12×10^{-4}	1.20	3.04×10^{-4}	9.21×10^4
7/60	1.39×10^5	2.01×10^{-4}	1.10	2.79×10^{-4}	1.0×10^5
6/60	2.15×10^5	1.30×10^{-4}	1.06	2.69×10^{-4}	1.04×10^5

TABLE 4.17

Sample Ref.No.	M_c Calculated from swelling measurements	q	δ	q	M_c Calculated from δ
LP/6/9/60	1.7×10^5	1.65×10^{-4}	2.61	6.6×10^{-4}	4.29×10^4
8/60	1.05×10^5	2.67×10^{-4}	2.3	5.81×10^{-4}	4.8×10^4
7/60	1.54×10^5	1.82×10^{-4}	2.08	5.27×10^{-4}	5.3×10^4
6/60	2.25×10^5	1.24×10^{-4}	1.88	4.77×10^{-4}	5.87×10^4
5/60	3.57×10^5	7.84×10^{-4}	1.24	3.15×10^{-4}	8.9×10^4
4/60	2.16×10^5	1.30×10^{-4}	1.30	3.29×10^{-4}	8.5×10^4
9/120	1.45×10^5	1.93×10^{-4}	1.92	4.87×10^{-4}	5.75×10^4
8/120	1.07×10^5	2.62×10^{-4}	2.11	5.33×10^{-4}	5.25×10^4
7/120	1.67×10^5	1.67×10^{-4}	1.86	4.71×10^{-4}	5.94×10^4
6/120	3.41×10^5	8.21×10^{-5}	1.68	4.25×10^{-4}	6.59×10^4
5/120	4.1×10^5	6.83×10^{-5}	1.25	3.15×10^{-4}	8.88×10^4
4/120	5.25×10^5	5.33×10^{-5}	1.11	2.82×10^{-4}	9.95×10^4
3/120	1.13×10^5	2.48×10^{-5}	1.01	2.56×10^{-4}	1.09×10^5
LP/7/9/120	6.05×10^5	4.6×10^{-4}	2.87	7.28×10^{-4}	3.85×10^4
8/120	7.58×10^5	3.69×10^{-4}	2.52	6.38×10^{-4}	4.39×10^4
7/120	1.2×10^5	2.33×10^{-4}	2.35	5.96×10^{-4}	4.7×10^4
6/120	1.41×10^5	1.99×10^{-4}	1.91	4.83×10^{-4}	5.79×10^4
5/120	3.08×10^5	9.09×10^{-5}	1.57	3.98×10^{-4}	7.03×10^4
4/120	-	-	1.01	2.57×10^{-4}	1.09×10^5

TABLE 4.18

Sample Ref.No.	M_c Calculated from swelling measurements	q	δ	q Calculated from δ	M_c Calculated from δ
PE/1/10/60	1.92×10^5	1.46×10^{-4}	1.34	3.39×10^{-4}	8.25×10^4
PE/1/9/60	-	-	1.28	3.23×10^{-4}	8.67×10^4
PE/1/8/60	5.37×10^4	5.2×10^{-4}	1.27	3.20×10^{-4}	8.74×10^4
PE/1/7/60	1.44×10^5	1.94×10^{-4}	1.34	3.39×10^{-4}	8.25×10^4
PE/1/6/60	1.63×10^5	1.72×10^{-4}	1.26	3.18×10^{-4}	8.8×10^4
PE/1/5/60	2.41×10^5	1.16×10^{-4}	1.14	2.89×10^{-4}	9.68×10^4
4/60	5.37×10^5	5.21×10^{-5}	1.06	2.68×10^{-4}	1.05×10^4
9/120	9.55×10^4	2.93×10^{-4}	1.28	3.24×10^{-4}	8.63×10^4
8/120	8.62×10^4	3.25×10^{-4}	1.35	3.4×10^{-4}	8.21×10^4
2/10/60	-	-	1.42	3.59×10^{-4}	7.8×10^4
9/60	3.32×10^5	8.43×10^{-5}	1.29	3.26×10^{-4}	8.59×10^4
8/60	1.12×10^5	2.5×10^{-4}	1.26	3.2×10^{-4}	8.76×10^4
7/60	1.19×10^5	2.35×10^{-4}	1.27	3.2×10^{-4}	8.74×10^4
6/60	2.00×10^5	1.4×10^{-4}	1.20	3.03×10^{-4}	9.23×10^4
5/60	1.82×10^5	1.54×10^{-4}	1.12	2.82×10^{-4}	9.9×10^4
4/60	4.87×10^5	5.75×10^{-5}	1.12	2.82×10^{-4}	9.92×10^4
3/60	-	-	1.01	2.55×10^{-4}	1.10×10^5
9/120	5.44×10^4	5.15×10^{-4}	1.45	3.69×10^{-4}	7.59×10^5
8/120	4.8×10^4	5.83×10^{-4}	1.69	4.27×10^{-4}	6.56×10^4

TABLE 4.19

Sample Ref.No.	M_c Calculated from swelling measurements	Q	δ	Q Calculated from δ	M_c
PE/3/9/60	6.98×10^4	4.01×10^{-4}	1.21	3.07×10^{-4}	9.13×10^4
8/60	1.34×10^5	2.07×10^{-4}	1.20	3.04×10^{-4}	9.22×10^4
7/60	1.45×10^5	1.93×10^{-4}	1.20	3.05×10^{-4}	9.17×10^4
6/60	1.64×10^5	1.71×10^{-4}	1.16	2.94×10^{-4}	9.54×10^4
5/60	2.84×10^5	9.86×10^{-5}	1.12	2.84×10^{-4}	9.87×10^4
4/60	3.24×10^5	8.64×10^{-5}	1.10	2.79×10^{-4}	1.00×10^5
3/60	-	-	1.01	2.55×10^{-4}	1.10×10^5
9/120	3.65×10^4	7.67×10^{-4}	1.46	3.69×10^{-4}	7.59×10^4
8/120	5.96×10^4	4.70×10^{-4}	1.16	2.94×10^{-4}	9.53×10^4
4/9/60	1.09×10^5	2.57×10^{-4}	1.15	2.92×10^{-4}	9.60×10^4
8/60	7.44×10^4	3.76×10^{-4}	1.15	2.90×10^{-4}	9.64×10^4
7/60	3.18×10^4	8.8×10^{-4}	1.18	2.99×10^{-4}	9.36×10^4
6/60	1.96×10^5	1.43×10^{-4}	1.13	2.87×10^{-4}	9.75×10^4
5/60	1.72×10^5	1.62×10^{-4}	1.08	2.74×10^{-4}	1.02×10^5
4/60	-	-	1.11	2.81×10^{-4}	9.95×10^4
3/60	-	-	1.01	2.55×10^{-4}	1.10×10^5
9/120	2.76×10^4	1.01×10^{-3}	1.74	4.41×10^{-4}	6.35×10^4
8/120	3.05×10^4	9.18×10^{-4}	1.74	4.40×10^{-4}	6.37×10^4

TABLE 4.20

Sample Ref.No.	M_c Calculated from swelling measurements	Q	δ	Q Calculated from δ	M_c Calculated from δ
PE/6/10/60	3.76×10^4	7.63×10^{-4}	1.70	4.30×10^{-4}	6.5×10^4
9/60	5.09×10^4	5.5×10^{-4}	1.53	3.89×10^{-4}	7.19×10^4
8/60	3.9×10^4	7.18×10^{-4}	1.54	3.91×10^{-4}	7.16×10^4
7/60	4.7×10^4	5.96×10^{-4}	1.28	3.23×10^{-4}	8.66×10^4
6/60	1.47×10^5	1.90×10^{-4}	1.25	3.15×10^{-4}	8.88×10^4
5/60	1.19×10^5	2.35×10^{-4}	1.09	2.75×10^{-4}	1.02×10^5
4/60	5.3×10^5	5.28×10^{-4}	1.07	2.72×10^{-4}	1.03×10^5
3/60	-	-	1.04	2.63×10^{-4}	1.06×10^5
9/120	3.24×10^4	8.64×10^{-4}	2.01	5.08×10^{-4}	5.5×10^4
8/120	7.0×10^4	4.0×10^{-4}	1.70	4.31×10^{-4}	6.5×10^4
7/10/60	3.81×10^4	7.35×10^{-4}	1.72	4.36×10^{-4}	6.43×10^4
9/60	5.06×10^4	5.53×10^{-4}	1.57	3.98×10^{-4}	7.04×10^4
8/60	2.84×10^4	9.86×10^{-4}	1.43	3.63×10^{-4}	7.72×10^4
7/60	5.74×10^4	4.88×10^{-4}	1.40	3.53×10^{-4}	6.45×10^4
6/60	3.52×10^4	7.95×10^{-4}	1.20	3.05×10^{-4}	9.18×10^4
5/60	1.30×10^5	2.15×10^{-4}	1.12	2.85×10^{-4}	9.84×10^4
4/60	-	-	1.06	2.67×10^{-4}	1.04×10^5
9/120	4.49×10^4	6.24×10^{-4}	1.74	4.40×10^{-4}	6.36×10^4
8/120	5.59×10^4	5.01×10^{-4}	1.72	4.35×10^{-4}	6.44×10^4
X/8/60	1.69×10^5	1.66×10^{-4}	1.10	2.88×10^{-4}	9.98×10^4

TABLE 4.21

Sample Ref. No.	M_c Calculated from swelling measurements	q	δ	q Calculated from δ	M_c
PE/M/D200	7.21×10^3	3.88×10^{-3}	2.52	6.38×10^{-4}	4.39×10^4
M/D100	7.65×10^3	3.66×10^{-3}	3.08	7.81×10^{-4}	3.59×10^4
M/D60	4.83×10^4	5.8×10^{-3}	1.72	4.36×10^{-4}	6.43×10^4
M/D40	7.43×10^4	3.77×10^{-4}	1.18	2.99×10^{-4}	9.35×10^4
M/D20	5.81×10^4	4.82×10^{-4}	1.33	3.39×10^{-4}	8.30×10^4
M/D12	1.42×10^4	1.97×10^{-4}	1.25	3.16×10^{-4}	8.87×10^4
M/D10	-	-	1.14	2.88×10^{-4}	9.72×10^4
M/D6	2.38×10^5	1.18×10^{-4}	1.03	2.61×10^{-4}	1.07×10^5
PE/D200	6.21×10^3	4.5×10^{-3}	3.02	7.64×10^{-4}	3.66×10^4
/D100	1.23×10^4	2.28×10^{-3}	2.92	7.39×10^{-4}	3.79×10^4
/D60	2.77×10^4	1.01×10^{-3}	1.55	3.94×10^{-4}	7.11×10^4
/D40	4.78×10^4	5.86×10^{-4}	1.28	3.24×10^{-4}	8.63×10^4
/D20	3.55×10^4	7.89×10^{-4}	1.20	3.03×10^{-4}	9.24×10^4
/D12	1.45×10^5	1.93×10^{-4}	1.25	3.17×10^{-4}	8.83×10^4
/D10	1.17×10^5	2.39×10^{-4}	1.34	3.39×10^{-4}	8.27×10^4
/D8	1.28×10^5	2.19×10^{-4}	1.23	3.11×10^{-4}	9.00×10^4
/D6	2.16×10^5	1.30×10^{-4}	1.06	2.69×10^{-4}	1.04×10^5

TABLE 4.22: % TAC w/w in gel measured by I.R. Analysis

Sample Ref. No.	Wg	% TAC w/w 1560 cm ⁻¹ peak	in Ref to 820 cm ⁻¹ peak
LP/1/9/60	0.432	0.345	0.405
8/60	0.35	0.379	0.404
7/60	0.32	0.366	0.414
6/60	0.22	0.294	0.325
5/60	0.007	-	-
9/120	0.50	0.257	0.328
8/120	0.47	0.219	0.262
7/120	0.36	0.231	0.289
6/120	0.32	0.182	0.251
5/120	0.07	-	-
OLP/1/9/60	0.22	0.350	0.40
8/60	0.19	0.384	0.49
7/60	0.049	0.461	0.48
6/60	0.045	0.383	0.49

TABLE 4.23: % TAC w/w in gel measured by I.R. Analysis

Sample Ref. No.	Wg	% TAC w/w in ref to	
		1560 cm^{-1} peak	820 cm^{-1} peak
LP/2/9/60	0.47	0.674	0.77
8/60	0.47	-	-
7/60	0.30	0.537	0.616
6/60	0.21	0.463	0.494
9/120	0.52	0.427	0.530
8/120	0.50	0.419	0.534
7/120	0.44	0.346	0.413
6/120	0.38	0.362	0.461
5/120	0.018	0.491	0.616
OLP/2/9/60	0.2	0.64	0.758
8/60	0.17	0.84	0.964
7/60	0.09	-	-
6/60	0.06	0.448	0.496

TABLE 4.24: % TAC w/w in gel measured by I.R. Analysis

Sample Ref. No.	Wg	% TAC w/w in ref to	
		1560 cm^{-1} peak	820 cm^{-1} peak
LP/6/9/60	0.62	0.304	0.354
8/60	0.56	0.318	0.35
7/60	0.52	0.335	0.415
6/60	0.47	0.197	0.367
5/60	0.20	0.316	0.38
4/60	0.23	0.209	0.239
9/120	0.148	0.106	0.158
8/120	0.53	0.219	0.290
7/120	0.46	0.154	0.202
6/120	0.40	-	-
5/120	0.20	0.038	0.041
4/120	0.10	-	-
9/120	0.65	0.401	0.471
8/120	0.60	0.438	0.512
7/120	0.58	0.401	0.467
6/120	0.48	0.392	0.484
5/120	0.36	0.468	0.587
4/120	0.01	-	-

TABLE 4.25: % TAC w/w in gel measured by I.R. Analysis

Sample Ref. No.	Wg	% TAC w/w in ref	
		1560 cm ⁻¹ peak	820cm ⁻¹ peak
PE/1/9/60	0.22	0.532	0.631
8/60	0.21	0.514	0.611
7/60	0.25	0.344	0.358
5/60	0.13	0.365	0.431
9/120	0.22	0.257	0.322
2/9/60	0.22	0.796	0.901
8/60	0.21	0.636	0.660
7/60	0.21	0.579	0.594
6/60	0.17	0.632	0.714
5/60	0.1	0.366	0.416
4/60	0.1	0.235	0.267
9/120	0.31	0.646	0.781
3/9/60	0.17	-	1.898
8/60	0.17	-	1.592
7/60	0.17	-	1.33
5/60	0.11	-	1.095
9/120	0.31	-	1.641
4/9/60	0.13	-	3.515
8/60	0.13	-	3.32
7/60	0.15	-	3.70
5/60	0.08	-	1.304
4/60	0.1	-	1.384
9/120	0.43	-	2.256
8/120	0.42	-	2.43

TABLE 4.26: % TAC w/w in gel measured by I.R. Analysis

Sample Ref. No.	Wg	% TAC w/w in Ref	
		1560 cm^{-1} peak	820 cm^{-1} peak
PE/6/10/60	0.41	0.351	0.400
9/60	0.35	0.32	0.42
8/60	0.35	0.545	0.64
7/60	0.14	-	-
6/60	0.20	0.585	0.770
5/60	0.08	0.354	0.42
9/120	0.50	0.314	0.400
8/120	0.42	0.311	0.390
7/9/60	0.36	0.687	0.783
8/60	0.30	0.940	0.96
7/60	0.28	0.908	0.95
6/60	0.17	0.763	0.86
5/60	0.11	0.450	0.559
9/120	0.43	0.518	0.648
8/120	0.42	0.509	0.634

4.5.7 Light Penetration through the polyethylene films

To study the effect of light penetration through different thicknesses of catalysed films, two experiments were made.

A. Measuring xanthone concentration in the polyethylene films.

The xanthone concentration was followed throughout the U.V. curing of two sets, each of four catalysed polyethylene films left on top of each other i.e. each set is a film of four layers.

The xanthone concentration was determined by using U.V. analysis and by considering the film thickness as the path length. The polyethylene films contained 1% TAC w/w. The xanthone concentration for the two sets are shown in table 4.27 and in table 2.28.

The films were irradiated at 60°C without using the radiation vessel described in the beginning of section 4.5. The distance between the lamp and film was 30 cm.

B. Measuring the MFI for cured films

The melt flow index is used as a rough guide for crosslinking and rapid assessment for layers of five polyethylene films, cured by light. The U.V. curing, which was carried out without the use of the radiation vessel, was continued for 25 minutes at 60°C.

TABLE 4.27 Xanthone concentration in the treated layers of polyethylene film.

Curing time minutes	% w/w xanthone sheet			
	A	B	C	D
0	0.17	0.16	0.16	0.17
5	0.15	0.16	0.16	0.17
10	0.14	0.15	0.16	0.17
15	0.13	0.14	0.155	0.16
20	0.12	0.138	0.15	0.158
25	0.116	0.13	0.143	0.152
30	0.113	0.127	0.14	0.146
35	0.113	0.126	0.137	0.143
40	0.113	0.123	0.133	0.139
45	0.113	0.118	0.131	0.137
50	0.113	0.118	0.128	0.135

The set containing of four layers thickness of

sheet A (top layer)	=	0.207 mm
' B	=	0.215 mm
' C	=	0.18 mm
' D	=	0.16 mm

TABLE 4.28 Xanthone concentration in the treated layers of polyethylene film.

Curing time minutes	% w/w xanthone sheet			
	A	B	C	D
0	0.045	0.054	0.054	0.057
5	0.030	0.044	0.050	0.055
10	0.019	0.031	0.046	0.048
15	0.013	0.023	0.037	0.043
20	0.0085	0.026	0.032	0.038
25	0.0064	0.016	0.025	0.031
30	0.0043	0.011	0.018	0.028
35	0.0043	0.0078	0.014	0.024
40	-	0.0077	0.012	0.019
45	-	0.0062	0.0088	0.014
50	-	0.0047	0.007	0.012
55	-	-	-	0.012
60	-	-	-	0.012

The set containing of four layers thickness of

sheet A (top layer) = 0.141 mm

' B = 0.215 mm

' C = 0.18mm

' D = 0.16 mm

The melt flow index (MFI) of the polymer is the weight of the polymer extruded in ten minutes at specific temperature. The MFI was measured for each individual layer of the 25 minutes curing time. Fig.(6.3) shows the MFI effect versus the thickness of the film.

The flow index of the starting material was 7.3 g/10 min. The additives were 0.2% w/w xanthone and 1% w/w TAC.

The MFI measurement, was carried out according to ASTM D1238. The MFI machine is a simple barrel and piston rheometer where the pressure for extrusion is supplied by a weight acting vertically on the piston. The weight used was 2.61 kg. The test was carried out at 190°C.

4.5.8 Post Curing of Polyethylene films

As found from previous sections, the gel content of around 50% was the highest one achieved. To study whether or not a higher gel content could be obtained, a few post U.V. irradiation was introduced to the films, after the primary curing of half an hour each. Before each cycle of post radiation, each film went through a treatment of 12 hours in TAC/xanthone/Toluene solution at 50°C, so that more of the additives will be introduced. They were then left in a vacuum oven for 12 hours to be dried from toluene and afterwards were irradiated by U.V. for half an hour.

The initial polyethylene film contained 0.1% w/w xanthone and 0.5% w/w TAC. The toluene solution of additives contained 0.1% w/v xanthone and 0.5% w/v TAC. The following table shows the different films and the gel content obtained in each case.

TABLE 4.29 Gel content of post treated Polyethylene films

Sample Ref.No.	No. of treatment in xanthone/TAC solution	No. of postcuring	% Gel content
PE/R0	0	0	15.27
PE/R1	1	1	25.85
PE/R2	2	2	38.44
PE/R3	3	3	41.23
PE/R4	4	4	46.43

The gel part of the above samples were analysed by elemental analysis, by taking specimens randomly from the same gel part of the individual samples. As far as the nitrogen content was concerned the results were not consistent as shown in the following table,

TABLE 4.30 Elemental Analysis for the gel part of cured polyethylene

Sample Ref.No.	Specimen	Carbon	% Hydrogen	Nitrogen
PE/R0	1	85.05	14.35	0.98
	2	85.55	14.33	Nil
PE/R1	1	85.04	14.23	0.78
	2	85.94	14.43	Nil
PE/R2	1	85.01	14.28	Nil
	2	85.45	14.29	Nil
PE/R3	1	85.02	14.03	1.64
	2	83.87	13.91	traces
PE/R4	1	84.07	13.76	0.42
	2	84.38	13.89	0.47

The elemental analysis showed the same inconsistency with the other gel samples.

The crosslinking density ' Q ' and the molecular weight between the crosslinks M_c were determined for these samples using the two different experimental data as in section 4.5.6.1, namely from the swelling measurements data and the gel content data. Table 4.31 shows the M_c and Q for these samples.

TABLE 4.31 M_c and Q for the post treated polyethylene films.

Sample Ref No.	M_c Calculated from swelling	Q	δ	Q Calculated from δ	M_c
PE/R0	9.81×10^4	2.845×10^{-4}	1.18	2.99×10^{-4}	9.37×10^4
PE/R1	5.04×10^4	5.56×10^{-4}	1.35	3.42×10^{-4}	8.19×10^4
PE/R2	3.64×10^4	7.69×10^{-4}	1.62	4.11×10^{-4}	6.81×10^4
PE/R3	1.40×10^4	2.01×10^{-3}	1.70	1.3×10^{-4}	6.5×10^4
PE/R4	1.45×10^4	1.93×10^{-3}	1.87	4.73×10^{-4}	5.92×10^4

4.5.9 The Effect of Crosslinking on the Tensile Strength
Elongation and Environmental Stress Cracking
Resistance [ESCR]

Preliminary tensile strength and elongation tests were carried out for samples of 2 mm thick, the tensile properties remaining unchanged.

The elongation was also slightly changed. No further tests were carried out since the primary results were not very encouraging.

Nevertheless, the following table shows the typical results obtained for one specimen using a R10 cutter to cut the polyethylene film. The tests were carried out at room temperature.

TABLE 4.32 Mechanical Properties of U.V. Cured Film

Sample	Yield stress kg/cm ²	% elongation
Blank polyethylene	76	585
Catalysed polyethylene (0.25% w/w xanthone + 1% w/w TAC) irradiated for one hour (30 minutes each side)	79	500

The environmental stress cracking tests were carried out on polyethylene samples which were catalysed with 0.2% w/w xanthone and 1% w/w TAC and also irradiated for 15 and 30 minutes.

The specimens used for the tests unnotched R10 specimens or that of 12.5 mm wide notches by 2 mm deep using a razor blade.

Different stresses were applied at room temperature to the samples in an isopropyl alcohol environment using blank polyethylene specimen as controls.

Fig.(6.23) shows that the resistance of the polyethylene film will be improved by U.V. curing.

4.5.10 The Characterization of the Sol Part by GPC

Charlesby (4,25,50) concluded many years ago that the radiolytic behaviour of polyethylene and other polymers could be most easily explained by assuming that both main chain scission and crosslinking occur randomly along the polymer chains. Whichever one of them or both takes place depends on the chemical structure of the polymers, not on the type of irradiation used.

In the case of polyethylene, Charlesby concluded that the distinct possibility of radiolytic chain scission was negligible or zero. At sufficiently high crosslink densities, provided that the chain scission probability is very low, the soluble fraction

consists almost solely of material that has not been affected by crosslinking.

Using high temperature gel permeation chromatography (GPC) an investigation of the changes in molecular weight distribution in the soluble fraction of U.V. irradiation polyethylene was undertaken. Also the analysis of the soluble fraction of γ -irradiated polyethylene was carried out. Unfortunately, due to the non-availability of the RAPRA instrument only a limited number of samples were analysed at I.C.I. (Corporate Labs).

GPC is a special type of liquid-solid solution chromatograph based on the permeation of solute molecules into a liquid gel particles. The separation of molecular species through the gel particles, occurs according to their size.

Molecules whose size is too great to allow them to enter the gel pores, pass through the column solely by way of the interstitial volume. Smaller particles permeate the beads to a greater or lesser extent depending upon their size and on the distribution of pore size available in gel particles.

Therefore the largest molecules emerge from the column first followed by smaller molecules which must follow a more circuitous path through the column. Details of GPC techniques are well covered by P.E. slide J.R.(50).

The actual machine used was manufactured by Applied Research laboratories Ltd. with the basic design and made operation, based on the work done by Hemming of the Corporate Laboratory (51).

The core of the instrument consisted of four columns packed with a porous glass medium known as 'Porosil'. The four 'porosil' columns had the following exclusion limits; 10^4 , 4×10^3 , 10^3 and 8×10 nm.

Orthodichlorobenzene (ODCB) was used as the solvent which was stabilised with 0.1% w/v Topanol OC. The sol part of polyethylene to be characterised was dissolved in ODCB and left overnight before the analysis was carried out. The instrument was maintained at 135°C . The elution volume from the GPC was measured by a drop counter while the polymer concentration was measured by Grubb-Parsons Infrared spectrometer which monitored the 'CH' stretching frequency at 3.42 microns.

Table (4.33) shows the weight average molecular weight ' \bar{M}_w ' number average molecular weight ' \bar{M}_n ' viscosity average molecular weight ' \bar{M}_v ' and the molecular weight distribution for the sol part of some selected samples. [\bar{M}_v value considered to 0.20].

TABLE 4.33 GPC Analysis for the Sol Part of Treated
Polyethylene Films

Sample Ref.No.	\bar{M}_n	\bar{M}_w	\bar{M}_w/\bar{M}_n	\bar{M}_v
Polyethylene standard	18100	110600	6.11	83000
PE/RO	14700	154800	10.53	96500
PE/R1	12700	115100	9.10	73600
PE/R2	11000	41000	3.73	32500
PE/R3	9800	32300	3.29	26600
PE/R4	7400	22400	3.00	19200
PE/D20	10200	85700	8.36	58800
PE/D40	8100	53500	6.63	37500
PE/D60	7200	32900	4.58	24900
PE/D100	4600	12400	2.68	10500
PE/D200	3800	11000	2.91	9100
PE/M/D20	10400	61700	5.94	45900
PE/M/D40	8700	48000	5.52	36300
PE/M/D60	6900	26000	3.76	20900
PE/M/D100	4100	11400	2.78	9600
PE/M/D200	4900	12000	2.45	9900

4.5.11 The Crosslinking Effect on Glass Transition and Melting Temperature, T_g and T_m

Using thermal analysis technique, namely, Differential scanning calorimetry (DSC), T_g and T_m were determined for untreated samples of polyethylene together with a few selected highly cured (U.V. and irradiated) polyethylene samples. Perkin-Elmer's DSC-2 instrument was used in each individual run. The scan was from 140 K, using liquid nitrogen, up to 400 K. Each specimen was cooled again and scanned for a second time. The scanning speed was 40 K/minute.

The analysis was carried out on a cured sheet, without separating the sol part from the gel part. The T_g value of (-103°C ± 2) was observed in all cases without any significant changes. The same applied to the T_m value of (111°C ± 3).

4.5.12 The Crosslinking Effect on the Degree of Crystallinity

X-ray diffraction was used to determine the effect of crosslinking on the crystallinity of the polyethylene. The analysis was carried out at I.C.I. Corporate Labs using Phillips PW 1056 diffractometer. The analysis was carried out on standard polyethylene sheets together with some selected highly cured samples by U.V. and γ -irradiation.

The percentage crystallinity observed for all samples were almost the same, ranging from 40-43% without any significant changes.

References

1. Charlesby, A. Nature 171, 167 (1953).
2. Lawton, E.J., et al. Nature 172, 76 (1953).
3. Karpov, V.L., Seggiya Akad. Nank S.S.S.R. Po Mirnomu Ispolzovaniyu Atommoi Energii Academy of Sciences of U.S.S.R., Moscow Page 1, (1955).
4. Charlesby, A., Proc. Roy. Soc. (London) A215, 187, (1952).
5. Dole, M. Report of Symposium IX "Chemistry and Physics of Radiation Dosimetry", Army Chemical Center, Maryland Page 120, (1950).
6. Chapiro, A. Radiation Chemistry of Polymeric Systems, Interscience, (1962).
7. Lawton, E.J., et al. J. Amer. Chem. Soc. 76, 3437 (1954).
8. Dole, M., et al., J. Amer. Chem. Soc. 76, 4304, (1954).
9. Miller, A., et al., J. Phys. Chem., 60, 599, (1956).
10. Harlen, F.W., et al., J. Polymer Sci. 18, 589, (1955).
11. Chapiro, A., J. Chim. Phys. 52, 246 (1955).
12. Alexander, P., et al., J. Polymer Sci. 22, 343, (1956).
13. Dole, M., The Radiation Chemistry of Macromolecules, Part 1, Academic Press (1972).
14. Lawton, E.J., et al., J. Polymer Sci. 32 257, 277, (1958).
15. Roedel, M.J., J. Amer. Chem. Soc. 75, 6110 (1953).
16. Bryant, W.M.D., Voter, R.C., J. Amer. Chem. Soc., 75, 6113 (1953).
17. Billmeyer, F.W., J. Amer. Chem. Soc., 75, 6118, 1953.
18. Willbourn, A.H., J. Polymer Sci., 34, 569 (1959).
19. Little, K., Nature 170, 1075 (1952).
20. Dole, M., Bodily, D.M., Advances in Chemistry Vol. 66 Amer. Chem. Soc., 1967.

21. Dole, M., et al., J. Phy. Chem., 66, 193, (1962).
22. Odian, G., et al., J. Polymer Sci., A2, 2835, (1964).
23. Charlesby, A., Campbell, D., Chem. Zvest. 26, 256 (1972)
Europ. Polymer J. 9 301 (1973).
Charlesby, A., Fydeler, P.J., Int. J. Radiat. Phys.
Chem., 4, 107 (1972).
24. Charlesby, A., Atomic Radiation of Polymers, Pergamon
(1960).
25. Maas, K.A., et al., Trans Faraday Soc., 60, 1202 (1964).
26. Ranby, B., et al., J. Polymer Sci., C12, 263 (1968).
27. Ranby, B., et al., Irradiation of Polymers, Advances in
Chemistry Series, Amer. Chem. Soc., 66 256 (1967).
28. Tsuji, K., Seiki, T., Polymer J., Vol. 2, 5, 606 (1971).
29. Takeshita, T., et al., J. Polymer Sci., A1, 10, 2315,
(1972).
30. Miltz, J., et al., J. App. Polymer Sci., 20, 1627, 1976.
31. Danneberg, E.M., et al., J. Polymer Sci., 31, 127, 1958.
32. Oster, G., et al., J. Polymer Sci., 34, 671, 1959.
33. Bonotto, S., J. Applied Polymer Science 9 3819 (1965).
34. Flory, P.J., Principles of Polymer Chemistry, Cornell
University Press, New York 1953.
35. Flory, P.J., J. Amer. Chem. Soc., 63, 3096, 1941, Chem.
Revs., 39 137 (1946).
36. Flory, P.J., J. Amer. Chem. Soc., 69, 30 (1947).
37. Charlesby, A., J. Polymer Sci., 11, 513, 1953, 14, 547
(1954).
38. Charlesby, A., Proc. Roy. Soc. (London) A222, 542, (1954).
39. Dusek, K., Prins, W., Advance Polymer Sci., 6, p1-102
(1969).

40. Case, L.C., J. Polymer Sci., 15, 397, (1963) (Branching in Polymer "Network Defects").
41. Stockmayer, Advancing Fronts in Chemistry Reinhold, (1945).
42. Stockmayer, J. Chem. Phys., 11, 45, 1943.
43. Kuhn, W., Grun, F., Kolloid Z. 101, 248, 1942.
44. Wall, F.T., J. Chem. Phys., 10, 132, 485, (1942), 11, 527 (1943).
45. Treloar, L.R.G., Trans Faraday Soc., 39, 36, 241, 1943, 40, 59, 109, 1944, 42, 83, 1946.
46. Treloar, L.R.G., Physics of Rubber Elasticity, Oxford Univ. Press, (1949).
47. Huggins, M.L., J. Chem. Phys., 9, 440, (1941), J. Phy. Chem., 46, 151, (1942), J. Am. Chem. Soc., 64, 1712, (1942).
48. Flory, P.J., J. Chem. Phys., 9, 660, 1941, 10, 51, 1942.
49. Orwoll, R.A., Rubber Chemistry and Technology, 50, 451, (1977).
50. Slade, J.R., Philip, E., Polymer Molecular Weight, Part I & II Dekker 1975.
51. Hemming, M., Thesis, Lancaster University 1973.
52. Johnson, B.L., Smith, J., Light Scattering from Dilute Polymer Solutions, Chapter 2 by M.B. Huglin, Academic Press, London (1972).

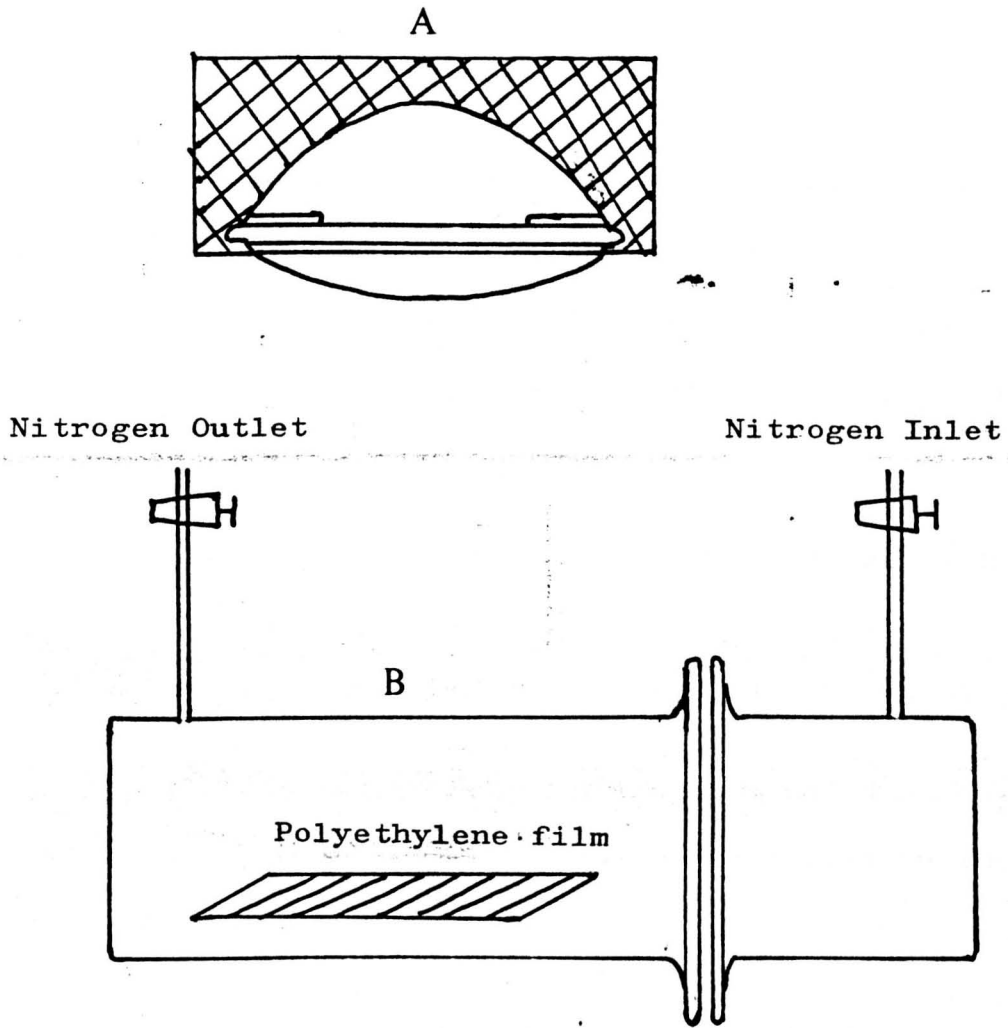


Fig. 4_3 The ultraviolet lamp (A) and the radiation vessel (B) used for curing and irradiating polyethylene sheets.

- A The ultraviolet lamp which was used for curing
- B The radiation vessel used for irradiating the polyethylene sheets

CHAPTER 5.THE CHARACTERIZATION OF CROSSLINKED POLYETHYLENE BY
RHEOLOGY STUDIES5.1 Theory

Crosslinking often affects the mechanical, thermal and flow properties. In this crosslinking system, it seems that there are significant changes in the resulting rheology of the polyethylene. Therefore, an extensive study of the system, using rheological techniques, will be presented in this Chapter.

Rheology is the science of deformation and flow. Polymers show a viscoelastic behaviour which may be divided into two terms, namely elasticity and viscosity.

The elastic properties are dealt with in accordance with Hooke's law, which is expressed in the following relation.

$$\text{Stress} \propto \text{Strain}$$

where stress is independent of the rate of strain.

The viscous properties are dealt with in accordance with Newton's law, which is expressed in the following relation.

$$\text{Stress} \propto \text{Rate of Strain}$$

where stress is independent of strain.

The behaviour of solids approaches Hooke's law for infinitesimal strains, although deviations may occur when a finite strain is imposed in which case a more complicated relationship will occur between stress and strain and it will be non-Hookean. Similarly, the behaviour of liquids approaches Newton's law for infinitesimal rates of strain. Some non-Newtonian flow will be exhibited when steady with finite strain rates. The deviation from the two laws depend on the individual materials. There will be possibilities of combinations of the two characteristics , e.g. liquid-like and solid like systems; such materials are known as viscoelastic. Linear viscoelastic behaviour is a function of time or frequency.

The relations between stress and strain, as a function of time, are described by rheological equations of state.

The viscoelastic properties of polymers are related to the nature and rates of the configurational rearrangements, e.g. branching, crosslinking, and they are also related to the molecular weight. The disposition and the interaction of the macromolecules in both their short range and their long range interrelations may be obtained from measuring the viscoelastic properties.

There are different types of flow which polymeric systems exhibit; Newtonian flow; Pseudo plastic; Bingham body, with yield stress and dilatant.

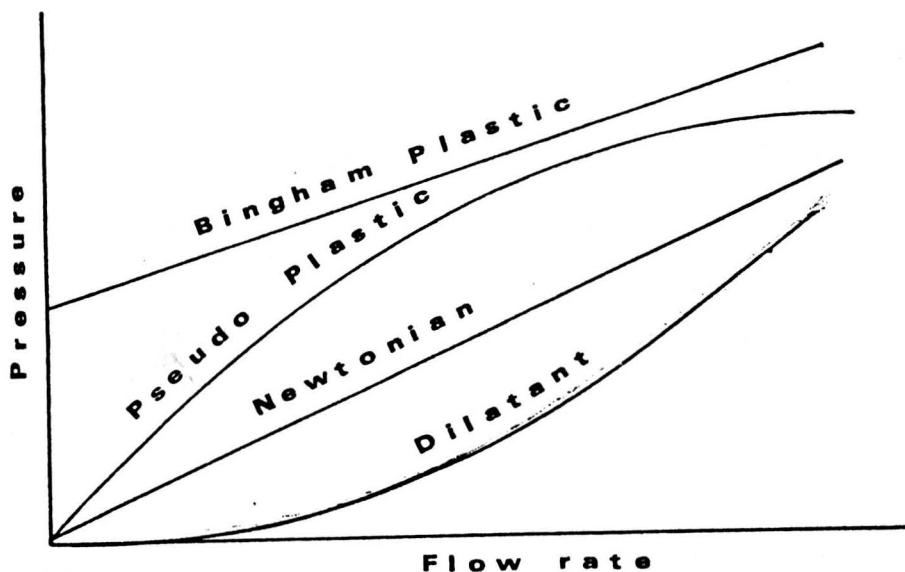


Fig.5.1 Different type of flow

Since changes in flow properties of crosslinked polyethylene has been described (1) as a function of melt viscosities and of melt flow index, it was thought to be a useful technique for characterization of the light cured polyethylene. Various moduli will be introduced for such a characterization, since they vary according to the nature of the polymer. Moduli such as stress relaxation modulus, storage modulus, the loss modulus, the dynamic viscosity, and the loss tangent could all be used for characterization and also comparison between light-cured polyethylene and the radiation cured polyethylene. This kind of comparison should be interesting since two different methods of crosslinking are involved.

A brief outline will now be given of these moduli which are to be studied.

The storage modulus $G'(\omega)$ is defined as the stress in phase with strain in sinusoidal shear deformation divided by the strain. It is a measure of the elastic stored energy that is recovered per cycle. $G'(\omega)$ is measured by varying the radian frequency ' ω '. For viscoelastic liquids, $G'(\omega)$ approaches zero with decreasing frequency. The stress relaxation modulus $G(t)$ is defined as the stress/strain ratio at constant deformation. $G(t)$ is measured as a function of time. At short time $G(t)$ appears to keep a limiting value due to its rigidity in the absence of backbone rearrangements. In the case of the crosslinked network, $G(t)$ almost keeps a constant value at long time intervals, whereas in the case of uncrosslinked polymers, $G(t)$ falls rapidly and eventually vanishes.

This may be explained in molecular terms due to the resumption of average random configurations by the macromolecule coils, which have been freed from the constraints originally imposed on them. The zone into which the $G(t)$ value falls is called the terminal zone.

Since $G(t)$ and $G'(\omega)$ are measures of stored elastic energy where $t = 1/\omega$, then

$$G(t) \cong G'(1/t) \quad \text{When } G(t) \text{ is changing very slowly.}$$

$G'(\omega)$ values may be approximate mirror images of those for $G(t)$ i.e. at long frequency, for uncrosslinked polymers, a sharp increase in $G'(\omega)$ where no change is expected when characterizing crosslinked polymers at high frequency.

The loss modulus $G''(\omega)$ is defined as the stress 90° out of phase with the strain divided by strain. $G''(\omega)$ measures the dissipated energy per cycle. Like $G'(\omega)$, $G''(\omega)$ will be measured as a function of the radian frequency.

The complex quantity for the storage modulus and the loss modulus will be represented by $|G|$ which is

$$|G| = \sqrt{G'^2 + G''^2}$$

Dynamic viscosity $|\eta|$ is defined as the ratio of stress in phase with rate of strain divided by the rate of strain.

A frequency dependent viscosity is

$$|\eta| = \frac{|G|}{\omega}$$

The loss tangent, ' $\tan \delta$ ' is dimensionless and has no physical magnitude but is a measure of the ratio of the energy lost to the energy stored in cyclic deformation i.e.

$$\tan \delta = \frac{G''}{G'}$$

Usually $\tan \delta$ is inversely proportional to the frequencies at low frequencies for uncrosslinked polymers. It has been found that $\tan \delta$ has different values in the transition zone for different types of polymers; e.g. for amorphous polymers whether crosslinked or not the $\tan \delta$ is approximately one and ranges from 0.2 to 3, for glassy and crystalline polymers; $\tan \delta$ is approximately 0.1 and for lightly crosslinked polymers the $\tan \delta$ has a very low value at low frequencies in the range of 0.01.

The loss tangent reveals molecular motions, small changes in polymer structure such as the presence of entanglement will modify the $\tan \delta$ value. It can be often more conveniently measured than any other viscoelastic function (1).

5.2 Instrumentation

As many industrial materials, e.g. polymers, cannot be classified as simply Newtonian, most conventional viscometers will not be of use since they are mostly designed for materials obeying the Newtonian law. To characterise non-Newtonian materials in a satisfactory way, an instrument with a different variable should be used. The rheogoniometer (Weissenberg) was developed as a research instrument to measure the stress rate of shear dependencies at every point in the fluid under test on both tangential and normal planes.

The basis of the Weissenberg Rheogoniometer is the

simple cone and plate viscometer (2). The lower plates of the instrument can be oscillated in a rotary direction over a range of frequencies.

There is facility of measuring the vernial force so that the movements and forces within the specimen in all three dimensions of space are measured at each instant of time during the test. This allows the determination of elasticity and viscosity over a very wide range.

The instrument is equipped with a temperature control so that tests could be carried out at different temperatures. However in this work the temperature was constant at 160°C for all the individual runs. The chambers used are arranged so that the specimen can be held in an atmosphere of inert gas.

The sample temperature was maintained at 160°C by two methods (a) a surrounding oven, and (b) a background heater. The background heater served two purposes, firstly as it operated by blowing hot nitrogen gas into the oven it provided an inert medium to minimise any possible degradation from occurring during the course of a measurement and secondly, the circulating effect maintained an even temperature throughout the oven. The response of the polymer to the applied oscillatory shear was measured by pressure transducers. Frictional losses were minimized by supporting the upper plate on an air bearing.

The output from the pressure transducers was fed into a data processing unit which not only calculated the shear modulus G but also the elastic G'_{ω} and viscous G''_{ω} components of the shear modulus.

The measurements were usually taken from each sample at different speeds, on the instrument equipped with a driving unit. Though about sixty different speeds were available on the instrument, the measurements used only five of these. Both continuous and oscillatory measurements were used on each providing both the desired moduli, $\tan \delta$ and viscoelastic behaviour of the polymer melt.

As described above, the Weissenberg Rheogoniometer is basically a simple cone and plate viscometer, therefore the theoretical considerations of this instrument are mainly developed from the simple cone and plate viscometer theory which has been dealt with in Weissenberg's papers (2).

5.3 Experimental

The specimens used for the rheological analysis at 160°C were cured sheets (without separating the gel from the sol part), in the form of small discs 25 mm in diameter and about 1 mm in thickness. To achieve such a thickness the cured sheets were folded. After allowing five minutes for temperature equilibration to occur, the $G'(\omega)$ and $G''(\omega)$ components were measured for each sample with a range of different frequencies. The first measure-

ment was repeated to check for any rheological change that may have occurred during the run.

Similar runs were carried out in different ranges of temperature and frequencies for U.V. cured polyethylene samples and irradiated samples.

Of
A set G'_{ω} , G''_{ω} values were measured for similar sample in reference to the time by keeping the frequency constant and constant shear.

Appendices A, B, C, D, E and F show G'_{ω} , G''_{ω} , $|G|$ and $\tan \delta$ for the different runs of each individual specimen.

Appendix A Rheology Analysis for LP/1 Batch Crosslinked
at 60°C and 120°C

Sample No. LP/1/9/60

ω	G'	G''	/G/	$ \eta $	Tan δ
1.0	9.7	4.6	10.7	10.735	0.4742
3.1	13.3	7.9	15.5	4.929	0.5986
10.0	18.1	9.7	20.5	2.054	0.5359
31.4	26.6	15.6	30.8	0.982	0.5868
100.0	38.0	23.9	44.9	0.449	0.6289
314.0	53.4	39.2	66.3	0.211	0.7337
1.0	9.3	4.4	10.3	10.288	0.4731

Sample No. LP/1/8/60

ω	G'	G''	/G/	$ \eta $	Tan δ
1.0	9.0	6.8	11.3	11.280	0.7556
3.1	13.8	9.2	16.6	5.282	0.6667
10.0	20.9	13.6	24.9	2.494	0.6507
31.4	31.1	20.5	37.2	1.186	0.6592
100.0	46.1	31.3	55.7	0.557	0.6790
314.0	67.9	50.1	84.4	0.269	0.7378
1.0	9.3	5.9	11.0	11.014	0.6344

Sample No. LP/1/7/60

ω	G'	G''	$/G/$	$ \eta $	Tan δ
1.0	6.6	4.6	8.0	8.045	0.6970
3.1	10.0	6.6	12.0	3.816	0.6600
10.0	15.5	10.1	18.5	1.850	0.6516
31.4	23.9	15.6	28.5	0.909	0.6527
100.0	36.2	24.5	43.7	0.437	0.6768
314.0	54.7	40.1	67.8	0.216	0.7331
1.0	6.6	4.1	7.8	7.770	0.6212

Sample No. LP/1/6/60

ω	G'	G''	$/G/$	$ \eta $	Tan δ
1.0	3.8	3.1	4.9	4.904	0.8158
3.1	6.6	5.4	8.5	2.716	0.8182
10.0	11.2	8.7	14.2	1.418	0.7768
31.4	18.6	14.2	23.4	0.745	0.7634
100.0	29.9	22.6	37.5	0.375	0.7559
314.0	45.3	39.1	59.8	0.191	0.8631
1.0	4.2	3.3	5.3	5.341	0.7857

Sample No. LP/1/5/60

ω	G'	G''	$/G/$	$ \eta $	Tan δ
1.0	1.9	2.2	2.9	2.907	1.1579
3.1	3.8	4.1	5.6	1.780	1.0789
10.0	7.3	7.1	10.2	1.018	0.9726
31.4	13.5	11.8	17.9	0.571	0.8741
100.0	23.4	19.8	30.7	0.307	0.8462
314.0	36.9	35.3	51.1	0.163	0.9566
1.0	2.6	2.3	3.5	3.471	0.8846

Sample No. LP/1/3/60

ω	G'	G''	$/G/$	$ \eta $	Tan δ
1.0	1.5	2.4	2.8	2.830	1.6000
3.1	3.5	4.8	5.9	1.892	1.3714
10.0	9.9	10.7	14.6	1.458	1.0808
31.4	15.1	15.1	21.4	0.680	1.0000
100.0	27.3	25.5	37.4	0.374	0.9341
314.0	44.8	44.1	62.9	0.200	0.9844
1.0	1.5	2.4	2.8	2.830	1.6000

Sample No. LP/1/9/120

ω	G'	G''	/G/	$ \eta $	Tan δ
1.0	6.8	5.3	8.6	8.621	0.7794
3.1	10.7	7.6	13.1	4.180	0.7103
10.0	17.0	11.3	20.4	2.041	0.6647
31.4	25.8	17.1	31.0	0.986	0.6628
100.0	38.8	26.9	47.2	0.472	0.6933
314.0	55.8	45.3	71.9	0.229	0.8118
1.0	7.3	4.8	8.7	8.737	0.6575

Sample No. LP/1/8/120

ω	G'	G''	/G/	$ \eta $	Tan δ
1.0	5.2	4.1	6.6	6.622	0.7885
3.1	8.4	6.3	10.5	3.344	0.7500
10.0	13.5	9.6	16.6	1.657	0.7111
31.4	21.2	14.8	25.9	0.823	0.6981
100.0	32.5	22.9	39.8	0.398	0.7046
314.0	48.2	38.3	61.6	0.196	0.7946
1.0	5.3	3.8	6.5	6.522	0.7170

Sample No. LP/1/7/120

ω	G'	G''	/G/	$ \eta $	Tan δ
1.0	3.5	3.5	4.9	4.950	1.0000
3.1	6.3	5.7	8.5	2.706	0.9048
10.0	10.8	9.2	14.2	1.419	0.8519
31.4	18.1	14.7	23.3	0.743	0.8122
100.0	29.3	23.9	37.8	0.378	0.8157
314.0	43.9	41.1	60.1	0.192	0.9362
1.0	3.7	3.4	5.0	5.025	0.9189

Sample No. LP/1/6/120

ω	G'	G''	/G/	$ \eta $	Tan δ
1.0	2.7	2.8	3.9	3.890	1.0370
3.1	4.7	4.8	6.7	2.139	1.0213
10.0	10.7	10.0	14.6	1.465	0.9346
31.4	15.0	13.1	19.9	0.634	0.8733
100.0	24.9	21.2	32.7	0.327	0.8514
314.0	40.7	35.2	53.8	0.171	0.8649
1.0	2.6	2.7	3.8	3.821	1.0769

Sample No. LP/1/5/120

ω	G'	G''	$/G/$	$ \eta $	Tan δ
1.0	1.7	2.4	2.9	2.941	1.4118
3.1	3.6	4.5	5.8	1.835	1.2500
10.0	7.3	7.9	10.8	1.076	1.0822
31.4	13.7	13.3	19.1	0.608	0.9708
100.0	24.5	21.0	32.3	0.323	0.8571
314.0	40.5	37.0	54.9	0.175	0.9136
1.0	1.7	2.4	2.9	2.941	1.4118

Sample No. LP/1/4/120

ω	G'	G''	$/G/$	$ \eta $	Tan δ
1.0	1.2	2.2	2.5	2.506	1.8333
3.1	2.8	4.4	5.2	1.661	1.5714
10.0	6.4	8.2	10.4	1.040	1.2812
31.4	13.1	14.4	19.5	0.620	1.0992
100.0	24.4	24.8	34.8	0.348	1.0164
314.0	40.7	43.6	59.6	0.190	1.0713
1.0	1.2	2.3	2.6	2.594	1.9167

Sample No. LP/1/3/120

ω	G'	G''	/G/	$ \eta $	Tan δ
1.0	0.8	1.5	1.7	1.700	1.8750
3.1	2.0	2.9	3.5	1.122	1.4500
10.0	4.5	5.5	7.1	0.711	1.2222
31.4	8.8	10.0	13.3	0.424	1.1364
100.0	16.3	17.2	23.7	0.237	1.0552
314.0	28.4	29.8	41.2	0.131	1.0493
1.0	0.8	1.5	1.7	1.700	1.8750

Sample No. LP/1/2/120

ω	G'	G''	/G/	$ \eta $	Tan δ
1.0	0.6	1.3	1.4	1.432	2.1667
3.1	1.6	2.7	3.1	1.000	1.6875
10.0	6.0	7.4	9.5	0.953	1.2333
31.4	8.1	9.3	12.3	0.393	1.1481
100.0	15.4	16.2	22.4	0.224	1.0519
314.0	26.5	27.9	38.5	0.123	1.0528
1.0	0.6	1.3	1.4	1.432	2.1667

Appendix B Rheology Analysis for OLP/1 series Crosslinked
at 60°C and 120°C.

Sample No. OLP/1/9/60

ω	G'	G''	/G/	$ \eta $	Tan δ
1.0	2.1	2.5	3.3	3.265	1.1905
3.1	3.8	4.3	5.7	1.828	1.1316
10.0	7.5	7.6	10.7	1.068	1.0133
31.4	13.2	12.2	18.0	0.572	0.9242
100.0	22.8	20.0	30.3	0.303	0.8772
314.0	36.9	35.6	51.3	0.163	0.9648
1.0	2.0	2.4	3.1	3.124	1.2000

Sample No. OLP/1/8/60

ω	G'	G''	/G/	$ \eta $	Tan δ
1.0	1.8	2.9	3.4	3.413	1.6111
3.1	3.8	5.0	6.3	2.000	1.3158
10.0	9.6	10.0	14.1	1.408	1.0729
31.4	14.8	15.0	21.0	0.671	1.0135
100.0	26.6	24.9	36.4	0.364	0.9361
314.0	45.0	41.6	61.3	0.195	0.9244
1.0	1.9	2.7	3.3	3.302	1.4211

Sample No. OLP/1/7/60

ω	G'	G''	$/G/$	$ \eta $	Tan δ
1.0	1.2	1.8	2.2	2.163	1.5000
3.1	2.6	3.5	4.4	1.389	1.3462
10.0	5.5	6.4	8.4	0.844	1.1636
31.4	10.6	11.2	15.4	0.491	1.0566
100.0	19.4	18.7	26.9	0.269	0.9639
314.0	33.2	32.7	46.6	0.148	0.9849
1.0	1.2	1.9	2.2	2.247	1.5833

Sample No. OLP/1/6/60

ω	G'	G''	$/G/$	$ \eta $	Tan δ
1.0	1.0	1.8	2.1	2.059	1.8000
3.1	2.3	3.6	4.3	1.361	1.5652
10.0	6.9	8.3	10.8	1.079	1.2029
31.4	10.7	12.1	16.2	0.514	1.1308
100.0	20.4	20.4	28.8	0.288	1.0000
314.0	35.6	36.2	50.8	0.162	0.0169
1.0	1.0	1.8	2.1	2.059	1.8000

Appendix C Rheology Analysis for LP/2 Series Crosslinked
at 60°C and 120°C.

Sample No. LP/2/9/60

ω	G'	G''	/G/	$ \eta $	Tan δ
1.0	10.5	2.9	10.9	10.893	0.2762
3.1	14.4	8.3	16.6	5.293	0.5764
10.0	21.0	11.5	23.9	2.394	0.5476
31.4	30.4	17.0	34.8	1.109	0.5592
100.0	44.0	26.1	51.2	0.512	0.5932
314.0	63.5	42.5	76.4	0.243	0.6693
1.0	10.6	5.1	11.8	11.763	0.4811

Sample No. LP/2/8/60

ω	G'	G''	/G/	$ \eta $	Tan δ
1.0	6.9	4.3	8.1	8.130	0.6232
3.1	10.0	6.1	11.7	3.730	0.6100
10.0	14.9	9.2	17.5	1.751	0.6174
31.4	22.3	14.3	26.5	0.844	0.6413
100.0	33.7	22.4	40.5	0.405	0.6647
314.0	49.7	37.8	62.4	0.199	0.7606
1.0	6.7	3.9	7.8	7.752	0.5821

Sample No. LP/2/7/60

ω	G'	G''	$/G/$	$ \eta $	Tan δ
1.0	3.8	4.1	5.6	5.590	1.0789
3.1	6.5	5.5	8.5	2.712	0.8462
10.0	11.3	9.0	14.4	1.445	0.7965
31.4	18.1	14.0	22.9	0.729	0.7735
100.0	29.1	22.7	36.9	0.369	0.7801
314.0	37.9	33.1	50.3	0.160	0.8734
1.0	4.0	3.2	5.1	5.122	0.8000

Sample No LP/2/6/60

ω	G'	G''	$/G/$	$ \eta $	Tan δ
1.0	3.6	2.8	4.6	4.561	0.7778
3.1	6.5	6.1	8.9	2.839	0.9385
10.0	16.7	14.9	22.4	2.238	0.8922
31.4	19.8	16.9	26.0	0.829	0.8535
100.0	36.0	29.0	46.2	0.462	0.8056
314.0	52.0	45.0	68.8	0.219	0.8654
1.0	3.8	3.5	5.2	5.166	0.9211

Sample No. LP/2/5/60

ω	G'	G''	$/G/$	$ \eta $	Tan δ
1.0	1.2	1.5	1.9	1.921	1.2500
3.1	2.6	3.0	4.0	1.264	1.1538
10.0	5.0	5.4	7.4	0.736	1.0800
31.4	9.4	9.5	13.4	0.426	1.0106
100.0	16.8	16.1	23.3	0.233	0.9583
314.0	27.1	29.6	40.1	0.128	1.0923
1.0	1.3	1.7	2.1	2.140	1.3077

Sample No. LP/2/4/60

ω	G'	G''	$/G/$	$ \eta $	Tan δ
1.0	1.6	2.4	2.9	2.884	1.5000
3.1	3.5	4.5	5.7	1.816	1.2857
10.0	7.2	7.9	10.7	1.069	1.0972
31.4	13.5	13.7	19.2	0.613	1.0148
100.0	24.5	22.5	33.3	0.333	0.9184
314.0	41.7	38.5	56.8	0.181	0.9233
1.0	1.7	2.4	2.9	2.941	1.4118

Sample No. LP/2/9/120

ω	G'	G''	$/G/$	$ \eta $	Tan δ
1.0	15.2	6.4	16.5	16.492	0.4211
3.1	20.6	9.3	22.6	7.198	0.4515
10.0	30.0	14.8	33.5	3.345	0.4933
31.4	39.1	18.6	43.3	1.379	0.4757
100.0	53.7	27.8	60.5	0.605	0.5177
314.0	73.6	46.4	87.0	0.277	0.6304
1.0	15.2	6.5	16.5	16.531	0.4276

Sample No. LP/2/8/120

ω	G'	G''	$/G/$	$ \eta $	Tan δ
1.0	8.1	4.4	9.2	9.218	0.5432
3.1	11.5	6.4	13.2	4.191	0.5565
10.0	16.7	9.5	19.2	1.921	0.5689
31.4	24.2	14.3	28.1	0.895	0.5909
100.0	35.2	22.6	41.8	0.418	0.6420
314.0	51.6	36.9	63.4	0.202	0.7151
1.0	8.3	4.2	9.3	9.302	0.5060

Sample No. LP/2/7/120

ω	G'	G''	$/G/$	$ \eta $	Tan δ
1.0	8.9	5.0	10.2	10.208	0.5618
3.1	12.2	7.5	14.3	4.561	0.6148
10.0	18.3	11.2	21.5	2.146	0.6120
31.4	27.3	17.1	32.2	1.026	0.6264
100.0	40.4	26.5	48.3	0.483	0.6559
314.0	58.7	44.0	73.4	0.234	0.7496
1.0	8.6	4.9	9.9	9.898	0.5698

Sample No. LP/2/6/120

ω	G'	G''	$/G/$	$ \eta $	Tan δ
1.0	5.5	4.2	6.9	6.920	0.7636
3.1	8.7	5.9	10.5	3.348	0.6782
10.0	13.7	9.2	16.5	1.650	0.6715
31.4	21.5	14.0	25.7	0.817	0.6512
100.0	32.7	22.4	39.6	0.396	0.6850
314.0	49.3	38.2	62.4	0.199	0.7748
1.0	5.9	3.9	7.1	7.072	0.6610

Sample No. LP/2/4/120

ω	G'	G''	$/G/$	$ \eta $	Tan δ
1.0	1.8	2.4	3.0	3.000	1.3333
3.1	3.7	4.7	6.0	1.905	1.2703
10.0	10.0	10.4	14.4	1.443	1.0400
31.4	14.7	14.3	20.5	0.653	0.9728
100.0	26.3	23.7	35.4	0.354	0.9011
314.0	44.4	40.6	60.2	0.192	0.9144
1.0	1.6	2.5	3.0	2.968	1.5625

Sample No. LP/2/3/120

ω	G'	G''	$/G/$	$ \eta $	Tan δ
1.0	1.4	2.2	2.6	2.608	1.5714
3.1	3.3	4.4	5.5	1.752	1.3333
10.0	7.1	8.1	10.8	1.077	1.1408
31.4	13.9	14.1	19.8	0.631	1.0144
100.0	25.0	23.8	34.5	0.345	0.9520
314.0	42.2	42.0	59.5	0.190	0.9953
1.0	1.4	2.3	2.7	2.693	1.6429

Appendix D Rheological analysis of the crosslinked LP/6 Series

Sample No. LP/6/9/60

ω	G'	G''	/G/	$ \eta $	Tan δ
1.0	13.7	4.9	14.5	14.550	0.3577
3.1	20.3	7.9	21.8	6.937	0.3892
10.0	29.7	13.8	32.7	3.275	0.4646
31.4	35.2	14.3	38.0	1.210	0.4062
100.0	47.9	21.5	52.5	0.525	0.4489
314.0	64.9	34.8	73.6	0.235	0.5362
1.0	15.8	5.5	16.7	16.730	0.3481

Sample No. LP/6/8/60

ω	G'	G''	/G/	$ \eta $	Tan δ
1.0	16.5	9.7	19.1	19.140	0.5879
3.1	20.5	8.2	22.1	7.032	0.4000
10.0	27.3	10.8	29.4	2.936	0.3956
31.4	35.0	17.0	38.9	1.239	0.4857
100.0	50.1	24.7	55.9	0.559	0.4930
314.0	67.9	42.4	80.1	0.255	0.6244
1.0	14.9	5.2	15.8	15.781	0.3490

Sample No. LP/6/7/60

ω	G'	G''	$/G/$	$ \eta $	Tan δ
1.0	8.6	6.8	11.0	10.964	0.7907
3.1	12.6	7.4	14.6	4.654	0.5873
10.0	18.6	11.3	21.8	2.176	0.6075
31.4	27.3	16.9	32.1	1.023	0.6190
100.0	40.6	26.2	48.3	0.483	0.6453
314.0	60.3	43.2	74.2	0.236	0.7164
1.0	8.6	4.8	9.8	9.849	0.5581

Sample No. LP/6/6/60

ω	G'	G''	$/G/$	$ \eta $	Tan δ
1.0	6.0	6.0	8.5	8.485	1.0000
3.1	9.0	6.6	11.2	3.554	0.7333
10.0	14.6	10.2	17.8	1.781	0.6986
31.4	23.0	15.8	27.9	0.889	0.6870
100.0	35.6	24.9	43.4	0.434	0.6994
314.0	52.6	42.9	67.9	0.216	0.8156
1.0	6.1	4.1	7.3	7.350	0.6721

Sample No. LP/6/5/60

ω	G'	G''	$/G/$	$ \eta $	Tan δ
1.0	2.8	4.1	5.0	4.965	1.4643
3.1	6.9	7.6	10.3	3.269	1.1014
10.0	13.2	12.7	18.3	1.832	0.9621
31.4	23.9	20.7	31.6	1.007	0.8661
100.0	40.3	33.6	52.5	0.525	0.8337
314.0	64.9	56.5	86.0	0.274	0.8706
1.0	3.5	4.2	5.5	5.467	1.2000

Sample No. LP/6/4/60

ω	G'	G''	$/G/$	$ \eta $	Tan δ
1.0	2.7	4.7	4.9	4.909	1.5185
3.1	5.6	6.8	8.8	2.805	1.2143
10.0	11.3	11.7	16.3	1.627	1.0354
31.4	21.0	19.5	28.7	0.913	0.9286
100.0	36.4	32.0	48.5	0.485	0.8791
314.0	60.3	53.0	80.3	0.256	0.8789
1.0	2.7	3.6	4.5	4.500	1.3333

Sample No. LP/6/9/120

ω	G'	G''	$/G/$	$ \eta $	Tan δ
1.0	23.1	6.5	24.0	23.997	0.2814
3.1	28.6	9.5	30.1	9.598	0.3322
10.0	36.1	12.7	38.3	3.827	0.3518
31.4	46.3	17.2	49.4	1.573	0.3715
100.0	59.7	24.9	64.7	0.647	0.4171
314.0	75.4	38.4	84.6	0.269	0.5093
1.0	23.1	6.5	24.0	23.997	0.2814

Sample No. LP/6/8/120

ω	G'	G''	$/G/$	$ \eta $	Tan δ
1.0	17.6	7.5	19.1	19.131	0.4261
3.1	24.4	10.2	26.4	8.422	0.4180
10.0	32.6	13.9	35.4	3.544	0.4264
31.4	43.8	19.1	47.8	1.522	0.4361
100.0	58.7	28.5	65.3	0.653	0.4855
314.0	79.3	44.4	90.9	0.289	0.5599
1.0	19.1	7.0	20.3	20.342	0.3665

Sample No. LP/6/7/120

ω	G'	G''	$/G/$	$ \eta $	Tan δ
1.0	10.6	6.8	12.6	12.594	0.6415
3.1	15.6	8.6	17.8	5.673	0.5513
10.0	22.7	12.3	25.8	2.582	0.5419
31.4	32.5	17.9	37.1	1.182	0.5508
100.0	46.1	27.1	53.5	0.535	0.5879
314.0	65.4	42.3	77.9	0.248	0.6468
1.0	11.2	6.0	12.7	12.706	0.5357

Sample No. LP/6/6/120

ω	G'	G''	$/G/$	$ \eta $	Tan δ
1.0	5.2	4.1	6.6	6.622	0.7885
3.1	9.5	6.2	11.3	3.613	0.6526
10.0	16.5	11.2	19.9	1.994	0.6788
31.4	22.6	14.0	26.6	0.847	0.6195
100.0	33.9	21.9	40.4	0.404	0.6460
314.0	49.0	38.3	62.2	0.198	0.7816
1.0	6.4	4.1	7.6	7.601	0.6406

Appendix E Rheological analysis of the crosslinked LP/7 series

Sample No. LP/7/9/120

ω	G'	G''	$/G/$	$ \eta $	Tan δ
1	25.8	8.2	27.1	27.1	0.318
3.1	31.8	11.3	33.7	10.73	0.355
10	41.2	14.8	43.8	43.8	0.359
31.4	53.4	20.3	57.1	1.82	0.38
100	70.4	29.1	76.2	0.762	0.41
314	80.3	41.6	90.4	0.298	0.52
1.0	26.4	8.1	27.6	27.6	0.307

Sample No. LP/7/8/120

ω	G'	G''	$/G/$	$ \eta $	Tan δ
1	12.2	6.5	13.8	13.8	0.533
3.1	17.6	9.1	19.8	6.31	0.517
10.0	25.2	12.6	28.1	2.81	0.5
31.4	35.6	18.1	39.9	1.27	0.508
100.0	49.8	27.1	56.7	0.567	0.54
314.1	69.3	43.1	81.6	0.26	0.62

Sample No. LP7/7/120

ω	G'	G''	$/G/$	$ \eta $	Tan δ
1	17.1	7.9	18.8	18.8	0.462
3.1	23.1	11.1	25.6	8.15	0.481
10.0	33.3	17.1	37.4	3.74	0.514
31.4	44.1	21.5	49.0	1.56	0.488
100.0	60.6	31.8	68.4	0.684	0.525
314.1	82.3	52.7	97.7	0.31	0.64
1	16.9	7.7	18.6	18.6	0.456

Sample No. LP/7/6/120

ω	G'	G''	$/G/$	$ \eta $	Tan δ
1	12.4	6.1	13.8	13.8	0.49
3.14	16.8	8.7	18.9	6.02	0.52
10.0	25.9	14.6	29.7	2.97	0.56
31.4	34.0	18.3	38.6	1.23	0.54
100.0	47.8	28.2	55.5	0.555	0.59
314	66.4	47.4	81.6	0.26	0.714

Sample No. LP/7/5/120

ω	G'	G''	/G/	$ \eta $	Tan δ
1	2.7	3.0	4.0	4.0	1.11
3.14	5.1	5.4	7.4	2.36	1.06
10.0	11.7	11.2	16.2	1.62	0.957
31.4	17.2	15.1	22.9	0.73	0.88
100.0	29.2	25.0	38.4	0.384	0.86
314	46.3	43.1	63.3	0.20	0.93
1	2.6	2.9	3.9	3.9	1.12

Sample No. LP/7/4/120

ω	G'	G''	/G/	$ \eta $	Tan δ
1	3.9	4.2	5.7	5.7	1.08
3.14	7.2	6.8	9.9	3.15	0.94
10.0	15.1	13.2	20.0	2.0	0.87
31.4	22.4	17.9	28.7	0.91	0.80
100.0	36.6	28.5	46.4	0.464	0.78
314	59.4	45.6	74.9	0.239	0.77
1	3.9	3.9	5.5	5.5	1

Appendix F Rheological analysis of the γ -irradiation polyethylene films

Sample No. PE/M/D200

ω	G'	G''	$/G/$	$ \eta $	Tan δ
1.0	7.5	1.6	7.7	7.669	0.2133
3.1	8.5	1.2	8.6	2.734	1.1412
10.0	9.6	1.7	9.7	0.975	0.1771
31.4	11.1	2.6	11.4	0.363	0.2342
100.0	13.4	4.7	14.2	0.142	0.3507
314.0	16.5	9.0	18.8	0.060	0.5455
1.0	10.6	0.8	10.6	10.630	0.0755

Sample No. PE/D200

ω	G'	G''	$/G/$	$ \eta $	Tan δ
1.0	2.0	1.6	2.6	2.561	0.8000
3.1	4.9	1.3	5.1	1.614	0.2653
10.0	6.2	1.7	6.4	0.643	0.2742
31.4	7.9	2.7	8.3	0.266	0.3418
100.0	10.2	4.4	11.1	0.111	0.4314
314.0	13.0	8.8	15.7	0.050	0.6769
1.0	7.2	0.9	7.3	7.256	0.1250

Sample No. PE/M/D100

ω	G'	G''	/G/	$ \eta $	Tan δ
1.0	25.8	1.1	25.8	25.823	0.0426
3.1	27.0	1.5	27.0	8.612	0.0556
10.0	27.8	1.4	27.8	2.784	0.0504
31.4	28.6	2.3	28.7	0.914	0.0804
100.0	29.9	3.9	30.2	0.302	0.1304
314.0	30.3	6.6	31.0	0.099	0.2178
1.0	27.6	1.3	27.6	27.631	0.0471

Sample No. PE/D100

ω	G'	G''	/G/	$ \eta $	Tan δ
1.0	20.8	0.6	20.8	20.809	0.0288
3.1	20.5	1.0	20.5	6.536	0.0488
10.0	21.4	1.4	21.4	2.145	0.0654
31.4	22.7	2.4	22.8	0.727	0.1057
100.0	24.7	4.1	25.0	0.250	0.1660
314.0	32.9	16.5	36.8	0.117	0.5015
1.0	21.4	0.7	21.4	21.411	0.0327

Sample No. PE/M/D60

ω	G'	G''	$/G/$	$ \eta $	Tan δ
1.0	3.4	1.8	3.8	3.847	0.5294
3.1	4.6	2.8	5.4	1.715	0.6087
10.0	6.7	4.2	7.9	0.791	0.6269
31.4	10.0	6.4	11.9	0.378	0.6400
100.0	14.9	10.1	18.0	0.180	0.6779
314.0	22.0	16.6	27.6	0.088	0.7545
1.0	3.6	1.8	4.0	4.025	0.5000
1.0	4.3	1.9	4.7	4.701	0.4419

Sample No. PE/D60

ω	G'	G''	$/G/$	$ \eta $	Tan δ
1.0	6.2	1.9	6.5	6.485	0.3065
3.1	7.6	3.8	8.5	2.706	0.5000
10.0	9.7	4.4	10.7	1.065	0.4536
31.4	13.1	6.4	14.6	0.464	0.4885
100.0	18.0	8.0	19.7	0.197	0.4444
314.0	25.0	18.0	30.8	0.098	0.7200
1.0	6.6	2.2	7.0	6.957	0.3333

Sample No. PE/M/D40

ω	G'	G''	/G/	$ \eta $	Tan δ
1.0	3.8	2.8	4.7	4.720	0.7368
3.1	4.9	3.1	5.8	1.847	0.6327
10.0	7.5	4.9	9.0	0.896	0.6533
31.4	10.7	7.6	13.1	0.418	0.7103
100.0	16.3	12.2	20.4	0.204	0.7485
314.0	23.9	22.2	32.6	0.104	0.9289
1.0	3.8	2.0	4.3	4.294	0.5263

Sample No. PE/D40

ω	G'	G''	/G/	$ \eta $	Tan δ
1.0	3.9	2.6	4.7	4.687	0.6667
3.1	6.6	3.9	7.7	2.441	0.5909
10.0	9.8	5.9	11.4	1.144	0.6020
31.4	14.9	9.3	17.6	0.559	0.6242
100.0	21.8	14.5	26.2	0.262	0.6651
314.0	33.2	24.6	41.3	0.132	0.7410
1.0	6.3	3.0	7.0	6.978	0.4762
1.0	6.4	3.3	7.2	7.201	0.5156

Sample No. PE/M/D20

ω	G'	G''	$/G/$	$ \eta $	Tan δ
1.0	7.2	3.2	7.9	7.879	0.4444
3.1	7.8	4.8	9.2	2.917	0.6154
10.0	11.4	7.0	13.4	1.338	0.6140
31.4	16.9	10.7	20.0	0.637	0.6331
100.0	25.0	16.7	30.1	0.301	0.6680
314.0	65.1	55.1	85.3	0.272	0.8464
1.0	5.5	2.9	6.2	6.218	0.5273

Sample No. PE/D20

ω	G'	G''	$/G/$	$ \eta $	Tan δ
1.0	6.3	1.2	6.4	6.413	0.1905
3.1	8.4	5.3	9.9	3.163	0.6310
10.0	15.5	10.9	18.9	1.895	0.7032
31.4	17.0	11.5	20.5	0.654	0.6765
100.0	26.1	18.0	31.7	0.317	0.6897
314.0	37.7	30.7	48.6	0.155	0.8143
1.0	5.3	3.0	6.1	6.090	0.5660
1.0	5.3	2.9	6.0	6.042	0.5472

Sample No. PE/M/D12

ω	G'	G''	$/G/$	$ \eta $	Tan δ
1.0	3.6	3.0	4.7	4.686	0.8333
3.1	6.1	4.6	7.6	2.433	0.7541
10.0	9.0	6.0	10.8	1.082	0.6667
31.4	15.0	10.0	18.0	0.574	0.6667
100.0	22.0	17.0	27.8	0.278	0.7727
314.0	34.0	28.0	44.0	0.140	0.8235
1.0	3.8	2.7	4.7	4.662	0.7105

Sample No. PE/D12

ω	G'	G''	$/G/$	$ \eta $	Tan δ
1.0	3.1	2.9	4.2	4.245	0.9355
3.1	6.1	4.3	7.5	2.377	0.7049
10.0	9.2	6.5	11.3	1.126	0.7065
31.4	14.2	9.8	17.3	0.549	0.6901
100.0	21.7	15.6	26.7	0.267	0.7189
314.0	32.1	26.1	41.4	0.132	0.8131
1.0	3.6	2.5	4.4	4.383	0.6944

Sample No. PE/M/D6

ω	G'	G''	$/G/$	$ \eta $	Tan δ
1.0	1.7	2.1	2.7	2.702	1.2353
3.1	3.2	3.6	4.8	1.534	1.1250
10.0	6.2	6.2	8.8	0.877	1.0000
31.4	11.0	10.5	15.2	0.484	0.9545
100.0	19.0	17.3	25.7	0.257	0.9105
314.0	32.0	29.3	43.4	0.138	0.9156
1.0	1.6	1.9	2.5	2.484	1.1875

Sample No. PE/D6

ω	G'	G''	$/G/$	$ \eta $	Tan δ
1.0	3.1	2.8	4.2	4.177	0.9032
3.1	4.8	4.5	6.6	2.095	0.9375
10.0	8.4	7.3	11.1	1.113	0.8690
31.4	14.2	11.9	18.5	0.590	0.8380
100.0	23.1	19.3	30.1	0.301	0.8355
314.0	35.8	32.9	48.6	0.155	0.9190
1.0	2.7	2.5	3.7	3.6800	0.9259

Sample No. PE/M/D4

ω	G'	G''	$/G/$	$ \eta $	Tan δ
1.0	1.9	2.6	3.2	3.220	1.3684
3.1	3.7	2.6	4.5	1.440	0.7027
10.0	10.1	10.2	14.4	1.435	1.0099
31.4	13.1	12.5	18.1	0.577	0.9542
100.0	22.6	20.7	30.6	0.306	0.9159
314.0	37.5	35.7	51.8	0.165	0.9520
1.0	1.7	2.2	2.8	2.780	1.2941

Sample No. PE/D4

ω	G'	G''	$/G/$	$ \eta $	Tan δ
1.0	1.6	2.4	2.9	2.884	1.5000
3.1	3.4	4.6	5.7	1.822	1.3529
10.0	7.2	8.4	11.1	1.106	1.1667
31.4	13.8	14.4	19.9	0.635	1.0435
100.0	25.1	24.1	34.8	0.348	0.9602
314.0	42.9	40.9	59.3	0.189	0.9534
1.0	1.6	2.4	2.9	2.884	1.5000

Sample No. PE/M/D1

ω	G'	G''	/G/	$ \eta $	Tan δ
1.0	1.2	2.2	2.5	2.506	1.8333
3.1	2.8	4.4	5.2	1.661	1.5714
10.0	6.4	8.2	10.4	1.040	1.2812
31.4	13.1	14.6	19.6	0.625	1.1145
100.0	24.2	24.9	34.7	0.347	1.0289
314.0	31.7	30.3	43.9	0.140	0.9558
1.0	1.1	2.2	2.5	2.460	2.0000

Sample No. PE/D1

ω	G'	G''	/G/	$ \eta $	Tan δ
1.0	0.7	1.3	1.5	1.476	1.8571
3.1	1.6	2.6	3.1	0.972	1.6250
10.0	3.9	5.2	6.5	0.650	1.3333
31.4	7.7	9.2	12.0	0.382	1.1948
100.0	14.6	16.1	21.7	0.217	1.1027
314.0	24.4	29.8	38.5	0.123	1.2213
1.0	0.6	1.3	1.4	1.432	2.1667

REFERENCES

1. Ferry, J.D., Viscoelastic Properties of Polymers, John Wiley (1970).
Rodriguez, F., Principles of Polymer Systems, McGraw-Hill (1970).
2. Walters, K. Basic Concepts & Formulae for the Rheogoniometer, Published by Sangamo Controls Ltd., Sussex, England 1968.

CHAPTER 6DISCUSSION AND CONCLUSIONS6.1 Discussion based on the results obtained from the polyethylene networks

The results obtained from the previous two chapters can be classified into three categories:- Gel characterization, Sol characterization and the polyethylene network as a whole.

Two points should be mentioned here, before discussing the characterization results obtained from the UV irradiated polyethylene. The first point is the the cross-linking process, with which this thesis deals, was carried out in the solid state i.e. polyethylene films. This means that reactants such as the TAC and Xanthone, which are incorporated in the matrix, will not be very mobile, but will have to diffuse from site to site.¹ However, it is possible that such foreign materials in a solid matrix are more free to move when the polyethylene is in the molten state.

In the case where the reactants are required to diffuse, the rate at which the reaction proceeds may be governed by the rate at which the reactants approach one another, and also to the collisions of their intermediates with surrounding molecules.

It should be noted that when UV radiation is used, the depth of penetration into the film must be considered. The rate of xanthone decomposition will depend mainly on the light intensity.

The following scheme can be envisaged for the irradiation of the polyethylene film.

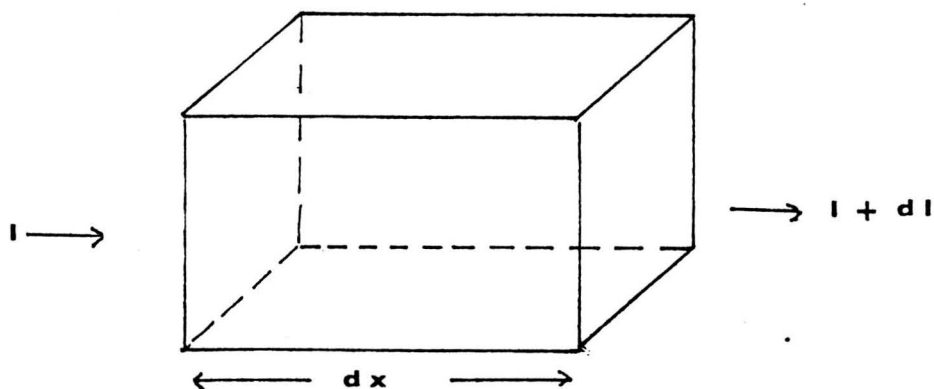


Fig. 6-1

where dx is the film thickness and dI will be numerically negative.

The effect of light penetration through different thicknesses is demonstrated in section 4.5.7 and is shown in Fig. 6.2. This shows the effect of film thickness on the decomposition of xanthone. Light penetrates layer by layer, decomposing xanthone at each stage.

This phenomenon and its effect on the crosslinking process is clearly shown in Fig. 6.3. The melt flow Index (MFI) values will normally be very low for a cross-linked polymer. As seen in Fig. 6.3 the top layer will have a very low MFI value of around 0.001 whereas the bottom layers have hardly been affected by the process.

This lack of light penetration throughout the film is mainly due to the low energy of light and also to the xanthone which absorbs most of the light in the top layer due to its high extinction coefficient.

This phenomenon is known in the photoinitiation process as the skin effect.

Since the irradiation is carried out in the solid state, the light intensity will decrease due to scattering from the different morphological sites in the matrix i.e. crystalline and amorphous phases (Fig. 6.4).

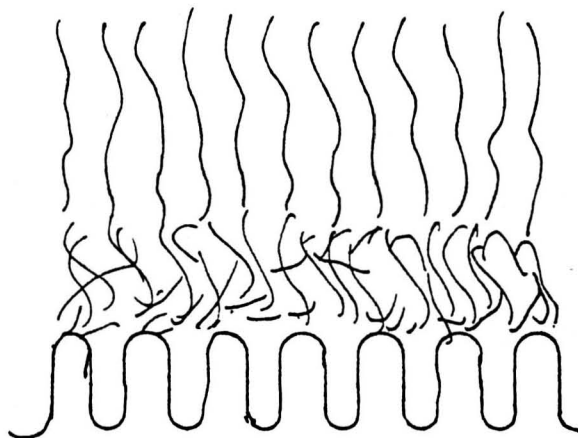


Fig. 6-4

The crystalline zone consists of ^{linear} $\langle \text{CH}_2 \rangle$ chain units. The other zone is the disordered amorphous phase, where the chain units $\langle \text{CH}_2 \rangle$ are in a non-ordered conformation and where branching is present. The third region is located at the diffuse boundary between the ordered and the disordered zones. The region is not regular in structure. When incorporating additives to such a polymer, they will reside mainly, if not, solely in the amorphous region since it is in a non-ordered state. So in our system where initiation is expected to originate where the xanthone is located, one would postulate that most of the reaction and crosslinking would only take place in the amorphous region.

6.1.1 Gel and Sol characterization results

From the gel content results shown in tables 4.2-4.12, it is quite clear that the maximum gel content was up but not exceeding 60%. Where the TAC initial concentration exceeds 1%, the gel content will drop. Where the xanthone concentration is increased from the 0.1% w/w to 0.25% w/w, the gel content increases. It was also noted that, whenever oxygen is present, the gel content decreases and when the irradiation temperature increases, the gel content also increases.

It should be noted that increases ⁱⁿ the irradiation time (i.e. greater than 30 minutes), produced no significant change in gel content.

For TAC containing systems, 5-10% gel formation will occur after approximately four minutes. When TAC was not present, the gel content for polyethylene did not exceed 10% which indicates that the TAC monomer plays a major part in this type of crosslinking. The slight increase in the gel content, when the process was carried out at 120°C, is due to the fact that most of the crystalline region will be destroyed at that temperature and the additives will have a chance to diffuse into the molten crystallites.

Figs. 6.5-6.7 show the IR spectra of the extracted gel for some selected UV irradiated samples. The gel obtained from crosslinking with TAC in the presence of the photoinitiators showed clearly the three distinct peaks of the polymerized TAC. The peaks were at 1560 cm⁻¹, 1140 cm⁻¹ and 820 cm⁻¹. These three peaks were obviously not noticed

when TAC was not incorporated e.g. in the gel from sample PE/X/8/60. Although the IR quantitative analysis for this system will not be very accurate, it was still carried out and the analysis was based on the two peaks at 1560 cm^{-1} and 820 cm^{-1} .

Figs. (6.8-6.11) compare the gel fraction and gel poly TAC content versus the irradiation time. It was clear from these figures that the poly TAC content in the gel increases with the initial TAC concentration in the polyethylene. Although the poly TAC content in the gel did not reach the original TAC concentration, the maximum content observed was around 3.5% w/w. It was also noted from Figs. (6.12, 6.13) that the gel fraction will be reduced, when the initial TAC concentration goes over 1% w/w. This clearly means that the TAC present in the polyethylene will polymerize and form a poly TAC network, which in turn, will be terminated at one stage between polyethylene molecules. The polyethylene network will then form.

Using the Flory-Huggins equation, to determine the M_c from the swelling measurements is far from ideal since no account was taken for the structural imperfections (as mentioned in 4.3.3). These would probably be present in our systems. However, the M_c values obtained from the swelling measurements and the gel fraction measurements (tables 4.14-4.21) were within the same range.

The M_c values were of the order $50,000 \pm 20,000$. Since this is almost half of the original polyethylene molecular weight, it is evident that only a small percentage of the carbon atoms in the polyethylene molecules actually take part in the crosslinking process. For a low radiation time, e.g. 15 minutes, the M_c values are around 120,000, which is in the same order as the molecular weight of the original polyethylene. Therefore, the percentage of carbon atoms taking part in the crosslinking process is very small. This again indicates that poly TAC formed will be the major factor for formation of the polyethylene network. It is very important to note that there is a considerable difference between UV and γ -irradiated polyethylene. In the latter process the M_c values were of the order 6000-7000, indications that a higher

percentage of the carbon atoms in polyethylene were involved in the crosslinking process.

Figs. 6.14-6.16 show the log crosslinking density to the gel fraction relationship. It shows that, when a higher concentration of crosslink agent is used, the crosslink density is greater, when the gel content is lowered.

This could be compared in Fig. 6.17 where it is shown that in the case of the γ -irradiated polyethylene, a higher gel content is needed to achieve high crosslinking density.

This fact is very clearly shown in the GPC analysis of the sol part in table 4.33. The molecular weight distribution (\bar{M}_w/\bar{M}_n) of "3" was determined for a UV irradiated network containing around 50% gel. Whereas a γ -irradiated polyethylene, the molecular weight distribution (\bar{M}_w/\bar{M}_n) was 2.45 for a network containing around 60% gel. Figure 6.18 shows how the higher end of the molecular weight will disappear with UV irradiation. At 50% gel content, the sol part will contain a high molecular weight fraction of \bar{M}_w about 2×10^5 . In figures 6.19 and 6.20, it is shown that the high molecular weight fraction disappeared with the γ -irradiated sample. At 60% gel content, the sol part contains only a high molecular weight fraction of \bar{M}_w about 1×10^5 .

For comparison, the polyethylene was subjected to ^{60}Co γ -irradiation with and without the TAC. Generally speaking, the gel fraction was about the same in both cases,

at medium doses of radiation. The polyethylene and TAC produced a slightly higher content of gel as shown in Figure 6.21. Cross and Lyons(2) analysed polyethylene/TAC crosslinking and found that the TAC inhibits gel formation at low doses. At higher doses, the gel formation is considerably increased. Cross and Lyons also reached the conclusion that, at TAC concentrations of 0.5-5.0 % each additive molecule crosslinks between 2.5 and 3 polymer molecules, whereas they indicated that allyl polymerization is not significant. In our studies IR analysis of the gel content of the UV irradiated system and γ -irradiated system showed that in the latter case, polymer crosslinked did not show any poly TAC in the gel as shown in Figure 6.22. In the UV irradiated polymer, the poly TAC content is very clearly present in the gel (Figures 6.5-6.7). This indicates that in the γ -irradiation crosslinking, TAC will not be incorporated in the gel formation as poly TAC. However, at low doses of γ -irradiation, namely < 10 Mrad, poly TAC was noticed in the gel part of the polyethylene network, thus confirming the results of Cross and Lyons.

The results obtained from the post-curing experiment, which involved the incorporation of additives by means of swelling after different times of UV irradiation, proves that the gel content will reach a maximum of 45%-50%. The polyethylene employed in this work contains 55-60% of amorphous material. The gel content corresponds to essentially 90% gelation of the amorphous regions and the crosslinking of the crystalline regions does not occur. This is consistent with the earlier statement, that most

of the additives will reside in the amorphous region. Even when further amounts of additives are introduced by means of swelling, they were expected to be absorbed only in the amorphous regions of the polyethylene, as was suggested by Richards³ and McCall.⁴

From the elemental analysis obtained for the gel samples, the nitrogen present in the network, which is an indication of poly TAC present, is scattered throughout the system. It means that the poly TAC is randomly incorporated in the network. This agrees with the observations noted when the gel samples were obtained using different UV irradiation times. For times less than 10 minutes, it was sometimes observed that the film showed areas of non-uniformity. However, with times greater than 10 minutes the thin sheet appeared completely homogeneous.

The molecular weights between crosslinks i.e., M_c , in the gel part of the post-cured irradiated polyethylene are shown in table 4.31. This indicates that for 25% gel there were small percentages of carbon atoms of the polymer involved in the crosslinking. On the otherhand there was a decrease in the number average molecular weight. \bar{M}_n , for the sol part and an increase in the weight average molecular weight \bar{M}_w as shown in table 4.33. This means that even at the total one hour irradiation, the gel content was 38% but there were few polymer molecules linked together which did not form a network i.e., were still soluble. However, after the one hour curing time, the samples started to show a reduction

in both the \bar{M}_n and \bar{M}_w , forming a narrower molecular weight distribution together with a reduction in the M_c values as shown in tables 4.33 and 4.31 respectively.

This means that, in the first instance crosslinking mainly involves TAC and a small percentage of carbon atoms from the polyethylene. At further stages more of the polyethylene's carbon atoms are involved in the network formation.

This agrees with the results obtained from the TAC content in the gel (tables 4.22-4.26) where in most cases the TAC, incorporated in the gel after the first five minutes of irradiation, will be $> 50\%$ of its original concentration. This only applies where the starting concentration of TAC is less than 1%.

This observation was similarly noticed by Odian and Bernstein⁵, when they were irradiating polyethylene in the presence of certain poly functional monomers by gamma radiation from ^{60}Co and electrons from a Van der Graaf accelerator.

It was generally noticed that when the initial TAC concentration in the polyethylene film exceeds the 1% w/w, the TAC was found to migrate to the surface of the polyethylene film, if a long enough period was allowed to elapse between pressing and irradiating the film. This is an indication that the system is not compatible, which will eventually lead to a two phase system even after forming the network.

6.12 Polyethylene network characterization results

As seen from section 4.5.9, the tensile strength and elongation tests did not show any significant differences between the untreated low density polyethylene and the one hour cured sheet.

From the x-ray diffraction and DSC analysis, it was noticed that there were no changes in the degree of crystallinity and T_m values respectively. These results indicate that the physical structure of the polyethylene after the UV irradiation was not affected. It was reported by Charlesby and coworkers⁶ Rejan⁷ and Collins and Culkins,⁸ that in most cases of γ -irradiated polymers, the mechanical properties are only significantly altered by high radiation doses. In the case of polyethylene the tensile strength was altered significantly above 100 mrad dose whereas the elongation was significantly altered above a 50 Mrad dose. At these doses the crystallinity was also affected. However in the UV system, although a moderate gel content was achieved, the degree of crystallinity was not affected and it was not sufficient to alter the mechanical properties.

The mechanical properties were also affected by other factors,⁹ such as molecular weight (\bar{M}_n) of the polymer. Comparing \bar{M}_n values of the sol part for the untreated polyethylene and the PE/I sample which was cured for one hour, it was observed that the \bar{M}_n values did not have a significantly large reduction which obviously indicates that the molecular weight has little direct effect on the yield stresses. Nevertheless, the molecular

weight changes will have a more definite effect on the other mechanical properties such as fatigue and environmental stress cracking.¹⁰ The T_g which was obtained from the DSC analysis, did not show any significant difference.

Factors which normally influence the glass transition temperature are the main chain structure of the amorphous zone and the side groups present in the zone. If there is any change in the main chain structure, this will produce changes in the molecular flexibility which in turn shows the effect in the T_g values. The nature of the side groups will influence the free volume in the zone. Free volume¹¹ is defined as an overall population of holes due to local density changes on a molecular scale. In general chemical crosslinking raises the temperature of the glass transition.⁹ For a very highly crosslinked material, there is no glass transition. This behaviour can be interpreted on the basis of changes in free volume, as chemical crosslinking brings adjacent chains closer together, reduces the free volume and hence raises the T_g .

It seems in our systems that the main chain structure has not been effected to the extent where it will affect the glass transition. The poly TAC involved in the chemical network is so small in size, the free volume has hardly been affected.

The environmental stress cracking (ESC) did show an improvement using the light cured treatment as shown

in Fig. 6.23. The ESC is defined as a delayed brittle failure of the polymer under stress in the presence of an active environment. The active environments that cause failure in polyethylene are polar liquids or waxes.

Although much is now known about the factors affecting stress cracking, the actual cause is still little understood.^{12, 13} Factors affecting stress cracking can be divided into three areas:- stress, environment and polymer characteristics.

As far as the polymer characteristics are concerned, three variables are important, molecular weight, melt index and crystallinity. The latter which usually increases the cracking will not be considered here as it was already found that there was no change in crystallinity on the polyethylene treated sheet. However, the melt index, which is usually related to the molecular weight of the polymer, will affect the ESC in a way that a low melt index means a higher viscosity. This is exactly consistent with our system, where the MFI values are usually very low for the irradiated polyethylene. However, the low MFI values will be due to an increase in the molecular weight and a narrowing of the molecular weight distribution.

Swelling of polymers introduces an additional stress into the polymer due to interaction with the solvent molecules. Brawn¹⁴ has proposed that this additional stress is reduced by crosslinking and hence will result in an improvement in the ESC characteristics. However, in our light cured system, it was found that the amorphous and the crystalline zones were little affected by the presence of

the microstructure of poly TAC. Therefore, it will be correct to say that the improvement in the ESC is due to the resistance of swelling in the amorphous phase.

6.1.3 Flow properties of the polyethylene network

The rheological studies carried out on the polyethylene sheets indicated an increase in visco elastic behaviour. In general, polymer melts have high viscosities due to restrictions in molecular motion as a result of chain entanglements. This situation also exists in the case of polymer networks. Furthermore, high elasticity depends on the length of the polymer chains. This results in a decrease in elasticity of network polymer since the chains are shortened due to crosslinks.

In general, the storage modulus, loss modulus and loss tangent for a polymer behave as shown in Fig. 6.24.⁹

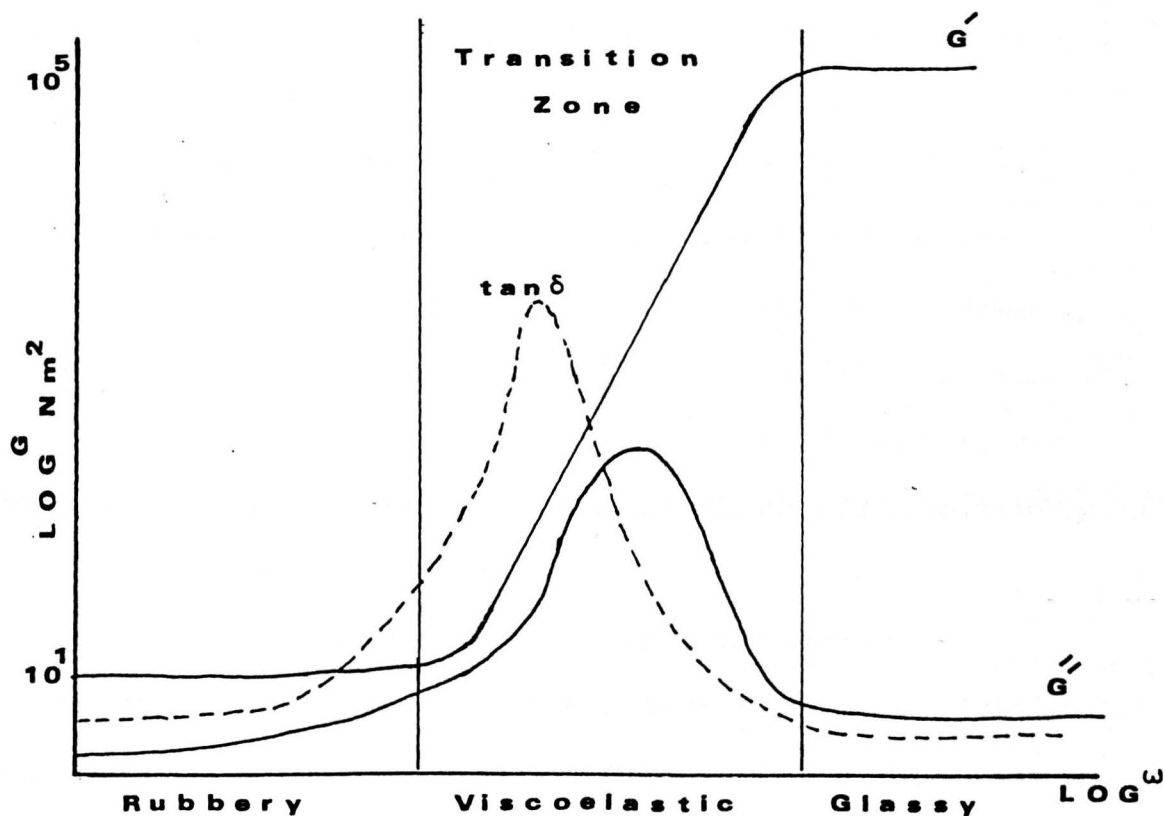


Fig. 6_24

At low frequencies, the polymer exhibits rubber-like characteristics since it has time to respond to the applied deformation. At high frequencies, the system becomes rigid (i.e. glassy) since molecular motion is too slow to follow the perturbation.

However, at intermediate frequencies we may have a mixture of two processes i.e. rubber like and glassy behaviour. This region is therefore, known as the viscoelastic zone.

The position of the transition zone with reference to the frequency scale varies among polymers. It was reported by Ferry¹⁵ that moderate crosslinking effects the transition zone only to a minor degree.

The viscosity study in chapter 5 was carried out at intermediate frequencies. However, the studies did not cover the whole frequency region. For the purpose of studying the effect of crosslinking on the system, it was sufficient to study only part of that region.

As seen from the data in chapter 5, it seems that the crosslinking process did change the viscoelastic properties of the polymer. In a UV crosslinked network, the storage and loss moduli will change in the transition zone (at intermediate frequencies). This is due to the short range configurational changes which will obviously increase with crosslinking.

Fig. 6.25, shows how the complex modulus and viscosity will increase with the degree of crosslinking. The other data for the different crosslinked films are shown in the Appendices of chapter 5, which clearly shows the

changes in the rheological parameters.

Fig. 6.26, shows the changes of the loss tangent ($\text{Tan } \delta$) with a range of frequencies for selected cross-linked films and untreated polyethylene films. Most of the crosslinked films show the behaviour of a UV cross-linked polymer as demonstrated by Ferry.¹⁵

In general, polymers containing both crystalline and amorphous regions, whether crosslinked or not, have a value of $\text{tan } \delta = 1$ as reported by Ferry.¹⁵

Fig. 6.27-6.29 show the complex modulus and viscosity will change by altering the temperature. As seen from these figures, the effect on the treated film is less severe compared to the effect on the untreated film.

The thermal stability is better demonstrated in Fig. 6.30 where the complex modulus and viscosity at constant frequency were plotted against temperature. Again it is clearly shown that with increasing temperature, the UV treated film maintains its flow properties reasonably well in comparison to the untreated film.

It was interesting to note the effect of ageing on the properties of UV and γ -irradiated systems. As shown in Fig. 6.31 the viscosity of the UV treated film is constant with respect to time. However, the γ -irradiated material shows a slight increase in viscosity with time. The changes in viscosity in the γ -irradiated system is due to the presence of trapped free radicals which at 160°C cause further crosslinking.

6.2 Conclusions

The incorporation of triallyl cyanurate (TAC) into UV treated polyethylene films causes only slight changes in some physical and mechanical properties (T_g and T_m), but significant changes in others such as viscous flow and environmental stress cracking. These latter appeared to be the result of a modification of the polymer molecular weight which occurred by the UV irradiation. The effect on these properties seems to reach a maximum at around 1% w/w incorporation of TAC even though higher levels were shown by infra-red analysis to contain an increased poly (TAC) level. Because of the skin effect it is best in practice, to work at xanthone levels below 0.5 w/w.

If the xanthone photoinitiation mechanism is established and the conclusions obtained from chapter 2 and 3 are applied to the low density polyethylene, then the crosslinking process taking place is reasonably clear.

In the case of the loaded polymer, with xanthone only, the photoinitiator will be activated by light, abstracting the hydrogen from the polyethylene backbone. At this stage the polymer will have a few free radical centers which will also migrate to a certain extent along the polymer molecules. These free radical centers will eventually be terminated by combination with another polymer molecules or within the same molecule to form a polymer network. However, such a process will give a low gel content as shown from the data obtained.

The picture will then be different if the TAC is present in the polymer together with the photoinitiator. The free radical centers will form within the polyethylene molecules due to hydrogen abstraction, and will again migrate throughout the polymer molecules.

These free radical centers, will diffuse and collide with the TAC molecules present within the polymer matrix. Their collisions will cause the initiation of the TAC monomer by one of the means suggested in chapter 2 and 3 i.e. hydrogen transfer, hydrogen abstraction, or by chain addition reactions. In any of these cases, the TAC will polymerize and will

eventually form a crosslinked poly TAC within the polymer matrix. This will occur by chain addition polymerization which involves propagation as well as termination steps. The crosslinked poly TAC formed will be dispersed within the polyethylene matrix. This picture is similar to the formation of the insoluble dispersion, which occurred in the model poly TAC/octane system. The polymerization of TAC will create, in addition to a network, a high functionality (active chain ends) polymer which will terminate at one stage by either colliding with another activated TAC molecule or by colliding with a polyethylene molecule. By this procedure, the polyethylene will be crosslinked in different centers according to the presence of TAC within the matrix.

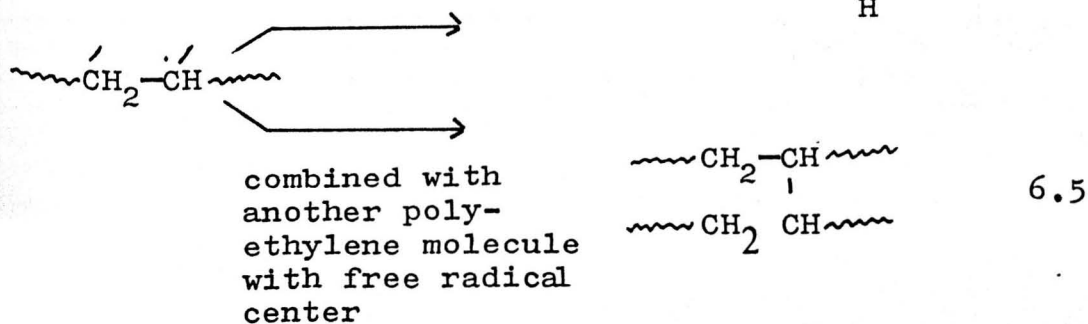
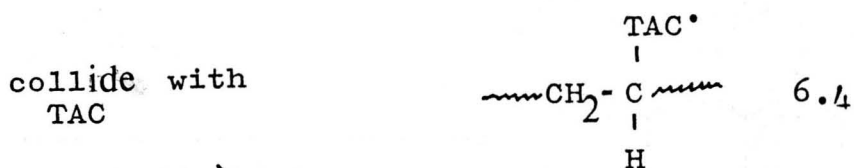
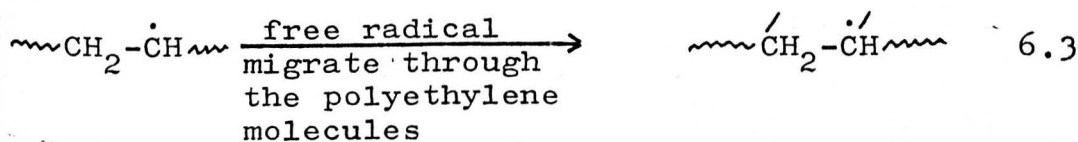
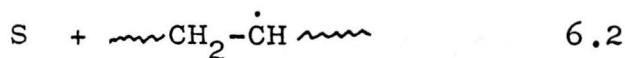
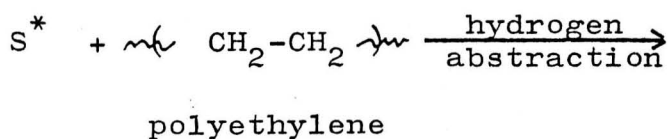
From the data obtained in chapter '1', it appears that this crosslinking process will mainly take place within the first ten minutes of the UV exposure to the loaded film. In this period the probability of collision between activated polymer molecules and the TAC molecule will be high. However, the higher concentration of TAC will cause a slight reduction in the gel content. This observation is consistent with a process whereby poly TAC terminates with its own species rather than with polyethylene molecule. Also with the higher TAC concentration, the possibility of chain transfer and forming the degradative allyl radical will be higher. This means a smaller short chain network with a possibility that more than one will link within the same polyethylene molecule.

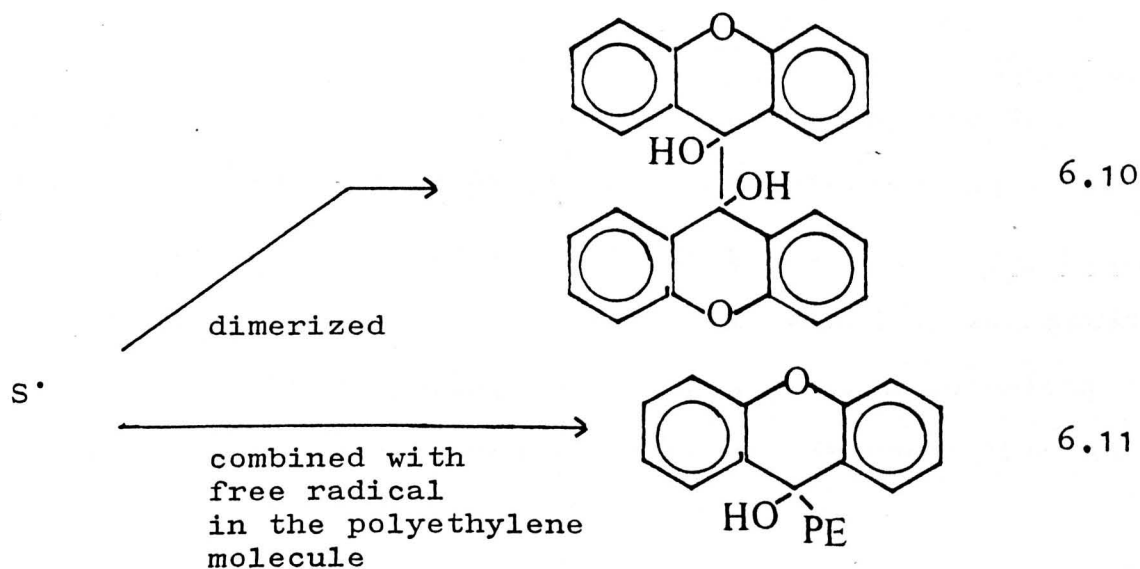
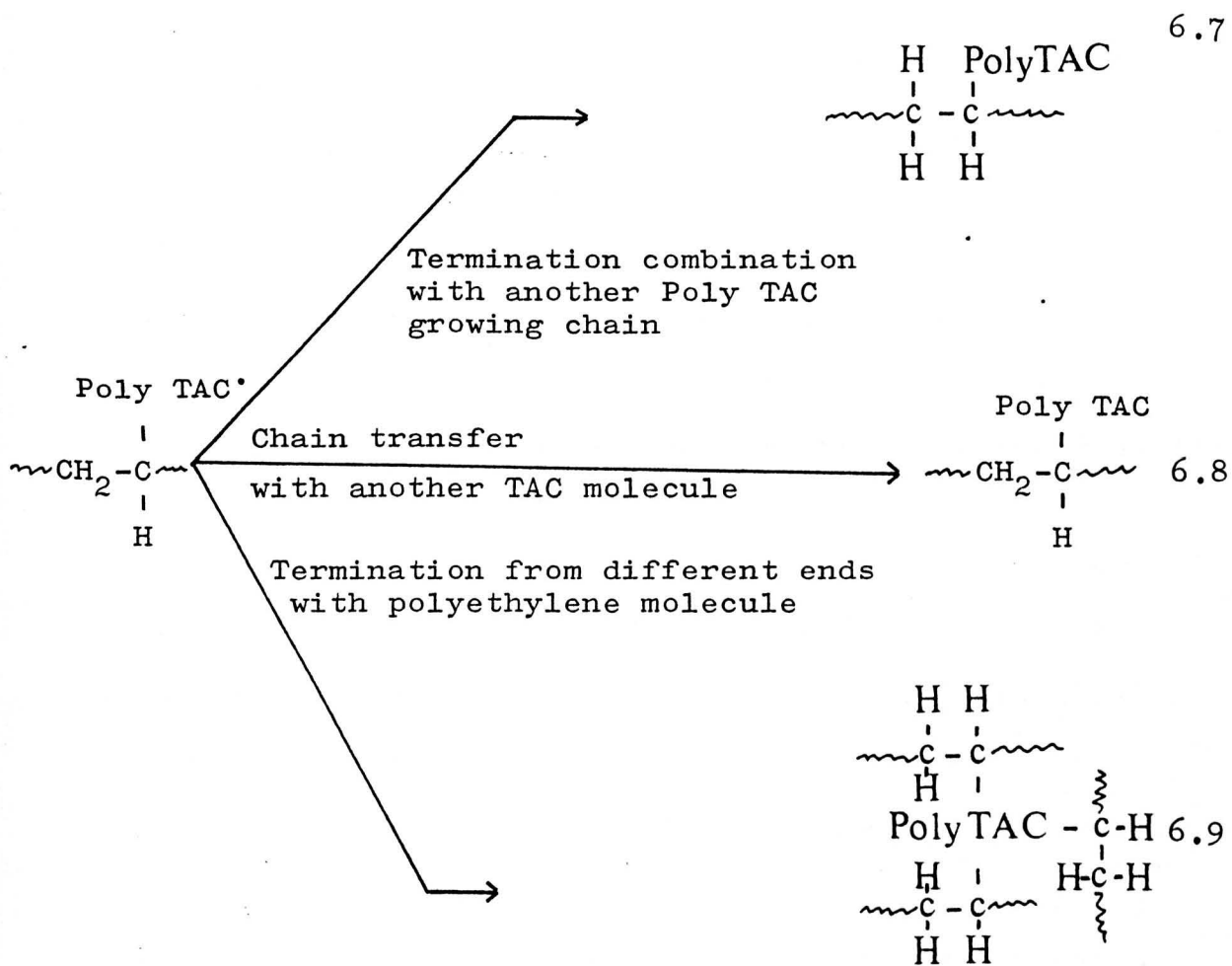
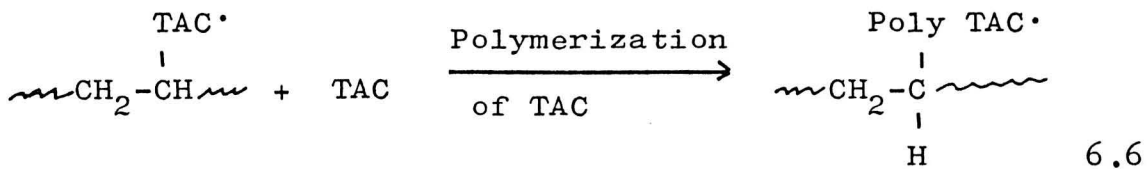
In general, the poly TAC network domain will be small. The network will indeed form due to the high functionality of the TAC resulting in low conversion. The possibility of chain transfer reactions and the formation of degradative radicals will limit the size of the network.

There was an attempt to see the gel part by electron microscopy, with the film stained with Osmium tetroxide. Unfortunately, circumstances prevented the carrying of such an analysis, which would no doubt have been very useful especially if separate domain of poly TAC could be seen. This would then have verified our assumption of such a domain in the polyethylene matrix.

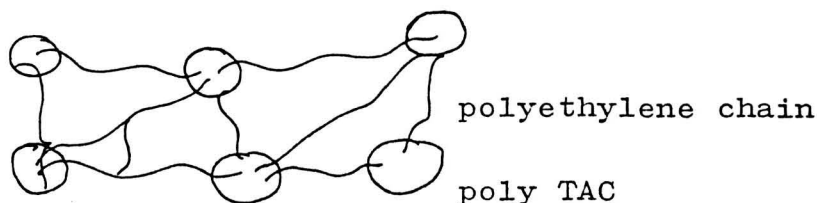
As was noticed from the incompatibility of the TAC in the polyethylene film, one could only assume that the polymer of such an incompatible additive, if formed within the polyethylene matrix would be a separate phase i.e., dispersed within the polymer.

The mechanism of the crosslinking process could be summarised, as follows in terms of the chemical equations:-





The final picture of the process could be represented by the following drawing.



- S* : Xanthone activated state
 S· : Xanthrol free radical
 TAC· : Free radical in one of the allyl groups in the TAC
 Poly TAC· : TAC growing polymer chain with the possibility of three dimension polymer due to the high functionality.

As could be seen from the above scheme, the more TAC present in the system, the more poly TAC microphase is spread within the polyethylene matrix. The overall gel content will be the same, since the same polyethylene molecules will be linked with the growing poly TAC network.

It should also be mentioned that the polyethylene molecules which are more likely to link to such a system will be the branched part of the polymer rather than the linear part i.e. the part which is present within the amorphous region. This statement is verified by the GPC analysis where the higher MW fraction of polyethylene disappears from the Sol part of the network.

For further work in this system, it would be worthwhile to investigate the morphology of the system in more detail and to analyse it by electron microscope. It could then be

used to verify the presence of such a separate domain in the network.

REFERENCES

1. Wintle, H.J. Theory of reactions in the Solid State Chapter 6 in "The radiation chemistry of Macromolecules" Vol. 1 by M. Dole, Academic Press 1972
2. Cross, P.E., Lyons, B.J. Trans. Faraday SOC 59, 2350 (1963).
3. Richards, R.B. ibid 12, 11 (1946).
4. McCall, D.W. J. Polymer Sci. 26, 151 (1957).
5. Odian, G., Bernstein, B.S. J. Polymer Sci. 2A, 2835 (1964).
6. Charlesby, A., Ross, M. Proc. Roy. Soc. (London) A217, 122, (1953).
Charlesby, A., et al ibid A218, 245 (1953).
7. Ryan, J.W., Nucleonics, 11, 52, 1953.
8. Collins, C.G., et al APEX-261, G.E. Technical Publication, Ohio (1956).
9. Ward, I.M., Mechanical Properties of Solid Polymer, Wiley 1971.
10. Vincent, P.I. Chapter 6 Thermoplastics properties & design Ed. by Ogorkiewicz, Wiley 1974.
11. Rodriguez, F. Principles of Polymer Systems, McGraw Hill 1970.
12. Howard, J.B. SPE Transactions 217, July 1964.
13. Howard, J.B. Polymer Eng. & Sci. 125, July 1965.
14. Brawn, H.R., Polymer 1186, 19, 1978.
15. Ferry, J.D. Viscoelastic Properties of Polymers, John Wiley (1970).
16. Bamford, C.H., et al., Advances in Chemistry Series 142 American Chem. Soc. 1975.

17. Bamford, C.H., et al. Polymer 12, 217 (1971).
18. Bamford, C.H. Recent advance in Polymer Blends Grafts & Blocks, Ed. Sperling L.H. Plenum, New York 1971.

Fig. 6-2A

Xanthone decomposition in the four layers of polyethylene sheets [set 1] during the UV radiation process

- ▼ Sheet A (top layer) 0.207 mm thick
- Sheet B (second top) 0.215 mm thick
- Sheet C (second bottom) 0.18 mm thick
- Sheet D (bottom layer) 0.16 mm thick

% Xanthone w/w

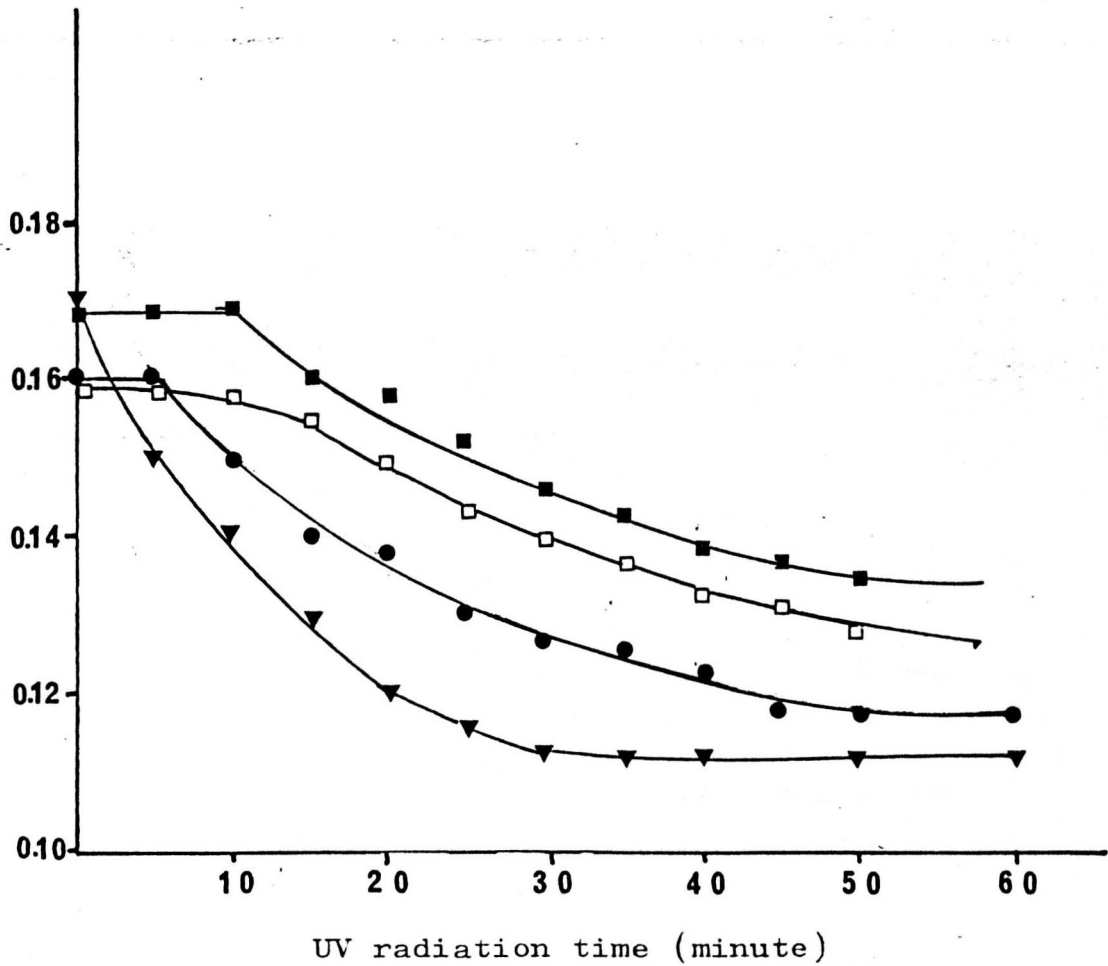
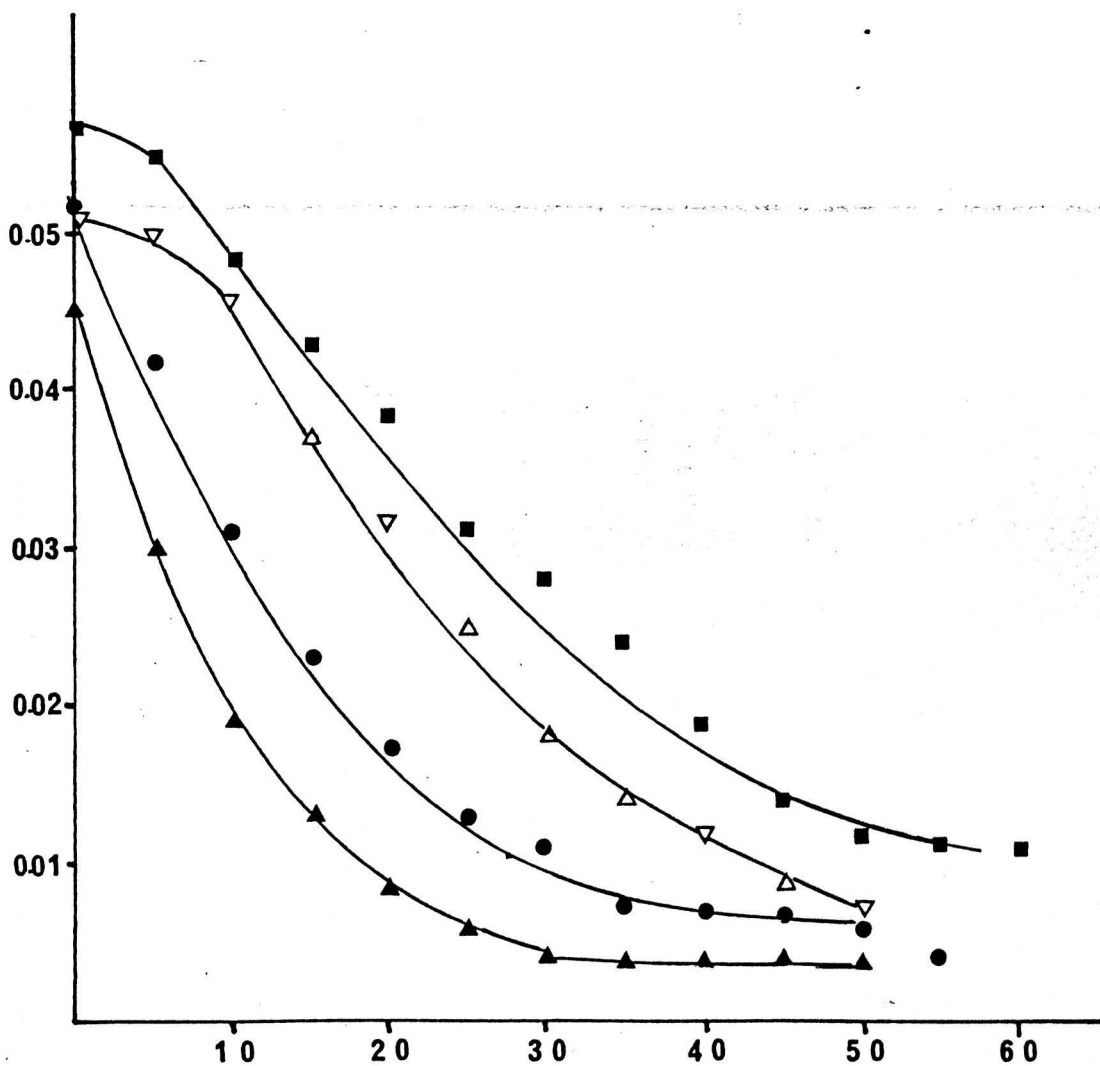


Fig. 6-2B Xanthone decomposition in the four layers of polyethylene sheets [set 2] during the UV radiation process

- ▲ ▲ Sheet A (top layer 0.171 mm thick)
- ● Sheet B (second top) 0.193 mm thick
- △ △ Sheet C (second bottom) 0.171 mm thick
- ■ Sheet D (bottom layer) 0.171 mm thick

% Xanthone w/w



UV radiation time (minute)

Fig. 6-3 Crosslinking effect on the melt flow index of the polyethylene in relation to the thickness of the polymer film.

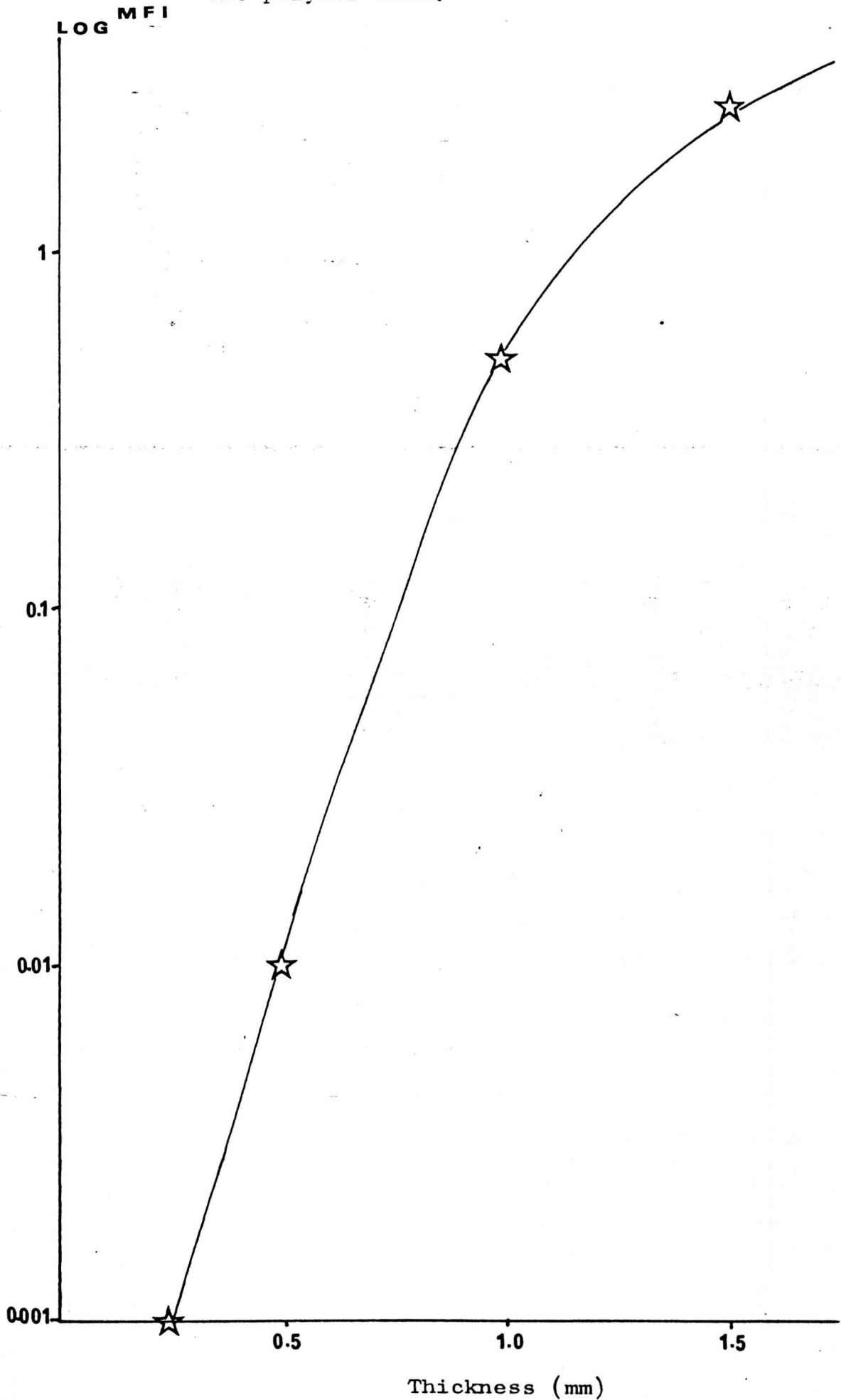


Fig. 6-5

IR spectrum of the gel part of polyethylene + TAC + Xanthone film,
UV radiated for five minutes.

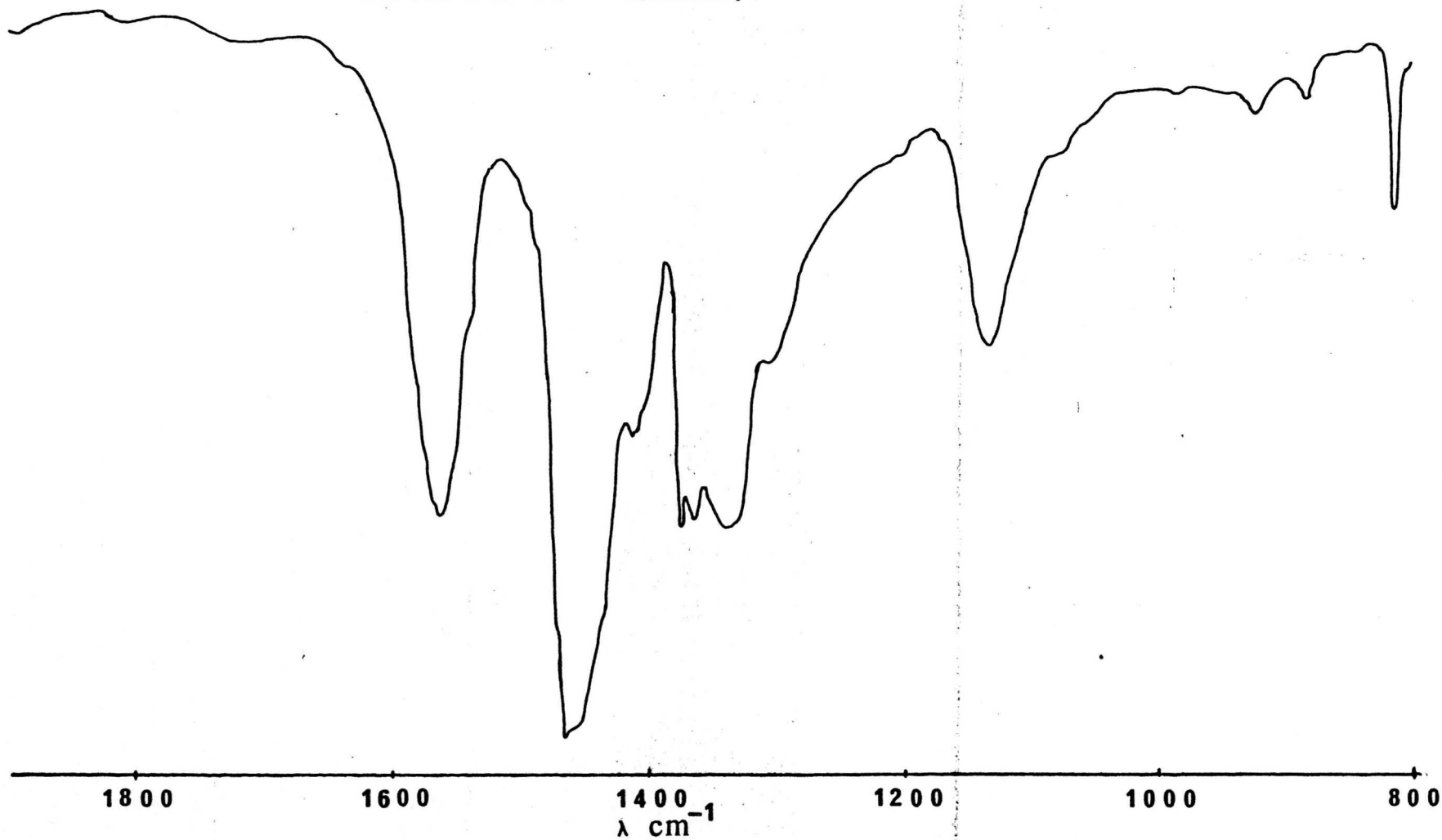


Fig. 6-6 IR spectrum of the gel part of polyethylene + TAC + Xanthone film,
UV radiated for half an hour.

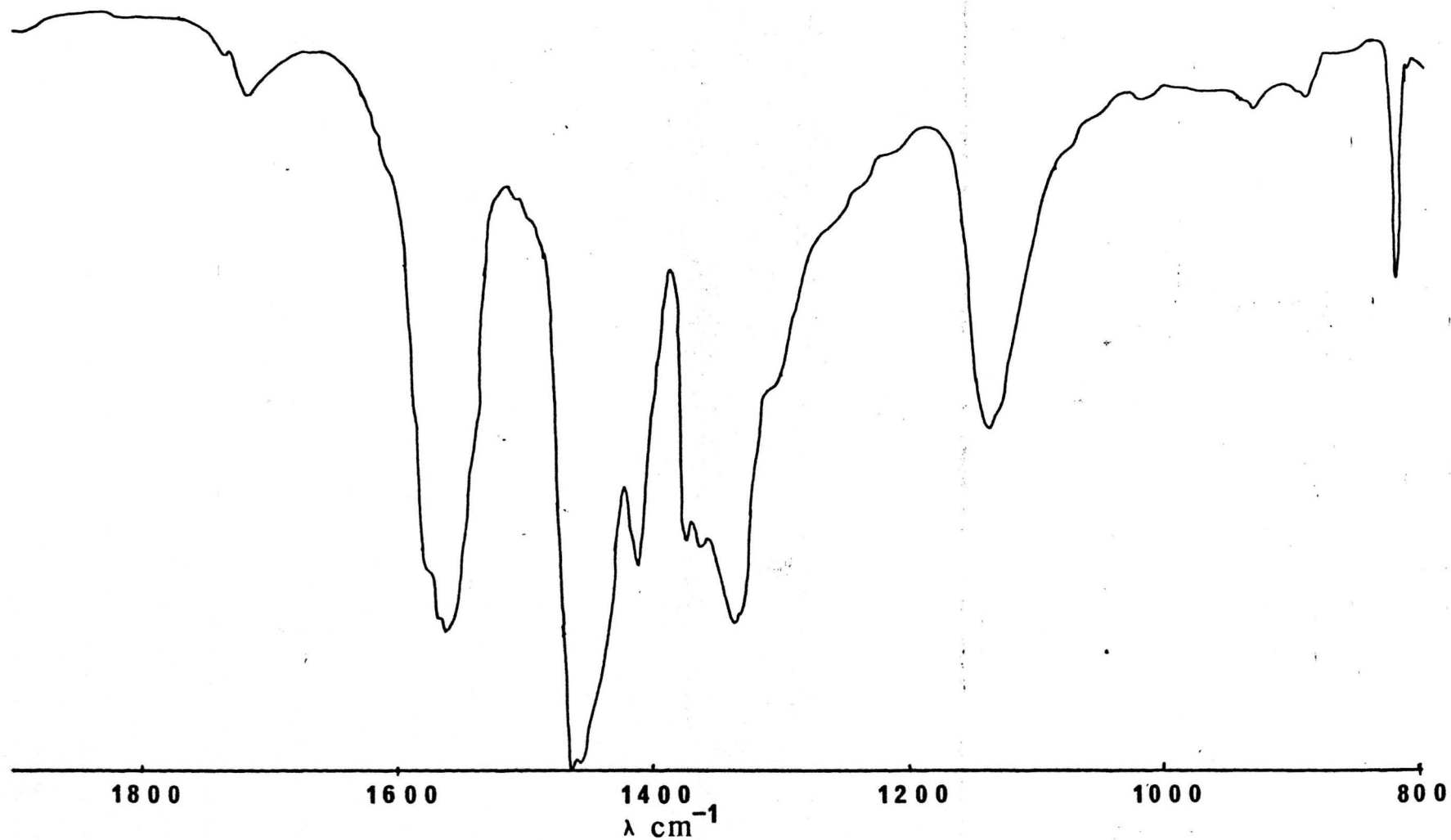


Fig. 6-7 IR spectrum of the gel part of polyethylene + Xanthone film, UV radiated for half an hour.

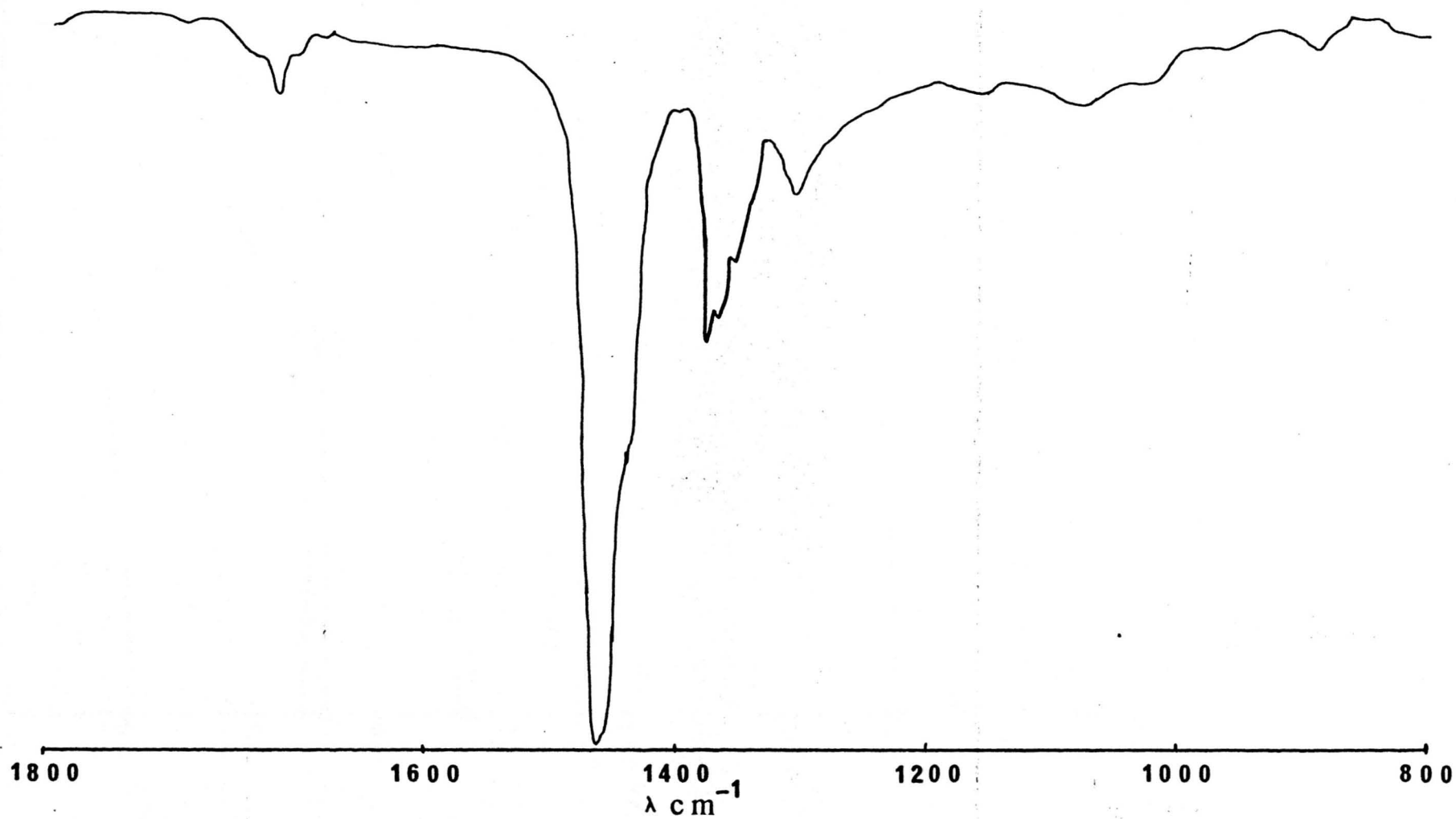


Fig. 6-8 Gel content and TAC % w/w in gel, in relation to the UV radiation time

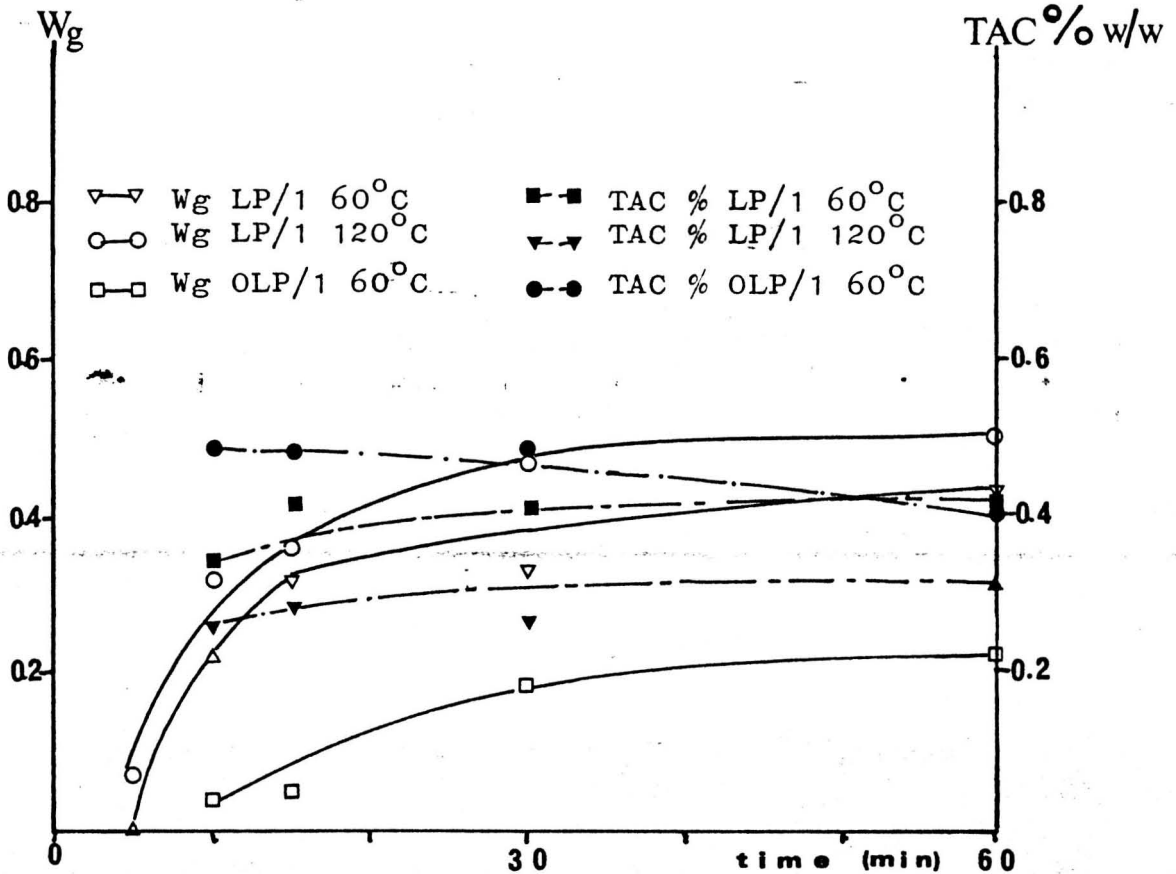


Fig. 6-9 Gel content and TAC % w/w in gel, in relation to the UV radiation time.

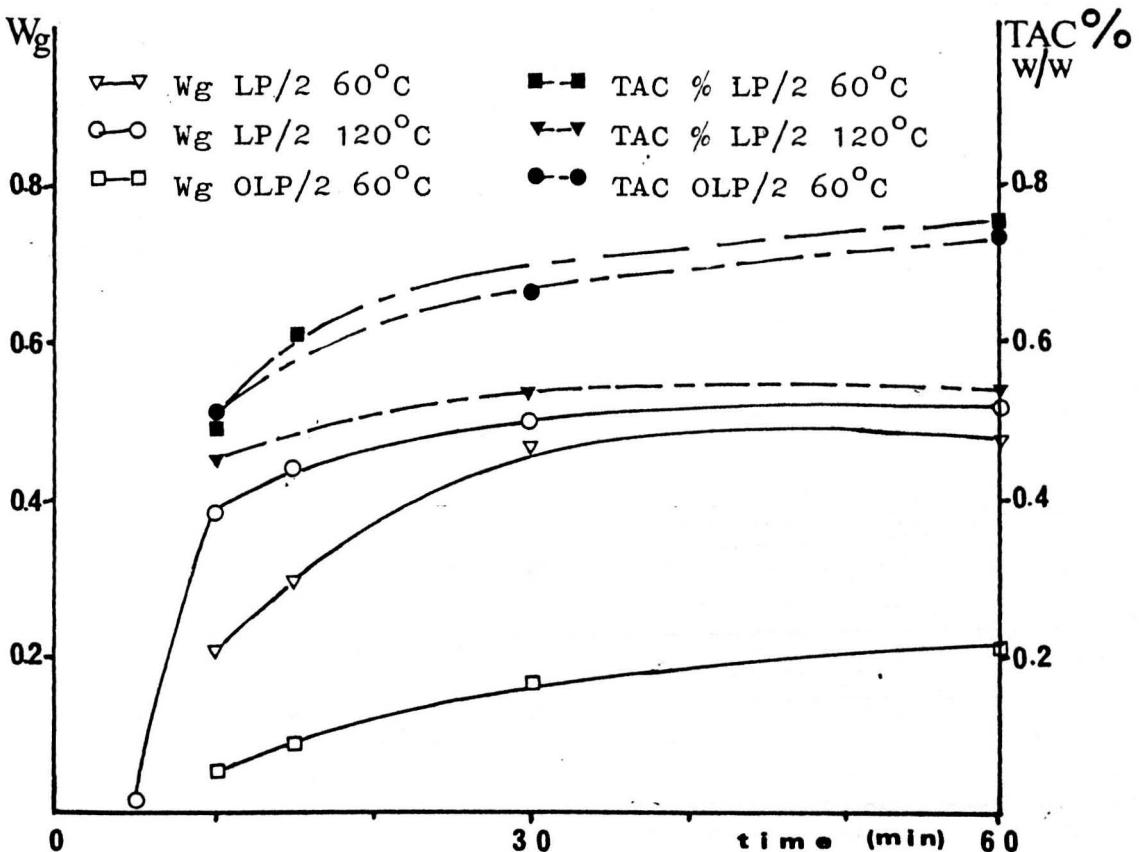


Fig. 6-10 Gel content and TAC % w/w in gel, in relation to the UV radiation time

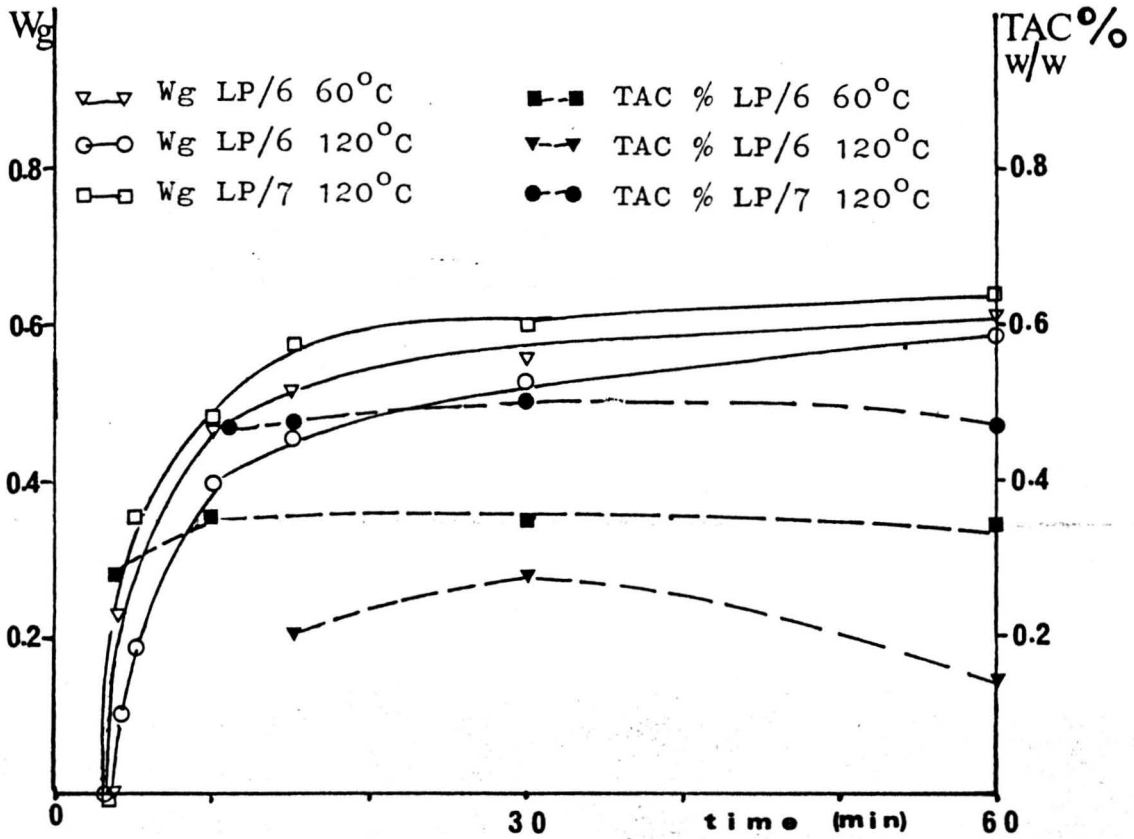


Fig. 6-11 Gel content of UV radiated polyethylene sheets at 60°C

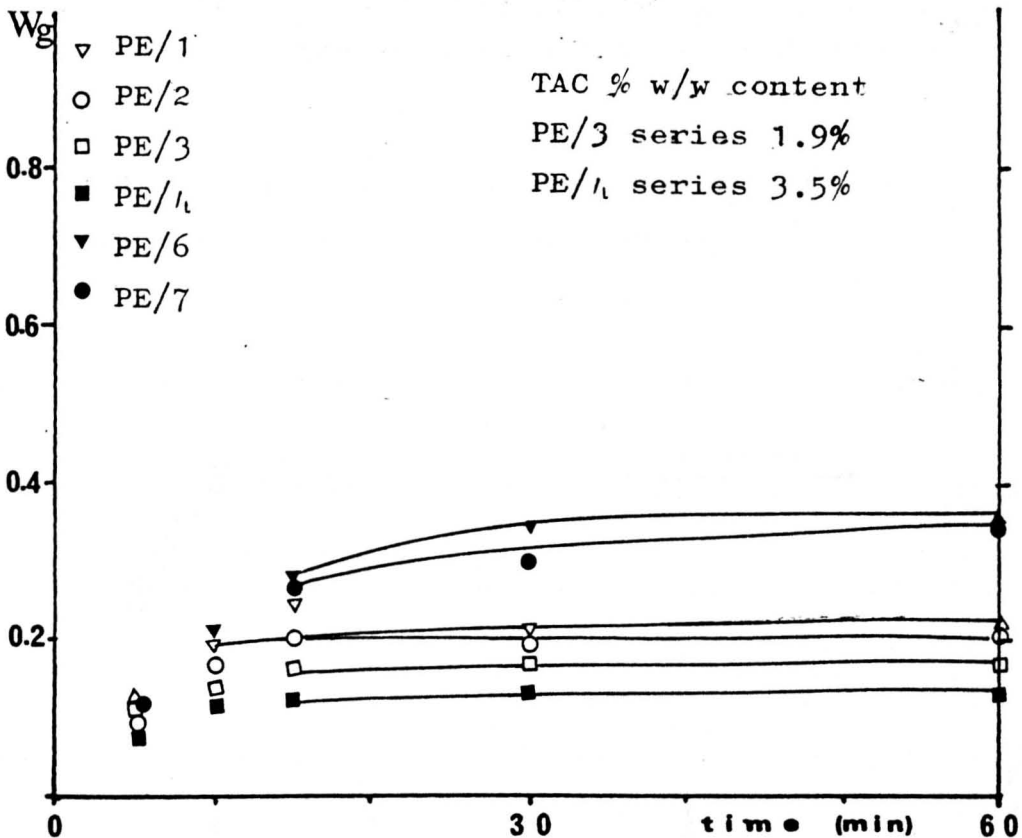


Fig. 6-12 Gel fraction after a 30 minute UV radiation in relation to the initial TAC % w/w concentration in the polyethylene sheets

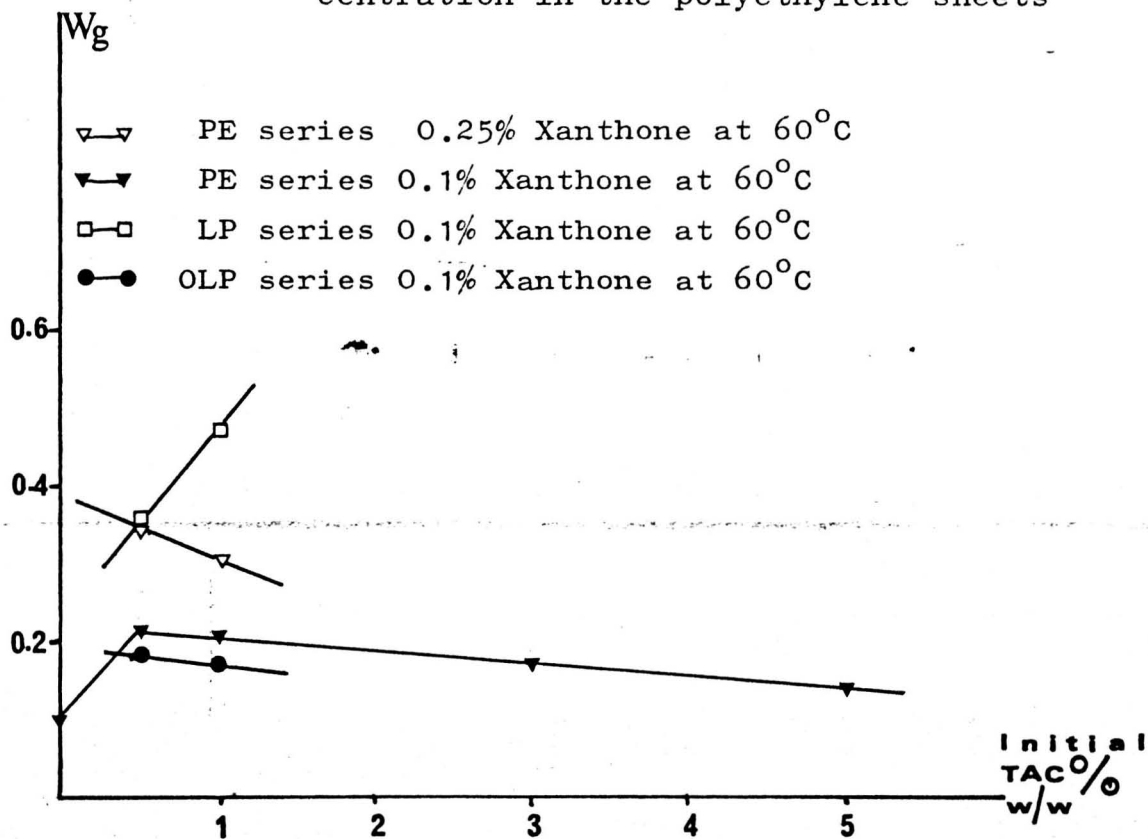


Fig. 6-13 Gel fraction after a 30 minute UV radiation in relation to the initial TAC % w/w concentration in polyethylene sheets

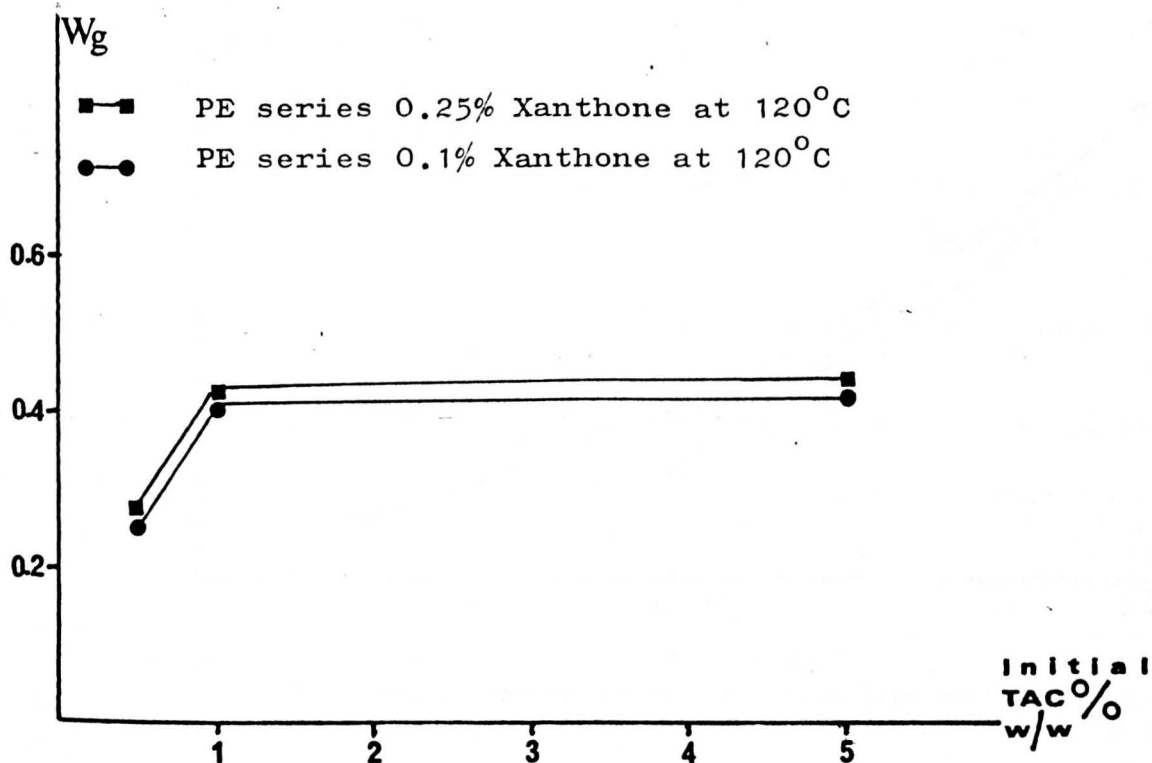
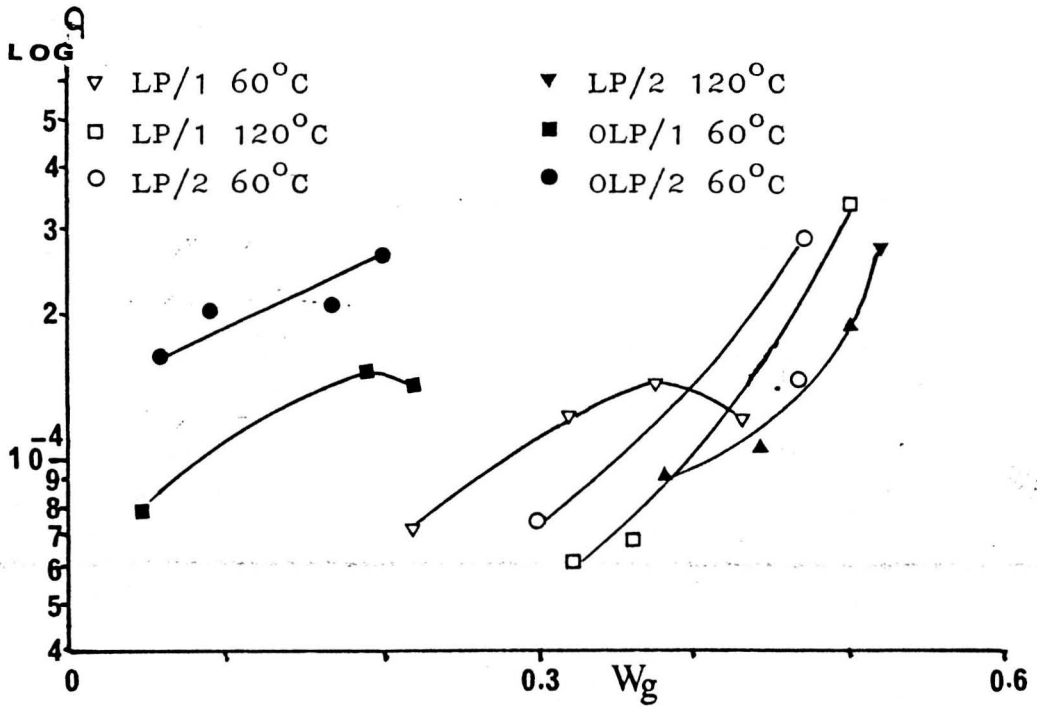
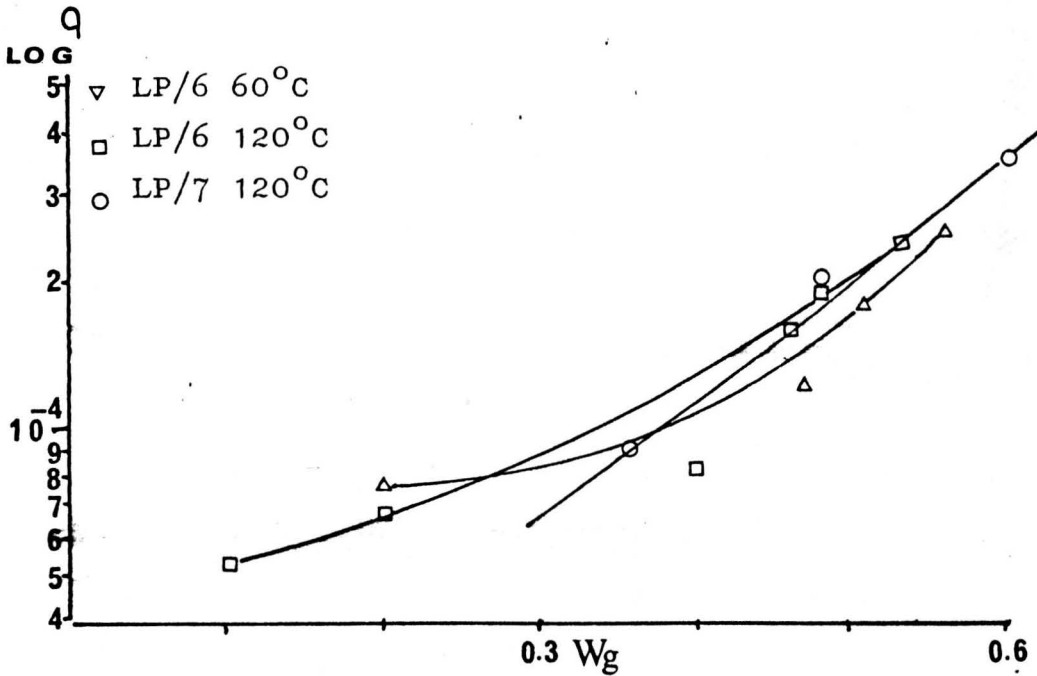


Fig. 6-14 The relationship between the crosslinking density and the gel fraction of the UV irradiated polyethylene sheets



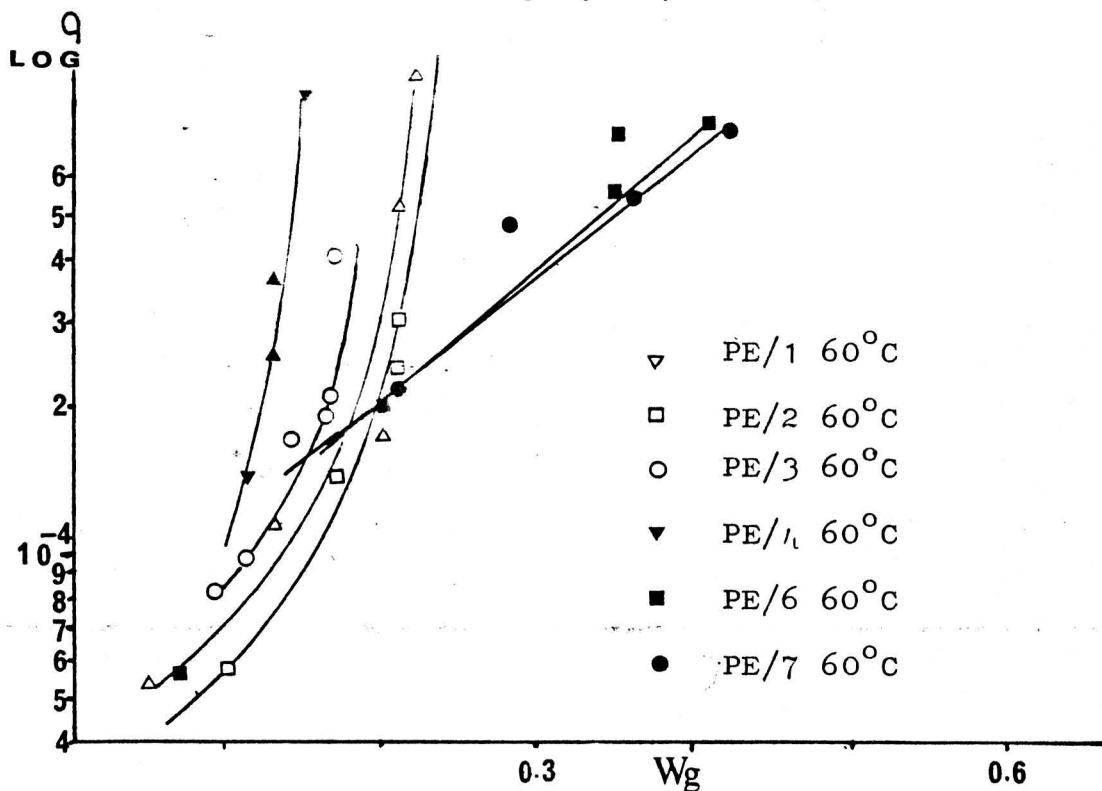
Q the crosslinking density from swelling measurements

Fig. 6-15 The relationship between the crosslinking density and the gel fraction of the UV irradiated polyethylene sheets



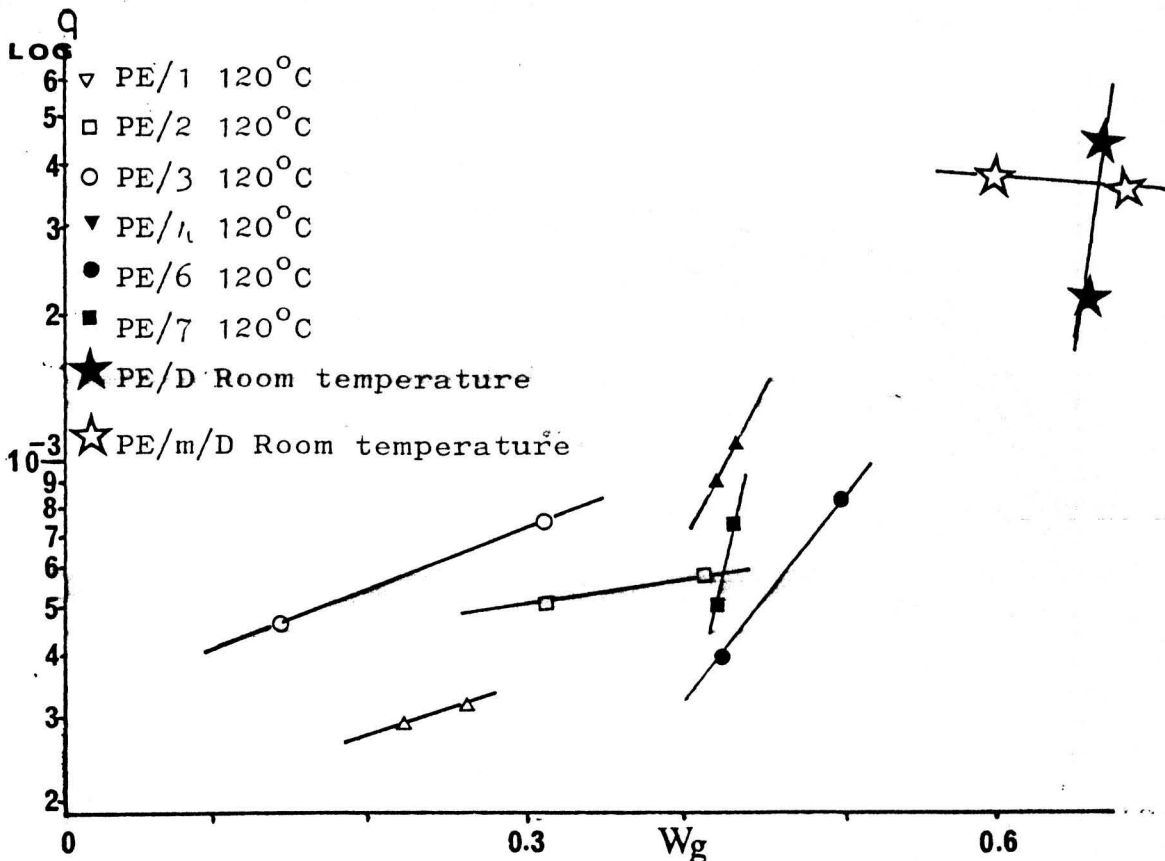
Q the crosslinking density from the swelling measurements

Fig. 6-16 The relationship between the crosslinking density and the gel fraction of the UV irradiated polyethylene sheets



Q the crosslinking density from the swelling measurements

Fig. 6-17 The relationship between the crosslinking density and the gel fraction of the UV and γ irradiated polyethylene sheets



Q The crosslinking density from the swelling measurements

Fig. 6-18

Gel permeation chromatography analysis of the post-treated polyethylene films.

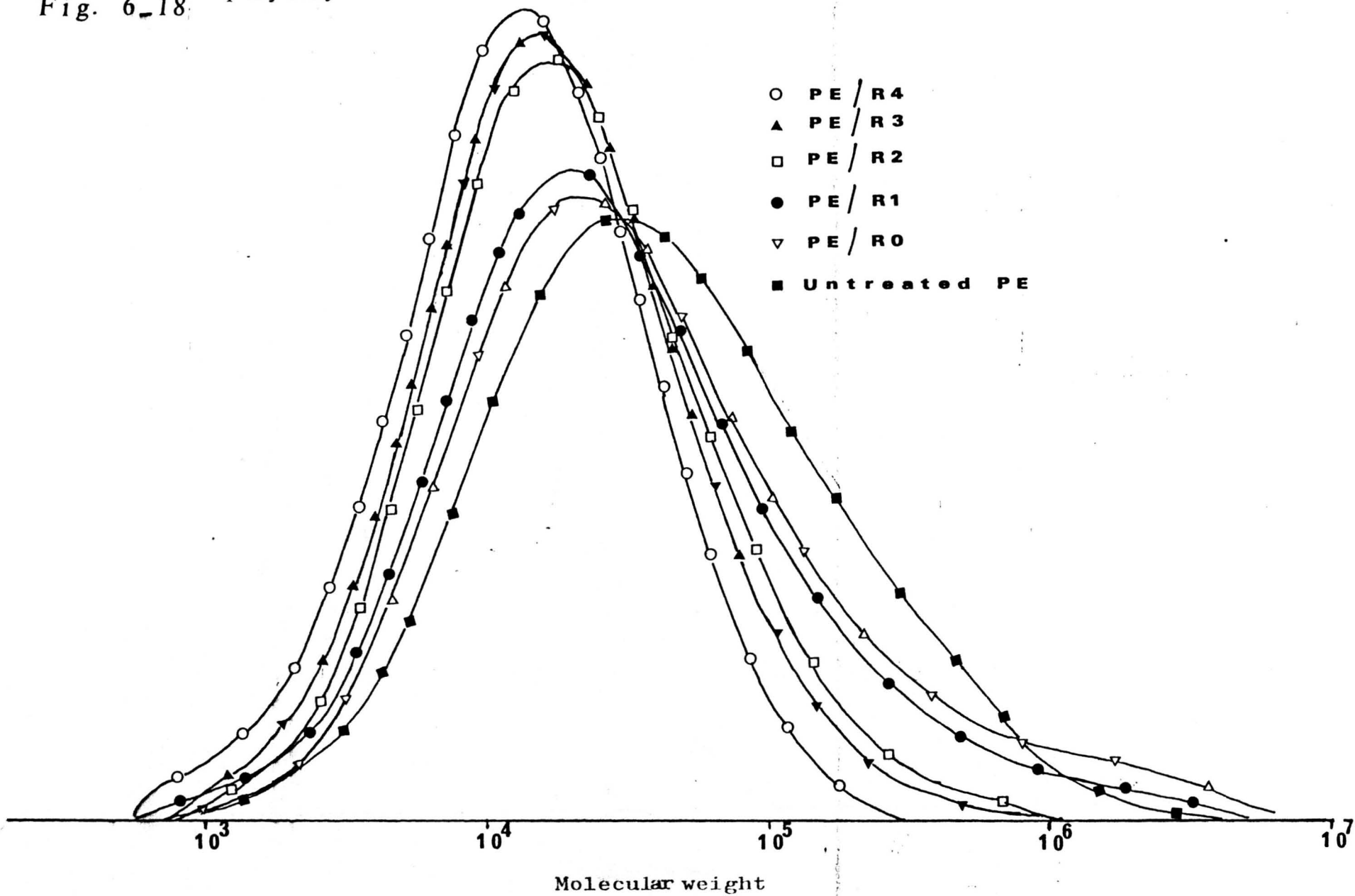


Fig. 6-19

Gel permeation chromatography analysis of the γ -irradiated polyethylene films

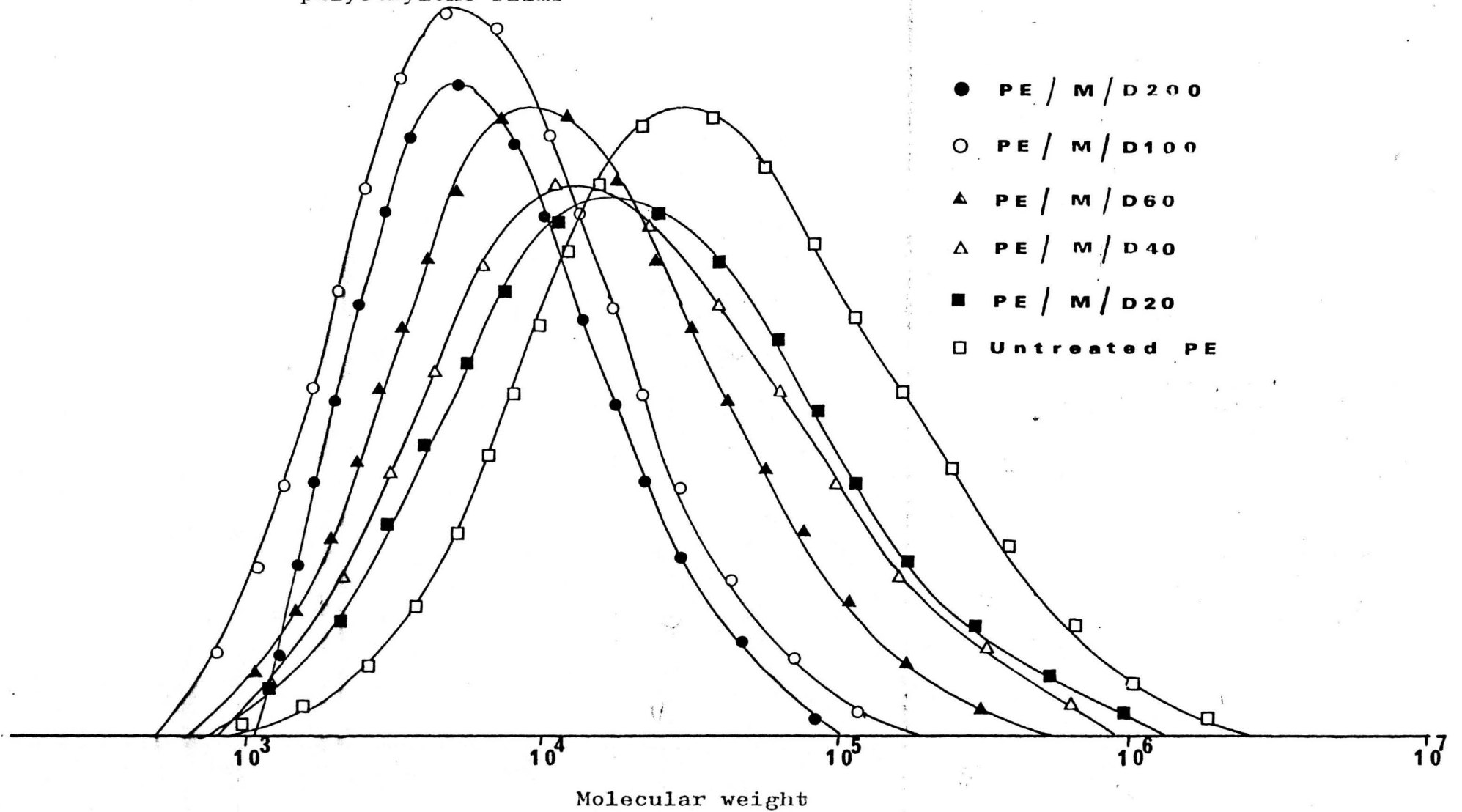


Fig. 6-20 Gel permeation chromatography analysis of the γ -irradiated polyethylene films

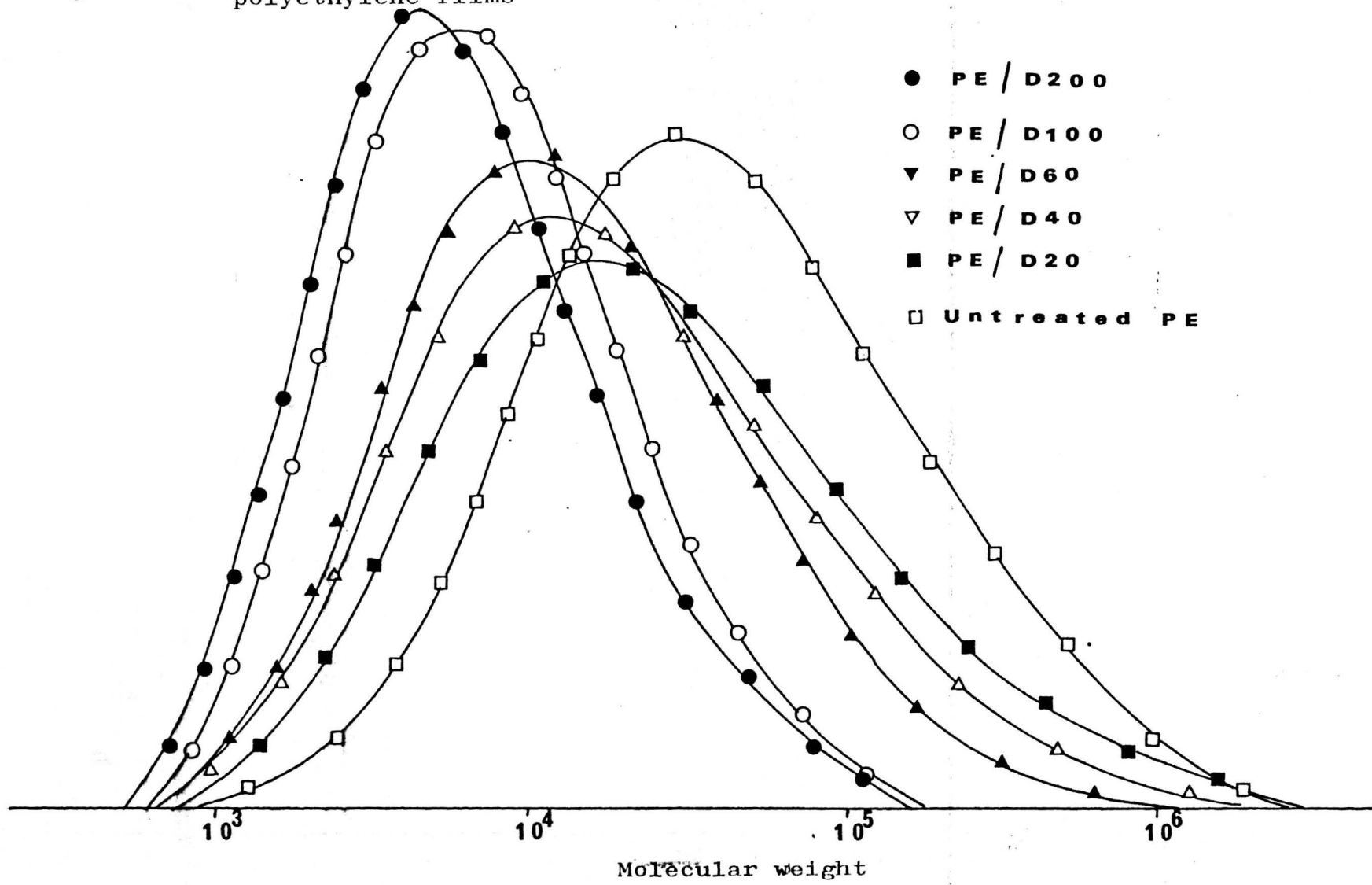


Fig. 6-21 Gel fraction of the γ -irradiated polyethylene films in relation to the dosage

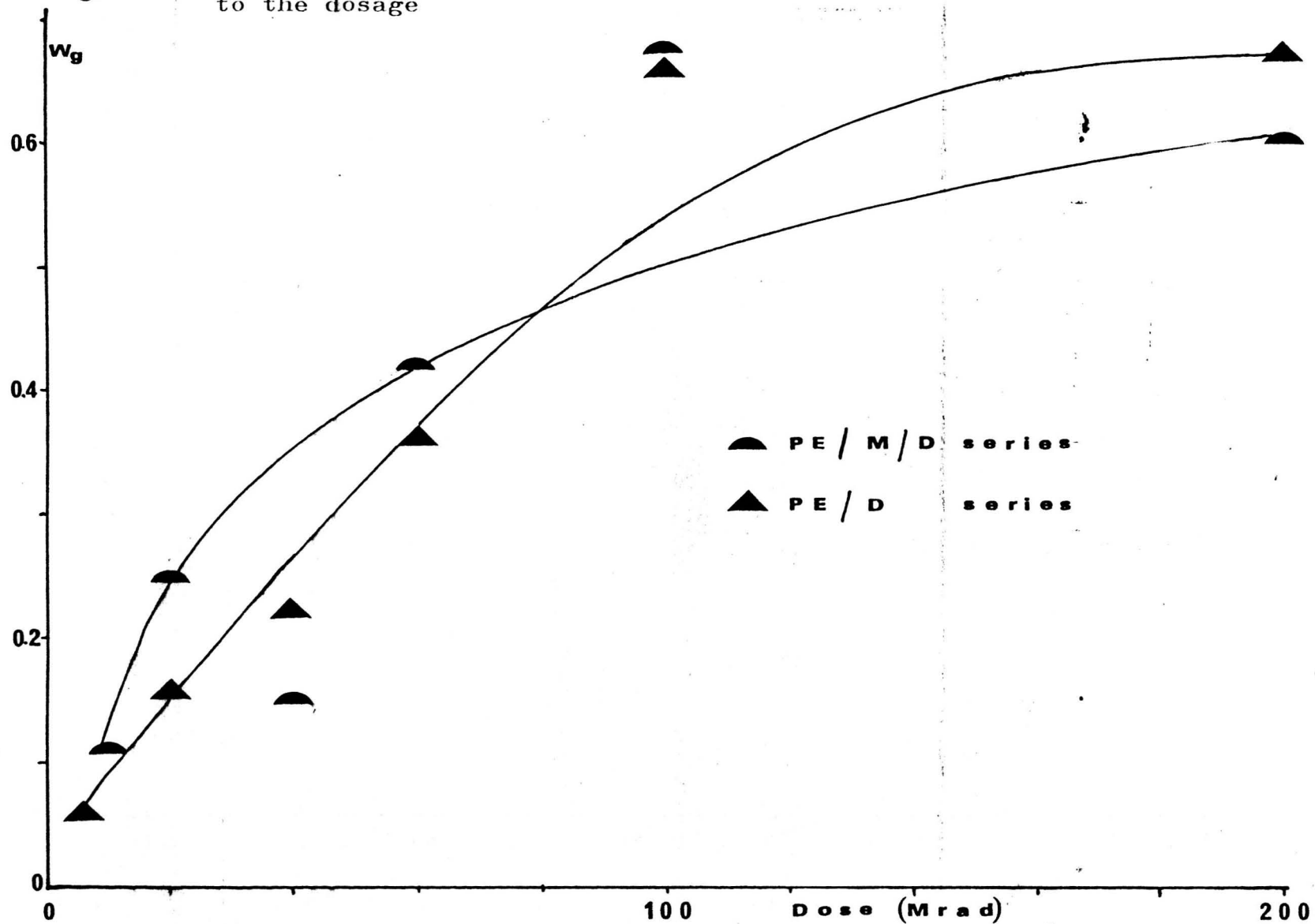
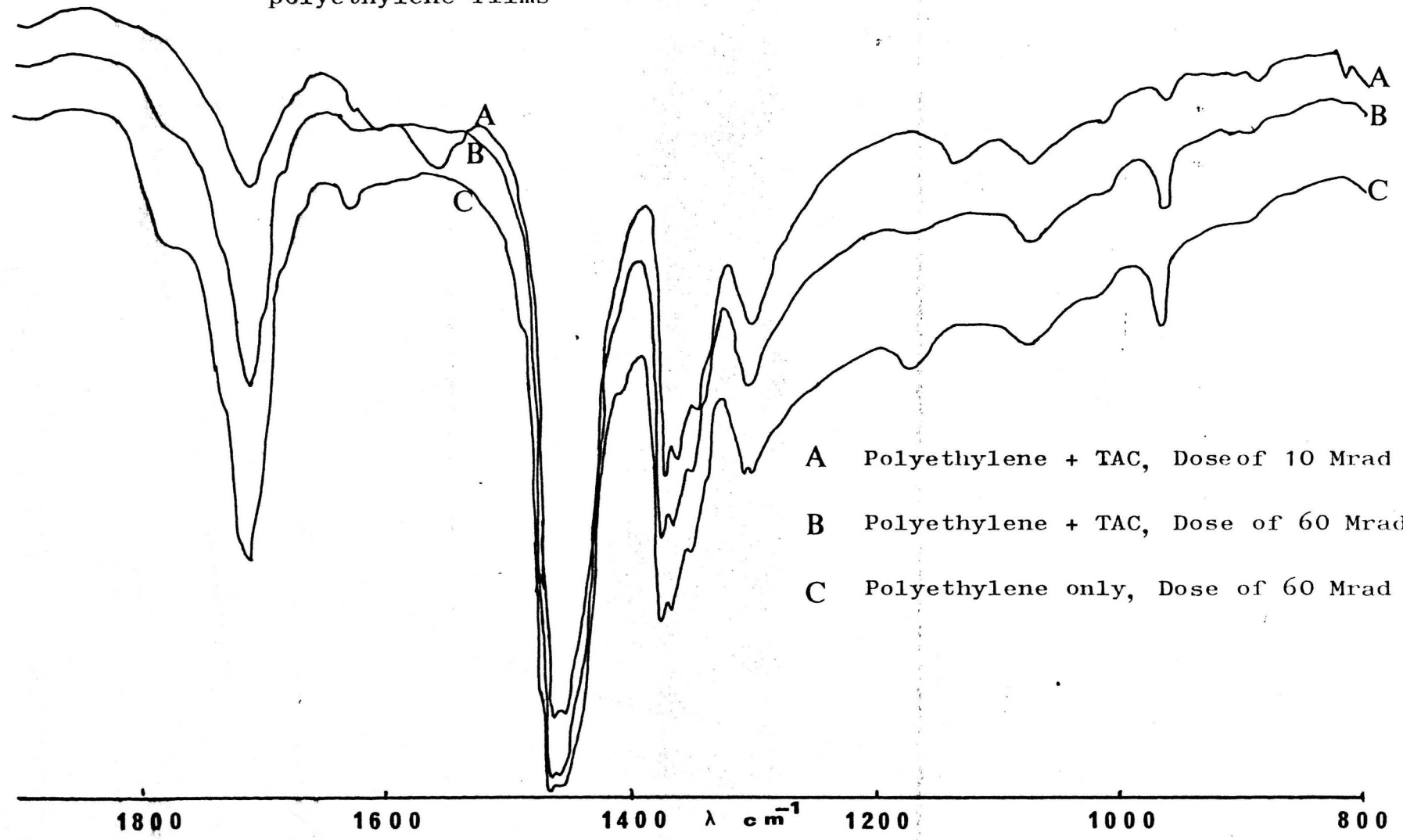


Fig. 6-22

IR spectra of the gel part of the γ -irradiated polyethylene films



- A Polyethylene + TAC, Dose of 10 Mrad
- B Polyethylene + TAC, Dose of 60 Mrad
- C Polyethylene only, Dose of 60 Mrad

Fig. 6-23 The environmental stress cracking [ESC] of the untreated and UV treated polyethylene films

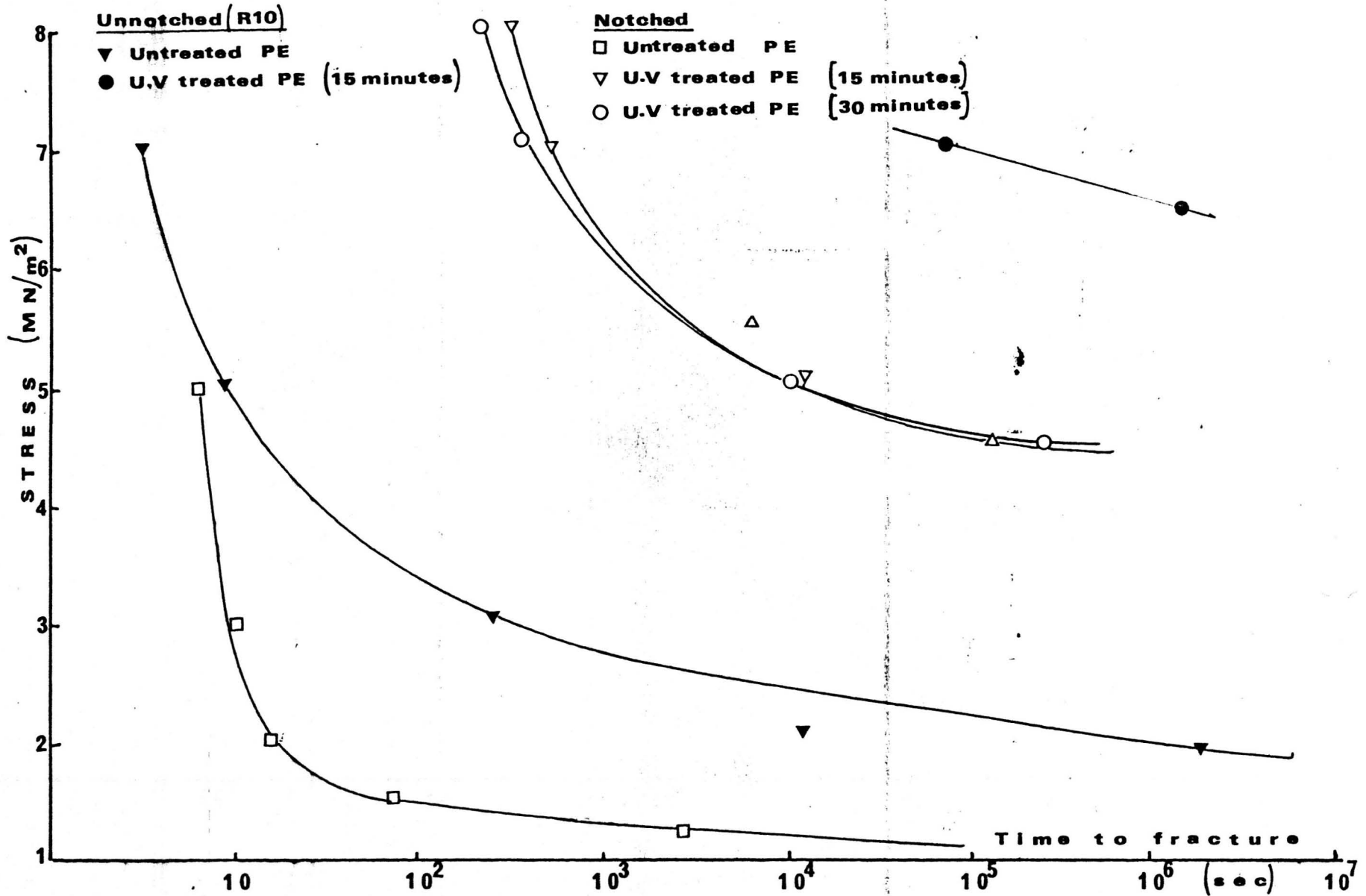


Fig. 6-25 The rheological behaviour of polyethylene sheets (treated and untreated) at 160°C.

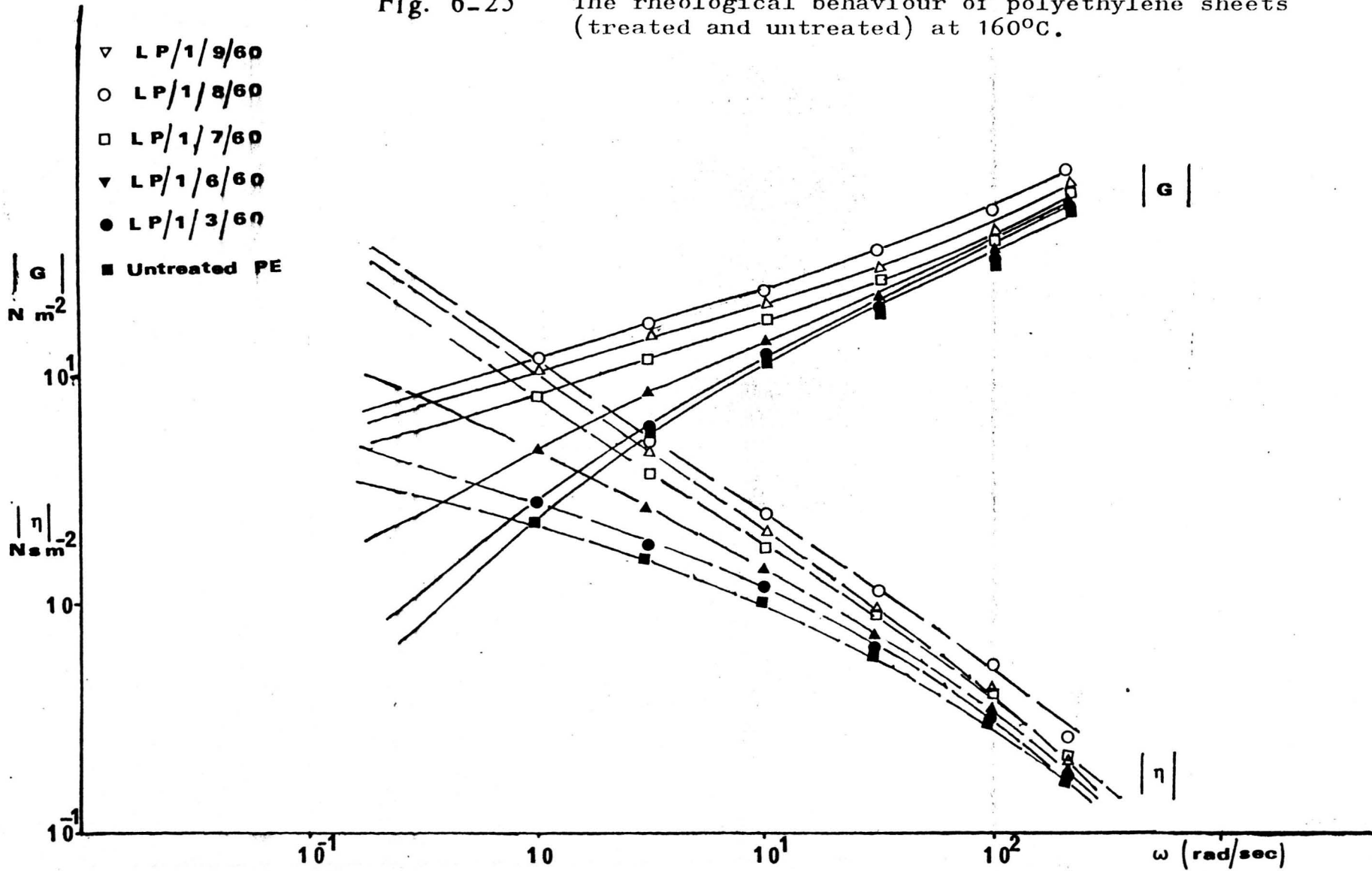


Fig. 6-26 The loss tangent ($\tan \delta$) of different polyethylene sheets (treated and untreated) at 160°C

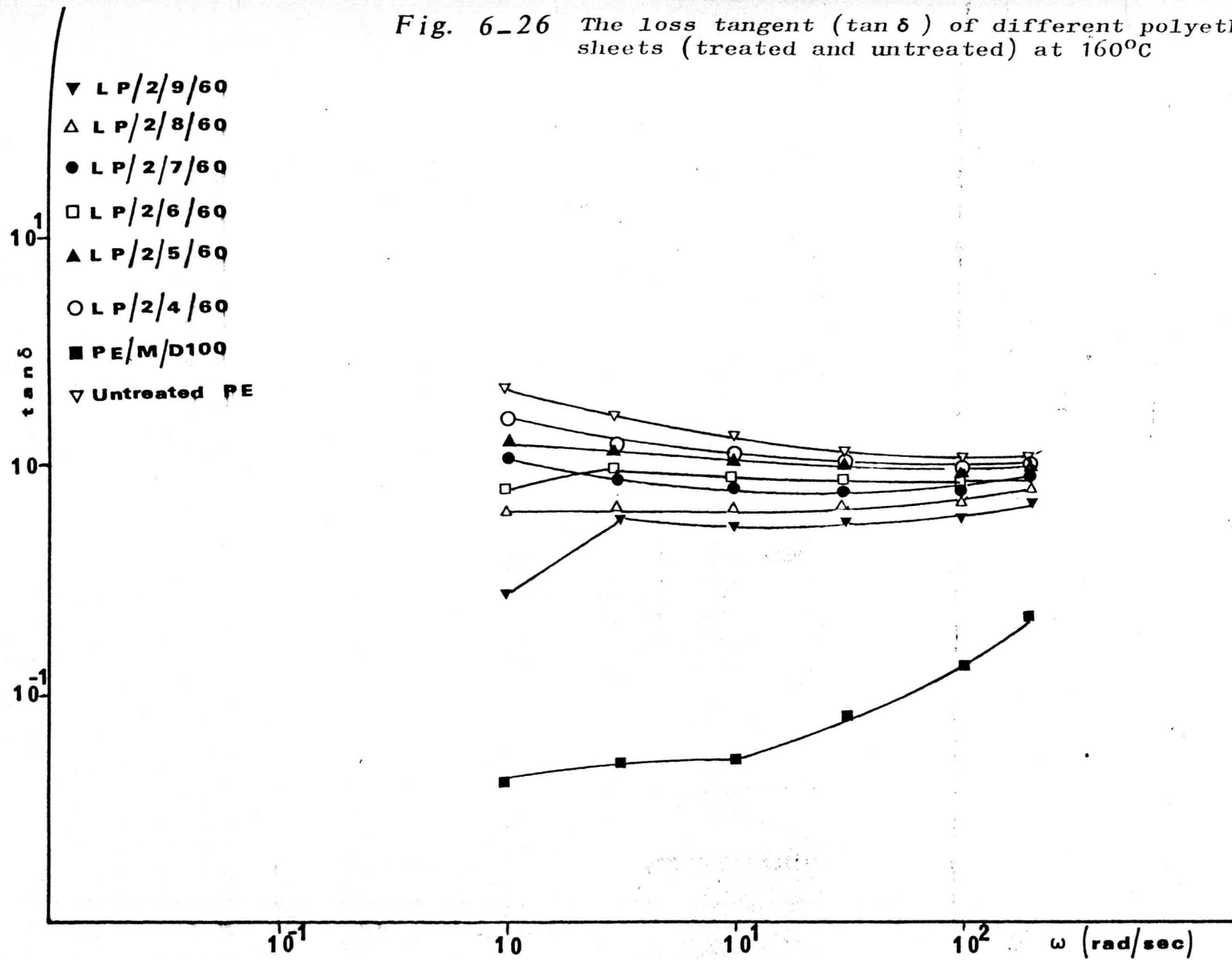


Fig. 6-27 The rheological behaviour of untreated polyethylene at different temperatures

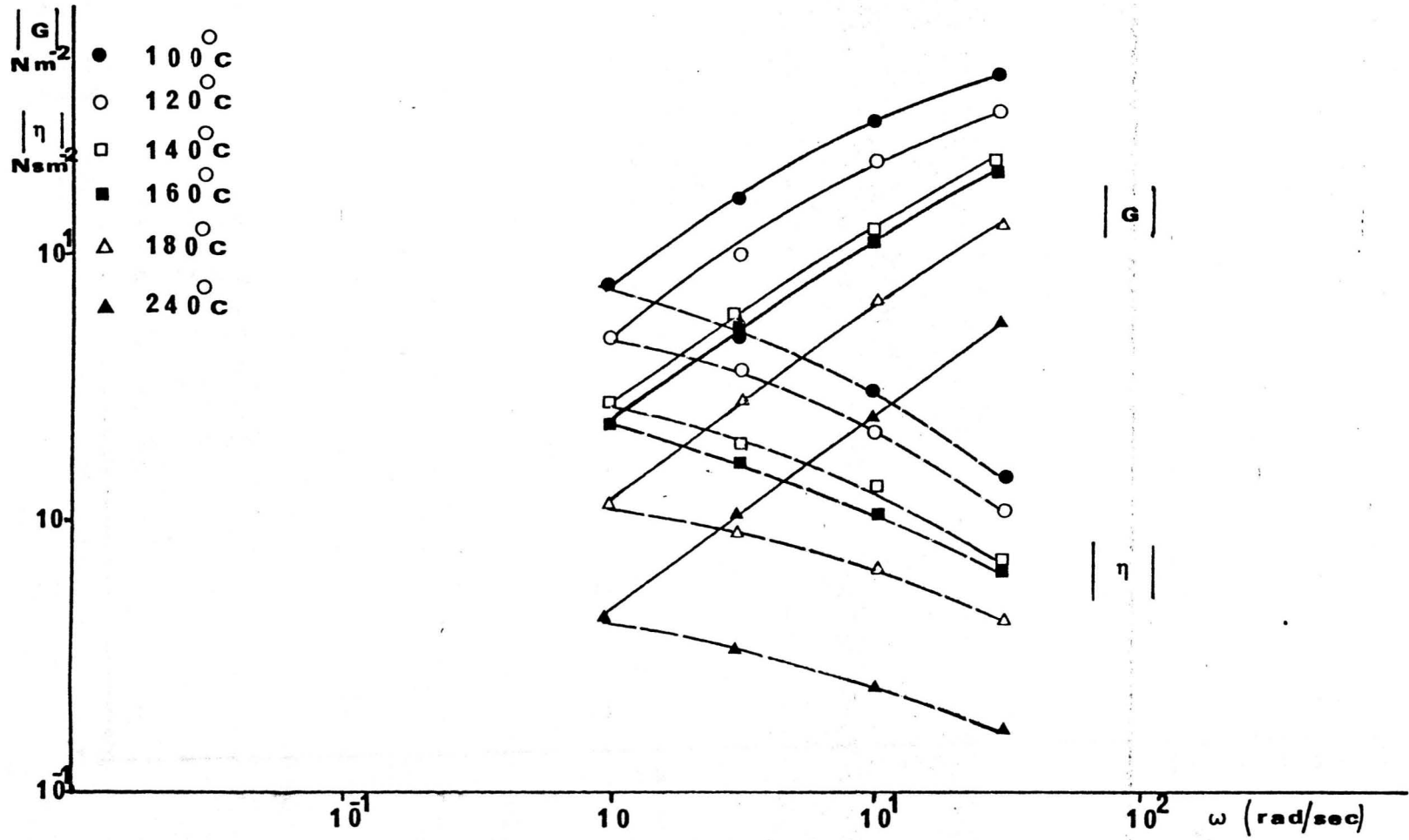


Fig. 6-28

The rheological behaviour of treated polyethylene sheets (LP/6/9/60) at different temperatures

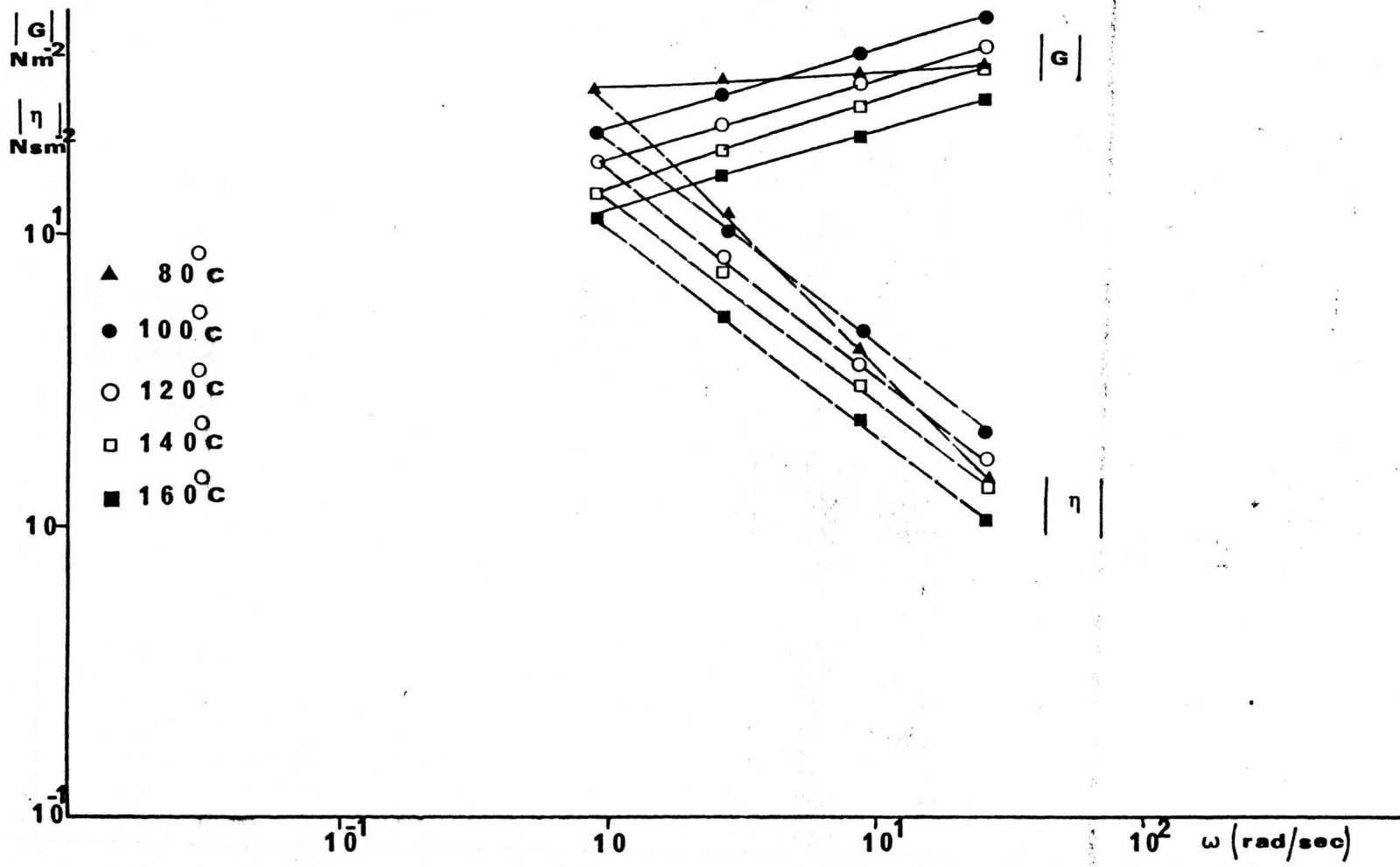


Fig. 6-29

The rheological behaviour of treated polyethylene sheets (LP/6/9/60) at different temperatures

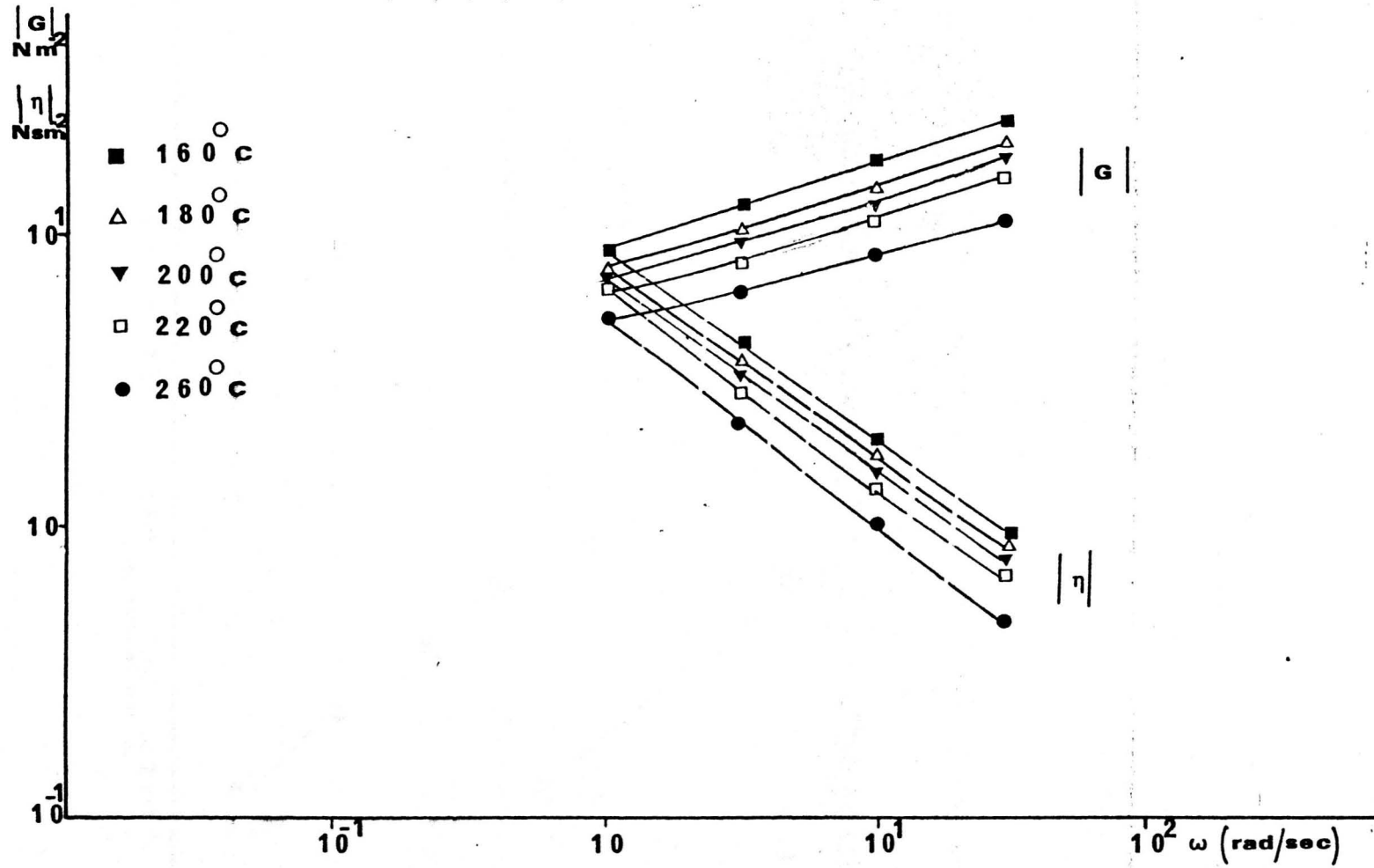


Fig. 6-30 The effect of temperature on the rheological behaviour of treated and untreated polyethylene at frequency $\omega = 3.14$ rad/sec

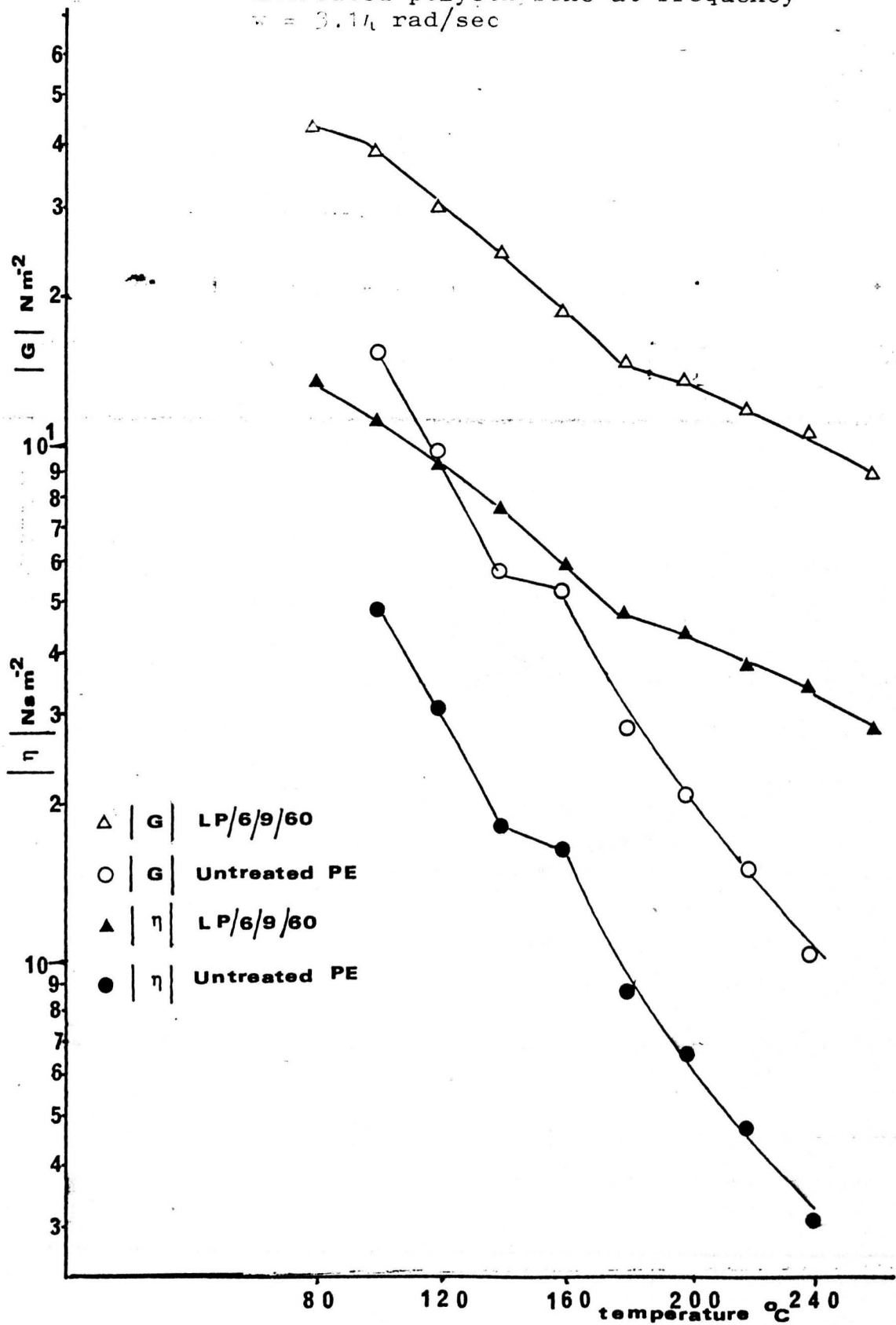


Fig. 6-31 The dynamic viscosity $|\eta|$ of treated and untreated polyethylene films at continuous shear (angular velocity $w = 1 \text{ rad/sec}$) and at temperature = 160°C

